Solvent tolerance mechanisms in Pseudomonas putida

Kusumawardhani, H.

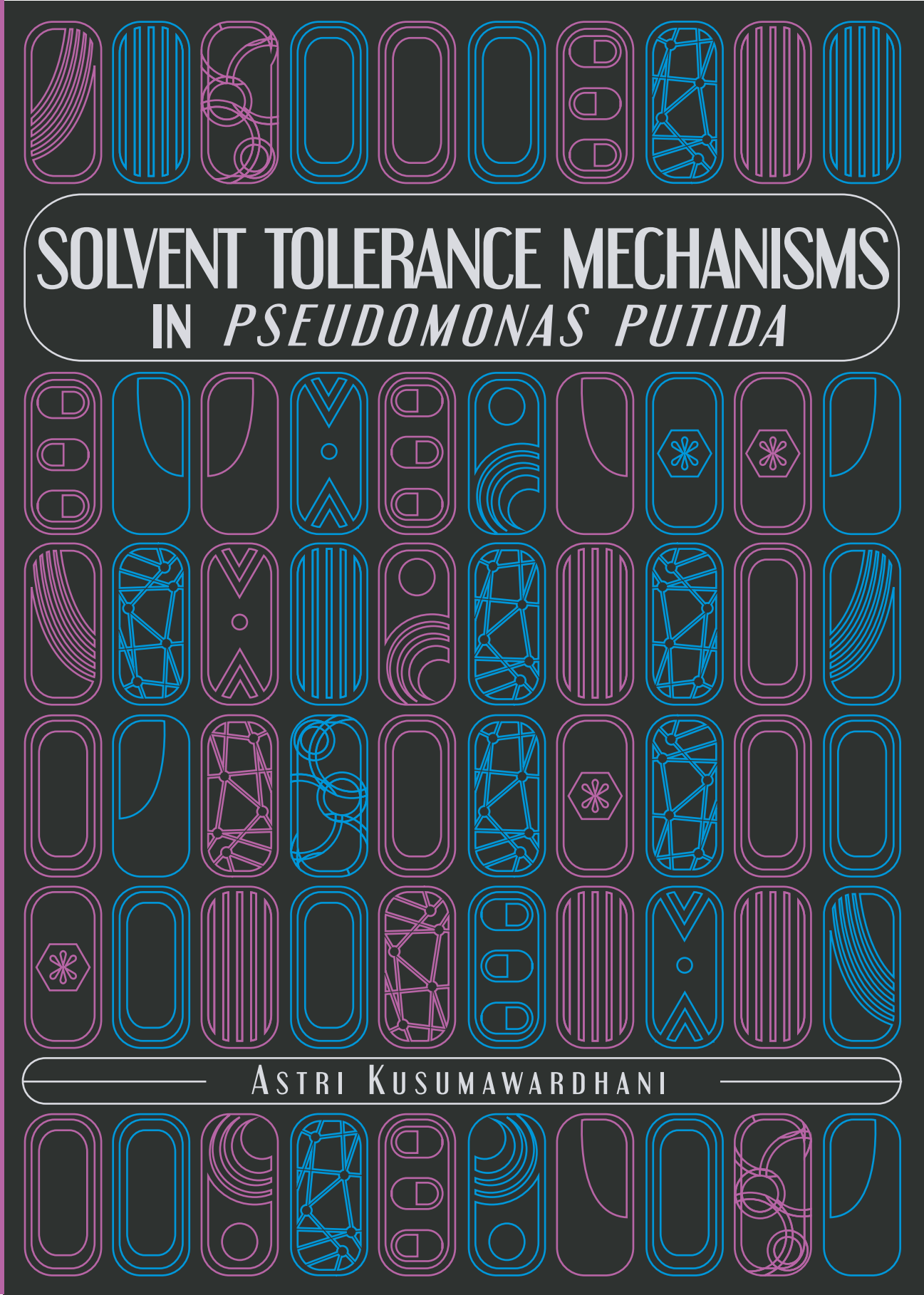

SOLVENT TOLERANCE MECHANISMS IN PSEUDOMONAS PUTIDA
ASTRI KUSUMAWARDHANI

Solvent tolerance mechanisms in *Pseudomonas putida*

Astri Kusumawardhani

ISBN:

Author: Hadiastri Kusumawardhani

Cover & Layout design: Raden Lerika Ratri Noorshanti, Hadiastri Kusumawardhani

Printing:

Funding statement: This work is financed by Indonesian Endowment Fund for Education (LPDP), The Ministry of Finance, Indonesia (grant number 20150322022595).

Solvent tolerance mechanisms in *Pseudomonas putida*

Proefschrift

ter verkrijging van

de graad van Doctor aan de Universiteit Leiden,

op gezag van Rector Magnificus Prof.dr.ir. H. Bijl,

volgens besluit van het College voor Promoties

te verdedigen op Donderdag 11 Maart 2021

klokke 16.15 uur

door

Hadiastri Kusumawardhani

geboren te Bandung, Indonesia

in 1991

Promotor: Prof. dr. J. H. De Winde

Co-promotor: Dr. Rohola Hosseini

Promotiecommissie: Prof. dr. Gilles P. van Wezel

Prof. dr. Ariane Briegel

Prof. dr. Nick Wierckx

Prof. dr. Miriam Agler-Rosenbaum

Dr. Hermann J. Heipieper

Table of Contents

CHAPTER 1

Aim and scope of this thesis

1

Pseudomonas putida S12 as a solvent-tolerant bacterial strain

Organic solvents are important in biocatalysis as precursors of various high-value chemicals, as end products and as in-situ product extractant (1). However, the usage of organic solvents in biocatalysis is challenging due to their toxicity to microbial cells. Organic solvents can cause the disruption of the bacterial cell membrane and lipid bilayer. Interestingly, some microorganisms can tolerate and assimilate toxic organic solvents in high concentrations. The first reported solvent-tolerant microorganism was *Pseudomonas putida* IH-2000 that can survive in 50% (vol/vol) of toluene (2). Following this discovery, several other solvent-tolerant *P. putida* strains were identified such as strain DOT-T1E and S12 (3, 4).

Pseudomonas putida is a diderm (Gram-negative), rod-shape bacterium belonging to the class Gamma proteobacteria and family Pseudomonadaceae. Several strains of *P. putida* were isolated from soil for utilizing organic solvent as its carbon source, for example strains mt-2 and DOT-T1E for toluene utilization and strain S12 for styrene utilization (3–5). Currently, *P. putida* S12 has been implemented for the production of high-value chemicals like phenol, p-hydroxybenzoate, and p-hydroxystyrene; all of which have solvent-like properties and therefore are generally toxic for most of microbial hosts (6–8). Moreover, this strain can also grow in a two-phase fermentation system using toxic organic solvents, thus making it excellent for industrial application.

Recently, whole genome sequencing has been performed on *P. putida* S12 (9). The genome of *P. putida* S12 consists of 5.8-mega base pairs chromosome (GeneBank Accession number CP009974) and a single copy of 583-kilo base pairs megaplasmid pTTS12 (GeneBank Accession number CP009975). A gene cluster encoding a solvent extrusion pump (*srpRSABC*) was revealed to be located on the plasmid pTTS12. However, the role of this megaplasmid in conferring solvent tolerance to *P. putida* S12 had not been described beyond the solvent extrusion pump SrpABC.

Several research questions are being addressed in this thesis. Initial efforts have been made to transfer genetic traits from solvent-tolerant bacteria to industrial production strains. Can such transfers be extended to more industrial strains? Moreover, will these engineered strains reach similar tolerance levels as native strains in combination with optimal production yields? In native solvent-tolerant strains, multiple efflux pumps operate simultaneously to prevent accumulation of organic solvents. However, simultaneous overexpression of multiple efflux pumps is disadvantageous in engineered strains due to membrane composition

changes and insertion machinery overload (10). How can expression levels be optimized for combinations of pumps operating simultaneously? Moreover, with many omics data becoming available to date, genetic traits responsible for solvent tolerance in different strains can be predicted. How to address the challenge of constructing a solvent tolerance model operating in different species?

Scope and outline of this thesis

This PhD project focuses mainly on the mechanism behind solvent tolerance of *P. putida* S12 and its genome stability. **Chapter 1** gives a general introduction on *P. putida* S12 as a model organism of solvent tolerance as well as its industrial relevance. Here, the gap of knowledge on the mechanisms of solvent tolerance and the outline of this thesis are described.

In **Chapter 2**, current knowledge and understanding of solvent-tolerant bacteria are described. Application and challenges in working with solvent-tolerant bacteria in biocatalysis are discussed. Furthermore, the emerging synthetic biology tools and advance in metabolic engineering regarding the solvent-tolerant bacteria are also discussed.

While *P. putida* S12 (ATCC 700801) is highly tolerant towards various organic solvents due to the presence of solvent extrusion pump (11, 12), it is unknown whether other parts of the megaplasmid plays a role in the solvent tolerance. **Chapter 3** and **Chapter 4** focus on the role of the megaplasmid in solvent tolerance. In **Chapter 3**, comparative analysis revealed that megaplasmid pTTS12 belongs to the incompatibility P-2 (IncP-2) plasmid group. Heavy-metal resistance is the main characteristic of the IncP-2 plasmid group and indeed, pTTS12 contains tellurite, chromate, and mercury resistance cassettes. In addition to the heavy-metal resistance cassettes, plasmid pTTS12 contains the solvent extrusion pump SrpABC, phenylpropionate and styrene-phenylacetate degradation pathways. Further observations on the modular functional build-up of these gene clusters in pTTS12 are described in **Chapter 3**.

In **Chapter 4**, a novel toxin-antitoxin (TA) SlvT-SlvA module is characterized. This TA module was found to be upregulated in the presence of toluene from previous transcriptomic data (13). SlvT-SlvA belongs to the COG5654-COG5642 TA family. Like other members of the COG5654 toxin family, SlvT can deplete cellular NAD^+, rendering the cells to stop growing in the absence of its antitoxin SlvA. The role of the SlvT-SlvA toxin-antitoxin pair in solvent tolerance and maintaining plasmid stability are discussed in **Chapter 4**.

In **Chapter 5**, the intrinsic solvent tolerance of *P. putida* S12 is addressed. Plasmid pTTS12 plays an important role in conferring solvent tolerance to *P. putida* S12. In the absence of this plasmid, *P. putida* S12 lost its ability to survive high concentration of toluene. Adaptive laboratory evolution (ALE) experiments were performed on the plasmid-cured *P. putida* S12 enabling growth on increasing concentrations of toluene. Eventually, evolved strains were able to grow on a high toluene concentration (10% (vol/vol)) even in the absence of megaplasmid pTTS12. Whole-genome and RNA sequencing analysis revealed the genetic interplay which allowed restoration of solvent tolerance in the plasmid-cured strains. Reverse engineering of the key mutations found in ALE experiment successfully reinstate the solvent tolerance trait in plasmid-cured *P. putida* S12, thus confirming intrinsic solvent tolerance of *P. putida* S12.

In **Chapter 6**, an **A**raC **f**amily transcriptional **r**egulator (proposed name Afr) encoded on RPPX_14685 locus is characterized. This locus carried a point mutation which leads to amino acid substitution of threonine (pos. 53) to proline, at its putative effector binding domain. This mutation occurred in all of the independent replicates of plasmid-curing experiments using intercalating agent, mitomycin C. Here, the genes regulated by Afr were identified and the role of Afr in enabling plasmid-curing and the recovery of solvent tolerance in ALE-derived strains are discussed.

Chapter 7 summarizes the interplay of the various mechanisms that contribute to the solvent tolerance in *P. putida* S12. Further research questions that need to be tackled and the trade-offs of the solvent tolerance trait are discussed.

In summary, the work described in this thesis illustrates the solvent tolerance mechanism in an industrially relevant strain of *Pseudomonas*; *P. putida* S12. One of the key challenges in the production of valuable chemicals using microbial cell factory is the unpredictability of yield due to product/intermediate toxicity. Therefore, biocatalysis of high-value chemicals require a robust microbial host, like solvent-tolerant bacteria. A profound analysis and understanding of solvent-tolerant mechanisms is therefore needed. This work may contribute in understanding the genetic and physiological interplay to confer and implement solvent tolerance traits in bacteria.

References

1. Kusumawardhani H, Hosseini R, de Winde JH. 2018. Solvent Tolerance in Bacteria: Fulfilling the Promise of the Biotech Era? Trends Biotechnol 36:1025–1039.
2. Inoue A, Horikoshi K. 1989. A *Pseudomonas* thrives in high concentrations of toluene. Nature 338:264–266.
3. Hartmans S, Smits JP, van der Werf MJ, Volkering F, de Bont JA. 1989. Metabolism of Styrene Oxide and 2-Phenylethanol in the Styrene-Degrading *Xanthobacter* Strain 124X. Appl Environ Microbiol 55:2850–2855.
4. Ramos JL, Duque E, Huertas MJ, Haïdour A. 1995. Isolation and expansion of the catabolic potential of a *Pseudomonas putida* strain able to grow in the presence of high concentrations of aromatic hydrocarbons. J Bacteriol 177:3911–3916.
5. Williams PA, Murray K. 1974. Metabolism of benzoate and the methylbenzoates by *Pseudomonas putida* (arvilla) mt-2: evidence for the existence of a TOL plasmid. J Bacteriol 120:416–423.
6. Wierckx NJP, Ballerstedt H, de Bont JAM, Wery J. 2005. Engineering of solvent-tolerant *Pseudomonas putida* S12 for bioproduction of phenol from glucose. Appl Environ Microbiol 71:8221–8227.
7. Verhoef S, Wierckx N, Westerhof RGM, de Winde JH, Ruijssenaars HJ. 2009. Bioproduction of p-hydroxystyrene from glucose by the solvent-tolerant bacterium *Pseudomonas putida* S12 in a two-phase water-decanol fermentation. Appl Environ Microbiol 75:931–936.
8. Verhoef S, Ruijssenaars HJ, de Bont JAM, Wery J. 2007. Bioproduction of p-hydroxybenzoate from renewable feedstock by solvent-tolerant *Pseudomonas putida* S12. J Biotechnol 132:49–56.
9. Kuepper J, Ruijssenaars HJ, Blank LM, de Winde JH, Wierckx N. 2015. Complete genome sequence of solvent-tolerant *Pseudomonas putida* S12 including megaplasmid pTTS12. J Biotechnol 200:17–18.
10. Turner WJ, Dunlop MJ. 2015. Trade-Offs in Improving Biofuel Tolerance Using Combinations of Efflux Pumps. ACS Synth Biol 4:1056–1063.
11. Kieboom J, de Bont JAM. 2001. Identification and molecular characterization of an efflux system involved in *Pseudomonas putida* S12 multidrug resistance. Microbiology 147:43–51.

12. Kieboom J, Dennis JJ, Zylstra GJ, de Bont JA. 1998. Active efflux of organic solvents by *Pseudomonas putida* S12 is induced by solvents. J Bacteriol 180:6769–6772.

13. Volkers RJM, Snoek LB, Ruijssenaars HJ, de Winde JH. 2015. Dynamic Response of *Pseudomonas putida* S12 to Sudden Addition of Toluene and the Potential Role of the Solvent Tolerance Gene trgI. PLoS One 10:e0132416.

CHAPTER 2 Introduction

Solvent Tolerance in Bacteria: Fulfilling the Promise of the Biotech Era?

Hadiastri Kusumawardhani, Rohola Hosseini, Johannes H. de Winde

Published in: Trends in Biotechnology (2018), 36 (10), 1025-1039.

DOI: 10.1016/j.tibtech.2018.04.007

Abstract

The challenge of sustainably producing highly valuable chemical compounds requires specialized microbial cell factories because the majority of these compounds can be toxic to microbial hosts. Therefore, solvent-tolerant bacteria are promising production hosts because of their intrinsic tolerance towards these compounds. Recent studies have helped to elucidate the molecular mechanisms involved in solvent tolerance. Advances in synthetic biological tools will enable further development of streamlined solvent tolerant production hosts and the transfer of solvent tolerant traits to established industrial strains. In this review, we outline challenges and opportunities to implement solvent tolerance in bacteria as a desired trait for industrial biotechnology.

Solvent tolerant bacteria are efficient biocatalysts

The transition of a fossil raw materials-based economy to a biobased economy is characterized by complex and ambitious systems innovations. Recent breakthrough developments in green chemistry and biotechnology are major drivers enabling production of biobased chemicals (1–4). Today, in the new Biotech Era, increased demands for bio-based “green” chemicals and pharmaceuticals are met with rapid product development benefitting from years of research in the microbial physiology and metabolic engineering fields. Biobased production of these compounds is becoming economically competitive with petrochemical-based production. Both environmental considerations and the need to further improve the competitiveness of the chemicals industry, promise to drive continued biotechnology developments and innovation in the production of biobased chemicals.

Biobased production of valuable chemicals and biopolymer compounds puts a challenge on the choice of microbial host strains (3–6). Many of these chemicals have hydrocarbon-solvent properties and thus exhibit toxicity towards the microbial hosts (7, 8). Furthermore, the production of more complex biobased products, such as o-cresol and 3-methylcathecol, requires toxic solvent-like compounds as substrates or intermediates (9, 10). Therefore, solvent tolerance becomes an essential trait for microbial host in the biobased production of valuable chemicals and biopolymer compounds. Several species of bacteria can grow and survive in the presence of hydrocarbon solvents (11) and can therefore be identified as promising and advantageous platforms for the production of such potentially toxic compounds, or for bioremediation. These bacteria can efficiently withstand or degrade various toxic solvent-like compounds (12, 13). Therefore, the application of solvent-tolerant bacteria in the biocatalytic production of (new) chemical building blocks is rapidly increasing (1–4). Using these solvent-tolerant bacteria in biotechnological production processes, however, requires a thorough understanding of solvent tolerance mechanisms involved. With recent advances in genome sequencing and omics studies of solvent-tolerant bacteria, unique clusters of genes have been identified that confer solvent tolerance traits (14–18). Better understanding of these solvent tolerance traits in combination with modern synthetic biology tools will enable further development of specialized biocatalysts, new applications, and improved production processes of high value compounds (19–27). In this review, we discuss recent findings in solvent tolerance mechanisms and new advances in synthetic biology tools that can help

to design microbial hosts and processes in industrial productions for a plethora of new and valuable compounds.

Table 2.1. Hydrocarbon solvents and their industrial relevance

Hydrocarbon solvent	Solvent class	Industrial relevance	$LogP_{o/w}$	Refs.
acetone	ether	solvent in cosmetic, pharmaceutical, medical, and domestic uses	-0.24	-
ethyl acetate	ester	solvent in coating formulation for epoxies, urethanes, acrylics, and vinyls.	0.73	-
n-butanol	short chain alkanol	biofuel	0.88	(28)
phenol	aromatics	precursor for plastics	1.5	(29)
butyl acetate	ester	product co-solvent (vanillin)	1.78	(3)
benzene	aromatics	substrate for the production of 3-methylcatechol	2	(30)
toluene	aromatics	substrate for the production of 3-methylcatechol, o-cresol, & p-hydroxybenzoate	2.69	(9, 30, 31)
styrene	aromatics	substrate for the production of (S)-styrene oxide	2.9	(32)
1-octanol	long chain alkanol	product co-solvent (phenol)	3	(29)
ethylbenzene	aromatics	production of paints, varnishes, and lacquers	3.3	-
cyclohexane	cyclic alkane	precursor to nylon, adipic acid, caprolactam	3.4	-
m-xylene	aromatics	substrate for the production of 3-methylcatechol	3.46	(10)
n-hexane	alkane	extraction solvent for vegetable oil, cleaning agent	3.9	-
1-decanol	long chain alkanol	product co-solvent (p-hydroxystyrene)	4.57	(6)

Current understanding of solvent tolerance mechanisms

Since the first discovery of solvent-tolerant bacterium *Pseudomonas putida* IH-2000 by Inoue and Horikoshi (12), the number of known solvent-tolerant strains has been rapidly expanding. Despite this growing number of identified solvent-tolerant bacteria, the current knowledge and understanding of solvent tolerance mechanisms has mostly been obtained from studying various strains of *P. putida* (14, 17, 18). But solvent-tolerant traits are not restricted to *P. putida*,

as exemplified for instance by *Exiguobacterium* sp., *Pseudoalteromonas* sp., *Vibrio* sp., *Marinomonas* sp., *Paracoccus denitrificans*, and *Halomonas* sp. (33–36). The discovery of new solvent-tolerant strains and their unique features may help to better understand the molecular and physiological mechanisms underlying bacterial solvent tolerance.

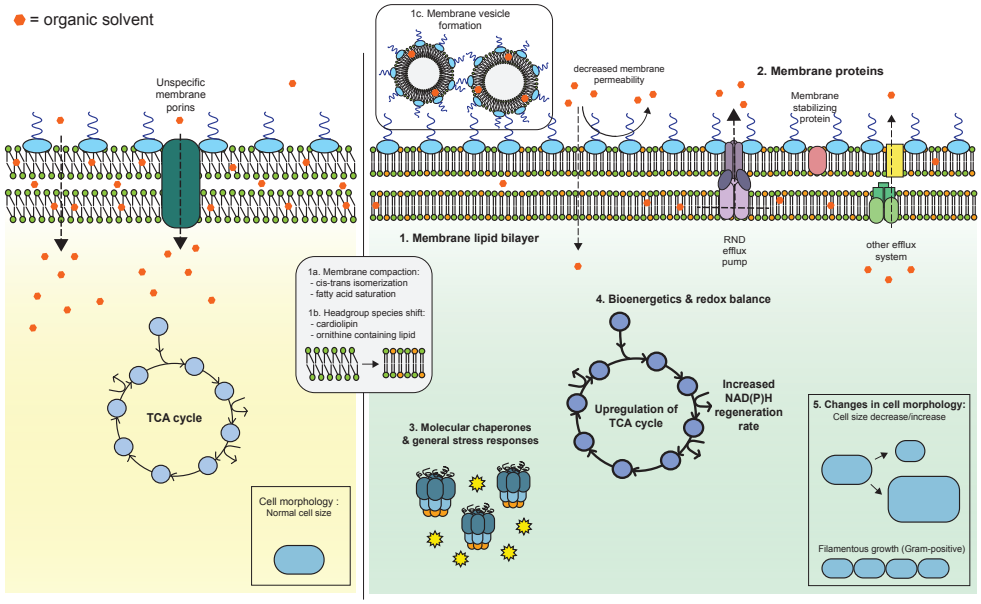

Fig. 2.1.Current understanding on solvent tolerance mechanism of bacteria

The left panel represents the state of a bacterium upon the addition of solvent and before solvent tolerance mechanisms are induced, and the right panel represents the state of the bacterium after solvent tolerance mechanisms are induced. Gram-negative and Gram-positive bacteria employ similar strategies to compensate for solvent exposure. The increase in membrane compaction [1] is a consensus for solvent tolerance mechanism between Gram-positive and Gram-negative bacteria by using multiple strategies [1a & 1b]. Resistance, nodulation, and division (RND) efflux pumps [2] and general stress responses [3] play important roles in both groups. Several mechanisms are also unique to certain species, such as the increase of bioenergetics and NAD(P)H regeneration rate in *Pseudomonas putida* [4], membrane vesicle formation in *P. putida* [1c], and filamentous growth in Gram-positive bacteria [5].

Hydrocarbon solvents with a log $P_{o/w}$ value in the range of 1 to 4 (Table 2.1) are toxic to microorganisms at very low concentration because these solvents bind and penetrate the cell membrane and severely affect cell permeability (37). Solvents with log $P_{o/w}$ value lower than 1, like short-chain alkanols (C2-C4), exhibit toxicity in high concentration. Short-chain alkanols directly interact with the phospholipid headgroups, while longer-chain alkanols (e.g.

C8) accumulate within the lipid bilayer of the membrane, 'competing' with the fatty acid acyl chains (38). Solvent-invoked membrane damage inhibits various important membrane functions, such as the permeability barrier function and the structural matrix scaffold for many metabolic and enzymatic reactions (39). Consequently, this membrane damages leads to disrupted cellular metabolism, growth inhibition, and eventually, cell death (11, 38).

Tolerance to hydrocarbon solvents is a multifactorial trait. Bacterial cells employ various strategies to change their physiology and gene expression to circumvent cellular damage caused by these solvents (Fig. 2.1). Tolerance mechanisms have been more extensively studied in gram-negative bacteria than in gram-positive bacteria, but similar mechanism have been observed for both groups (40, 41).

Membrane fluidity

In the presence of a hydrocarbon solvent, tolerant Gram-negative bacteria respond by changing their cell membrane composition towards saturated and trans-unsaturated fatty acids (7, 42). The formation of trans-unsaturated fatty acid is catalysed by a periplasmic, haem-containing cis-trans isomerase (Cti) (43). In *P. putida* DOT-T1E, Cti is constitutively expressed at a constant level during log-growth and stationary-phase cells and moderately upregulated in the presence of toluene (42). Recently, a working model of Cti activity was proposed by Eberlein and colleagues (44): initially, Cti activity is regulated by the limited accessibility to cis fatty acid under nonstressed condition due to membrane rigidity. The membrane bilayer becomes more fluid upon interaction with hydrocarbon solvents, enabling hydrophilic Cti to reach cis fatty acids and isomerize them into trans fatty acid. Saturated and trans-unsaturated fatty acids increase membrane rigidity, exemplified by a higher phase-transition temperature. This rigid membrane structure provides resistance to hydrocarbon solvents by decreasing solvent influx and accumulation in the membrane. Similarly, Gram-positive bacteria also shift their membrane composition towards a more rigid structure in presence of hydrocarbon solvents by a concentration-dependent decrease in anteiso/iso branched fatty acid ratio. This modification in branched fatty acid promotes a more compact membrane structure, resulting in reduced accumulation of hydrocarbon solvents (43, 45).

Phospholipid headgroup species

The phospholipid headgroup constituents found in Pseudomonads are phosphatidyl-ethanolamine (PE), phosphatidylglycerol (PG), and cardiolipin (CL). Those phospholipid headgroups, especially CL, appear to play an important role in aiding Pseudomonads in their adaptation against hydrocarbon solvents (46). Recently, an increase in CL-containing lipids was reported in strains of *P. putida* S12 and *Pseudomonas taiwanensis* VLB120 grown in the presence of n-butanol (35). Accordingly, CL-containing lipids are important for the function of the efflux pumps in *P. putida* DOT-T1E (42).

Recent metabolomic analyses of *P. putida* DOT-T1E showed that the intracellular ornithine concentration increases in response to toluene exposure (47). Ornithine-containing lipids are known to play an important role in stabilizing the outer membrane and the negative charge of lipopolysaccharides (LPS), as well as in the stress response towards abiotic conditions such as elevated temperature and acidic environment (48).

Membrane vesicle formation

Outer membrane vesicle (OMV) is a spherical compartment released from the outer membrane of bacteria (consisting phospholipids, LPSs, and small amounts of outer membrane proteins) as a response to various stress condition encountered in the environment (49). Encapsulation of hydrocarbon solvents by the formation of membrane vesicles is an effective defence mechanism in solvent tolerant *P. putida* strains in the presence of toluene (50). By forming these membrane vesicles, the cells effectively discard toluene adhering to the outer membrane. In *P. putida* DOT-T1E, the formation of OMVs contributes to a rapid and extreme rise in cell surface hydrophobicity, which prepare the cells for biofilm formation as a protective response towards solvent-induced stress (51, 52). Membrane vesicles also play a role in releasing lipids with lesser degrees of saturation, enabling rapid lipid turnover as a response to the presence of hydrocarbon solvents (52).

Resistance, nodulation and division (RND) efflux pump and membrane proteins

Adaptive cell membrane properties constitute a robust mechanism against toxic hydrocarbon solvents. However, decreased membrane permeability does not necessarily generate sufficient tolerance in the presence of hydrocarbon solvent (53). Therefore, cells need an effective mechanism to actively extrude accumulating toxic solvents.

In both Gram-positive and Gram-negative bacteria, the most important membrane proteins in terms of solvent tolerance are the RND efflux pumps (35, 53–55). The RND efflux pumps can extrude a broad range of compounds with little chemical resemblance to each other. They are frequently associated with resistance to a broad spectrum of antibiotics and heavy metals (54, 56). Some RND efflux pumps are specifically induced by (and only extrude) hydrocarbon solvents and are not induced by, for example, hydrophobic antibiotics. Illustrative examples are SrpABC from *P. putida* S12 and TtgDEF from *P. putida* DOT-T1E (53, 55). Recent knowledge and advances in the field of these efflux pumps, their role, control mechanisms, and cross-resistance with antibiotics and efflux properties have recently been extensively reviewed (57, 58).

Novel recent findings have pointed to differential expression of membrane porins and other secretion systems in solvent-tolerant *Pseudomonads* exposed to solvents (14, 15, 59). Unspecific outer membrane porins are downregulated in the presence of toluene to prevent influx of toluene (14, 15, 59). A membrane protein OprH is found to be upregulated to stabilize cell membrane and decrease the uptake of toluene (15, 59). Hence, alongside the RND efflux pumps, other membrane proteins may play important roles in constituting solvent tolerance.

Molecular chaperones and general stress responses

The presence of hydrocarbon solvents invokes similar stress responses in both Gram-positive and Gram-negative bacteria (15, 16, 60). In several bacterial species confronted with hydrocarbon solvents, general stress response regulators such as the heat shock protein and the cold shock protein are upregulated (15, 16). Other members of the general stress response system may be induced by the presence of toluene, such as molecular chaperones, oxida-

tive stress response components, and other resistance proteins in Gram-negative *P. putida* DOT-T1E and *P. putida* S12 as well as in Gram-positive *B. subtilis* (16, 60). Accordingly, the toluene-repressed gene (*trgI*) of *P. putida* S12 was found to control a large number of protein modification and chaperone genes (18).

Bioenergetics and redox balance

Several studies in *P. putida* have indicated that in the presence of hydrocarbon solvents, tricarboxylic acid (TCA) cycle components are upregulated, the NAD(P)H regeneration rate is increased, and growth is reduced (14–16, 18, 61). Differential expression of TCA cycle-related proteins modulates the NAD(P)H concentration, and therefore the redox balance, throughout the solvent stress (15). Upregulation of the TCA cycle and concomitant increase of the NAD(P)H regeneration rate enable the cells to cope with the energetic potential loss connected with rapid solvent extrusion through the efflux pumps (15, 61). As a representative illustration, the ATP content, cellular concentration of potassium and adenine nucleotides, and the adenylate energy charge were all similar in cells of *P. putida* DOT-T1E grown in the presence or absence of 1-decanol (51). These findings reflected the efficient metabolic and energetic adaptation of solvent-tolerant bacteria during their exposure to toxic hydrocarbon solvents.

Changes in cell morphology

Both Gram-positive and Gram-negative bacteria exhibit changes in cell morphology and in cell size as a response to the presence of hydrocarbon solvents (62–65). For example, decrease in cell size was observed in *P. aeruginosa* and *Enterobacter sp.* upon the exposure to hydrocarbon solvents (63, 65). However, conflicting observations were reported in *Bacillus lichineformis* S-86, *P. putida* P8, and *Enterobacter sp.* VKGH12 which have shown increases in cell volume in the presence of hydrocarbon solvents (41, 64). Additionally, in the presence of 0.6% 3-methylbutan-1-ol, *B. lichineformis* S-86 was reported to exhibit filamentous growth (62). By decreasing cell-size, cell surface-to-volume ratio increases, contributing to a more efficient uptake of nutrient. With the decreased cell surface-to-volume ratio, cell surface exposure is reduced and solvent extrusion can be more effective.

Applications of solvent-tolerant bacteria in biocatalysis of valuable compounds

Employing bacteria for biocatalysis is currently a preferred method for industrial synthesis of various biochemicals, pharmaceuticals, and enantiomerically pure intermediates. Indeed, such synthesis routes require co-enzymes and co-factors, and stepwise/multiple enzymatic reactions that may be readily available within the microorganism of choice (38). In the bio-production of industrial chemicals, the production process is often hampered by the toxicity of the substrate or the product, which may severely affect the product yield (3, 6). Solvent-tolerant bacteria are favored for the biocatalytic production of many valuable compounds, since they are far less prone to inhibition by toxic compounds, so the desired yields can be better achieved. Valuable compounds that can be readily produced through the use of solvent-tolerant bacteria include simple aromatic compounds such as phenol or p-hydroxybenzoate, as well as more complicated compounds such as 2,5-furandicarboxylic acid (FDCA), enantiomerically specific (s)-2-octanol, and pharmaceutically active 15β-hydroxytestosterone (Table 2.2). Recently, the biobased production of a major building-block chemical FDCA, a promising 'green' alternative to terephthalate in the production of polyesters, from 5-hydroxymethyl-furfural (HMF) was achieved in the noted solvent-tolerant strain *P. putida* S12. Hence, solvent-tolerant traits of microbial production strains can enable the use of hydrocarbon solvents and solvent-like compounds as substrate and intermediates for the production of high-value compounds. In addition, the unique features of solvent-tolerant bacteria allow tolerance towards a broad range of potentially toxic compounds and make them highly suitable for implementation in two-phase bioreactors production set-up (3, 66). The main challenges that arise in using solvent-tolerant bacteria in biocatalysis are maintaining product yield and system complexity.

Solvent-tolerant bacteria are well suited for biocatalytic production in two-phase biocatalysis systems, as reviewed previously (38). This system can significantly improve production yield by reducing substrate and/or product toxicity (3, 6). The use of a hydrocarbon solvent as the second phase has several advantages, including reduced reaction inhibition, reduced toxicity towards the microbial host and the prevention of product hydrolysis (3). Moreover, the second hydrocarbon phase acts as a simultaneous extraction step, thus simplifying downstream processing and purification and increasing the yield of poorly water-soluble products (29). Hydrocarbon solvents having log $P_{o/w}$ values in the range of 1 to 4 are considered

suitable for product extraction and substrate reservoir in a two-phase biocatalysis system, and solvent-tolerant bacteria can survive and exhibit biocatalytic activity under these circumstances. Known bacterial index values have been extensively listed in previous articles (11, 67). Predominantly Gram-negative bacteria have index values in the ideal two-phase biocatalysis range from 1 to 4.

Several examples demonstrate increased product titre and optimized production of valuable chemicals in two-phase biocatalysis system (3, 6, 68). Production of p-hydroxystyrene in *P. putida* S12 was established with by introducing the *pal* (L-phenylalanine/L-tyrosine ammonia lyase) and *pdc* (p-coumaric acid decarboxylase) genes in combination with inactivating the *fcs* gene (6). A product titre of 4.5 mM with a yield of 6.7% (C-mol p-hydroxystyrene/C-mol glucose) and maximum volumetric productivity of 0.4 mM h^{-1} was initially achieved. However, due to the toxicity of p-hydroxystyrene, cell growth and production was inhibited. Using decanol as a second phase, the toxicity of the product p-hydroxystyrene was significantly reduced, which resulted in a p-hydroxystyrene titer of 147 mM (17.6 g l^{-1}), a fourfold increase compared with a standard fed-batch production. The maximum volumetric productivity was also increased to reach 0.75 mM h^{-1}. Similarly, production of p-hydroxystyrene from p-coumaric acid from corn cob hydrolysate using recombinant *Escherichia coli* and simultaneous extraction by n-hexane as the second phase clearly improved product titre (68). Another example is the bioproduction of vanillin from isoeugenol, which can be inhibited by two major phenomena: the toxicity of isoeugenol and vanillin to microbial host, and the low solubility of isoeugenol in water (3). The solvent-tolerant Gram-positive bacterium *Brevibacillus agri* 13 can produce vanillin from 2 g l^{-1} isoeugenol with a yield of 7.6% (Cmol vanillin/Cmol isoeugenol) in a single-phase system. Using butyl-acetate (30% v/v) as an second-phase with 10 g l^{-1} isoeugenol increases the production yield to 17.2% with product titer of 1.7 g l^{-1} after 48 hours of fermentation. Here, the reduction of isoeugenol and vanillin toxicity in combination with the simultaneous extraction of vanillin by the second phase result in increased product formation.

Table 2.2. Biocatalysis using solvent tolerant bacteria

Product	Biocatalyst	System	Challenge(s) in production process	Product titer (mM)	Yield ($Cmol_p/Cmol_s$)	Productivity	Comparison	Ref.
p-Hydroxybenzoate	*P. putida* S12 expressing *pal* gene from *Rhodosporium toruloides*	Fed batch whole-cell biocatalysis system	Toxic aromatic product	12.9	8.5%	0.168 (mmol h^{-1} $gCDW^{-1}$)	-	(5)
FDCA (2,5-furandicarboxylic acid)	*P. putida* S12 expressing hmfH gene from *Cupriavidus basilensis* HMF14	Fed batch whole-cell biocatalysis system	Toxic aromatic substrate	192.83	97%	0.096 ± 0.004 (mmol h^{-1} $gCDW^{-1}$)	-	(4, 97)
Anthranilate	*P. putida* KT2440 expressing *trpDC* with futher optimization of anthranilate production pathway	Fed batch whole-cell biocatalysis system	Toxic aromatic product	11.23	3.6 ± 0.5%	N/A	1.83 mM, without further optimization of the anthranilate production pathway	(2)
(S)-2-Octanol	*P. putida* DSM 12264 expressing CYP154A8	Fed batch whole-cell biocatalysis system	Hydrocarbon solvent as product	15.7 (87% ee)	N/A	0.172 (mmol h^{-1} $gCDW^{-1}$)	2.2 mM, 58% ee in *E. coli* system expressing CYP154A8	(66)
3-Methylcathecol	*P. putida* DOT-T1E containing pWW0 plasmid from *P. putida* KT2440	Two phase batch whole-cell biocatalysis system with aliphatic alcohol as the second phase	Second-phase for product reservoir	70	N/A	4.83 (mM h^{-1})	3 mM, using the same strain without the two phase system	(10)
Phenol	*P. taiwanensis* VLB120 with minimal genomic modification and expressing *tpl* gene from *Pantoea agglomerans*	Fed batch whole-cell biocatalysis system	Toxic product	3.62	18.5 ± 0.2%,	0.09 ± 0.00 (mM h^{-1})	1.5 mM in *P. putida* S12	(1)
p-Hydroxystyrene	*P. putida* S12 expressing *pal* gene from *Rhodosporium toruloides* and *pdc* gene from *Lactobacillus plantarum*	Two phase fed batch whole-cell biocatalysis system with decanol as the	Toxic product and second-phase for product reservoir	147	4.1%,	0.75 (mM h^{-1})	21 mM, using the same strain without the two phase system	(6)
Vanillin	*B. agri* 13	Two phase batch whole-cell biocatalysis system with butyl acetate as the second phase	Second phase for toxic product and substrate reservoir	11.17	27.8%	N/A	< 6.5 mM l^{-1}, on *Bacillus subtilis*, *Pseudomonas chlororaphis*, and recombinant *E. coli* without two phase system	(3)
1-Naphthol	*E. coli* TG1 pBS(kan)TOM-Green expressing srpABC operon from *P. putida* S12	Two phase batch whole-cell biocatalysis system with lauryl acetate as the second phase	Toxic aromatic product	9.91	N/A	3.81 (mmol $gCDW^{-1}$)	0.27 mM , without two phase system	(83)

The case of FDCA

A recent study identified and characterized a fully biobased enzymatic route for the production of 2,5-furandicarboxylic acid (FDCA) directly from 5-hydroxymethylfurfural (HMF) [86]. HMF, like furfural, is an intrinsically toxic furanic aldehyde occurring in lignocellulosic hydrolysates (Fig. 2.2). FDCA has been proclaimed by the USA Department of Energy as 1 of 12 priority chemicals for the realization of a biobased green chemistry industry (69). It is regarded an important platform compound for the synthesis of a variety of aromatic chemical building blocks, including as a biobased alternative for the monomer terephthalic acid in polymeric polyethylene terephthalate (PET) (70–73). Polymerisation of ethylene glycol and FDCA yields polyethylene furanoate (PEF), which has improved barrier, thermal and mechanical properties compared with PET (72).

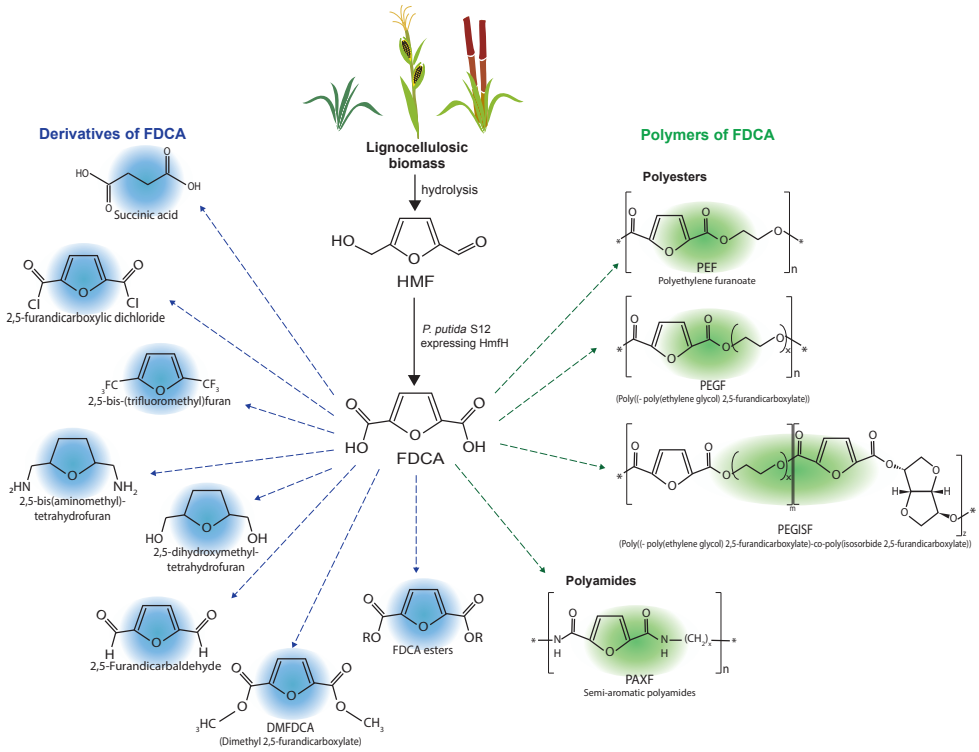

Fig. 2.2. Potential applications of FDCA, from lignocellulosic biomass to biopolymers

Expression of a novel, specific HMF/furfural oxidoreductase from the soil bacterium *Cupriavidus basilensis* in the solvent-tolerant industrial host bacterium *Pseudomonas puti-*

da enabled efficient high-yield production of FDCA from HMF (4). In this process, *P. putida* proves to be an efficient whole-cell biocatalyst. The company Corbion is currently developing a cost-effective production route for FDCA, based on this novel enzymatic route (http://www.corbion.com/bioplastics/products/fdca-for-pef).

Challenges in biocatalysis using solvent tolerant bacteria

The primary complication with using solvent-tolerant bacteria in industrial biotechnology is the unpredictable product yield caused by host interference issues (19, 74, 75). Adapting native biocatalytic pathways often provokes imbalances in pathway flux, the accumulation of toxic intermediates, and reduced cellular fitness, again causing unpredictable product yields (76). Genome streamlining reduces host interference, resulting in increased biomass and growth rate and subsequently leading to optimizing production chassis (19). Imbalances in pathway fluxes, bottlenecking enzymes, and accumulation of toxic intermediates can be mitigated by optimizing metabolic pathways (5, 29, 76, 77). And the development of synthetic biology tools is becoming crucial to support the implementation of solvent-tolerant bacteria in biocatalysis (20, 78).

Another advantage of solvent-tolerant bacteria is their easier implementation in two-phase bioreactor systems. However, other challenges may arise in two-phase bioreactor systems, such as increased system complexity, problems with waste disposal, and the hazardous risk of using flammable solvents (79). By applying heat treatment or a continuous-plate centrifuge, a solvent emulsion in an aqueous phase can be degraded or, preferably, be avoided, resulting in a clear solvent that can be processed by further downstream treatment. Distillation may be applied in the downstream process specifically to purify volatile product from its volatile substrate. Schmid and colleagues developed a safe and efficient pilot-scale two-phase bioreactor containing flammable solvent (79). Finally, exogenously supplemented glycerol provides effective protection and thus improves bacterial growth in a two-phase bioreactor system (80).

Synthetic biology and engineering towards advanced biocatalysts

Host interference issues can be overcome by reducing the complexity of the genome in the

microbial chassis by genome streamlining (74). Genome streamlining is widely used in engineering industrial bacterial strains (75, 81). This approach has resulted in increased biomass formation, reduced doubling times, increased product yield, and ultimately optimized production systems (19). Metabolic pathway optimization can resolve imbalances in pathway fluxes and reduce accumulation of toxic intermediates to restore cellular fitness (76, 82). Transferring solvent-tolerant traits to a preferred industrial host strain is also a plausible strategy (83). In combination, these strategies comprise promising approaches to exploit the solvent tolerance features of bacteria for producing a wide range of valuable compounds with a high degree of predictability and robustness (Fig. 2.3). Existing and novel tools for synthetic biology and the rapidly accumulating genome sequencing data of solvent-tolerant bacteria, drive the opportunities to implement these strategies.

Molecular synthetic tools for improving solvent-tolerant process design and application

Synthetic molecular tools are crucial aspects for developing a robust industrial bacterial strains. BioBricks was developed as flexible exchangeable DNA fragments that can be combined to fully synthesized biological tools suitable for common industrial strains like *E. coli* (78). The Standard European Vector Architecture (SEVA) established a reliable and efficient vector repository accompanied by a simple and user-friendly database mainly implemented in solvent-tolerant *P. putida* and other industrial strains (20). A plasmid system, GeneGuard, was constructed to overcome the safety concerns including unwanted horizontal gene transfer by host-mutual dependency, based on using SEVA plasmids (24).

Optimizing a robust bacterial chassis requires both precise genome editing tools and the ability to incorporate new features into its genome. The CRISPR/Cas system has become a standard tool in editing bacterial genomes (84). Using SEVA plasmids as its backbone, a recombination event between free homologous DNA sequences, allowing an accurate genome editing, was developed for a wide variety of Gram-negative bacteria (21).

Transposon tools for specific transgene introduction, in combination with promoter libraries for *P. putida* cell factories, have been developed as an alternative to the use of multi copy plasmids (22, 23, 85). The developed mini-Tn5 vector offers the advantages of maintaining introduced genes without selective pressure, construct stability, recurrent use of the

system, and introducing a relatively large DNA sequence (22). The mini-Tn7 transposon system can integrate with a high frequency in a specific location as a unidirectional single copy of gene that is suitable in various studies for gene expression, characterization of certain genes, and gene complementation (23). Finally, a novel broad range system for the transfer and expression of biosynthetic pathways (TREX) was developed using this transposon system to include all functional elements that are essential for efficient introduction and expression of pathway clusters in different bacteria (86).

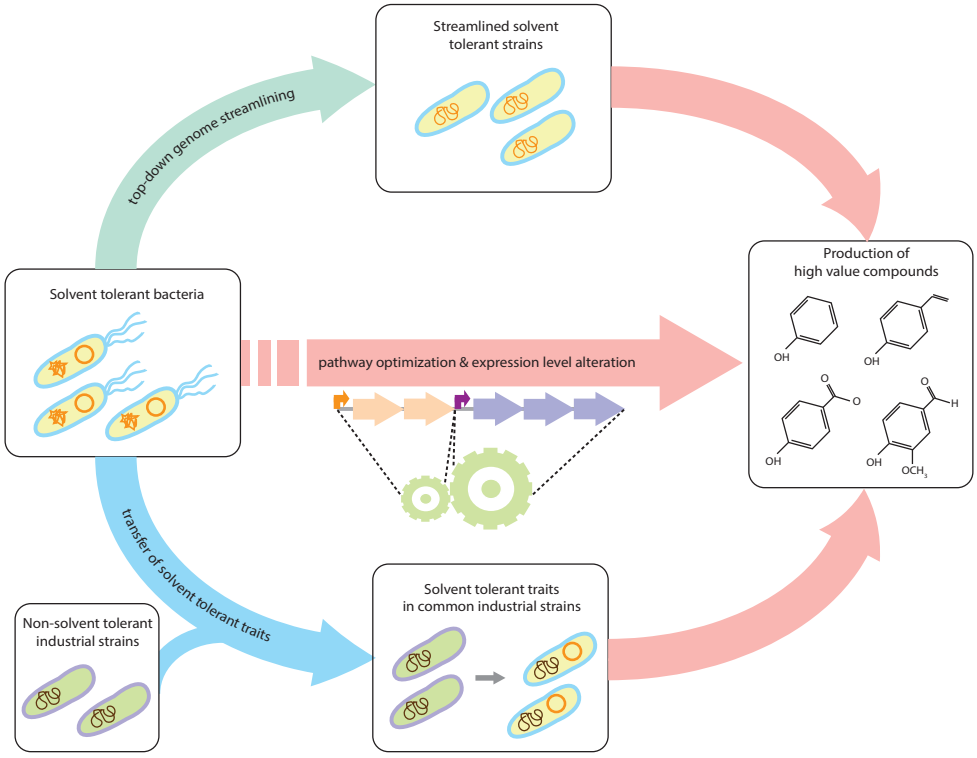

Fig. 2.3. Synthetic biology and engineering towards advanced solvent-tolerant biocatalysts

Three optimization strategies on biocatalysis using solvent-tolerant bacteria are employed to solve problem of host interference, which can cause an unpredictable yield of products. Pathway flux imbalance can be reduced by identifying bottlenecking enzymes and altering the expression level of the bioproduction pathway (red arrows). Genome streamlining can be applied to reduce the genome complexity of solvent-tolerant strains (green arrow). Introducing solvent tolerance-related genes into an existing industrial strain is also proven to be a promising approach (blue arrow). Synthetic biology tools are useful in pathway optimization, altering the expression level of bioproduction, strain optimization, and conferring solvent-tolerant traits.

Pathway optimization and adaptation of enzyme expression

Metabolic pathways can be optimized by characterizing enzyme expression, identifying bottlenecking enzymes, and subsequently optimizing the expression and activity of enzymes through modulation of transcription, translation and specific enzyme characteristics (76, 82). As an example, transcriptomics and proteomics studies of p-hydroxybenzoate-producing *P. putida* S12 identified critical components of the tyrosine degradation pathway (5, 77). Subsequent deletion of the *hpd* gene involved in p-hydroxybenzoate degradation led to a 22% increase of p-hydroxybenzoate production. In another case, by overproducing the pyruvate dehydrogenase subunit gene *acoA* or deleting the glucose dehydrogenase gene *gcd* to overcome bottlenecking, production of polyhydroxyalkanoate (PHA) in *P. putida* KT2440 was increased by 33% and 121%, respectively (87).

In combination with rapidly emerging synthetic biology tools, pathway optimization is a powerful strategy in designing optimized bacterial strains for application in industrial biotechnology. The highest yield in microbial phenol production reported so far was achieved by implementing pathway optimization on solvent-tolerant *P. taiwanensis* VLB120 (1). To optimize phenol production, catabolic routes toward aromatic compounds and shikimate pathway intermediates are inactivated. This inactivation is accomplished by the deletion of five genes: *pobA*, *hpd*, *quiC*, *quiC1*, and *quiC2,* along with the subsequent loss of megaplasmid pSTY. This process yields *P. taiwanensis* VLB120Δ5, which is unable to grow on 4-hydroxybenzoate, tyrosine, and quinate. The introduction of a codon-optimized tyrosine-phenol lyase (TPL) gene from *Pantoea agglomerans* facilitates tyrosine transformation into phenol. Metabolic flux towards phenol production is further increased using forward- and reverse-engineering from leads indicated by previous mutagenesis of phenol-producing *P. putida* S12 (88) and the addition of bottlenecking enzymes AroG and TyrA. *P. taiwanensis* VLB120Δ5-TPL36 achieved the yield of 15.6% and 18.5% (Cmol/Cmol) of phenol in minimal medium from glucose and glycerol, respectively, without requiring additional complex nutrient.

Synthetic promoter libraries can optimize the expression of several modules in a metabolic pathway (23). Using synthetic promoters, the production of rhamnolipids in *P. putida* KT2440 was significantly increased, reaching a yield of 40% rhamnolipids on sugar (89, 90). These examples present further proof that pathway optimization is a highly promising

approach to resolving pathway flux imbalance and improving biomass and product yield in solvent-tolerant bacterial industrial host strains.

Top-down strategies in genome streamlining

Genome streamlining has been implemented in various industrial host strains, such as *E. coli* and *Streptomyces* species (75, 81). Top-down genome streamlining deletes from microbial chassis multiple genes or gene clusters that are predicted to be inessential for the microbes, consume high amount of energy, contribute to the degradation of products or intermediates, or reduce metabolic flux towards the product of interest (75). Alternatively, the bottom-up strategy attempts to design a production chassis from scratch based on minimum requirements for a functioning microbial chassis. The top-down strategy significantly increased the biomass yield and the maximum specific rate for protein synthesis in the streamlined hosts *P. putida* EM329 and *P. putida* EM383, compared with the parental strain *P. putida* KT2440 (19, 91). One early example was *Pseudomonas arvilla* mt-2, described by Murray and colleagues in 1972 as a fascinating strain of *Pseudomonas* able to grow on benzoate, m-toluate (3-methylbenzoate) or p-toluate (4-methylbenzoate) as its sole carbon source (92). A derivative of this strain, *P. putida* KT2440, has been cured of the endogenous megaplasmid pWW0 present in the parental strain *P. putida* mt-2. Since then, *P. putida* KT2440 has proven to be a suitable host for gene cloning due to its deficiency in endogenous DNA restriction, so it can efficiently receive plasmid DNA for gene cloning purposes (93). *P. putida* KT2440 is a generally regarded as safe (GRAS) strain of *P. putida*[1]. The genome of *P. putida* KT2440 comprises of a 6,181,873-bp single circular chromosome (25).

In the process of optimizing *P. putida* KT2440 towards a robust industrial chassis, 11 chromosomal regions comprising 300 genes, including mobile elements, were found to be responsible for genetic instability or massive energy spillage (19). Together, these genes comprise a 170 kb genome segment encoding two transposons (Tn7 and Tn4652), prophages, two type I DNAses (*endA-1* and *endA-2*), an operon encoding type I DNA restriction-modification system (hsdRMS operon), and the 69-kb complete flagellar operon. Mobile elements play a significant role in the adaptation during solvent exposure, but mobile elements are

[1] **Correction:** *P. putida* KT2440 is classified by the FDA as HV1 certified, indicating it is safe to use in a P1 or ML1 environment. (98)

also responsible for genetic instability (94). Removing all of these genes resulted in a new optimized strain of *P. putida* EM42. To further diminish the probability of genetic instability, *recA* was deleted, resulting in *P. putida* EM383. This streamlined *P. putida* EM383 was shown to be superior to *P. putida* KT2440, as it exhibited a reduced lag phase, increased biomass formation, and increased redox charge, leading to exceptional tolerance against redox stress and reactive oxygen species damage.

Optimization of industrial host strains with solvent tolerance traits

Improving tolerance against toxic compounds is an important step towards developing a robust bacterial chassis for the industrial production of a wide range of valuable compounds. Using a modular semisynthetic system, overexpression of heat shock proteins GrpE, GroESL, and ClpB in *E. coli* generated a stress response that increased tolerance towards ethanol, n-butanol, and other toxic compounds (95). An engineered *E. coli* TG1-derived strain expressing the solvent efflux pump SrpABC from *P. putida* S12 was employed for 1-naphthol production in a two-phase fermentation (83). Although 1-naphtol production did not reach the same levels as in *P. putida* S12, this result demonstrated the successful transfer of the *Pseudomonas* solvent extrusion pump gene cluster, providing the engineered *E. coli* strain with a genuine solvent-tolerant trait.

The introduction of multiple efflux pumps may promise further advantages, but overexpression of efflux pumps may severely inhibit cell growth (96). As demonstrated by Turner and Dunlop, certain combinations of different efflux pumps can be highly toxic, even at basal expression levels of the pump proteins. Another successful example of optimizing solvent tolerance relates to bacterial fatty acid modification. Introducing cyclopropane fatty acid synthase (Cfa) from the solvent-tolerant strain *Enterococcus faecalis* CM4A into *E. coli* clearly increased tolerance towards n-butanol (34). Cfa activity maintains the fluidity of the cell membrane upon exposure to toxic hydrocarbon solvents. Further understanding of the roles of and interplay between solvent-tolerant mechanisms will enable the transfer of solvent-tolerant traits into suitable industrial host strains.

Concluding Remarks and Future Perspectives

Increased insight into solvent tolerance mechanisms is an important basis for biotechnological production of challenging compounds. An increasingly wider variety of compounds will be produced in microbial hosts due to the transition to a biobased economy. However, biobased production of added-value compounds, many of which are aromatics, is still challenging because of the inherently toxic nature of most of these compounds. Solvent-tolerant strains indeed represent a promising solution to this problem. A deeper understanding of the interplay in solvent tolerance mechanisms is still required to further increase the applicability of solvent-tolerant traits in industrial production.

With the help of modern synthetic biology tools, top-down genome streamlining of solvent-tolerant strains is essential to reduce host interference and increase production yields. In this approach, the challenge is to identify minimal gene clusters required for solvent tolerance and biosynthetic capacity which should not be disrupted. Implementing specific synthetic biological tools, like efficient gene editing for introducing heterologous genetic feature, or adjustable transcriptional regulators for pathway optimization, will enable the rapid generation of optimized production strains.

Transferring solvent tolerance traits into existing industrial strains may be a promising alternative strategy to optimize biobased production. The required synthetic biology tools are already available for established industrial strains. The challenge in this strategy is in obtaining the desired expression level of exogenous gene clusters in their new hosts. Once again, this highlights the necessity for thorough analysis and understanding of solvent tolerance mechanisms and the interplay of these mechanisms that orchestrate the tolerance toward solvents.

References

1. Wynands B, Lenzen C, Otto M, Koch F, Blank LM, Wierckx N. 2018. Metabolic engineering of *Pseudomonas taiwanensis* VLB120 with minimal genomic modifications for high-yield phenol production. Metab Eng 47:121–133.

2. Kuepper J, Dickler J, Biggel M, Behnken S, Jäger G, Wierckx N, Blank LM. 2015. Metabolic Engineering of *Pseudomonas putida* KT2440 to Produce Anthranilate from Glucose. Front Microbiol 6:1310.

3. Wangrangsimagul N, Klinsakul K, Vangnai AS, Wongkongkatep J, Inprakhon P, Honda K, Ohtake H, Kato J, Pongtharangkul T. 2012. Bioproduction of vanillin using an organic solvent-tolerant *Brevibacillus agri* 13. Appl Microbiol Biotechnol 93:555–563.

4. Koopman F, Wierckx N, de Winde JH, Ruijssenaars HJ. 2010. Efficient whole-cell biotransformation of 5-(hydroxymethyl)furfural into FDCA, 2,5-furandicarboxylic acid. Bioresour Technol 101:6291–6296.

5. Verhoef S, Ruijssenaars HJ, de Bont JAM, Wery J. 2007. Bioproduction of p-hydroxybenzoate from renewable feedstock by solvent-tolerant *Pseudomonas putida* S12. J Biotechnol 132:49–56.

6. Verhoef S, Wierckx N, Westerhof RGM, de Winde JH, Ruijssenaars HJ. 2009. Bioproduction of p-hydroxystyrene from glucose by the solvent-tolerant bacterium *Pseudomonas putida* S12 in a two-phase water-decanol fermentation. Appl Environ Microbiol 75:931–936.

7. Rühl J, Hein E-M, Hayen H, Schmid A, Blank LM. 2012. The glycerophospholipid inventory of *Pseudomonas putida* is conserved between strains and enables growth condition-related alterations. Microb Biotechnol 5:45–58.

8. Alsaker K V, Paredes C, Papoutsakis ET. 2010. Metabolite stress and tolerance in the production of biofuels and chemicals: gene-expression-based systems analysis of butanol, butyrate, and acetate stresses in the anaerobe *Clostridium acetobutylicum*. Biotechnol Bioeng 105:1131–1147.

9. Faizal I, Dozen K, Hong CS, Kuroda A, Takiguchi N, Ohtake H, Takeda K, Tsunekawa H, Kato J. 2005. Isolation and characterization of solvent-tolerant *Pseudomonas*

putida strain T-57, and its application to biotransformation of toluene to cresol in a two-phase (organic-aqueous) system. J Ind Microbiol Biotechnol 32:542–547.

10. Rojas A, Duque E, Schmid A, Hurtado A, Ramos JL, Segura A. 2004. Biotransformation in double-phase systems: physiological responses of *Pseudomonas putida* DOT-T1E to a double phase made of aliphatic alcohols and biosynthesis of substituted catechols. Appl Environ Microbiol 70:3637–3643.

11. Inoue A, Horikoshi K. 1991. Estimation of solvent-tolerance of bacteria by the solvent parameter log P. J Ferment Bioeng 71:194–196.

12. Inoue A, Horikoshi K. 1989. A *Pseudomonas* thrives in high concentrations of toluene. Nature 338:264–266.

13. Nitisakulkan T, Oku S, Kudo D, Nakashimada Y, Tajima T, Vangnai AS, Kato J. 2014. Degradation of chloroanilines by toluene dioxygenase from *Pseudomonas putida* T57. J Biosci Bioeng 117:292–297.

14. Molina-Santiago C, Udaondo Z, Gómez-Lozano M, Molin S, Ramos JL. 2017. Global transcriptional response of solvent-sensitive and solvent-tolerant *Pseudomonas putida* strains exposed to toluene. Environ Microbiol 19:645–658.

15. Volkers RJM, de Jong AL, Hulst AG, van Baar BLM, de Bont JAM, Wery J. 2006. Chemostat-based proteomic analysis of toluene-affected *Pseudomonas putida* S12. Environ Microbiol 8:1674–1679.

16. Segura A, Godoy P, van Dillewijn P, Hurtado A, Arroyo N, Santacruz S, Ramos J-L. 2005. Proteomic analysis reveals the participation of energy- and stress-related proteins in the response of *Pseudomonas putida* DOT-T1E to toluene. J Bacteriol 187:5937–5945.

17. Cuenca MDS, Roca A, Molina-Santiago C, Duque E, Armengaud J, Gómez-García MR, Ramos JL. 2016. Understanding butanol tolerance and assimilation in *Pseudomonas putida* BIRD-1: an integrated omics approach. Microb Biotechnol 9:100–115.

18. Volkers RJM, Snoek LB, Ruijssenaars HJ, de Winde JH. 2015. Dynamic Response of *Pseudomonas putida* S12 to Sudden Addition of Toluene and the Potential Role of the Solvent Tolerance Gene trgI. PLoS One 10:e0132416.

19. Martínez-García E, Nikel PI, Aparicio T, de Lorenzo V. 2014. Pseudomonas 2.0: genetic upgrading of *P. putida* KT2440 as an enhanced host for heterologous gene expression. Microb Cell Fact 13:159.

20. Silva-Rocha R, Martínez-García E, Calles B, Chavarría M, Arce-Rodríguez A, de las Heras A, Páez-Espino AD, Durante-Rodríguez G, Kim J, Nikel PI, Platero R, de Lorenzo V. 2013. The Standard European Vector Architecture (SEVA): a coherent platform for the analysis and deployment of complex prokaryotic phenotypes. Nucleic Acids Res 41:D666–D675.

21. Martínez-García E, de Lorenzo V. 2011. Engineering multiple genomic deletions in Gram-negative bacteria: analysis of the multi-resistant antibiotic profile of *Pseudomonas putida* KT2440. Environ Microbiol 13:2702–2716.

22. Martínez-García E, Aparicio T, de Lorenzo V, Nikel PI. 2014. New transposon tools tailored for metabolic engineering of gram-negative microbial cell factories. Front Bioeng Biotechnol 2:46.

23. Zobel S, Benedetti I, Eisenbach L, de Lorenzo V, Wierckx N, Blank LM. 2015. Tn7-Based Device for Calibrated Heterologous Gene Expression in *Pseudomonas putida*. ACS Synth Biol 4:1341–1351.

24. Wright O, Delmans M, Stan G-B, Ellis T. 2015. GeneGuard: A modular plasmid system designed for biosafety. ACS Synth Biol 4:307–316.

25. Belda E, van Heck RGA, Lopez-Sanchez MJ, Cruveiller S, Barbe V, Fraser C, Klenk H-P, Petersen J, Morgat A, Nikel PI, Vallenet D, Rouy Z, Sekowska A, Martins Dos Santos VAP, de Lorenzo V, Danchin A, Médigue C. 2016. The revisited genome of *Pseudomonas putida* KT2440 enlightens its value as a robust metabolic chassis. Environ Microbiol 18: 3403-3424.

26. Chavarría M, Nikel PI, Pérez-Pantoja D, de Lorenzo V. 2013. The Entner-Doudoroff pathway empowers *Pseudomonas putida* KT2440 with a high tolerance to oxidative stress. Environ Microbiol 15:1772–1785.

27. Sudarsan S, Dethlefsen S, Blank LM, Siemann-Herzberg M, Schmid A. 2014. The functional structure of central carbon metabolism in *Pseudomonas putida* KT2440.

Appl Environ Microbiol 80:5292–5303.

28. Xin F, Chen T, Jiang Y, Lu J, Dong W, Zhang W, Ma J, Zhang M, Jiang M. 2017. Enhanced biobutanol production with high yield from crude glycerol by acetone uncoupled *Clostridium sp.* strain CT7. Bioresour Technol 244:575–581.

29. Wierckx NJP, Ballerstedt H, de Bont JAM, Wery J. 2005. Engineering of solvent-tolerant *Pseudomonas putida* S12 for bioproduction of phenol from glucose. Appl Environ Microbiol 71:8221–8227.

30. Dobslaw D, Engesser KH. 2015. Degradation of toluene by ortho cleavage enzymes in *Burkholderia fungorum* FLU100. Microb Biotechnol 8:143–154.

31. Ramos-González MI, Ben-Bassat A, Campos MJ, Ramos JL. 2003. Genetic engineering of a highly solvent-tolerant *Pseudomonas putida* strain for biotransformation of toluene to p-hydroxybenzoate. Appl Environ Microbiol 69:5120–5127.

32. Park JB, Bühler B, Panke S, Witholt B, Schmid A. 2007. Carbon metabolism and product inhibition determine the epoxidation efficiency of solvent-tolerant *Pseudomonas sp.* strain VLB120ΔC. Biotechnol Bioeng 98:1219–1229.

33. Geng Y, Deng Y, Chen F, Jin H, Tao K, Hou T. 2014. Biodegradation of Isopropanol by a Solvent-Tolerant *Paracoccus denitrificans* Strain. Prep Biochem Biotechnol 45:491–499.

34. Kanno M, Katayama T, Tamaki H, Mitani Y, Meng X-Y, Hori T, Narihiro T, Morita N, Hoshino T, Yumoto I, Kimura N, Hanada S, Kamagata Y. 2013. Isolation of Butanol- and Isobutanol-Tolerant Bacteria and Physiological Characterization of Their Butanol Tolerance. Appl Environ Microbiol 79:6998–7005.

35. Kongpol A, Kato J, Tajima T, Vangnai AS. 2012. Characterization of acetonitrile-tolerant marine bacterium *Exiguobacterium sp.* SBH81 and its tolerance mechanism. Microbes Environ 27:30–35.

36. Segura A, Hurtado A, Rivera B, Lazaroaie MM. 2008. Isolation of new toluene-tolerant marine strains of bacteria and characterization of their solvent-tolerance properties. J Appl Microbiol 104:1408–1416.

37. Kabelitz N, Santos PM, Heipieper HJ. 2003. Effect of aliphatic alcohols on growth and degree of saturation of membrane lipids in *Acinetobacter calcoaceticus*. FEMS Microbiol Lett 220:223–227.

38. Heipieper HJ, Neumann G, Cornelissen S, Meinhardt F. 2007. Solvent-tolerant bacteria for biotransformations in two-phase fermentation systems. Appl Microbiol Biotechnol 74:961–973.

39. Sikkema J, de Bont JA, Poolman B. 1995. Mechanisms of membrane toxicity of hydrocarbons. Microbiol Rev 59:201–222.

40. Ramos J-LL, Sol Cuenca M, Molina-Santiago C, Segura A, Duque E, Gómez-García MR, Udaondo Z, Roca A. 2015. Mechanisms of solvent resistance mediated by interplay of cellular factors in *Pseudomonas putida*. FEMS Microbiol Lett 39:555–566.

41. Torres S, Baigorí MD, Swathy SL, Pandey A, Castro GR. 2009. Enzymatic synthesis of banana flavour (isoamyl acetate) by *Bacillus licheniformis* S-86 esterase. Food Res Int 42:454–460.

42. Bernal P, Segura A, Ramos JL. 2007. Compensatory role of the cis-trans-isomerase and cardiolipin synthase in the membrane fluidity of *Pseudomonas putida* DOT-T1E. Environ Microbiol 9:1658–1664.

43. Zhang Y-M, Rock CO. 2008. Membrane lipid homeostasis in bacteria. Nat Rev Microbiol 6:222–233.

44. Eberlein C, Baumgarten T, Starke S, Heipieper HJ. 2018. Immediate response mechanisms of Gram-negative solvent-tolerant bacteria to cope with environmental stress: *cis-trans* isomerization of unsaturated fatty acids and outer membrane vesicle secretion. Appl Microbiol Biotechnol 102:2583–2593.

45. Unell M, Kabelitz N, Jansson JK, Heipieper HJ. 2007. Adaptation of the psychrotroph *Arthrobacter chlorophenolicus* A6 to growth temperature and the presence of phenols by changes in the anteiso/iso ratio of branched fatty acids. FEMS Microbiol Lett 266:138–143.

46. Kondakova T, D'Heygère F, Feuilloley MJ, Orange N, Heipieper HJ, Duclairoir Poc C. 2015. Glycerophospholipid synthesis and functions in *Pseudomonas*. Chem Phys

Lipids 190:27–42.

47. Sayqal A, Xu Y, Trivedi DK, AlMasoud N, Ellis DI, Rattray NJW, Goodacre R. 2016. Metabolomics Analysis Reveals the Participation of Efflux Pumps and Ornithine in the Response of *Pseudomonas putida* DOT-T1E Cells to Challenge with Propranolol. PLoS One 11:e0156509.

48. Vences-Guzmán MÁ, Geiger O, Sohlenkamp C. 2012. Ornithine lipids and their structural modifications: from A to E and beyond. FEMS Microbiol Lett 335:1–10.

49. Schwechheimer C, Kuehn MJ. 2015. Outer-membrane vesicles from Gram-negative bacteria: Biogenesis and functions. Nat Rev Microbiol 13:605–619.

50. Kobayashi H, Uematsu K, Hirayama H, Horikoshi K. 2000. Novel Toluene Elimination System in a Toluene-Tolerant Microorganism. J Bacteriol 182:6451–6455.

51. Neumann G, Cornelissen S, van Breukelen F, Hunger S, Lippold H, Loffhagen N, Wick LY, Heipieper HJ. 2006. Energetics and surface properties of *Pseudomonas putida* DOT-T1E in a two-phase fermentation system with 1-decanol as second phase. Appl Environ Microbiol 72:4232–4238.

52. Baumgarten T, Sperling S, Seifert J, von Bergen M, Steiniger F, Wick LY, Heipieper HJ. 2012. Membrane vesicle formation as a multiple-stress response mechanism enhances *Pseudomonas putida* DOT-T1E cell surface hydrophobicity and biofilm formation. Appl Environ Microbiol 78:6217–6224.

53. Ramos JL, Duque E, Godoy P, Segura A. 1998. Efflux pumps involved in toluene tolerance in *Pseudomonas putida* DOT-T1E. J Bacteriol 180:3323–3329.

54. Du D, Wang Z, James NR, Voss JE, Klimont E, Ohene-Agyei T, Venter H, Chiu W, Luisi BF. 2014. Structure of the AcrAB-TolC multidrug efflux pump. Nature 509:512–515.

55. Isken S, Santos PMAC, de Bont JAM. 1997. Effect of solvent adaptation on the antibiotic resistance in *Pseudomonas putida*. Appl Microbiol Biotechnol 48:642–647.

56. Watanabe R, Doukyu N. 2012. Contributions of mutations in acrR and marR genes to organic solvent tolerance in *Escherichia coli*. AMB Express 2:58.

57. Blair JMA, Piddock LJ V. 2016. How to Measure Export via Bacterial Multidrug Resis-

tance Efflux Pumps. MBio 7:e00840-16.

58. Godoy P, Molina Henares AJ, de la Torre J, Duque E, Ramos JL. 2010. Characterization of the RND family of multidrug efflux pumps: in silico to in vivo confirmation of four functionally distinct subgroups. Microb Biotechnol 3:691–700.

59. Wijte D, van Baar BLM, Heck AJR, Altelaar AFM. 2011. Probing the proteome response to toluene exposure in the solvent tolerant *Pseudomonas putida* S12. J Proteome Res 10:394–403.

60. Seydlová G, Halada P, Fišer R, Toman O, Ulrych A, Svobodová J. 2012. DnaK and GroEL chaperones are recruited to the *Bacillus subtilis* membrane after short-term ethanol stress. J Appl Microbiol 112:765–774.

61. Blank LM, Ionidis G, Ebert BE, Bühler B, Schmid A. 2008. Metabolic response of *Pseudomonas putida* during redox biocatalysis in the presence of a second octanol phase. FEBS J 275:5173–5190.

62. Torres S, Pandey A, Castro GR. 2011. Organic solvent adaptation of Gram positive bacteria: Applications and biotechnological potentials. Biotechnol Adv 29:442–452.

63. Gaur R, Khare SK. 2009. Cellular response mechanisms in *Pseudomonas aeruginosa* PseA during growth in organic solvents. Lett Appl Microbiol 49:372–377.

64. Neumann G, Veeranagouda Y, Karegoudar TB, Sahin zlem, M usezahl I, Kabelitz N, Kappelmeyer U, Heipieper HJ. 2005. Cells of *Pseudomonas putida* and *Enterobacter sp.* adapt to toxic organic compounds by increasing their size. Extremophiles 9:163–168.

65. Veeranagouda Y, Karegoudar TB, Neumann G, Heipieper HJ. 2006. Enterobactersp. VKGH12 growing with n-butanol as the sole carbon source and cells to which the alcohol is added as pure toxin show considerable differences in their adaptive responses. FEMS Microbiol Lett 254:48–54.

66. Tieves F, Erenburg IN, Mahmoud O, Urlacher VB. 2016. Synthesis of chiral 2-alkanols from n-alkanes by a *P. putida* whole-cell biocatalyst. Biotechnol Bioeng.

67. Sardessai Y, Bhosle S. 2002. Tolerance of bacteria to organic solvents. Res Microbiol

153:263–268.

68. Salgado JM, Rodríguez-Solana R, Curiel JA, de Las Rivas B, Muñoz R, Domínguez JM. 2014. Bioproduction of 4-vinylphenol from corn cob alkaline hydrolyzate in two-phase extractive fermentation using free or immobilized recombinant *E. coli* expressing pad gene. Enzyme Microb Technol 58–59:22–28.

69. Bozell JJ, Petersen GR. 2010. Technology development for the production of biobased products from biorefinery carbohydrates—the US Department of Energy's "top 10" revisited. Green Chem 12:539–554.

70. Sousa AF, Coelho JFJ, Silvestre AJD. 2016. Renewable-based poly((ether)ester)s from 2,5-furandicarboxylic acid. Polymer (Guildf) 98:129–135.

71. Jiang Y, Maniar D, Woortman AJJ, Loos K. 2016. Enzymatic synthesis of 2,5-furandicarboxylic acid-based semi-aromatic polyamides: enzymatic polymerization kinetics, effect of diamine chain length and thermal properties. RSC Adv 6:67941–67953.

72. De Jong E, Dam MA, Sipos L, Gruter GJM. 2012. Furandicarboxylic acid (FDCA), A versatile building block for a very interesting class of polyesters. ACS Symp Ser 1105:1–13.

73. Lewkowski J. 2001. Synthesis, chemistry and applications of 5-hydroxymethyl-furfural and its derivatives. ARKIVOC 2001:17.

74. Leprince A, van Passel MW, dos Santos VAPM. 2012. Streamlining genomes: toward the generation of simplified and stabilized microbial systems. Curr Opin Biotechnol 23:651–658.

75. Beites T, Mendes MV. 2015. Chassis optimization as a cornerstone for the application of synthetic biology based strategies in microbial secondary metabolism. Front Microbiol 6.

76. Ajikumar PK, Xiao W-H, Tyo KEJ, Wang Y, Simeon F, Leonard E, Mucha O, Phon TH, Pfeifer B, Stephanopoulos G. 2010. Isoprenoid Pathway Optimization for Taxol Precursor Overproduction in Escherichia coli. Science 330:70–74.

77. Verhoef S, Ballerstedt H, Volkers RJM, de Winde JH, Ruijssenaars HJ. 2010. Com-

parative transcriptomics and proteomics of p-hydroxybenzoate producing *Pseudomonas putida* S12: novel responses and implications for strain improvement. Appl Microbiol Biotechnol 87:679–690.

78. Shetty RP, Endy D, Knight TF. 2008. Engineering BioBrick vectors from BioBrick parts. J Biol Eng 2:5.

79. Schmid A, Kollmer A, Sonnleitner B, Witholt B. 1999. Development of equipment and procedures for the safe operation of aerobic bacterial bioprocesses in the presence of bulk amounts of flammable organic solvents. Bioprocess Eng 20:91–100.

80. Choi HJ, Lim BR, Park YJ, Joo WH. 2017. Improvement in solvent tolerance by exogenous glycerol in *Pseudomonas sp.* BCNU 106. Lett Appl Microbiol 65:147–152.

81. Mizoguchi H, Mori H, Fujio T. 2007. *Escherichia coli* minimum genome factory. Biotechnol Appl Biochem 46:157–167.

82. Chubukov V, Mukhopadhyay A, Petzold CJ, Keasling JD, Martín HG. 2016. Synthetic and systems biology for microbial production of commodity chemicals. npj Syst Biol Appl 2:16009.

83. Janardhan Garikipati SVB, Peeples TL. 2015. Solvent resistance pumps of *Pseudomonas putida* S12: Applications in 1-naphthol production and biocatalyst engineering. J Biotechnol 210:91–99.

84. Aparicio T, de Lorenzo V, Martínez-García E. 2017. CRISPR/Cas9-Based Counterselection Boosts Recombineering Efficiency in *Pseudomonas putida*. Biotechnol J 13:e1700161.

85. Elmore JR, Furches A, Wolff GN, Gorday K, Guss AM. 2017. Development of a high efficiency integration system and promoter library for rapid modification of *Pseudomonas putida* KT2440. Metab Eng Commun 5:1–8.

86. Loeschcke A, Markert A, Wilhelm S, Wirtz A, Rosenau F, Jaeger K-E, Drepper T. 2012. TREX: A Universal Tool for the Transfer and Expression of Biosynthetic Pathways in Bacteria. ACS Synth Biol 2:22–33.

87. Borrero-de Acuña JM, Bielecka A, Häussler S, Schobert M, Jahn M, Wittmann C,

Jahn D, Poblete-Castro I. 2014. Production of medium chain length polyhydroxyalkanoate in metabolic flux optimized *Pseudomonas putida*. Microb Cell Fact 13:88.

88. Wierckx NJP, Ballerstedt H, De Bont JAM, De Winde JH, Ruijssenaars HJ, Wery J. 2008. Transcriptome analysis of a phenol-producing *Pseudomonas putida* S12 construct: Genetic and physiological basis for improved production. J Bacteriol 190:2822–2830.

89. Tiso T, Sabelhaus P, Behrens B, Wittgens A, Rosenau F, Hayen H, Blank LM. 2016. Creating metabolic demand as an engineering strategy in *Pseudomonas putida* – Rhamnolipid synthesis as an example. Metab Eng Commun 3:234–244.

90. Wigneswaran V, Nielsen KF, Sternberg C, Jensen PR, Folkesson A, Jelsbak L. 2016. Biofilm as a production platform for heterologous production of rhamnolipids by the non-pathogenic strain *Pseudomonas putida* KT2440. Microb Cell Fact 15:181.

91. Lieder S, Nikel PI, de Lorenzo V, Takors R. 2015. Genome reduction boosts heterologous gene expression in *Pseudomonas putida*. Microb Cell Fact 14:23.

92. Murray K, Duggleby CJ, Sala-Trepat JM, Williams PA. 1972. The metabolism of benzoate and methylbenzoates via the meta-cleavage pathway by *Pseudomonas arvilla* mt-2. Eur J Biochem 28:301–310.

93. Bagdasarian M, Lurz R, Rückert B, Franklin FCH, Bagdasarian MM, Frey J, Timmis KN. 1981. Specific-purpose plasmid cloning vectors II. Broad host range, high copy number, RSF 1010-derived vectors, and a host-vector system for gene cloning in *Pseudomonas*. Gene 16:237–247.

94. Hosseini R, Kuepper J, Koebbing S, Blank LM, Wierckx N, de Winde JH. 2017. Regulation of solvent tolerance in *Pseudomonas putida* S12 mediated by mobile elements. Microb Biotechnol 10:1558–1568.

95. Zingaro KA, Papoutsakis ET. 2012. Toward a semisynthetic stress response system to engineer microbial solvent tolerance. MBio 3:e00308-12.

96. Turner WJ, Dunlop MJ. 2015. Trade-Offs in Improving Biofuel Tolerance Using Combinations of Efflux Pumps. ACS Synth Biol 4:1056–1063.

97. Koopman F, Wierckx N, de Winde JH, Ruijssenaars HJ. 2010. Identification and characterization of the furfural and 5-(hydroxymethyl)furfural degradation pathways of *Cupriavidus basilensis* HMF14. Proc Natl Acad Sci 107:4919–4924.

98. Kampers LFC, Volkers RJM, Martins dos Santos VAP. 2019. *Pseudomonas putida* KT2440 is HV1 certified, not GRAS. Microb Biotechnol 12:845–848.

CHAPTER 3

Comparative analysis reveals the modular functional build-up of megaplasmid pTTS12 of *Pseudomonas putida* S12: a paradigm for transferable traits, plasmid stability and inheritance?

Hadiastri Kusumawardhani†, Rohola Hosseini†, Johannes H. de Winde

†H. K. and R. H. contributed equally to this work.

Submitted for publication.

DOI: 10.1101/2020.06.19.162511

Abstract

The *Pseudomonas putida* S12 genome contains 583 kbp megaplasmid pTTS12 that carries over 600 genes enabling tolerance to various stress conditions, including the solvent extrusion pump SrpABC. We performed a comparative analysis of pTTS12 against 28915 plasmids from NCBI databases. We investigated putative roles of genes encoded on pTTS12 and further elaborated on its role in the establishment and maintenance of several stress conditions, specifically focusing on solvent tolerance in *P. putida* strains. The backbone of pTTS12 was found to be closely related to that of the carbapenem-resistance plasmid pOZ176, member of the IncP-2 incompatibility group, although remarkably the carbapenem resistance cassette is absent from pTTS12. Megaplasmid pTTS12 contains multiple transposon-flanked cassettes mediating resistance to various heavy metals such as tellurite, chromate (Tn7), and mercury (Tn5053 and Tn5563). Additionally, pTTS12 also contains a P-type, Type IV secretion system (T4SS) supporting self-transfer to other *P. putida* strains. This study increases our understanding in the build-up of IncP-2 plasmids and several promising exchangeable gene clusters to construct robust microbial hosts for biotechnology applications.

Importance

Originating from various environmental niches, large numbers of bacterial plasmids have been found carrying heavy metal and antibiotic resistance genes, degradation pathways and specific transporters for organic solvents or aromatic compounds. Such genes may constitute promising candidates for novel synthetic biology applications. Our systematic analysis of gene clusters encoded on megaplasmid pTTS12 underscores that a large portion of its genes is involved in stress response increasing survival under harsh conditions like heavy metal and organic solvent resistance. We show that pTTS12 belongs to the IncP-2 plasmid family. Comparative analysis of pTTS12 provides thorough insight into the structural and functional build-up of members of the IncP-2 plasmid family. pTTS12 is highly stable and carries a complex arrangement of transposable elements containing heavy metal resistance clusters as well as distinct aromatic degradation pathways and solvent-extrusion pump. This offers interesting insight into the evolution of solvent tolerance in the *P. putida* family.

Introduction

Megaplasmids as transferable vehicles of environmental resistance genes

Bacteria may use plasmids as autonomous, self-replicating elements driving horizontal transfer of genes (HGT) that confer resistance to otherwise detrimental conditions. As such, these extrachromosomal entities often confer advantageous characteristics for the host strain (1–3). The rapid spread of resistance genes through these, usually large conjugative plasmids is further facilitated by the presence of a variety of mobile genetic elements such as transposons, integrons and insertion sequences (IS's) (4–7). The spread of multidrug resistance (MDR) via mobile genetic elements has been the subject of investigation for a number of years (8). Despite those efforts, the role and functioning of megaplasmids is still poorly understood. Recent studies highlighted the role of megaplasmids in the spread of MDR in the opportunistic pathogen *Pseudomonas aeruginosa* (1, 2). Strains of its close relative, *Pseudomonas putida,* have been known to harbor large conjugational plasmids, conferring resistance to environmental threats (3, 9). Plasmids of the *Pseudomonas* family are classified by incompatibility groups, that exhibit various modes of compatibility and transferability (10). We have chosen to study the recently identified megaplasmid pTTS12 of *Pseudomonas putida* S12 in comparison with a number of other large plasmids of the *Pseudomonas* family, in order to elucidate key elements governing HGT, stability and essential functions.

Solvent tolerance in *Pseudomonas putida* S12; resistance as a benefit for biotechnology

Pseudomonas putida S12 is a gram-negative soil bacterium which was isolated on styrene as a sole carbon source (11). This strain shows a remarkable tolerance towards non-metabolized organic solvents (e.g. toluene) (12). Such high tolerance towards organic solvents presents a beneficial trait and advantage for bioproduction of aromatics and biofuel (13, 14). Due to its solvent tolerance and versatile metabolism, *P. putida* S12 excels as a microbial host for production of valuable chemicals (15–19). Removal of organic solvent molecules from the bacterial cell membrane is essential and carried out by SrpABC, a resistance-nodulation-cell division (RND) family efflux pump (12, 20). Membrane compaction and the upregulation of chaperones, general stress responses, and TCA cycle-related enzymes support a further in-

trinsic solvent tolerance in *P. putida* S12 (21–24).

We recently found through whole-genome sequencing that the genome of *P. putida* S12 consists of a 5.8 Mbp chromosome and a 583 kbp single-copy megaplasmid pTTS12 (25). Interestingly, both the SrpABC RND-efflux pump and the styrene degradation pathway which are major distinctive features of *P. putida* S12, are encoded on this megaplasmid. The genome of *P. putida* S12 contains a large number of several types of mobile elements, spread over both chromosome and megaplasmid pTTS12 (25–27). Some of these insertion sequences were shown to be involved in the regulation and adaptation towards stress conditions, for example during the solvent stress (4, 28). Like *P. putida* S12, related solvent-tolerant *P. putida* DOT-T1E and *Pseudomonas taiwanensis* VLB120 have been shown to harbor megaplasmids of 121 kb and 312 kb, respectively (29, 30). Indeed, those plasmids encode RND-type efflux pumps and biodegradative pathways for aromatic compounds, similar to *P. putida* S12. To further characterize pTTS12, we here performed a comparative analysis against a large number of other megaplasmids from Refseq and Nuccore databases. With this analysis, we aimed at identifying the origin of the pTTS12 plasmid and understanding the build-up of environmental-stress related gene clusters in pTTS12.

Results

Comparative analysis of megaplasmid pTTS12

The 583 Kbps megaplasmid pTTS12 (GenBank accession no. CP009975) is a single-copy plasmid encoded in *P. putida* S12 (25). For this paper, annotations for pTTS12 were further extended and the overall sequence was corrected based on our previous observations of an additional seven ISS12 mobile elements (4). pTTS12 encodes 609 genes of which 583 are single copy and 15 genes are duplicated at least once. These genes were divided into 232 putative operons for subsequent ordered genes in forward or reverse strand with less than 20 bps distance. The operons were clustered together based on the function of genes encoded within these clusters.

Comparative analysis was performed with 28915 plasmids larger than 2 kb in length, acquired from the Refseq database (https://www.ncbi.nlm.nih.gov/refseq/) combined with additional sequences from the Nuccore database (https://www.ncbi.nlm.nih.gov/nuccore/). The top 50 plasmids encoding homologues of pTTS12 proteins are visualized in a circular plot using CGView (31) as shown on Fig. 3.1, and listed in Table 3.1. In Fig. 3.1, the outer purple

line represents pTTS12 with forward coding genes on top of the line and the reverse coding gene sequences below the line. Each of the subsequent 50 inner circles represents a single plasmid and is colored based on the family of its host. In case no homologous protein was identified for a pTTS12 counterpart, that space on the circle was left blank. The extended circular plot of the top 500 plasmids encoding homologues of pTTS12 can be found in Fig. 3.S1.

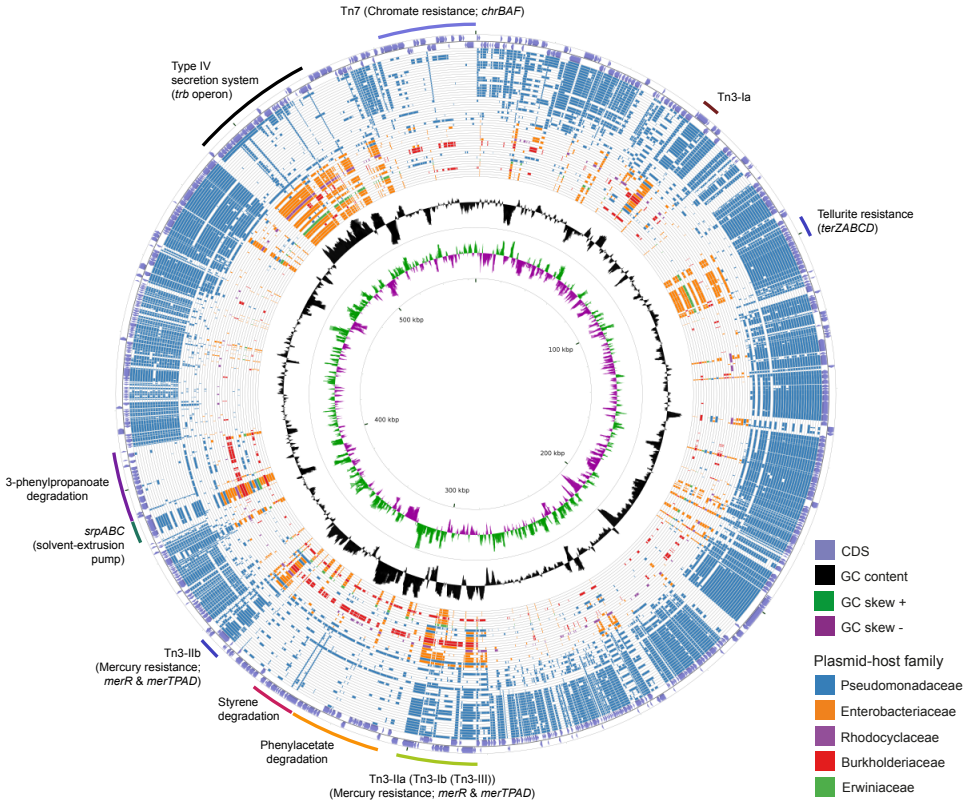

Fig. 3.1. Circular plot of the top 50 plasmids with the highest identity scores to pTTS12

pTTS12 coding sequences (CDS) were aligned to 28915 other plasmids available at NCBI Refseq and Nuccore databases. The outer light purple ring represents the CDS of plus and minus strand of pTTS12. In the inner ring, the GC content is represented in black and the positive and negative GC skew are represented in green and purple respectively. The plasmids are ordered based on their similarity and coverage to pTTS12 CDS from outermost to innermost of the plot with each ring representing a single plasmid as listed in Table 3.1. Ring colors represent different plasmid-host families; Pseudomonadaceae (blue), Enterobacteriaceae (orange), Rhodocyclaceae (purple), Burkholderiaceae (red), and Erwiniaceae (green). The position of the gene clusters of interest are annotated in the figure. An extended circular plot of the top 500 plasmids with highest identity scores to pTTS12 are shown in Fig. 3.S1.

The majority of plasmids highly similar to pTTS12 were found in *Pseudomonas* type strains (Table 3.1). The relative identity scores presented in Table 3.1 were calculated as a percentage of total scores of each plasmid divided by the total identity score obtained for pTTS12 itself. The plasmid most similar to pTTS12 is pOZ176 from *P. aeruginosa* PA96 which was previously categorized as a member of incompatibility group P-2 (IncP-2). pOZ176 and pTTS12 share no less than 71% similarity of their encoded genes indicating that these plasmids share a similar IncP-2 backbone. However, while pOZ176 encodes a carbapenem-resistance gene cluster typical for several pathogenic *P. aeruginosa* strains (2), pTTS12 of *P. putida* S12 does not share this feature.

Table 3.1. List of 50 plasmids with the highest similarity scores to pTTS12. pTTS12 coding sequences (CDS) were aligned to other megaplasmids available at NCBI databases. The relative similarity score was calculated by dividing total scores for each plasmid by total score obtained for pTTS12 itself.

Rank	Strain	Plasmid	Taxid	Length (bp)	Relative similarity
	Pseudomonas putida S12	pTTS12	1215087	583900	100.00%
1	*Pseudomonas aeruginosa* PA96	pOZ176	145792	500839	72.54%
2	*Pseudomonas aeruginosa* strain FFUP_PS_37	pJB37	287	464804	69.30%
3	*Pseudomonas aeruginosa* strain AR_0356	unnamed2	287	438531	67.97%
4	*Pseudomonas aeruginosa* strain AR441	unnamed3	287	438529	66.23%
5	*Pseudomonas putida* strain SY153	pSY153-MDR	303	468170	64.70%
6	*Pseudomonas aeruginosa* strain T2436	pBT2436	287	422811	64.69%
7	*Pseudomonas koreensis* strain P19E3	p1	198620	467568	64.44%
8	*Pseudomonas putida* strain 12969	p12969-DIM	303	409102	64.43%
9	*Pseudomonas aeruginosa* strain T2101	pBT2101	287	439744	64.43%
10	*Pseudomonas aeruginosa* strain PA298	pBM908	287	395774	63.99%
11	*Pseudomonas aeruginosa* isolate RW109	RW109	287	555265	63.75%
12	*Pseudomonas aeruginosa* strain PA121617	pBM413	287	423017	63.20%
13	*Pseudomonas aeruginosa* strain PABL048	pPABL048	287	414954	62.82%
14	*Pseudomonas aeruginosa*	p727-IMP	287	430173	62.75%
15	*Pseudomonas aeruginosa* strain AR439	unnamed2	287	437392	62.00%
16	*Pseudomonas citronellolis* strain SJTE-3	pRBL16	53408	370338	61.12%
17	*Pseudomonas aeruginosa*	p12939-PER	287	496436	60.86%
18	*Pseudomonas aeruginosa*	pA681-IMP	287	397519	59.50%
19	*Pseudomonas aeruginosa*	pR31014-IMP	287	374000	55.58%

Rank	Strain	Plasmid	Taxid	Length (bp)	Relative similarity
20	*Pseudomonas taiwanensis* VLB120	pSTY	69328	321653	21.65%
21	*Pseudomonas fluorescens* SBW25	pQBR103	216595	425094	20.48%
22	*Pseudomonas syringae pv. maculicola* str. ES4326	pPma4326F	629265	387260	20.16%
23	*Pseudomonas putida* strain KF715	pKF715A	303	483376	16.63%
24	*Pseudomonas stutzeri* strain YC-YH1	pYCY1	316	225945	16.06%
25	*Pseudomonas fluorescens* SBW25	pQBR57	216595	307330	14.45%
26	*Pseudomonas aeruginosa* strain PA83	unnamed1	287	398087	14.42%
27	*Pseudomonas aeruginosa* strain DN1	unnamed1	287	317349	14.24%
28	*Pseudomonas monteilii* strain FDAAR-GOS_171	unnamed	76759	60588	13.85%
29	*Salmonella enterica* strain 8025	p8025	28901	311280	11.99%
30	*Pseudomonas luteola* strain FDAAR-GOS_637	unnamed1	47886	585976	10.92%
31	*Enterobacter hormaechei subsp. steigerwaltii* strain 34998	p34998	299766	239973	10.39%
32	*Enterobacter hormaechei* strain A1	pIn-cHI2-1502264	158836	309444	10.37%
33	*Leclercia adecarboxylata* strain Lec-476	pLec-476	83655	311758	10.06%
34	*Enterobacter hormaechei subsp. hoffmannii* strain AR_0365	unnamed1	1812934	328871	9.98%
35	*Azospira sp.* I09	pAZI09	1765049	397391	9.98%
36	*Citrobacter freundii* strain SL151	unnamed1	546	229406	9.89%
37	*Cupriavidus metallidurans* strain FDAAR-GOS_675	unnamed3	119219	2586495	9.54%
38	*Cupriavidus metallidurans* CH34	megaplasmid	266264	2580084	9.53%
39	*Enterobacter hormaechei subsp. hormaechei* strain 34983	p34983	301105	328905	9.41%
40	*Escherichia coli* strain CFSAN064035	pGMI17-003_1	562	310064	9.19%
41	*Pseudomonas sp.* XWY-1	pXWY	2069256	394537	9.15%
42	*Klebsiella oxytoca* strain CAV1374	pKPC_CAV1374	571	332956	9.12%
43	*Pseudomonas veronii* 1YdBTEX2	pPVE	1295141	373858	9.06%
44	*Pantoea sp.* PSNIH2	pPSP-75c	1484157	378808	9.04%
45	*Klebsiella michiganensis* strain AR375	unnamed2	1134687	340462	8.96%
46	*Citrobacter freundii* complex sp. CFNIH9	pCFR-eb27	2077149	355789	8.82%
47	*Ralstonia solanacearum* strain HA4-1	HA4-1MP	305	1947245	8.82%
48	*Enterobacteriaceae bacterium* ENNIH1	pENT-1f0b	2066051	302640	8.78%
49	*Leclercia sp.* LSNIH1	pLEC-1cb1	1920114	341250	8.74%
50	*Leclercia sp.* LSNIH3	pLEC-7c0d	1920116	330021	8.74%

Surprisingly, pTTS12 shares only 21% of sequence similarity with the pSTY plasmid of *P. taiwanensis* VLB120. The major and only gene clusters shared between pTTS12 and pSTY are involved in styrene degradation, phenylpropionic acid degradation, and solvent efflux pump (SrpABC). Interestingly, the genes shared between pTTS12 and pSTY are absent in all other *Pseudomonas* plasmids, except for the solvent efflux pump gene cluster which is similar with TtgGHI efflux pump from the pGRT-1 plasmid of *P. putida* DOT-T1E. The regions encoding solvent efflux pump and phenylpropionic acid degradation are clustered together and have identical synteny in pTTS12 and pSTY (Fig. 3.S2). However, the plasmids do not share any mobile genetic elements surrounding this cluster that might indicate a mechanism of acquisition or transfer. The similarity of the styrene degradation clusters and solvent efflux pump - phenylpropionic acid degradation clusters between pTTS12 and pSTY were 99% and 80%, respectively.

Between 8% to 12% of encoded proteins from pTTS12 can also be found in other genera than *Pseudomonas* (Table 3.1). Several plasmids from *Salmonella*, *Enterobacter*, *Citrobacter*, *Leclersia*, *Klebsiella*, *Pantoea*, *Polaromonas*, and *Cupriavidus* species shared homologous proteins involved in the T4SS conjugation, replication machinery, and plasmid maintenance. Like other IncP-2 plasmids, pTTS12 contains multiple transposable elements, particularly Tn3 mobile elements (Fig. 3.1). This mobile element encodes for heavy metal resistance genes that are predominantly present in IncP-2 plasmids. Additionally, pTTS12 carries a unique Tn7-element consisting of several chromate resistance genes.

Distinctive conjugation machinery of pTTS12

Megaplasmid pTTS12 contains a P-type T4SS (Type IV secretion system) conjugation system (RPPX_28670-RPPX_28725), sharing synteny with the prototype *trb* operon from *A. tumefaciens* pTiC58 (Fig. 3.2A). For an operational T4SS conjugation machinery, a T4SS gene cluster, type IV coupling protein (T4CP) and a relaxase protein are required (32). An additional *traG* (RPPX_28650), which may serve as a T4CP, is located upstream of the T4SS cluster. Further upstream of the T4SS and T4CP, a putative virD2-like gene (RPPX_28750) and an operon consisting of *parB, parA* and *repA* (RPPX_28765-28775) are encoded on pTTS12. The putative virD2-like gene (RPPX_28750) may play a role as a relaxase which is important for the transferability of pTTS12.

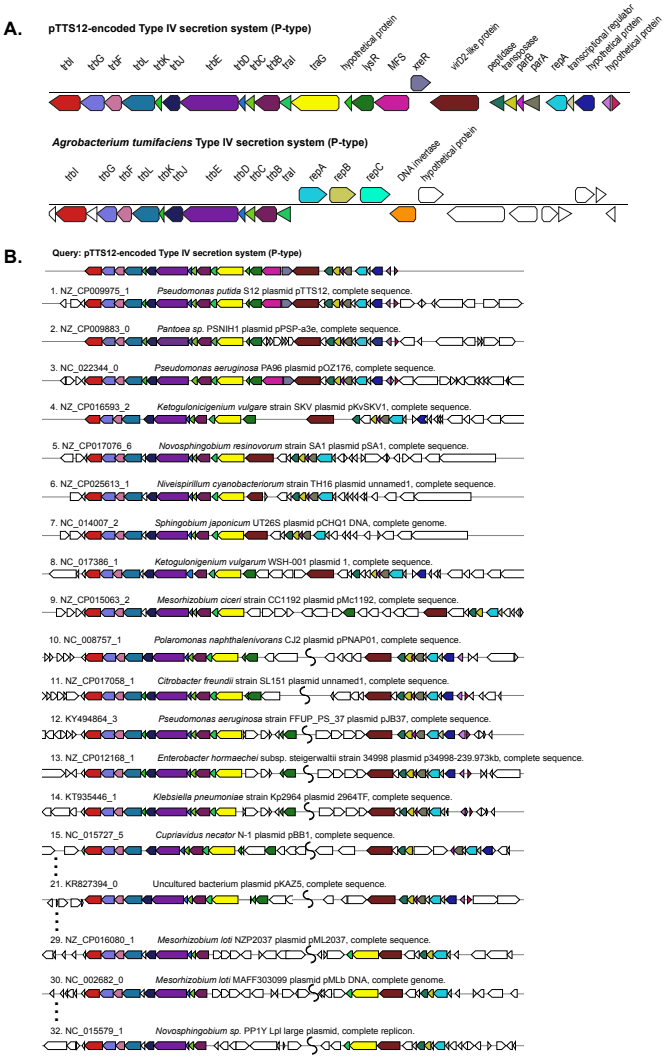

Fig. 3.2. Structure and synteny of pTTS12 conjugation system

A. The arrangement of the T4SS gene cluster found in pTTS12 and the prototype *trb* operon from *Agrobacterium tumefaciens* (pTiC58). The colors represent different genes in the cluster and same colors are assigned for the homologous genes. The gene names are indicated above the respective clusters. pTTS12/T4SS and the *trb* operon of pTiC58 share synteny for 11 genes (*trbI* to *traI*), while other parts are clearly different.

B. Synteny plot of the T4SS gene cluster of pTTS12 for plasmid conjugation, replication and partitioning compared with other plasmids. This visualization was generated using multigeneblast software (49). The numbers refer to the order of decreasing synteny. For the sake of clarity, several plots were removed from this figure, indicated by the dots. The colors represent different genes in the cluster corresponding to color-coding in panel A. Putative coupling-protein (T4CP) *traG* is indicated in yellow and the putative relaxase *virD2*-like protein is indicated in brown.

T4SS, *traG*, and upstream genes involved in replication and partitioning shared synteny with the T4SS clusters on other plasmids such as *Pantoea sp.* PSNIH1 (pPSP-a3e), *Pseudomonas aeruginosa* PA96 (pOZ1760), and *Ketogulonicigenium vulgare* SKV (pKvSKV1) (Fig. 3.2B). Typically, *traG* (T4CP) is coupled to the same operon of T4SS while the region encoding replication and partitioning may be separated (Fig. 3.2B), in some cases relatively far. It is interesting to note that in two *Mesorhizobium loti* strains and *Novosphingobium sp.* PP1Y, the T4SS operon and *traG-traI* are completely separated (Fig. 3.2B). Instead, VirD2-like protein (relaxase), *traG* (T4CP) and *traI* formed a single operon.

Most of the Pseudomonadaceae-family plasmids do not contain this *trb* operon (Fig. 3.1) except for pTTS12, pOZ176 from *P. aeruginosa* PA96, pJB37 from *P. aeruginosa* FFUP_PS_37 and an unnamed plasmid from *P. aeruginosa* PA83. Therefore, this conjugative operon may not be common in IncP-2 plasmid family. However, this *trb* operon is abundant among Enterobacteriaceae-family plasmids (Fig. 3.1).

Distribution of transposable elements conferring heavy metal resistance

pTTS12 as well as many other highly similar plasmids contain a multitude of mobile genetic elements, such as ISS12 and Tn3-family transposases. pTTS12 harbors five copies of Tn3-family transposable elements; two copies of Tn3-I with highest identity to Tn4656, two copies of Tn3-II that are highly similar to Tn5053 and a single copy of Tn3-III with highest similarity to Tn5563 (Fig. 3.3A). Tn3-I is an identical transposase (RPPX_RS27515, *tnpR* and RPPX_RS27515, *tnpA*) to Tn4656 encoded on pWW53 plasmid from *P. putida* MT53. Moreover, the 39-bps inverted repeat (IR) sequences found on both ends of these two elements are highly identical with only a single mismatch difference. In addition to *tnpA* and *tnpR*, this Tn3-element contains a putative methyl-accepting chemotaxis protein (*mcpT*-2) and an insertion sequence IS256. Tn3-II of pTTS12 is identical (99.8% similarity) to Tn5053 of *Xanthomonas sp.* W17 encoding a mercury resistance gene cluster *merR* and *merTPAD* (7). This Tn3-II has 25 bp inverted repeats, bracketing the ends and 5 bp directed repeats (DR). Tn3-III is identical to Tn5563, that is found in several other plasmids, eg. pAMBL of *P. aeruginosa*, pSTY of *P. taiwanensis* VLB-120 and pRA2 of *P. alcaligenes*. The Tn3-III has identical 38 bps IRs bracketing the element, also identical to IRs found for this element in other plasmids. This element contains several genes such as *merR*, *merTP*, *pilT* and a gene with a PIN nuclease domain.

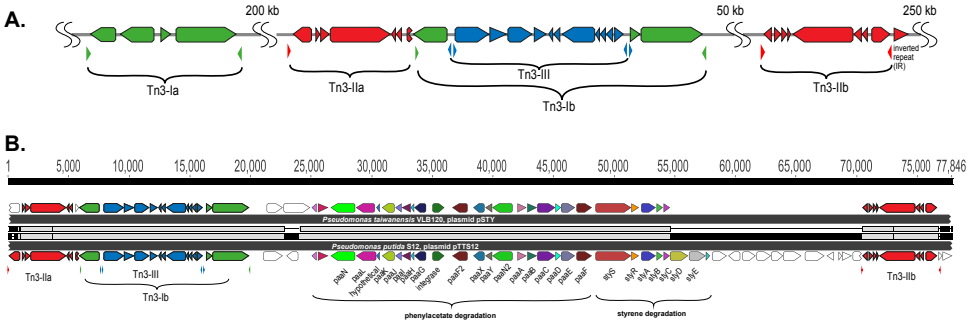

Fig. 3.3. Tn3 transposon family elements responsible for horizontal gene transfer of styrene and phenylacetate degradation pathway.

A. Genetic organization of the three different Tn3-family transposable elements in pTTS12. Colors represent the three different Tn3 transposon families; Tn3-I with highest identity to Tn4656 (green), Tn3-IIa and b with highest identity to Tn5053 (red) and Tn3-III with highest identity to Tn5563 (blue) . The inverted repeats (IRs) flanking each element are marked by small lowered triangles in the same colours, accordingly.

B. Alignment of the Tn3-mediated horizontal gene transfer of the styrene and phenylacetate degradation cluster in pTTS12 (bottom) and pSTY from *Pseudomonas taiwanensis* VLB120 (top). Colors represent the different genes constituting styrene-phenylacetate degradation cluster and the three Tn3 transposable elements, corresponding to the color-coding in panel A. Gene names are indicated.

The Tn4656 and Tn5563 are both duplicated and rearranged on the megaplasmid together with Tn5053. This rearrangement resulted in a highly characteristic sequence, which partially resulted from insertion of Tn5053 transposition in the second copy of Tn4656 (Tn4656-II), between the *mcpT*-2 and *tnpR* loci (Fig. 3.3). The IRs as well as DRs of Tn5053 indicate the insertion site of this element. The IRs of Tn4656-II are well preserved bracketing both elements. Other parts of this sequence consist of the second copy of Tn5563 (Tn5563-II), which is truncated at the right end by insertion of Tn4656-II in *merT* and thus truncated the 5' end of *merT* sequence, can be identified. Due to this truncation, the IRs of Tn4656-II cannot be found on the right side of the element anymore except for the right IR of initial Tn4656, which is located 58 kbps upstream of this element.

The unique rearrangement of the three different Tn3 elements in pTTS12 surprisingly is also present on pSTY of *P. taiwanesis* VLB120, including an additional copy of Tn5563. In between these two Tn5563-elements, both megaplasmids contain the complete styrene degradation pathway, enabling both strains to grow on styrene as sole carbon source (25, 30). Detailed comparison of the regions between the two Tn5563 elements from pTTS12 and

pSTY reveals a high similarity between Tn5563-I and Tn5563-II (Fig. 3.3B). This sequence is around 77 kbps and 60 kbps for pTTS12 and pSTY respectively, including the IRs bracketing both sequences.

In addition to Tn3-elements, a unique Tn7-like element (20 kbps) is also encoded on pTTS12 (Fig. 3.1). Interestingly, an identical transposable element is also encoded on the chromosome of *P. putida* S12. This element contains several transposase genes at both ends and a putative chromate resistance gene cluster (locus tag RPPX_28930-29030). The putative chromate resistance gene cluster was identified based on homology search using BLAST and alignments to other plasmids. RPPX_28995, RPPX_28990, and RPPX_29000 were identified to encode for a chromate resistance efflux pump ChrA, and two regulatory proteins ChrB and ChrF respectively similar to the chromate resistance gene cluster carried by pMOL28 of *Cupriavidus metallidurans* CH34 (33).

Conjugative megaplasmid pTTS12 is highly stable in *P. putida* KT2440

To characterize the conjugative transferability of pTTS12, we performed biparental mating between *P. putida* S12.1 and *P. putida* KT-BG35. *P. putida* KT-BG35 is a strain derived from *P. putida* KT2440, does not harbour a megaplasmid and carries a gentamicin resistant marker and green fluorescence protein (GFP) at its *attn*7 site (34). The transfer was performed using biparental mating between *P. putida* S12.1 containing pTTS12 with kanamycin resistant marker and *P. putida* KT-BG35. Transconjugant colonies resistant to both kanamycin and gentamicin occurred at the frequency of 4.20 (± 0.51) x 10^{-7}. After appropriate selection on agar plates, the identity of transconjugant colonies was confirmed by observing GFP expression of the colonies derived from *P. putida* KT-BG35. Additionally, transfer of entire pTTS12 was confirmed using PCR. Amplification of several regions of pTTS12 using primer pairs 53,496_Fw-56,596_Rv, 200,497_Fw-203,602_Rv, and 286,448_Fw-289,462_Rv resulted in an expected band of 3 kbp in transconjugant colonies. All 15 randomly selected colonies chosen for colony PCR showed correct bands. This confirmed the transfer of entire pTTS12 into *P. putida* KT-BG35 and the resulting strains will further be referred to as *P. putida* KTpS12. Several attempts to transfer pTTS12 into *E. coli* strains represented by *E. coli* MV1190 and *E. coli* XL1-Blue by biparental mating did not result in any successful transconjugant colonies.

The putative relaxase gene, *virD2*, was identified on pTTS12 (locus tag RPPX_28750). To confirm this finding, we created a complete deletion of *virD2* gene and compared the self-transfer frequency of pTTS12 Δ*virD2* and wild-type pTTS12 into *P. putida* KT2440. The transfer frequency of pTTS12 Δ*virD2* was 4.16 (± 0.08) x 10^{-7}, which was not significantly different (p-value 0.8867) compared to the transferability of the wild-type pTTS12 from *P. putida* S12 to *P. putida* KT2440.

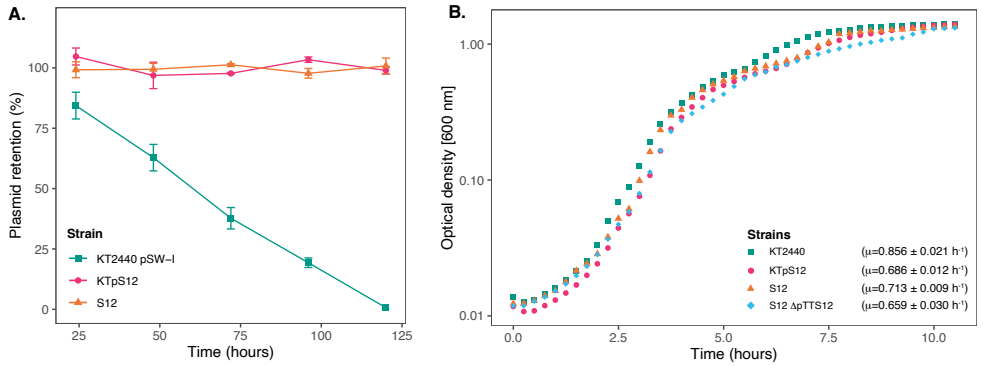

Fig. 3.4. Megaplasmid pTTS12 is highly stable in *P. putida* strains and reduces maximal growth rate in *P. putida* KT2440.

A. Plasmid retention of pTTS12 in *P. putida* KT2440 and *P. putida* S12 on liquid LB without selection pressure for approximately 50 generations. Colors and shapes indicate the different strains with green squares indicating *P. putida* KT2440 pSW-II, magenta circles indicating *P. putida* KTpS12, and orange triangles indicating *P. putida* S12 (containing pTTS12). Plasmid pSW-II in *P. putida* KT2440 was used as a control for loss of unstable plasmid. pTTS12 is stably maintained in both *P. putida* S12 and *P. putida* KTpS12.

B. Growth curve of *P. putida* KT2440, *P. putida* KTpTTS12 *P. putida* S12, and *P. putida* S12 ΔpTTS12. Growth was followed on liquid LB at 30 °C, 200 rpm shaking. Growth curves represent data obtained from three biological replicates for each strain, starting from OD_{600nm} = 0.05. Green squares indicate *P. putida* KT2440 pSW-II, magenta circles indicate *P. putida* KTpS12, orange triangles indicate *P. putida* S12 (containing pTTS12), and blue diamond indicate *P. putida* S12 ΔpTTS12. Maximum growth rates calculated for each strais are indicated within the figure.

The stability of pTTS12 in *P. putida* KTpS12 and *P. putida* S12 was examined for 5 passages in the absence of antibiotic selective pressure (approximately 10 generations/ passage step). No plasmid loss was observed from either *P. putida* KTpS12 or *P. putida* S12 growing without selective pressure while the negative control pSW-2 showed a steady plasmid loss (Fig. 3.4A). Serendipitous deletion of pTTS12 was not found in *P. putida* S12 and *P. putida* KTpS12 either. Hence, pTTS12 is a stable megaplasmid in both *P. putida* S12 and *P.*

putida KT2440.

The occurrence of large plasmids in bacteria is known to cause metabolic burden, which is reflected in reduced bacterial growth rate (μ). *P. putida* KTpS12 exhibited a lower maximum growth rate compared to *P. putida* KT2440, 0.686 ± 0.012 and 0.856 ± 0.021 h^{-1} respectively (Fig. 3.4B). However, *P. putida* S12 and *P. putida* S12 ΔpTTS12 did not show a significant maximum growth rate difference (0.713 ± 0.009 and 0.659 ± 0.030 h^{-1} respectively). The length of lag-phase and biomass yield at stationary phase remained unaffected with pTTS12 present in both *P. putida* S12 and KTpS12. Apparently, the presence pTTS12 imposes a only slight metabolic burden in *P. putida* KT2440, but not in S12.

Phenotypic features of pTTS12 and attained solvent tolerance in P. putida KT2440

P. putida S12 is intrinsically tolerant to an assortment of environmental xenobiotics. The majority of these characteristic traits are encoded on pTTS12; the styrene degradation operon *styABCDE*, the tellurite resistance operon *terZABCDE* and a solvent efflux pump *srpABC*. To explore functionality of pTTS12 following conjugative transfer, these characteristic traits were investigated in *P. putida* KTpS12 (Fig. 3.5). Activity of the styrene degradation operon in *P. putida* KTpS12 was tested by growing on minimal media with styrene as carbon source and inspecting transformation of indole into indigo. Similarly as observed in *P. putida* S12, *P. putida* KTpS12 was able to transform indole into indigo, whereas wild-type KT2440 was not, indicating activity of styrene monooxygenase (*styA*) and styrene oxide isomerase (*styB*) in these strains (Fig. 3.5A). In addition, *P. putida* KTpS12 was able to grow on minimal media supplemented with styrene as carbon source or minimal media agar plates incubated in styrene atmosphere (data not shown).

Potassium tellurite (K_2TeO_3) exhibits antimicrobial activity and tellurite resistance in bacteria is achieved through reduction of tellurite (TeO_3^{2-}) into a less toxic metallic tellurium (Te^0), hence the formation of black colonies in the presence of tellurite (35). The resistance genes on pTTS12 are encoded as an operon *terZABCDE* (RPPX_26360-26385). To investigate whether this gene cluster is able to increase resistance towards tellurite in *P. putida* KT2440, the minimum inhibitory concentration (MIC) was determined for the three different stains (Fig. 3.5B). The MIC of potassium tellurite for *P. putida* KT2440 was 16 fold less compared to *P. putida* S12, 12.5 mg $liter^{-1}$ and 200 mg $liter^{-1}$ respectively. Interestingly, *P. putida*

KTpS12 showed an 8 fold increase in tellurite resistance (MIC 100 mg liter^{-1}) compared to its parental strain *P. putida* KT2440.

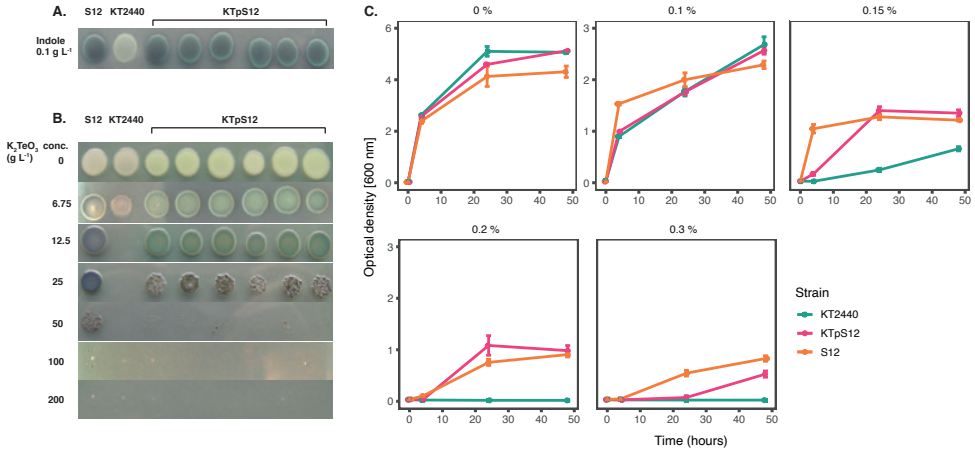

Fig. 3.5. Transfer of pTTS12 phenotypic characteristics.

A. Production of indigo from indole indicating activity of styrene monooxygenase (StyA) and styrene oxide isomerase (StyB) . Minimal medium (M9) was supplemented with indole which, in the presence of StyAB enzymes encoded on pTTS12, is converted into indigo. Positive control *P. putida* S12 showed indigo coloration, whereas negative control *P. putida* KT2440 remained white. *P. putida* KTpS12 showed indigo coloration indicating activity of pTTS12-encoded *styAB*.

B. Growth of *P. putida* strains in the presence of potassium tellurite (K_2TeO_3). Minimum inhibitory concentration (MIC) of positive control *P. putida* S12 was 200 g liter^{-1} whereas the MIC of the wild-type *P. putida* KT2440 was 12.5 g liter^{-1}. The MIC of *P. putida* KTpS12 was 100 g liter^{-1} indicating the presence and activity of the *ter* operon on pTTS12.

C. Growth of *P. putida* strains on increasing concentrations of toluene. Optical density (OD_{600nm}) of the cultures was measured at 4, 24, and 48-hour time points with starting point of OD_{600nm} = 0.1. The y-axis range is different between the first panel (0-6) and the other panels (0-3). Green squares indicate *P. putida* KT2440 pSW-II, magenta circles indicate *P. putida* KTpS12, and orange triangles indicate *P. putida* S12 (containing pTTS12). *P. putida* KTpS12 showed an increase in solvent tolerance indicating the presence and acivity of the *srp* operon from pTTS12.

The solvent efflux pump *srpABC* encoded on the megaplasmid pTTS12, enables survival and growth of *P. putida* S12 in non-utilized organic solvents (36). In order to investigate the effect of induced tolerance toward organic solvents due to the introduction of pTTS12 in *P. putida* KTpS12, a growth assay was performed in the presence of different toluene concentrations (Fig. 3.5C). *P. putida* KT2440 was able to grow in LB liquid media supplemented

with toluene up to a maximum of 0.15 % (vol/vol) concentration, although suffering from a significant growth reduction compared to *P. putida* S12. With the introduction of pTTS12, *P. putida* KTpS12 tolerance toward toluene increased to 0.30 % (vol/vol). Similar concentration was obtained for *P. putida* S12, while *P. putida* KTpS12 exhibited slightly slower growth in the presence of toluene. These observations indicated that the introduction of megaplasmid pTTS12 provided a full set of characteristic features to *P. putida* KT2440.

Discussion

Megaplasmid pTTS12 defines an environment-adaptive and type-specific family of IncP-2 plasmids, carrying distinct accessory gene clusters

Megaplasmid pTTS12 of *P. putida* S12 is closely related to other plasmids in proteobacteria, especially within the *Pseudomonas* genus. In this study we demonstrated high similarity of the pTTS12 'backbone' with pOZ176 from *P. aeruginosa* PA96 (2) and several other IncP-2 plasmids, such as pQBR103 of *Pseudomonas fluorescens* SBW25 (37). pOZ176 has been categorized within incompatibility group IncP-2 based on its replication, partitioning, and transfer machinery along with conferring tellurite resistance as a key feature of IncP-2 plasmid (2, 5). Indeed, pTTS12 encodes typical characteristics of IncP-2 plasmids, such as heavy metal resistance (tellurite, mercury, and chromate) and plasmid maintenance via the *parA*/*parB*/*repA* system (10, 38). pTTS12 clearly conferred tellurite resistance when transferred to tellurite-susceptible *P. putida* KT2440, confirming this IncP-2 characteristic phenotype. Interestingly, despite high similarity between pTTS12 and pOZ176, pTTS12 lacks the Tn6016 bla_{IMP-9}-carrying class 1 integron cassette which is an important trait of pOZ176 conferring resistance to aminoglycosides and carbapenems (2, 5). On the other hand, pOZ176 lacks the solvent efflux pump, styrene degradation pathway, and phenylpropionic acid degradation pathway which are main characteristics of pTTS12. This demonstrates that very similar megaplasmid backbones may carry resistance to a diversity of xenobiotics, metabolic functions, or virulence gene clusters (39). Whereas the traits disseminated by pTTS12 and pOZ176 respectively, are highly divergent and distinctive, a similar observation of environment-adaptive traits conferred by flexible and diverse accessory gene clusters contained on IncP-2 plasmids was recently reported for *P. aeruginosa* plasmids pBT2436 and pBT2101, carrying multiple MDR cassettes (1).

Convergent distribution of plasmid-encoded solvent tolerance gene clusters

pTTS12 shares its unique features of styrene and phenyl-propanoate degradation pathway with *P. taiwanensis* VLB120 and the solvent extrusion pump SrpABC with TtgGHI from *P. taiwanensis* VLB120 and *P. putida* DOT-T1E. These solvent tolerant strains were isolated independent of each other, although in different geographical locations; *P. putida* S12 and *P. taiwanensis* VLB120 were isolated for their ability to utilize styrene as sole carbon source (11, 40). *P. putida* DOT-T1E was isolated for its ability to degrade toluene (9). Hence, these plasmids isolated from different environmental sources show convergent distribution of highly similar gene clusters with similar features related to environmental stresses (e.g. organic solvents) on different plasmid backbones. In *P. taiwanensis* VLB120, the arrangement of gene clusters encoding the styrene degradation pathway and solvent efflux pump - phenylpropionic acid degradation pathway is highly similar to pTTS12, with 99% and 80% similarity, respectively. This moreover, indicates that exchange of the styrene degradation pathway occurred more recently than exchange of the efflux pump/phenylpropionic acid degradation cluster. Alternatively, these clusters may have been acquired independently.

The styrene degradation gene cluster is encoded within a unique arrangement of Tn3 family transposases shared by pTTS12 and pSTY from *P. taiwanensis* VLB120 (Fig. 3.3). Due to the transposition of Tn3-Ib, Tn3-IIa lost its right flank inverted repeat (IR). Because of this arrangement, Tn3-IIa can only “jump” while carrying the entire Tn3 and styrene-phenylacetate degradation clusters using the right flank of Tn3-IIb IR. This may explain the occurrence of the styrene-phenylacetate degradation cluster distinctive arrangement shared between pTTS12 and pSTY. Although we could not find evidence of mobile genetic elements carrying the efflux pump and the phenylpropionic acid degradation gene clusters on pSTY and pTTS12, it is well possible that the exchange originally occurred via such route.

Transferability of pTTS12

pTTS12 contains a P-Type type IV secretion system (T4SS) with synteny similar to the prototype *trb* operon of the *A. tumefaciens* pTiC58 system (32, 41). Indeed, our experiments showed that pTTS12 is transferable towards other *P. putida* strains with a frequency of 4.20 (± 0.51) x 10^{-7}. A putative relaxase, responsible for creating a nick prior to plasmid transfer via the conjugative bridge, was predicted to be encoded by *virD2* (locus tag RPPX_28750). However, complete deletion of *virD2* did not resulted in a significant reduction of transfer frequency,

compared to the wild-type pTTS12. This may indicate the presence of other relaxase(s) which act in-trans with the P-type T4SS to mediate the nicking of plasmid DNA and subsequently aided the plasmid transfer process. *P. putida* S12 contains other T4SS within its genome which share synteny with the I-type T4SS represented by Dot/Icm from *L. pneumophila* (Fig. 3.S3), although it is unclear whether Dot/Icm can support the transfer of pTTS12 (42).

Amelioration of pTTS12 reduces fitness cost and promotes plasmid persistence in *P. putida* S12

We observed that in its original host *P. putida* S12 on rich media, pTTS12 did not impose an apparent metabolic burden whereas in another strain as *P. putida* KT2440, pTTS12 caused a 20% reduction of maximum growth rate. We previously reported on the occurrence of metabolic burden caused by pTTS12 in *P. putida* S12 in the presence of toluene (43). In addition to the relatively low metabolic burden, pTTS12 was very stable in both *P. putida* S12 and *P. putida* KT2440 (Fig. 3.4A). Several mechanisms may be involved in the reduced fitness cost and the stability of pTTS12 in *P. putida* S12.

Conjugative transfer may impose substantial cost and burden due to the energy investment on pili formation during conjugation (39, 44). Indeed, pTTS12 showed a substantially lower conjugation rate (4.20 x 10^{-7} transfer frequency) after 24 hours in comparison to other IncP-2 plasmids (10^{-1} to 10^{-4} transfer frequency after 2 hours) (38). Downregulation of plasmid genes appeared to be involved in the amelioration of pTTS12. The expression of plasmid-encoded resistance genes, like the solvent extrusion pump, can typically be a source of metabolic burden imposed by plasmids (45). pTTS12 contains multiple types of mobile genetic elements, with ISS12 being the most abundant (4, 27). Substantial duplication of the ISS12 mobile element has previously been reported to interrupt *srpA*, encoding the periplasmic subunit of the solvent efflux pump (4). In the prolonged absence of organic solvent, expression and maintenance of the solvent efflux pump may be costly for the bacterial cell, hence, interruption of the *srp* efflux pump gene cluster may further reduce the plasmid burden of pTTS12. In addition to these mechanisms, we recently described the contribution of a toxin-antitoxin module SlvT-SlvA to the stability of pTTS12 (43).

Future outlook

IncP-2 family plasmids are widely distributed among environmental and clinical *Pseudomonas* isolates. These plasmids contain variable regions encoding MDR, xenobiotics extrusion

pumps, degradation pathways, and heavy metal resistance cassettes. In contrast to the dynamic variable regions, the core backbone of these plasmids shows a general conservation. It is interesting to discover the minimal backbone of IncP-2, which enables Pseudomonads to scavenge gene clusters important for its survival both in environmental and clinical set-up, as a model of horizontal gene transfer. Ultimately, IncP-2 plasmid backbone may be promising for biotechnological and bioremediation applications due to its stability and relatively low metabolic burden. Moreover, these plasmids have been described to exchange their traits, thus creating hybrid plasmids when they occur within the same host (38). The mechanisms for such exchange are poorly understood and may well involve transposition and conjugation as suggested by the shared and type-specific characteristics of pTTS12 and pOZ176 as described in this study. Further clarification of these mechanisms is important to shed light on the rapid dissemination of bacterial tolerance and resistance to antibiotics and chemical stresses in the environment.

Successful attempts have been made in exploiting traits from environmental plasmids for standardized components in synthetic biology (46). Environmental plasmids are exchangeable between different hosts and may express their genetic features in various genomic and metabolic backgrounds. Moreover, they are an excellent source of novel biological parts such as origin of replication, metabolic pathway, resistance marker, and regulated promoters. New sequencing technologies and comparative genomics analyses support the identification of the genes enabling these features. Here, we demonstrated that pTTS12 contains promising exchangeable gene clusters and building blocks to construct robust microbial hosts for high-value biotechnology applications.

Materials and methods

Cultivation of *P. putida*

Table 3.2. Bacterial strains and plasmids used in this study

Strain/plasmid	Relevant characteristics	Ref.
E. coli DH5α	*sup* E44, Δ*lacU*169 (Φ*lacZ*ΔM15), *recA*1, *endA*1, *hsdR*17, *thi*-1, *gyrA*96, *relA*1	(52)
E. coli DH5α λpir	*sup* E44, Δ*lacU*169 (Φ*lacZ*ΔM15), *recA*1, *endA*1, *hsdR*17, *thi*-1, *gyrA*96, *relA*1, λpir phage lysogen	(53)
E. coli HB101	*recA pro leu hsdR* Sm^R	(54)

Strain/plasmid	Relevant characteristics	Ref.
E. coli XL-1 Blue	endA1 gyrA96(nalR) thi-1 recA1 relA1 lac glnV44 F'[::Tn10 proAB+ lacIq Δ(lacZ)M15] hsdR17(rK- mK+) Tc^R	Stratagene
E. coli MV1190	delta(lacproAB) thi supE44 delta(sr1recA)306::Tn10 [F':traD36 proAB lacIq delta(lacZ)M15] Tc^R	ATCC
P. putida KT2440	Derived from wild-type *P. putida* mt-2, ΔpWW0	(55)
P. putida S12	Wild-type *P. putida* S12 (ATCC 700801), harboring megaplasmid pTTS12	(11)
P. putida S12.1	*P. putida* S12; Km^R on pTTS12	This paper
P. putida KT-BG35	*P. putida* KT2440; Gm^R, *msfgfp*::Tn7	This paper
P. putida KTpS12	*P. putida* KT2440, Gm^R, *msfgfp*::Tn7, pTTS12, Km^R	This paper
pRK2013	RK2-Tra^+, RK2-Mob^+, Km^R, *ori* ColE1	(56)
pTTS12	A 583 kbp megaplasmid of *P. putida* S12	(25)
pTnS-1	Ap^R, *ori* R6K, TnSABCD operon	(57)
pBG35	Km^R, Gm^R, *ori* R6K, pBG-derived	(34)
pEMG	Km^R, Ap^R, *ori* R6K, *lacZ*α MCS flanked by two I-SceI sites	(48)

Strains and plasmids used in this report were listed in Table 3.2. All *P. putida* strains were grown in Lysogeny Broth (LB) containing 10 g $liter^{-1}$ tryptone, 5 g $liter^{-1}$ yeast extract and 5 g $liter^{-1}$ sodium chloride at 30 °C with 200 rpm shaking. *E. coli* strains were cultivated in LB at 37 °C with 250 rpm shaking in a horizontal shaker (Innova 4330, New Brunswick Scientific). For solid cultivation, 1.5 % (wt/vol) agar was added to LB. M9 minimal medium used in this report was supplemented with 2 mg $liter^{-1}$ $MgSO_4$ and 0.2% (wt/vol) of citrate as sole carbon source (11). Bacterial growth was observed by optical density measurement at 600 nm (OD_{600nm}) using a spectrophotometer (Ultrospec 2100 pro, Amersham Biosciences). Maximum growth rate and other parameters were calculated using growthcurver R-package ver.0.3.0 (47). Solvent tolerance analysis was performed by growing *P. putida* strains in LB starting from OD_{600nm} = 0.1 in Boston bottles with Mininert bottle caps. When required, potassium tellurite (6.75 - 200 mg $liter^{-1}$), indole (100 mg $liter^{-1}$), gentamicin (25 mg $liter^{-1}$), ampicillin (100 mg $liter^{-1}$), tetracycline (25 mg $liter^{-1}$), and kanamycin (50 mg $liter^{-1}$) were added to the media.

DNA methods

All PCR reaction were performed using Phire polymerase (Thermo Fischer) according to the manufacturer's manual. All primers are listed in Table 3.3 and were obtained from Sigma-Aldrich. PCR reactions were visualized and analyzed by gel electrophoresis on 1 % (wt/vol) TBE agarose gels containing 5 mg $liter^{-1}$ ethidium bromide in an electric field (110V, 0.5x TBE running buffer).

Table 3.3. Primers used in this study

Primer	Sequence	Target
glmS_Fw	AGTCAGAGTTACGGAATTGTAGG	*P. putida* KT2440 (Tn7 site)
glmS_Rv	GTCGAGAAAATTGCCGAGCT	*P. putida* KT2440 (Tn7 site)
53,496_Fw	ACTTCGACCAATGCCCCATT	*P. putida* S12 pTTS12
56,596_Rv	GGACACCCTCATCCTTAGCG	*P. putida* S12 pTTS12
200,497_Fw	GTGTATCGAAGGGCCTCCAC	*P. putida* S12 pTTS12
203,602_Rv	TCGACGATGCAGACAGATCG	*P. putida* S12 pTTS12
286,448_Fw	AACACCGAAGATGGGGCTTT	*P. putida* S12 pTTS12
289,462_Rv	GCAGGTCGACAAGCAAGTTG	*P. putida* S12 pTTS12
4,963,661_Fw	ATCACCCAGCTGAGCCATTC	*P. putida* S12 chromosome
4,966,726_Rv	CTGCCGGATAACAAAGCAGC	*P. putida* S12 chromosome
90285_Fw	TTT**TCTAGA**TGCTGAGCAGTT CCTTCAGG	Construction of pEMG-TS for Km^R marker in pTTS12, with XbaI restriction site
90825_Rv	TTT**CCCGGG**AGGAAGGGAAG CAAACTCCG	Construction of pEMG-TS for Km^R marker in pTTS12, with XmaI restriction site
TS1_28750_Fw	AATCT**GAATTC**GGACGTATTG GGCTTCAATG	Construction of pEMG-Δ28750 for deleting the putative relaxase, with EcoRI restriction site
TS1_28750_Rv	GAAAGCCTGTCTGCACATGG CTATCGACTCATCATTCACCG	Construction of pEMG-Δ28750 for deleting the putative relaxase
TS2_28750_Fw	CGGTGAATGATGAGTCGATCA TGTGCAGACAGGCTTTC	Construction of pEMG-Δ28750 for deleting the putative relaxase
TS2_28750_Rv	AACCC**GGATCC**GTTCGACA GCCGCTATTTC	Construction of pEMG-Δ28750 for deleting the putative relaxase, with BamHI restriction site
test_28750_Fw	CCTGATGCACGATTTACCG	Confirming the deletion of the putative relaxase (ΔRPPX_28750)
test_28750_Fw	CTACCTGCCGGTACACATT	Confirming the deletion of the putative relaxase (ΔRPPX_28750)

Megaplasmid pTTS12 transfer into *P. putida* KT2440 and *E. coli* strains

Gentamicin resistance and GFP containing cassette were incorporated into *P. putida* KT2440 chromosome at the Tn7 site using pBG35 plasmid resulting in the strain *P. putida* KT-BG35 as previously described (34). Correct transformants were additionally verified by observing the gentamicin resistance, GFP expression and colony PCR of *P. putida* KT2440 chromosome sequence. Kanamycin resistance gene was introduced into the megaplasmid pTTS12 by integrating plasmid pEMG using homologous recombination resulting in *P. putida* S12.1 as previously described (48). A single homologous recombination site was obtained by PCR with 90285_Fw and 90825_Rv primer pair and this fragment was used to construct pEMG-TS plasmid. Correct integration into *P. putida* S12 was verified by observing kanamycin resistance

and colony PCR using primers 4,963,661_Fw-4,966,726_Rv.

The transfer of pTTS12 into *P. putida* KT-BG35, *E. coli* XL1-Blue or *E. coli* MV1190 were performed by biparental mating between *P. putida* S12.1 and the recipient strain on LB agar for 24 hours at 30 °C. The correct transformants were selected using LB agar supplemented with gentamicin and kanamycin for *P. putida* KT-BG35 or with tetracycline and kanamycin for *E. coli* strains. Additionally, transformants were verified using colony PCR (53,496_Fw-56,596_Rv, 200,497_Fw-203,602_Rv, and 286,448_Fw-289,462_Rv). Plasmid transfer rate was determined by comparing the event of successful plasmid transconjugant with the colony formation unit (cfu) of the recipient strain (*P. putida* KT-BG35, *E. coli* XL1-Blue or *E. coli* MV1190) after biparental mating (Gm^R/Tc^R). Plasmid stability was determined by calculating the event of megaplasmid loss in *P. putida* KTpS12 grown in liquid media without supplementation of kanamycin as the selective pressure for pTTS12. Plasmid pSW-2 was used as a control for megaplasmid loss events (48).

Sequence analyses

All plasmid sequences were downloaded from NCBI database, 22389 plasmid sequences from Refseq database (retrieved 8 March 2020) and complemented with few plasmid sequences from NUCORE that were omitted from Refseq. The CGviewer (31) was used to generate circular plots of entire pTTS12 with standard settings and MultiGeneBlast tool (49) was used to generate synteny plots of specific regions and operons. Further analysis was performed using Geneious software (BioMatters), and selected sequences were aligned using MAFFT (50) for DNA sequences or MUSCLE (51) for protein sequences.

References

1. Cazares A, Moore MP, Hall JPJ, Wright LL, Grimes M, Emond-Rhéault JG, Pongchaikul P, Santanirand P, Levesque RC, Fothergill JL, Winstanley C. 2020. A megaplasmid family driving dissemination of multidrug resistance in *Pseudomonas*. Nat Commun 11:1370.
2. Xiong J, Alexander DC, Ma JH, Déraspe M, Low DE, Jamieson FB, Roy PH. 2013. Complete Sequence of pOZ176, a 500-Kilobase IncP-2 Plasmid Encoding IMP-9-Mediated Carbapenem Resistance, from Outbreak Isolate *Pseudomonas aeruginosa* 96. Antimicrob Agents Chemother 57:3775–3782.
3. Molina L, Duque E, Gómez MJ, Krell T, Lacal J, García Puente A, García V, Matilla MA, Ramos J-L, Segura A. 2011. The pGRT1 plasmid of *Pseudomonas putida* DOT-T1E encodes functions relevant for survival under harsh conditions in the environment. Environ Microbiol 13:2315–2327.
4. Hosseini R, Kuepper J, Koebbing S, Blank LM, Wierckx N, de Winde JH. 2017. Regulation of solvent tolerance in *Pseudomonas putida* S12 mediated by mobile elements. Microb Biotechnol 10:1558–1568.
5. Xiong J, Hynes MF, Ye H, Chen H, Yang Y, M'Zali F, Hawkey PM. 2006. bla_{IMP-9} and its association with large plasmids carried by *Pseudomonas aeruginosa* isolates from the People's Republic of China. Antimicrob Agents Chemother.
6. Nojiri H, Shintani M, Omori T. 2004. Divergence of mobile genetic elements involved in the distribution of xenobiotic-catabolic capacity. Appl Microbiol Biotechnol 64:154–174.
7. Kholodii GY, Yurieva O V., Lomovskaya OL, Gorlenko ZM, Mindlin SZ, Nikiforov VG. 1993. Tn5053, a mercury resistance transposon with integron's ends. J Mol Biol 230:1103–1107.
8. Partridge SR, Kwong SM, Firth N, Jensen SO. 2018. Mobile genetic elements associated with antimicrobial resistance. Clin Microbiol Rev 31:e00088-17.
9. Ramos JL, Duque E, Huertas MJ, Haïdour A. 1995. Isolation and expansion of the catabolic potential of a *Pseudomonas putida* strain able to grow in the presence of high concentrations of aromatic hydrocarbons. J Bacteriol 177:3911–3916.
10. Shintani M, Sanchez ZK, Kimbara K. 2015. Genomics of microbial plasmids: classification and identification based on replication and transfer systems and host taxono-

my. Front Microbiol 6:242.

11. Hartmans S, van der Werf MJ, de Bont JA. 1990. Bacterial degradation of styrene involving a novel flavin adenine dinucleotide-dependent styrene monooxygenase. Appl Environ Microbiol 56:1347–1351.
12. Kieboom J, Dennis JJ, de Bont JAM, Zylstra GJ. 1998. Identification and Molecular Characterization of an Efflux Pump Involved in *Pseudomonas putida* S12 Solvent Tolerance. J Biol Chem 273:85–91.
13. Kusumawardhani H, Hosseini R, de Winde JH. 2018. Solvent Tolerance in Bacteria: Fulfilling the Promise of the Biotech Era? Trends Biotechnol 36:1025–1039.
14. Mukhopadhyay A. 2015. Tolerance engineering in bacteria for the production of advanced biofuels and chemicals. Trends Microbiol 23:498–508.
15. Janardhan Garikipati SVB, Peeples TL. 2015. Solvent resistance pumps of *Pseudomonas putida* S12: Applications in 1-naphthol production and biocatalyst engineering. J Biotechnol 210:91–99.
16. Koopman F, Wierckx N, de Winde JH, Ruijssenaars HJ. 2010. Efficient whole-cell biotransformation of 5-(hydroxymethyl)furfural into FDCA, 2,5-furandicarboxylic acid. Bioresour Technol 101:6291–6296.
17. Verhoef S, Wierckx N, Westerhof RGM, de Winde JH, Ruijssenaars HJ. 2009. Bioproduction of p-hydroxystyrene from glucose by the solvent-tolerant bacterium *Pseudomonas putida* S12 in a two-phase water-decanol fermentation. Appl Environ Microbiol 75:931–936.
18. Verhoef S, Ruijssenaars HJ, de Bont JAM, Wery J. 2007. Bioproduction of p-hydroxybenzoate from renewable feedstock by solvent-tolerant *Pseudomonas putida* S12. J Biotechnol 132:49–56.
19. Wierckx NJP, Ballerstedt H, de Bont JAM, Wery J. 2005. Engineering of solvent-tolerant Pseudomonas putida S12 for bioproduction of phenol from glucose. Appl Environ Microbiol 71:8221–8227.
20. Kieboom J, Dennis JJ, Zylstra GJ, de Bont JA. 1998. Active efflux of organic solvents by *Pseudomonas putida* S12 is induced by solvents. J Bacteriol 180:6769–6772.
21. Volkers RJM, Snoek LB, Ruijssenaars HJ, de Winde JH. 2015. Dynamic Response of *Pseudomonas putida* S12 to Sudden Addition of Toluene and the Potential Role of the Solvent Tolerance Gene trgI. PLoS One 10:e0132416.

22. Rühl J, Hein E-M, Hayen H, Schmid A, Blank LM. 2012. The glycerophospholipid inventory of Pseudomonas putida is conserved between strains and enables growth condition-related alterations. Microb Biotechnol 5:45–58.

23. Wijte D, van Baar BLM, Heck AJR, Altelaar AFM. 2011. Probing the proteome response to toluene exposure in the solvent tolerant *Pseudomonas putida* S12. J Proteome Res 10:394–403.

24. Volkers RJM, de Jong AL, Hulst AG, van Baar BLM, de Bont JAM, Wery J. 2006. Chemostat-based proteomic analysis of toluene-affected *Pseudomonas putida* S12. Environ Microbiol 8:1674–1679.

25. Kuepper J, Ruijssenaars HJ, Blank LM, de Winde JH, Wierckx N. 2015. Complete genome sequence of solvent-tolerant *Pseudomonas putida* S12 including megaplasmid pTTS12. J Biotechnol 200:17–18.

26. Volkers RJM, Ballerstedt H, de Winde JH, Ruijssenaars HJ. 2010. Isolation and genetic characterization of an improved benzene-tolerant mutant of *Pseudomonas putida* S12. Environ Microbiol Rep 2:456–460.

27. Wery J, Hidayat B, Kieboom J, de Bont JA. 2001. An insertion sequence prepares *Pseudomonas putida* S12 for severe solvent stress. J Biol Chem 276:5700–5706.

28. Sun X, Dennis JJ. 2009. A Novel Insertion Sequence Derepresses Efflux Pump Expression and Preadapts *Pseudomonas putida* S12 for Extreme Solvent Stress. J Bacteriol 191:6773–6777.

29. Rodríguez-Herva JJ, García V, Hurtado A, Segura A, Ramos JL. 2007. The ttgGHI solvent efflux pump operon of *Pseudomonas putida* DOT-T1E is located on a large self-transmissible plasmid. Environ Microbiol 9:1550–1561.

30. Köhler KAK, Rückert C, Schatschneider S, Vorhölter FJ, Szczepanowski R, Blank LM, Niehaus K, Goesmann A, Pühler A, Kalinowski J, Schmid A. 2013. Complete genome sequence of *Pseudomonas sp.* strain VLB120 a solvent tolerant, styrene degrading bacterium, isolated from forest soil. J Biotechnol 168:729–730.

31. Stothard P, Wishart DS. 2005. Circular genome visualization and exploration using CGView. Bioinformatics 21:537–539.

32. Christie PJ, Whitaker N, González-Rivera C. 2014. Mechanism and structure of the bacterial type IV secretion systems. Biochim Biophys Acta - Mol Cell Res 1843:1578–1591.

33. Monchy S, Benotmane MA, Janssen P, Vallaeys T, Taghavi S, Van Der Lelie D, Mergeay M. 2007. Plasmids pMOL28 and pMOL30 of *Cupriavidus metallidurans* are specialized in the maximal viable response to heavy metals. J Bacteriol 189:7417–7425.
34. Zobel S, Benedetti I, Eisenbach L, de Lorenzo V, Wierckx N, Blank LM. 2015. Tn7-Based Device for Calibrated Heterologous Gene Expression in *Pseudomonas putida*. ACS Synth Biol 4:1341–1351.
35. Taylor DE. 1999. Bacterial tellurite resistance. Trends Microbiol 7:111–115.
36. Kieboom J, de Bont JAM. 2001. Identification and molecular characterization of an efflux system involved in *Pseudomonas putida* S12 multidrug resistance. Microbiology 147:43–51.
37. Hall JPJ, Harrison E, Lilley AK, Paterson S, Spiers AJ, Brockhurst MA. 2015. Environmentally co-occurring mercury resistance plasmids are genetically and phenotypically diverse and confer variable context-dependent fitness effects. Environ Microbiol 17:5008–5022.
38. Jacoby GA, Sutton L, Knobel L, Mammen P. 1983. Properties of IncP-2 plasmids of *Pseudomonas spp.* Antimicrob Agents Chemother 24:168–175.
39. Harrison E, Brockhurst MA. 2012. Plasmid-mediated horizontal gene transfer is a coevolutionary process. Trends Microbiol 20:262–267.
40. Panke S, Witholt B, Schmid A, Wubbolts MG. 1998. Towards a biocatalyst for (S)-styrene oxide production: characterization of the styrene degradation pathway of *Pseudomonas sp.* strain VLB120. Appl Environ Microbiol 64:2032–2043.
41. Li PL, Hwang I, Miyagi H, True H, Farrand SK. 1999. Essential components of the Ti plasmid trb system, a type IV macromolecular transporter. J Bacteriol 181:5033–5041.
42. Nagai H, Kubori T. 2011. Type IVB secretion systems of Legionella and other gram-negative bacteria. Front Microbiol 2:136.
43. Kusumawardhani H, van Dijk D, Hosseini R, de Winde JH. 2020. A novel toxin-antitoxin module SlvT–SlvA regulates megaplasmid stability and incites solvent tolerance in *Pseudomonas putida* S12. Appl Environ Microbiol 86:e00686-20.
44. Turner PE, Cooper VS, Lenski RE. 1998. Tradeoff Between Horizontal and Vertical Modes of Transmission in Bacterial Plasmids. Evolution (N Y) 52:315–329.
45. R. Craig MacLean, Milan AS. 2015. Microbial Evolution: Towards Resolving the Plas-

mid Paradox. Curr Biol 25:R764–R767.

46. Martínez-García E, Benedetti I, Hueso A, de Lorenzo V. 2015. Mining Environmental Plasmids for Synthetic Biology Parts and Devices. Microbiol Spectr 3:PLAS-0033-2014.

47. Sprouffske K, Wagner A. 2016. Growthcurver: An R package for obtaining interpretable metrics from microbial growth curves. BMC Bioinformatics 17:172.

48. Martínez-García E, de Lorenzo V. 2011. Engineering multiple genomic deletions in Gram-negative bacteria: analysis of the multi-resistant antibiotic profile of *Pseudomonas putida* KT2440. Environ Microbiol 13:2702–2716.

49. Medema MH, Takano E, Breitling R. 2013. Detecting sequence homology at the gene cluster level with multigeneblast. Mol Biol Evol 30:1218–1223.

50. Katoh K, Standley DM. 2013. MAFFT multiple sequence alignment software version 7: Improvements in performance and usability. Mol Biol Evol 30:772–780.

51. Edgar RC. 2004. MUSCLE: A multiple sequence alignment method with reduced time and space complexity. BMC Bioinformatics 5:113.

52. Bethesda Research Laboratories. 1986. *E. coli* DH5 alpha competent cells. Focus - Bethesda Res Lab 8:9.

53. Herrero M, De Lorenzo V, Timmis KN. 1990. Transposon vectors containing non-antibiotic resistance selection markers for cloning and stable chromosomal insertion of foreign genes in gram-negative bacteria. J Bacteriol 172:6557–6567.

54. Boyer HW, Roulland-dussoix D. 1969. A complementation analysis of the restriction and modification of DNA in *Escherichia coli*. J Mol Biol 41:459–472.

55. Bagdasarian M, Lurz R, Rückert B, Franklin FCH, Bagdasarian MM, Frey J, Timmis KN. 1981. Specific-purpose plasmid cloning vectors II. Broad host range, high copy number, RSF 1010-derived vectors, and a host-vector system for gene cloning in *Pseudomonas*. Gene 16:237–247.

56. Figurski DH, Helinski DR. 1979. Replication of an origin-containing derivative of plasmid RK2 dependent on a plasmid function provided in trans. Proc Natl Acad Sci 76:1648–1652.

57. Choi K-H, Gaynor JB, White KG, Lopez C, Bosio CM, Karkhoff-Schweizer RR, Schweizer HP. 2005. A Tn7-based broad-range bacterial cloning and expression system. Nat Methods 2:443–448.

Supplementary Materials

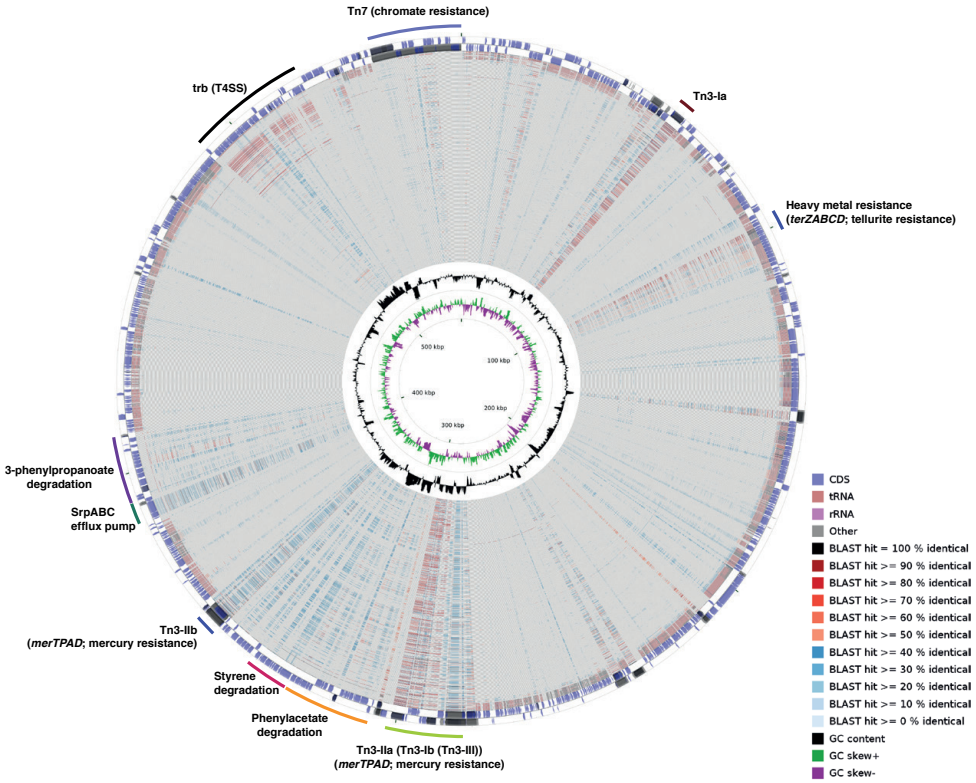

Fig. 3.S1-A. CDS alignment of the top 500 plasmids with highest similarity score to pTTS12.

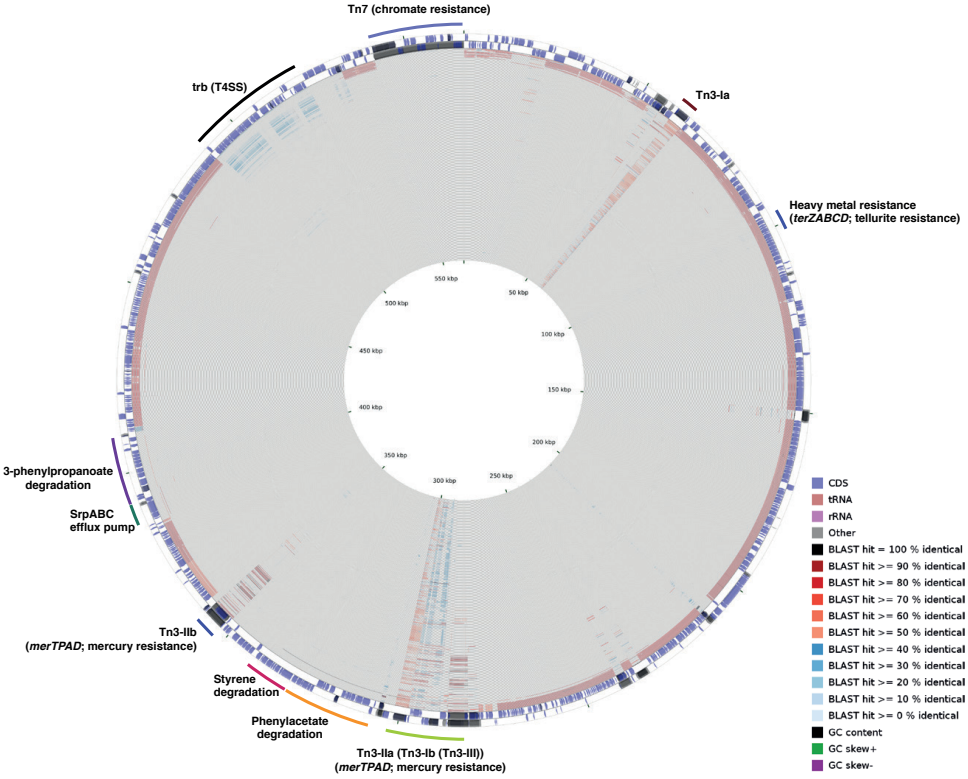

Fig. 3.S1-B. DNA alignment of the top 500 plasmids with highest similarity score to pTTS12.

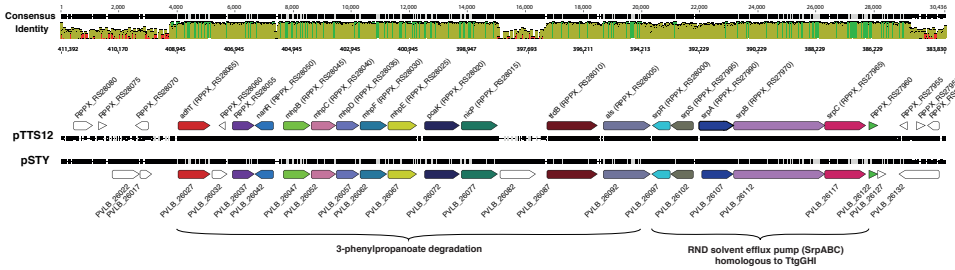

Fig. 3.S2. Comparison of the regions encoding 3-phenylpropionate degradation and solvent efflux pump between pTTS12 from Pseudomonas putida S12 and pSTY from Pseudomonas taiwanensis VLB120 reveals identical syntheny and high similarity.

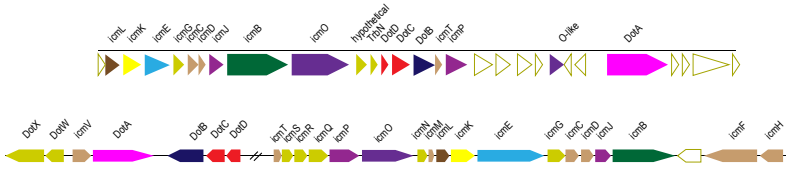

Protein	*C. burnetii* Ident./Sim.a	P. putida S12 Identity/similarity	P. putida S12 locustag	L. pneumophila Locustag	Length aminoacid	Length aminoacid 2	pTTS12 Identity (%)	pTTS12 similarity (%)
IcmT	47.1/63.2	15/33	RPPX_RS13055	lpl0483	73	87	15	33
IcmS	52.6/67.5	/	–	lpl0484	–			
IcmR	–	/	–	lpl0485	–			
IcmQb	22.6/34.0	/	–	lpl0486	–			
IcmP/DotM	36.5/50.3	18/38	RPPX_RS13060	lpl0487	377	437	18	38
IcmO/DotL	59.6/70.9	28/42	RPPX_RS13025	lpl0488	784	984	28	42
IcmN/DotK	24.8/32.7	/	–	lpl0489	–			
IcmM/DotJc	–	/	–	lpl0490	–			
IcmL/DotIc	35.8/48.5	18/41	RPPX_RS12985	lpl0491	213	255	18	41
IcmK/DotH	48.2/58.6	26/40	RPPX_RS12990	lpl0492	361	338	26	40
IcmE/DotGd	44.2/51.4	13/21	RPPX_RS12995	lpl0493	476	1049	13	21
IcmG/DotF	27.1/42.4	16/29	RPPX_RS13000	lpl0494	270	208	16	29
IcmC/DotEe	27.7/47.1	22/38	RPPX_RS13005	lpl0495	195	195	22	38
IcmD/DotPe	20.8/34.0	17/30	RPPX_RS13010	lpl0496	133	127	17	30
IcmJ/DotN	51.2/61.9	22/42	RPPX_RS13015	lpl0497	209	249	22	42
IcmB/DotO	62.2/73.7	34/54	RPPX_RS13020	lpl0498	1010	1021	34	54
IcmFf	23.1/34.4	/	–	lpl0500	–			
IcmH	27.7/37.6	/	–	lpl0501	–			
DotD	39.2/48.5	13/33	RPPX_RS13050	lpl2601	164	162	13	33
DotC	40.1/51.1	27/47	RPPX_RS13045	lpl2602	304	295	27	47
DotB	63.4/74.8	34/53	RPPX_RS13040	lpl2603	378	400	34	53
DotA	25.0/34.4	17/30	RPPX_RS13100	lpl2613	1048	995	17	30
IcmV	27.1/44.5	/	–	lpl2614	–			
IcmW	58.6/68.4	/	–	lpl2615	–			
IcmX	21.9/30.2	/	–	lpl2616	–			

Fig. 3.S3. Type 4 secretion system encoded on P. putida S12 chromosome belongs to I-type, similar to prototype L. pneumophila Dot/Icm system and R64.

CHAPTER 4

A novel toxin-antitoxin module SlvT–SlvA regulates megaplasmid stability and incites solvent tolerance in *Pseudomonas putida* S12

Hadiastri Kusumawardhani, David van Dijk, Rohola Hosseini, Johannes H. de Winde

Published in: Applied and Environmental Microbiology (2020), 86 (13), e00686-20.
DOI: 10.1128/AEM.00686-20

Abstract

Pseudomonas putida S12 is highly tolerant of organic solvents in saturating concentrations, rendering this microorganism suitable for the industrial production of various aromatic compounds. Previous studies revealed that *P. putida* S12 contains a single-copy 583 kbp megaplasmid pTTS12. pTTS12 carries several important operons and gene clusters facilitating *P. putida* S12 survival and growth in the presence of toxic compounds or other environmental stresses. We wished to revisit and further scrutinize the role of pTTS12 in conferring solvent tolerance. To this end, we cured the megaplasmid from *P. putida* S12 and conclusively confirmed that the SrpABC efflux pump is the major determinant of solvent tolerance on the megaplasmid pTTS12. In addition, we identified a novel toxin-antitoxin module (proposed gene names *slvT* and *slvA,* respectively) encoded on pTTS12 which contributes to the solvent tolerance phenotype and is important for conferring stability to the megaplasmid. Chromosomal introduction of the *srp* operon in combination with the *slv*AT gene pair created a solvent tolerance phenotype in non-solvent-tolerant strains such as *P. putida* KT2440, *Escherichia coli* TG1, and *E. coli* BL21(DE3).

Importance

Sustainable alternatives for high-value chemicals can be achieved by using renewable feedstocks in bacterial biocatalysis. However, during bioproduction of such chemicals and biopolymers, aromatic compounds that function as products, substrates or intermediates in the production process may exert toxicity to microbial host cells and limit the production yield. Therefore, solvent tolerance is a highly preferable trait for microbial hosts in the biobased production of aromatic chemicals and biopolymers. In this study, we revisit the essential role of megaplasmid pTTS12 from solvent-tolerant *Pseudomonas putida* S12 for molecular adaptation to an organic solvent. In addition to the solvent extrusion pump (SrpABC), we identified a novel toxin-antitoxin module (SlvAT) which contributes to short-term tolerance in moderate solvent concentrations, as well as to the stability of pTTS12. These two gene clusters were successfully expressed in non-solvent-tolerant strains of *P. putida* and *Escherichia coli* strains to confer and enhance solvent tolerance.

Introduction

One of the main challenges in the production of aromatic compounds is chemical stress caused by the added substrates, pathway intermediates, or products. These chemicals, often exhibiting characteristics of organic solvents, are toxic to microbial hosts and may negatively impact product yields. They adhere to the cell membranes, alter membrane permeability, and cause membrane damage (1, 2). *Pseudomonas putida* S12 exhibits exceptional solvent tolerance characteristics, enabling this strain to withstand toxic organic solvents in saturating concentrations (3, 4). Consequently, a growing list of valuable compounds has successfully been produced using *P. putida* S12 as a biocatalyst by exploiting its solvent tolerance (5–9).

Following the completion of its full genome sequence and subsequent transcriptome and proteome analyses, several genes have been identified that may play important roles in controlling and maintaining solvent tolerance of *P. putida* S12 (10–12). As previously reported, an important solvent tolerance trait of *P. putida* S12 is conferred through the resistance-nodulation-division (RND)-family efflux pump SrpABC, which actively removes organic solvent molecules from the cells (13, 14). Initial attempts to heterologously express the SrpABC efflux pump in *Escherichia coli* enabled the instigation of solvent tolerance and production of 1-naphtol (15, 16). Importantly, the SrpABC efflux pump is encoded on the megaplasmid pTTS12 of *P. putida* S12 (12).

The 583-kbp megaplasmid pTTS12 is a stable single-copy plasmid specific to *P. putida* S12 (12). It harbors several important operons and gene clusters enabling *P. putida* S12 to tolerate, resist and survive the presence of various toxic compounds or otherwise harsh environmental conditions. Several examples include the presence of a complete styrene degradation pathway gene cluster, the RND efflux pump specialized for organic solvents (SrpABC), and several gene clusters conferring heavy metal resistance (12, 17, 18). In addition, through analysis using TADB2.0, a toxin-antitoxin database (19, 20), pTTS12 is predicted to contain three toxin-antitoxin modules. Toxin-antitoxin modules recently have been recognized as important determinants of resistance towards various stress conditions, like nutritional stress and exposure to sublethal concentration of chemical stressor (21, 22). Toxin-antitoxin modules identified in pTTS12 consist of an uncharacterized RPPX_26255-RPPX_26260 system and two identical copies of a VapBC system (23). RPPX_26255 and RPPX_26260 belong to a newly characterized type II toxin-antitoxin pair, COG5654-COG5642. While toxin-antitoxin systems are known to preserve plasmid stability through postsegregational killing of plas-

mid-free daughter cells (24), RPPX_26255-RPPX_26260 was also previously shown to be upregulated during organic solvent exposure, suggesting its role in solvent tolerance (11).

In the manuscript, we further address the role of pTTS12 in conferring solvent tolerance of *P. putida* S12. Curing pTTS12 from its host strain might cause a reduction in solvent tolerance, while complementation of the *srp* operon into the cured strain may fully or partially restore solvent tolerance. Furthermore, we wished to identify additional genes or gene clusters on pTTS12 and putative mechanisms that might also play a role in conferring solvent tolerance to *P. putida* and non-solvent-tolerant *E. coli*.

Results

Megaplasmid pTTS12 is essential for solvent tolerance in *P. putida* S12

To further analyze the role of the megaplasmid of *P. putida* S12 in solvent tolerance, pTTS12 was removed from *P. putida* S12 using mitomycin C. This method was selected due to its reported effectiveness in removing plasmids from *Pseudomonas sp.* (25), although previous attempts regarded plasmids that were significantly smaller in size than pTTS12 (26). After treatment with mitomycin C (10 to 50 mg liter^{-1}), liquid cultures were plated on M9 minimal medium supplemented with indole to select for plasmid-cured colonies. Megaplasmid pTTS12 encodes two key enzymes, namely, styrene monooxygenase (SMO) and styrene oxide isomerase (SOI) that are responsible for the formation of indigo coloration from indole. This conversion results in indigo coloration in spot assays for wild-type *P. putida* S12 whereas white colonies are formed in the absence of megaplasmid pTTS12. With the removal of pTTS12, loss of indigo coloration and, hence, of indigo conversion was observed in all three plasmid-cured strains and the negative control *P. putida* KT2440 (Fig. 4.1A).

With mitomycin C concentration of 30 mg liter^{-1}, 2.4% (3 out of 122) of the obtained colonies appeared to be completely cured from the megaplasmid, underscoring the high genetic stability of the plasmid. No colonies survived the addition of 40 and 50 mg liter^{-1} of mitomycin C, whereas all the colonies that survived the addition of 10 and 20 mg liter^{-1} of mitomycin C retained the megaplasmid. Three independent colonies cured from the megaplasmid were isolated as *P. putida* S12-6, *P. putida* S12-10, and *P. putida* S12-22. The complete loss of the megaplasmid was further confirmed by phenotypic analysis (Fig. 4.1), and by full-genome sequencing. Several operons involved in heavy metal resistance were previously reported

in the pTTS12 (12). The *terZABCD* operon contributes to tellurite resistance in wild-type *P. putida* S12 with minimum inhibitory concentrations (MICs) as high as 200 mg liter^{-1} (Fig. 4.1B). In the megaplasmid-cured strains, a severe reduction of tellurite resistance was observed, decreasing the potassium tellurite MIC to 50 mg liter^{-1} (Fig. 4.1B).

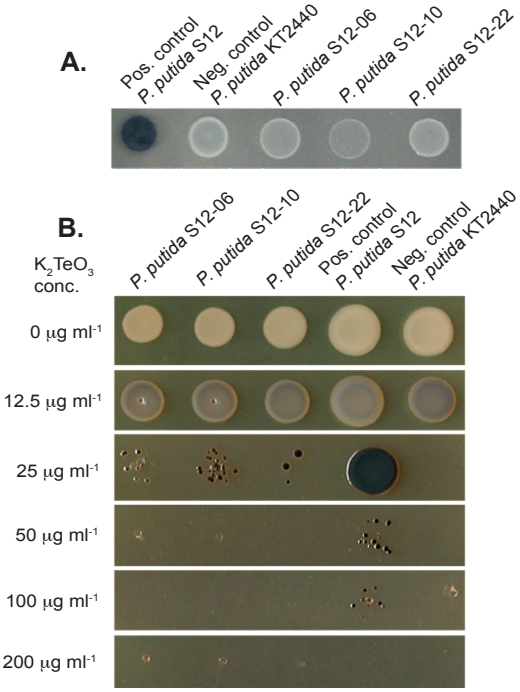

Fig. 4.1. Curing of the megaplasmid pTTS12 from *P. putida* S12.

A. Activity of styrene monooxygenase (SMO) and styrene oxide isomerase (SOI) for indigo formation from indole in *P. putida* strains. Enzyme activity was lost in the megaplasmid-cured genotype S12 ΔpTTS12 (white colonies). Indole (100 mg liter^{-1}) was supplemented in M9 minimum medium.

B. K_2TeO_3 resistance of *P. putida* strains on lysogeny broth (LB) agar. Tellurite resistance was reduced in the megaplasmid-cured genotype S12 ΔpTTS12 (MIC 50 mg liter^{-1}).

Genomic DNA sequencing confirmed a complete loss of pTTS12 from *P. putida* genotypes S12-6, S12-10, and S12-22 without any plasmid-derived fragment being inserted within the chromosome, and genomic alterations by mitomycin C treatment were minimal. Complementation of pTTS12 into the plasmid-cured *P. putida* S12 genotypes restored the indole-indigo transformation and high tellurite resistance to a similar level as the wild-type strain (see Fig. 4.S1 in the supplemental material). Repeated megaplasmid curing experi-

ments indicated that *P. putida* S12 can survive the addition of 30 mg liter^{-1} mitomycin C with the frequency of (2.48 ± 0.58) x 10^{-8}. Among these survivors, only 2% of the colony population lost the megaplasmid, confirming the genetic stability of pTTS12. In addition, attempts to cure the plasmid by introducing double-strand breaks as described by Wynands and colleagues (27) were not successful due to the pTTS12 stability.

Growth comparison in solid and liquid culture in the presence of toluene was performed to analyze the effect of megaplasmid curing in constituting solvent tolerance trait of *P. putida* S12. In contrast with wild-type *P. putida* S12, the plasmid-cured genotypes were unable to grow under toluene atmosphere conditions (data not shown). In liquid LB medium, plasmid-cured *P. putida* S12 genotypes were able to tolerate 0.15% (vol/vol) toluene, whereas the wild-type *P. putida* S12 could grow in the presence of 0.30% (vol/vol) toluene (Fig. 4.2). In the megaplasmid-complemented *P. putida* S12-C genotypes, solvent tolerance was restored to the wildtype level (Fig. 4.S1-D). Hence, the absence of megaplasmid pTTS12 caused a significant reduction of solvent tolerance in *P. putida* S12.

The SrpABC efflux pump and gene pair RPPX_26255-26260 are the main constituents of solvent tolerance encoded on pTTS12

The significant reduction of solvent tolerance in plasmid-cured *P. putida* S12 underscored the important role of megaplasmid pTTS12 in solvent tolerance. Besides encoding the efflux pump SrpABC enabling efficient intermembrane solvent removal (12, 13), pTTS12 carries more than 600 genes and, hence, may contain additional genes involved in solvent tolerance. Two adjacent hypothetical genes, RPPX_26255 and RPPX_26260, were previously reported to be upregulated in a transcriptomic study as a short-term response to toluene addition (11). We propose to name the RPPX_26255-RPPX_26260 gene pair as "*slv"* due to its elevated expression in the presence of solvent. In a first attempt to identify additional potential solvent tolerance regions of pTTS12, we deleted the *srp*ABC genes (Δ*srp*), RPPX_26255-26260 genes (Δ*slv*), and the combination of both gene clusters (Δ*srp* Δ*slv*) from pTTS12 in wild-type *P. putida* S12.

All strains were compared for growth under increasing toluene concentrations in liquid LB medium (Fig. 4.2). In the presence of low concentrations of toluene (0.1% [vol/vol]), all genotypes showed similar growth. With the addition of 0.15% (vol/vol) toluene, S12 Δ*slv*, S12 Δ*srp* and S12 Δ*srp* Δ*slv* exhibited slower growth and reached a lower optical density at 600

nm (OD_{600}) than the wild-type S12 strain. S12 Δ*slv* and S12 Δ*srp* achieved a higher OD_{600} in batch growth than S12 ΔpTTS12 and S12 Δ*srp* Δ*slv* due to the presence of the SrpABC efflux pump or RPPX_26255-RPPX_26260 gene pair.

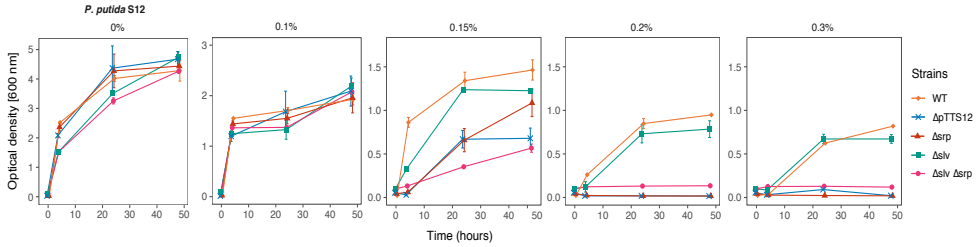

Fig. 4.2. Megaplasmid pTTS12 determines the solvent tolerance trait of *P. putida* S12.

Solvent tolerance analysis was performed on wild-type *P. putida* S12, *P. putida* S12 ΔpTTS12 (genotypes S12-6, S12-10, and S12-22), *P. putida* S12 Δsrp, *P. putida* S12 Δslv, and *P. putida* S12 Δsrp Δslv growing in liquid LB media with 0%, 0.10%, 0.15%, 0.20% and 0.30% (vol/vol) toluene. The removal of the megaplasmid pTTS12 clearly caused a significant reduction in the solvent tolerance of ***P. putida*** S12 ΔpTTS12. Deletion of srpABC (Δsrp), RPPX_26255-26260 (Δslv), and the combination of these gene clusters (Δsrp Δslv) resulted in a lower solvent tolerance. This figure displays the means of three biological replicates, and error bars indicate standard deviation. The range of y axes are different in the first panel (0 to 5), second panel (0 to 3) and third to fifth panels (0 to 1.5).

Interestingly, S12 Δ*srp* Δ*slv* (still containing pTSS12) exhibited diminished growth compared with S12 ΔpTTS12. This may be an indication of megaplasmid burden in the absence of essential genes for solvent tolerance. With 0.2% and 0.3% (vol/vol) toluene added to the medium, S12 Δ*srp,* S12 Δ*srp* Δ*slv*, and S12 ΔpTTS12 were unable to grow, while wild-type S12 and S12 Δ*slv* were able to grow, although S12 Δ*slv* reached a lower OD_{600}. Taken together, these results demonstrate an important role for both the SrpABC efflux pump and the *slv* gene pair in conferring solvent tolerance. We chose *P. putida* S12-6 for further experiments representing megaplasmid-cured *P. putida* S12.

Solvent tolerance can be exerted by ectopic expression of the SrpABC efflux pump and *slv* gene pair in Gram-negative bacteria

The functionality of the *srp* operon and *slv* gene pair was explored in the model Gram-negative non-solvent-tolerant strains *P. putida* KT2440, *E. coli* TG1 and *E. coli* BL21(DE3). We complemented *srpRSABC* (*srp* operon), *slv* gene pair, and a combination of both gene clus-

ters into *P. putida* S12-6, *P. putida* KT2440, *E. coli* TG1, and *E. coli* BL21(DE3) using mini-Tn7 transposition. These strains were chosen due to their common application as model industrial strains while lacking solvent tolerance. *P. putida* KT2440 is another robust microbial host for metabolic engineering due to its adaptation toward physicochemical stresses; however, contrary to P. putida S12, this strain is not solvent-tolerant (28). *E. coli* BL21(DE3), derived from strain B, is the common *E. coli* lab strain optimized for protein production due to its lacking Lon and OmpT proteases and encoding T7 RNA polymerase (29). *E. coli* TG1 was previously reported to successfully produce 1-naphtol with the expression of SrpABC (15, 16), and therefore, this strain was included in this study as a comparison.

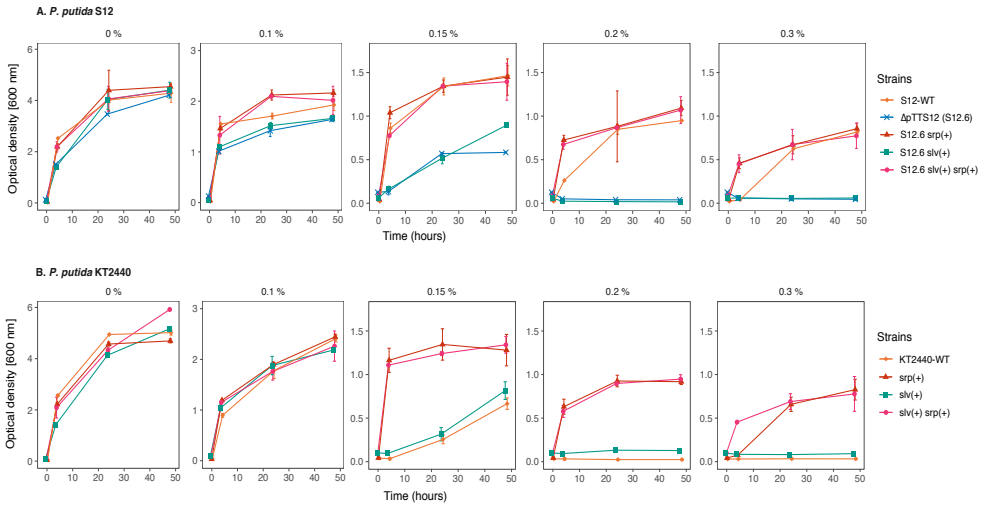

Fig. 4.3. Chromosomal introduction of *srp* and *slv* gene clusters increased solvent tolerance in *P. putida* genotypes.

Solvent tolerance analysis of the genotypes with chromosomal introduction of *srp* operon (*srpRSABC*), *slv* gene pair (RPPX_26255-RPPX_26260), and the combination of these gene clusters into *P. putida* S12 ΔpTTS12 (represented by strain S12-6) (A) and wild-type *P. putida* KT2440 (B) in liquid LB with 0%, 0.10%, 0.15%, 0.20% and 0.30% (vol/vol) of toluene. Wild-type *P. putida* S12 was taken as a solvent-tolerant control strain. This figure displays the mean of three independent replicates, and error bars indicate standard deviation. The range of y axes are different in the first panel (0 to 6), second panel (0 to 3) and third to fifth panels (0 to 1.5).

The chromosomal introduction of *slv* into S12-6 and KT2440 improved growth of the resulting strains at 0.15% (vol/vol) toluene compared with S12-6 and KT2440 (Fig. 4.3). The introduction of *srp* or a combination of *slv* and *srp* enables S12-6 and KT2440 to grow in the

presence of 0.3% (vol/vol) toluene. In KT2440, the introduction of both *slv* and *srp* resulted in a faster growth in the presence of 0.3% (vol/vol) toluene than the addition of only *srp* (Fig. 4.3B). Interestingly, the growth of S12-6 *srp*,*slv* and S12-6 *srp* is better than wild-type S12 (Fig. 4.3A). The observed faster growth of S12-6 *srp*,*slv* and S12-6 *srp* may be due to more efficient growth in the presence of toluene, supported by a chromosomally introduced *srp* operon, than its original megaplasmid localization. Indeed, replication of this large megaplasmid is likely to require additional maintenance energy. To corroborate this, we complemented the megaplasmid lacking the solvent pump (Tc^R::*srpABC*) into *P. putida* S12-6 *srp* resulting in *P. putida* S12-9. Indeed, *P. putida* S12-9 showed further reduced growth in the presence of 0.20 and 0.30 % (vol/vol) toluene (Fig. 4.S2), indicating the metabolic burden of carrying the megaplasmid. We conclude that the SrpABC efflux pump can be regarded as the major contributor to solvent tolerance from pTTS12. The *slv* gene pair appears to promote tolerance of *P. putida* S12 at least under moderate solvent concentrations.

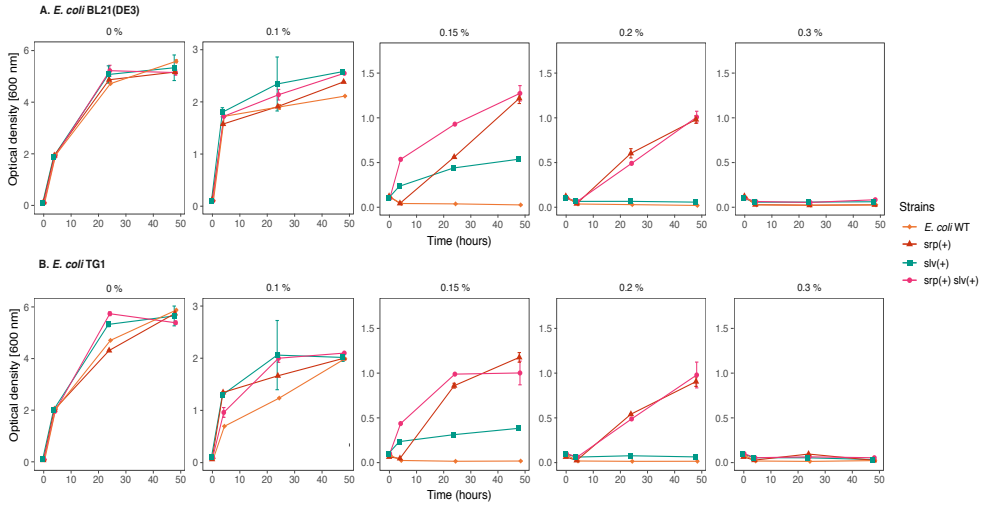

Fig. 4.4. Chromosomal introduction of *srp* and *slv* gene clusters increased solvent tolerance in *E. coli* strains.

Solvent tolerance analysis of the strains with chromosomal introduction of *srp* operon (*srpRSABC*), *slv* gene pair (RPPX_26255-RPPX_26260), and the combination of these gene clusters into *E. coli* BL21(DE3) (A) and *E. coli* TG1 (B) in liquid LB with 0%, 0.10%, 0.15%, 0.20% and 0.30% (vol/vol) of toluene. This figure displays the mean of three independent replicates, and error bars indicate standard deviation. The range of y axes are different in the first panel (0 to 6), second panel (0 to 3) and third to fifth panels (0 to 1.5).

The intrinsic solvent tolerance of *E. coli* strains was observed to be clearly lower than that of *P. putida* (Fig. 4.4). The wild-type *E. coli* strains were able to withstand a maximum 0.10% (vol/vol) toluene, whereas plasmid-cured *P. putida* S12-6 and *P. putida* KT2440 were able to grow in the presence of 0.15% (vol/vol) toluene. With the introduction of *slv* and *srp* in both *E. coli* strains, solvent tolerance was increased up to 0.15% and 0.2% (vol/vol) toluene respectively (Fig. 4.4). A combination of *slv* and *srp* also increased tolerance to 0.20% (vol/vol) toluene, while showing a better growth than the chromosomal introduction of only *srp*. However, none of these strains were able to grow in the presence of 0.30% (vol/vol) toluene.

qPCR analysis of SrpABC expression (Table 4.S1) in *P. putida* S12, *P. putida* KT2440, *E. coli* TG1, and *E. coli* BL21(DE3) confirmed that *srp*A, *srp*B, and *srp*C were expressed at basal levels in all strains. In the presence of 0.10% toluene, the expression of *srp*A, *srp*B, and *srp*C was clearly upregulated in all strains. Thus, the lower solvent tolerance conferred by introducing SrpABC efflux pump in *E. coli* strains was not due to lower expression of the *srp* genes. An analysis of the codon adaptation index (CAI) (http://genomes.urv.es/CAIcal/) (30) showed that for both the *P. putida* and *E. coli* strains, the CAI values of the srp operon are suboptimal, cleary below 0.8 to 1.0 (Table 4.S2). Interestingly, the CAI values were higher for *E. coli* (0.664) than for *P. putida* (0.465), predicting a better protein translation efficiency of the *srp* operon in *E. coli*. Hence, reduced translation efficiency is not likely to be the cause of lower performance of the *srp* operon in *E. coli* strains for generating solvent tolerance. Overall, our results indicate that, in addition to the solvent efflux pump, *P. putida* S12 and *P. putida* KT2440 are intrinsically more robust than *E. coli* TG1 and *E. coli* BL21(DE3) in the presence of toluene.

The *slv* gene pair constitutes a novel toxin-antitoxin system

BLASTp analysis was initiated to further characterize RPPX_26255 and RPPX_26260. This analysis indicated that RPPX_26260 and RPPX_26255 likely represent a novel toxin-antitoxin (TA) system. Through a database search on TADB2.0 (19, 20), we found that RPPX_26260 is a toxin of COG5654 family typically encodes a RES domain-containing protein, which has a conserved arginine (R) – glutamine (E) – serine (S) motif providing a putative active site; and RPPX_26255 is an antitoxin of COG5642 family. Based on its involvement in solvent tolerance, we propose naming the toxin-encoding RPPX_26260 as *slvT* and the antitoxin-encoding RPPX_26255 as *slvA*.

Makarova and colleague identified putative toxin-antitoxin pairs through genome mining of reference sequences in the NCBI database (31). They identified 169 pairs of the COG5654-COG5642 TA system from the reference sequences (Table 4.S3). Here, we constructed a phylogenetic tree of the COG5654-COG5642 TA system, including SlvA (GenBank accession no. AJA16859.1) and SlvT (AJA16860.1), as shown in Fig. 4.5A and 4.6A. SlvA and SlvT cluster with other plasmid-borne toxin-antitoxin from *Burkholderia vietnamensis* G4, *Methylibium petroleiphilum* PM1, *Rhodospirillum rubrum* ATCC 11170, *Xanthobacter autotrophicus* Py2, *Sinorhizobium meliloti* 1021, *Sinorhizobium medicae* WSM419, and *Gloeobacter violaceus* PCC7421. Multiple alignments of SlvAT against the COG5654-COG5642 TA system are shown in Fig. 4.5B and 4.6B.

Of the 169 TA pairs of the COG5654-COG5642 TA system, three TA pairs have recently been characterized, namely, ParST from *Sphingobium sp.* YBL2 (GenBank accession no. AJR25281.1 and AJR25280.1)(32), PP_2433-2434 from *P. putida* KT2440 (NP_744581.1 and NP_744582.1)(33), and MbcAT from *Mycobacterium tuberculosis* H37Rv (NP_216506.1 and NP216505.1)(34), as indicated by bold text and asterisks in Fig. 4.5A and 4.6A. A 3D-model prediction of SlvT and SlvA proteins using the I-TASSER suite for protein structure and function prediction (35), indicated that SlvT and SlvA showed the highest structural similarity to the MbcAT system from *Mycobacterium tuberculosis* (Fig. 4.5C, 4.6C, and 4.S3), which is reported to be expressed during stress conditions (34). Amino acid conservation between SlvAT and these few characterized toxin-antitoxin pairs is relatively low, as they do not belong to the same clade (Fig. 4.5A and 4.6A). However, 100% conservation is clearly observed on the putative active side residues, namely, arginine (R) 35, tyrosine (Y) 45, and glutamine (E) 56, and only 75% consensus is shown on serine (S) 133 residue (Fig. 4.S3).

According to the model with highest TM score, SlvT is predicted to consist of four beta sheets and four alpha helices. As such, SlvT shows structural similarity with diphtheria toxin which functions as an ADP-ribosyl transferase enzyme. Diphtheria toxin can degrade NAD^+ into nicotinamide and ADP ribose (36). A similar function was recently identified for COG5654 family toxins from *P. putida* KT2440, *M. tuberculosis*, and *Sphingobium sp* (32–34).

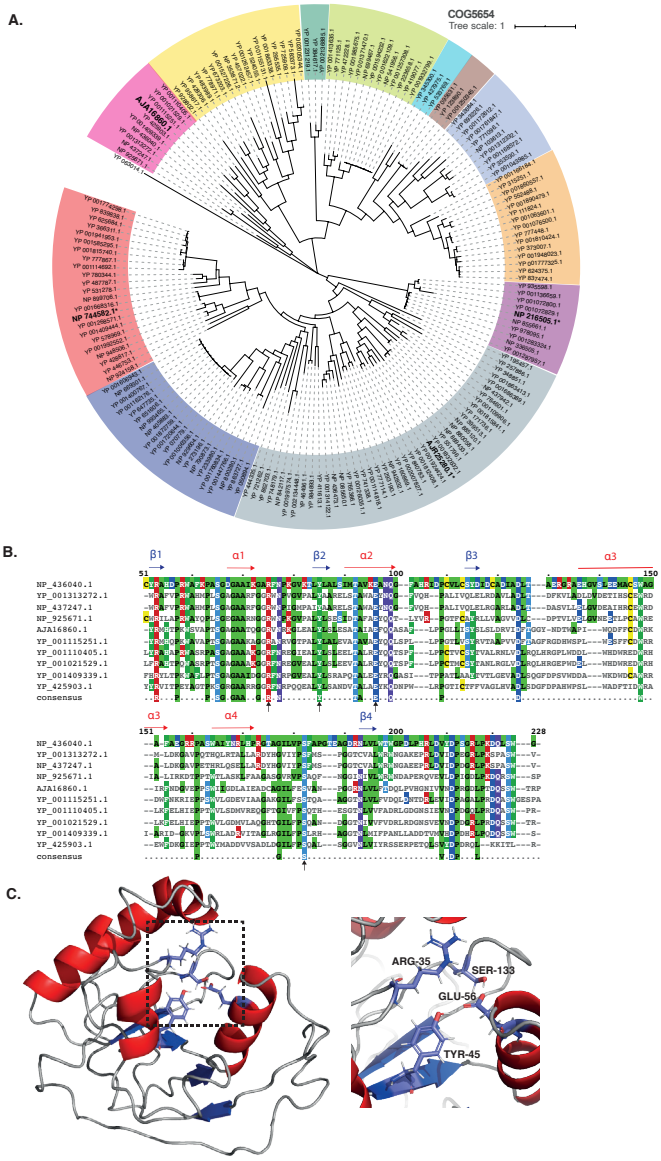

Fig. 4.5. Bioinformatics analysis of SlvT as a member of COG5654 toxin family

A. Phylogenetic tree (neighbour joining tree with 100 bootstraps) of COG5654 family toxin from reference sequences identified by Makarova and colleagues (31). Different colours correspond to the different toxin-antitoxin module clades. Asterisks (*) and bold text indicate the characterized toxin proteins, namely, ParT from *Sphingobium sp.* YBL2 (GenBank accession no. AJR25280.1), PP_2434 from *P. putida* KT2440 (NP_744582.1), MbcT from *Mycobacterium tuberculosis* H37Rv (NP_216505.1), and SlvT from *P. putida* S12 (AJA16860.1).

B. Multiple sequence alignment of the COG5654 toxin SlvT from *P. putida* S12 with several putative COG5654 family toxin proteins which belong in the same clade. Putative active site residues are indicated by black arrows.

C. Protein structure modelling of SlvT using I-TASSER server (35), which exhibits high structural similarity with MbcT from *Mycobacterium tuberculosis* H37Rv. Shown are the close ups of putative active sites of the SlvT toxin (Arg-35, Tyr-45, Glu-56, and Ser-133).

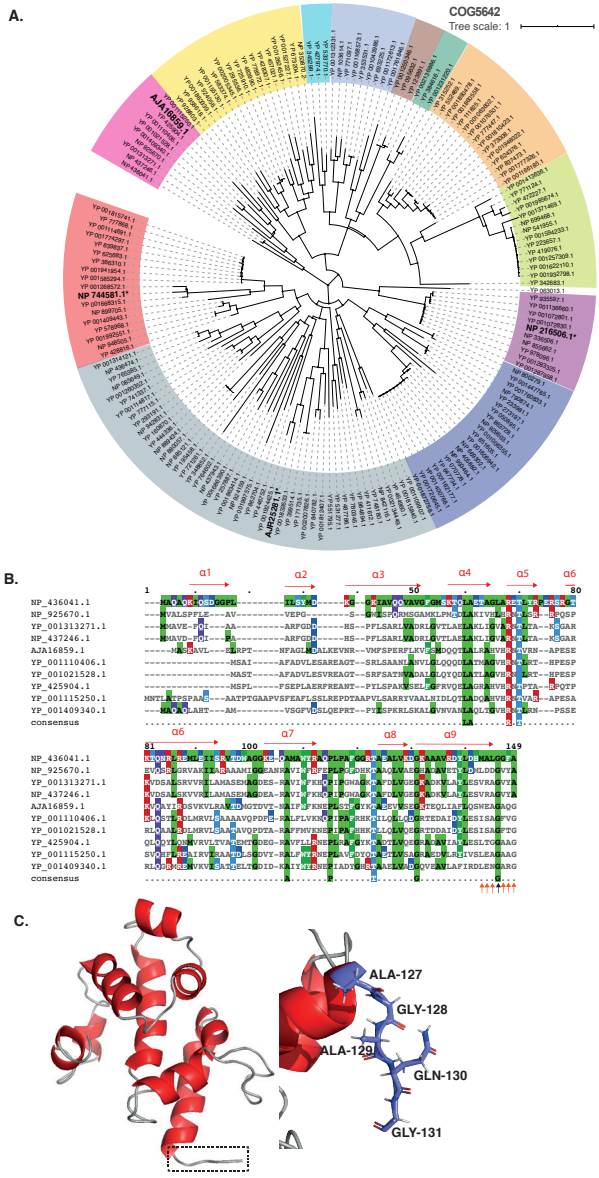

Fig. 4.6. Bioinformatics analysis of SlvA as a member of COG5642 toxin family

A. Phylogenetic tree (neighbour joining tree with 100 bootstrap) of COG5642 family antitoxin from reference sequences identified by Makarova and colleagues (31). Different colours correspond to the different toxin-antitoxin module clades. Asterisks (*) and bold text indicate the characterized antitoxin proteins, namely, ParS from

Sphingobium sp. YBL2 (GenBank accession no. AJR25281.1), PP_2433 from *P. putida* KT2440 (NP_744581.1), MbcA from *Mycobacterium tuberculosis* H37Rv (NP_216506.1), and SlvA from *P. putida* S12 (AJA16859.1).

B. Multiple sequence alignment of the COG5654 toxin SlvA from *P. putida* S12 with several putative COG5642 family antitoxin proteins which belong in the same clade. Putative active site residues are indicated by orange and black arrows.

C. Protein structure modelling of SlvA using I-TASSER server (30) which exhibits high structural similarity with MbcA from *Mycobacterium tuberculosis* H37Rv. Shown are the close up of antitoxin putative C-terminal binding site to block SlvT toxin active site (Ala-127, Gly-128, Ala-129, Gln-130, and Gly-131).

slvT toxin causes cell growth arrest by depleting cellular NAD^+

To prove that *slvAT* presents a pair of toxin and antitoxin, *slvA* and *slvT* were cloned separately in pUK21 (lac-inducible promoter) and pBAD18 (ara-inducible promoter), respectively. The two constructs were cloned into *E. coli* BL21(DE3). The growth of the resulting strains was monitored during conditional expression of the *slvA* and *slvT* genes (Fig. 4.7A). At the mid-log growth phase, a final concentration of 0.8% arabinose was added to the culture (*), inducing expression of *slvT*. After 2 h of induction, growth of this strain ceased, while the uninduced control culture continued to grow. Upon addition of 2 mM isopropyl-β-D-thiogalactopyranoside (IPTG) (**), growth of the *slvT*-induced culture was immediately restored, reaching a similar OD_{600} as the uninduced culture.

Bacterial cell division was further studied by flow cytometer analyses during the expression of *slvT* and *slvA*. After approximately 6 h of growth (indicated by grey arrow in Fig. 4.7A), samples were taken from control, arabinose, and arabinose + IPTG-induced liquid culture. Cell morphology was analyzed by light microscopy, and the DNA content of the individual cells in the culture was measured using a flow cytometer with SYBR green II staining (Fig. 4.7B). Indeed, an absence of dividing cells and lower DNA content were observed during the induction of only *slvT* toxin with arabinose (Fig. 4.7B). Subsequent addition of IPTG to induce *slvA* expression was shown to restore cell division and to an upshift of DNA content similar to that of control strain (Fig. 4.7B). While the expression of *slvT* was not observed to be lethal to bacterial strain, this experiment showed that the expression of the *slvT* toxin stalled DNA replication and, subsequently, cell division. The induction of *slvA* subsequently restored bacterial DNA replication and cell division.

To corroborate a putative target of SlvT, concentrations of NAD^+ were measured during the induction experiment (Fig. 4.7C). Before the addition of arabinose to induce *slvT*

(orange arrow on Fig. 4.7A), NAD^+ was measured and compared to the strain harboring empty pUK21 and pBAD18 (Fig. 4.7B). On average, at this time point, the NAD^+ level is similar between the *slvAT*-bearing strain and the control strain. NAD^+ was measured again after arabinose induction when the growth of the induced strain has diminished (blue arrow on Fig. 4.7A). At this time point, the measured NAD^+ was 32% (±14.47) of the control strain. After the induction of *slvA*, NAD^+ was immediately restored to a level of 77% (±9.97) compared to the control strain. Thus, the induction of *slvT* caused a depletion of NAD^+, while induction of *slvA* immediately increased NAD^+ level, indicating that *slvAT* is a pair of toxin-antitoxin which controls its toxicity through NAD^+ depletion.

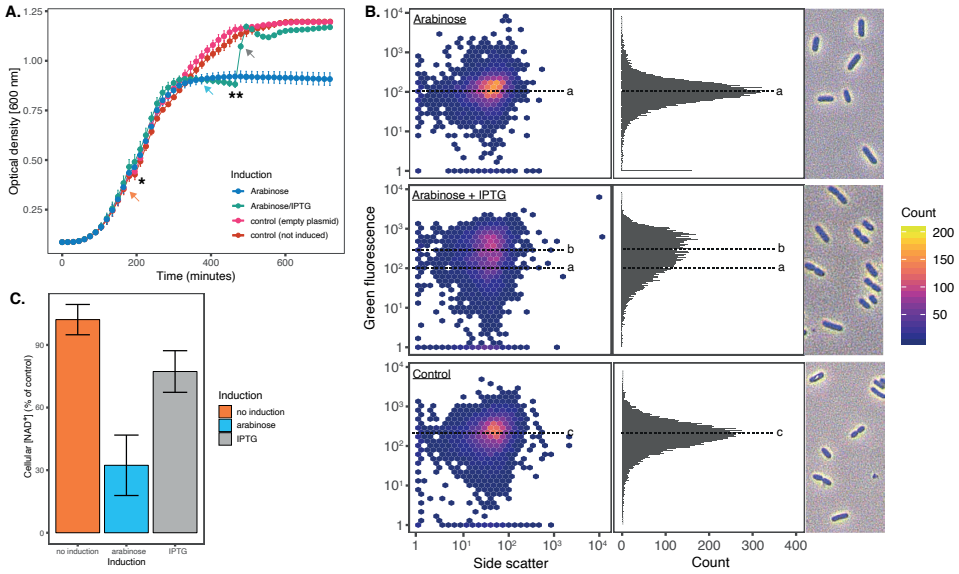

Fig. 4.7. Heterologous expression of SlvAT in *E. coli* BL21(DE3)

A. Growth curves of *E. coli* BL21(DE3) harbouring pBAD18-slvT and pUK21-slvA, showing growth reduction after the induction of toxin by a total concentration of 0.8 % arabinose (*) and growth restoration after antitoxin induction by a total concentration of 2 mM IPTG (**). Samples were taken at the time points indicated by coloured arrows for cellular NAD^+ measurement.

B. Flow cytometry analysis of DNA content and cell morphology visualization on *E. coli* BL21(DE3) during *slvT* and *slvAT* expression. Median value of green fluorescence representing DNA content during *slvT* expression (118.202), *slvAT* expression (236.056), and control (208.406) are indicated by **a**, **b**, and **c**, respectively. Samples were taken at the time point indicated by grey arrow in A.

C. Cellular NAD^+ measurements during the expression of the toxin-antitoxin module. Induction of toxin SlvT caused a reduction in cellular NAD^+ level to 32.32% (±14.47%) of the control strain, while the expression of SlvA

restored cellular NAD^+ level to 77.27% (±9.97%) of the control strain.

slvAT regulates megaplasmid pTTS12 stability

In addition to its role in solvent tolerance, localization of the *slvAT* pair on megaplasmid pTTS12 may have an implications for plasmid stability. pTTS12 is a very stable megaplasmid that cannot be spontaneously cured from *P. putida* S12 and cannot be removed by introducing double-strand breaks (see above). We deleted *slvT* and *slvAT* from the megaplasmid to study their impact in pTTS12 stability. With the deletion of *slvT* and *slvAT*, the survival rate during treatment with mitomycin C improved significantly, reaching (1.01 ± 0.17) x 10^{-4} and (1.25 ± 0.81) x 10^{-4}, respectively, while the wild-type S12 had a survival rate of (2.48 ± 0.58) x 10^{-8}.

We determined the curing rate of pTTS12 from the surviving colonies. In wild-type S12, the curing rate was 2% (see also above), while in Δ*slvT* and Δ*slvAT* mutants, the curing rate increased to 41.3% (± 4.1%) and 79.3% (± 10%), respectively, underscoring an important role for *slvAT* in megaplasmid stability. We attempted to cure the megaplasmid from the colonies by introducing a double strand break (DSB), as previously described on *Pseudomonas taiwanensis* VLB120 (27, 37). This indeed was not possible in wild-type S12 and Δ*slvT* strains; however, the Δ*slvAT* mutant now showed plasmid curing by a DSB, resulting in a curing rate of 34.3% (± 16.4%).

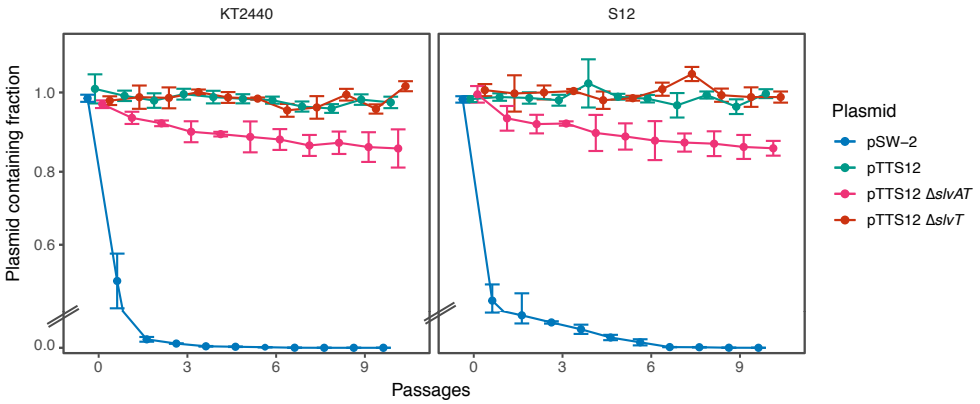

Fig. 4.8. SlvAT is important for pTTS12 maintenance in *P. putida*.

pTTS12 (variant with Km^R) maintenance in *P. putida* S12 and *P. putida* KT2440 growing in LB liquid medium without antibiotic selection for 10 passages (approximately 10 generations per passage). pSW-2 was taken as negative control for plasmid stability in *P. putida*. This experiment was performed with three biological replicates,

and error bars represent standard deviation.

Since Δ*slvT* and Δ*slvAT* may compromise megaplasmid stability, we now performed megaplasmid stability tests by growing S12 and KT2440 harboring pSW-2 (negative control) (37), pTTS12 (positive control), pTTS12 Δ*slvT*, and pTTS12 Δ*slvAT* in LB medium with 10 passages (± 10 generations/passage step) as shown in Fig. 4.8. Both KT2440 and S12 easily lost the negative-control plasmid pSW-2 (Fig. 4.8). Plasmid pTTS12 was not lost during this test, confirming that pTTS12 is indeed a stable plasmid. Furthermore, the Δ*slvT* genotypes also did not show a loss of the megaplasmid. Interestingly, the Δ*slvAT* genotypes spontaneously lost the megaplasmid, confirming that the *slvAT* module is not only important to promote solvent tolerance but also determines megaplasmid stability in *P. putida* S12 and KT2440.

Discussion

Revisiting the role of pTTS12 and SrpABC efflux pump in solvent tolerance

In this study, we conclusively confirm the role of SrpABC efflux pump carried on pTTS12 and identify a novel toxin-antitoxin module playing an additional role in conveying solvent tolerance to P. putida S12 (Fig. 4.9). Notably, megaplasmids may cause a metabolic burden to their host strains, and they can be a source of genetic instability (11). Our results show that, indeed, pTTS12 imposed a metabolic burden in the presence of an organic solvent (Fig. 4.S2). This plasmid is very large and contains many genes that are not related to solvent tolerance. Hence, it may be interesting for biotechnological purposes to reduce plasmid size and, consequently, metabolic burden. In addition, a streamlined and minimal genome size is desirable for reducing host interference and genome complexity (12, 13).

We investigated the heterologous expression of the SrpABC efflux pump in strains of both *P. putida* and *E. coli*, which successfully enhanced their solvent tolerance in these strains (Fig. 4.3 and 4.4). Previous reports on the implementation of SrpABC in whole-cell biocatalysis successfully increased the production of 1-naphtol in *E. coli* TG1 (15, 16). Production was still higher using *P. putida* S12, as this strain could better cope with substrate (naphthalene) toxicity, while both *P. putida* S12 and *E. coli* TG1 showed similar tolerance to the product 1-naphtol (16). In our experiments, the *E. coli* strains clearly showed a smaller increase in toluene tolerance than the *P. putida* strains, although *srpABC* was expressed at a basal level and upregulated in the presence of 0.10 % (vol/vol). These results indicate that besides hav-

ing an efficient solvent efflux pump, *P. putida* S12 and *P. putida* KT2440 are inherently more robust in the presence of toluene and, presumably, other organic solvents than *E. coli* TG1 and *E. coli* BL21(DE3). The absence of cis-trans isomerase (*cti*), resulting in the inability to switch from *cis*- to *trans*-fatty acid in *E. coli* (38), may contribute to this difference in solvent tolerance. Additionally, *P. putida* typically has a high NAD(P)H regeneration capacity (39, 40) which can contribute to the maintenance of proton motive force during solvent extrusion by RND efflux pump. Further detailed investigation is required to reveal the exact basis for its intrinsic robustness.

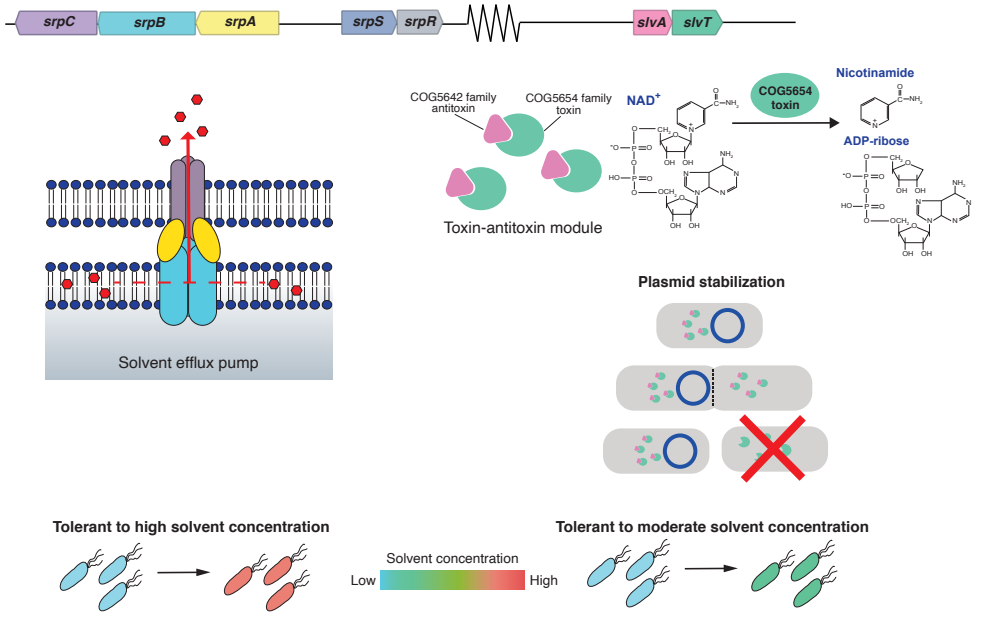

Fig. 4.9. Schematic representation of the gene clusters involved in solvent tolerance from megaplasmid pTTS12.

The SrpABC efflux pump is the major contributor of solvent tolerance trait from the megaplasmid pTTS12. This efflux pump is able to efficiently extrude solvents from membrane lipid bilayer. A COG5654-COG5642 family toxin-antitoxin module (SlvT and SlvA, respectively) promoted the growth of *P. putida* S12 in the presence of a moderate solvent concentration and stabilized pTTS12 plasmid. In the absence of SlvA, SlvT causes toxicity by conferring cellular NAD^+ depletion and, subsequently, halt DNA replication and cell division.

Identification of the novel antitoxin-toxin module SlvAT

In *P. putida* S12, deletion of *srpABC* genes still resulted in higher solvent tolerance than the pTTS12-cured genotypes (Fig. 4.2, panel 3). This finding indicated that within pTTS12 there were other gene(s) which may play a role in solvent tolerance. Two genes of unknown

function were upregulated in a transcriptome analysis of toluene-shocked *P. putida*, namely, RPPX_26255 and RPPX_26260, suggesting a putative role in solvent tolerance (11). Here, we confirmed this finding and demonstrated that these genes together form a novel toxin-antitoxin module (Fig. 4.7). SlvT exerts toxicity by degradation of NAD^+, like other toxins of the COG5654-family, and expression of antitoxin SlvA immediately restored NAD^+ levels. Depletion of NAD^+ interfered with DNA replication and caused an arrest of cell division similar to another recently described COG5654-COG5642 family toxin-antitoxin pair (33). Indeed, the SlvAT toxin-antitoxin module was shown to be important for the stability of pTTS12 (Fig. 4.8).

Based on TADB2.0 analysis, pTTS12 encodes three TA pairs, namely, SlvAT and two identical copies of VapBC. VapBC was first identified from a virulence plasmid of *Salmonella sp.* and is known to prevent the loss of plasmid during nutrient-limiting condition (39). A previous report showed that VapBC can stabilize/retain approximately 90% of pUC plasmid in *E. coli* within 300 h of growth (40), which is similar to our result although demonstrated in a much smaller plasmid and under the control of the lac operon. Serendipitous plasmid loss due to double-strand break was reported in pSTY, which carries two identical copies of VapBC (27). Here, we observed a similar phenomenon in pTTS12 Δ*slvAT*. Hence, in the absence of SlvAT, two copies of VapBC were not sufficient to prevent the loss of pTTS12 on rich media without selection pressure and by double-strand break, indicating a major role for SlvAT.

A putative role of toxin-antitoxin module SlvAT in solvent tolerance

Toxin-antitoxin modules are known to be important in antibiotic persistent strains as a trigger to enter and exit the dormant state, causing the cell to become unaffected by the antibiotic (21, 40, 41). Among *Pseudomonas* species, several toxin-antitoxin modules are reported to be involved in survival strategies, such as stress response, biofilm formation, and antimicrobial persistence (33, 41, 42). Previous transcriptomic studies reported upregulation of the *slvAT* locus as a response towards toluene addition and its expression at 10 to 30 minutes after toluene addition (11). Here, we show that SlvAT improves solvent tolerance in *P. putida* and *E. coli* strains independent of pTTS12 or SrpABC efflux pump. We hypothesize that SlvAT plays a role as a rapid response towards toluene addition. Activation of SlvT toxin may halt bacterial growth, and this allows physiological adaptation and adjustments to take place (e.g., expression of extrusion pumps and membrane compaction) before resuming its growth and cell division in the presence of toxic organic solvent. It is interesting to note that *P. putida* S12

and KT2440 both carry another COG5654-COG5642 family toxin-antitoxin pair in their chromosome (locus tag RPPX_19375-RPPX_19380 and PP_2433-PP_2434, respectively). In *P. putida* S12, this TA module is not being induced during solvent stress, rendering it unlikely to play a role in solvent tolerance.

The putative regulation mechanism of toxin-antitoxin module SlvAT in *P. putida S12*

Expression of the *slvAT* locus with its native promoter region seemed to exert a similar physiological effect in solvent tolerance both in *E. coli* and *P. putida* (Fig. 4.3 and Fig. 4.4). Typically, toxin-antitoxin can regulate its own expression by antitoxin binding to the promoter region (21). Unstable antitoxin is encoded upstream of the stable toxin, giving a transcriptional advantage for production of antitoxin (43). While this study presents the role of SlvAT module as a response to solvent stress, this toxin-antitoxin module may play a role in the response to various other stresses since pTTS12 itself encodes several modules involved in different stress response. It would be interesting to further study whether organic solvents directly induce the expression of *slvAT* locus or intermediate signalling pathways are required. Several type II toxin-antitoxin modules are known to be regulated by proteases, such as Lon and Clp (44). These proteases degrade antitoxin protein, promoting toxin activity, and thus upregulate the expression of the toxin-antitoxin locus. Indeed, our preliminary transcriptomic data show upregulation of specific protease-encoding loci after toluene addition. These may constitute putative regulatory proteases to the SlvAT module. Future research on the dynamics of *slvAT* locus regulation is required for revealing the details of the control mechanisms operating in vivo.

Conclusions

In summary, our experiments confirmed that the SrpABC efflux pump is the major contributor of solvent tolerance on the megaplasmid pTTS12 which can be transferred to other non-solvent-tolerant host microbes. In addition, the megaplasmid carries the novel toxin-antitoxin system SlvAT (RPPX_26255 and RPPX_26260) which promotes rapid solvent tolerance in *P. putida* S12 and is important for maintaining the plasmid stability of pTTS12. Chromosomal introduction of the *srpRSABC* operon genes in combination with *slvAT* confers a clear solvent tolerance phenotype in other industrial strains previously lacking this phenotype, such as *P. putida* KT2440, *E. coli* TG1, and *E. coli* BL21(DE3). Taken together, our findings shows that

both SrpABC and SlvAT constitute suitable candidate loci for exchange with various microbial hosts for increasing tolerance towards toxic compounds.

Materials and Methods

Strains and culture conditions

Strains and plasmids used in this paper are listed in Table 4.1. All *P. putida* strains were grown in Lysogeny Broth (LB) at 30 °C with 200 rpm shaking. *E. coli* strains were cultivated in LB at 37 °C with 250 rpm shaking. For solid cultivation, 1.5 % (wt/vol) agar was added to LB. M9 minimal medium was supplemented with 2 mg liter^{-1} $MgSO_4$ and 0.2 % of citrate as sole carbon source (45). Toluene atmosphere growth was evaluated on solid LB in a glass plate incubated in an exicator with toluene supplied through the gas phase at 30 °C. Solvent tolerance analysis was performed by growing *P. putida* S12 genotypes in LB starting from OD_{600} of 0.1 in Boston bottles with Mininert bottle caps. When required, gentamicin (25 mg liter^{-1}), ampicillin (100 mg L^{-1}), kanamycin (50 mg liter^{-1}), indole (100 g liter^{-1}), potassium tellurite (6.75 to 200 mg liter^{-1}), arabinose (0.8% wt/vol), and IPTG (2 mM) were added to the medium.

Table 4.1. Strains and plasmids used in this paper

Strain	Characteristics	Ref.
P. putida S12	Wild-type *P. putida* S12 (ATCC 700801), harboring megaplasmid pTTS12	(3)
P. putida S12-1	*P. putida* S12, harboring megaplasmid pTTS12 with Km^R marker	This paper
P. putida S12-6/ S12-10/ S12-22	ΔpTTS12	This paper
P. putida S12-9	ΔpTTS12, Gm^R *srpRSABC*::Tn7, complemented with megaplasmid pTTS12 (Tc^R::*srpABC*)	This paper
P. putida S12-C	*P. putida* ΔpTTS12 (S12-6/ S12-10/ S12-22), complemented with megaplasmid pTTS12	This paper
P. putida KT2440	Derived from wild-type *P. putida* mt-2, ΔpWW0	(48)
E. coli HB101	*recA pro leu hsdR* Sm^R	(49)
E. coli BL21(DE3)	*E. coli* B, F^- *ompT gal dcm lon hsdS*$_B$($r_B^-m_B^-$) λ(DE3) [*lacI lacUV5-T7p07 ind1 sam7 nin5*]) [*malB*$^+$]$_{K\text{-}12}$(λ^S)	(29)
E. coli DH5α λpir	*sup* E44, Δ*lacU*169 (Φ*lacZ*ΔM15), *recA*1, *endA*1, *hsdR*17, *thi*-1, *gyrA*96, *relA*1, λpir phage lysogen	(50)
E. coli TG1	*E. coli* K-12, *glnV44 thi-1* Δ*(lac-proAB)* Δ*(mcrB-hsdSM)5*($r_K^-m_K^-$) F′ [*traD36 proAB*$^+$ *lacI*^{q} *lacZΔM15*]	Lucigen
E. coli WM3064	*thrB1004 pro thi rpsL hsdS lacZ*ΔM15 RP4-1360 Δ(*araBAD*)567 Δ*dapA1341*::[erm pir]	William Metcalf

Plasmid		
pRK2013	RK2-Tra$^+$, RK2-Mob$^+$, Km^R, *ori* ColE1	(51)
pEMG	Km^R, Ap^R, *ori* R6K, *lacZ*α MCS flanked by two I-SceI sites	(37)
pEMG-Δ*srpABC*	pEMG plasmid for constructing *P. putida* S12 Δ*srpABC*	This paper
pEMG-Δ*slvAT*	pEMG plasmid for constructing *P. putida* S12 Δ*slvAT*	This paper
pEMG-Δ*slvT*	pEMG plasmid for constructing *P. putida* S12 Δ*slvT*	This paper
pSW-2	Gm^R, *ori* RK2, *xylS*, Pm ® I-sceI	(37)
pBG35	Km^R, Gm^R, *ori* R6K, pBG-derived	(46)
pBG-srp	Km^R, Gm^R, *ori* R6K, pBG-derived, contains *srp* operon (RPPX_27995-27965)	This paper
pBG-slv	Km^R, Gm^R, *ori* R6K, pBG-derived, contains *slv* gene pair (RPPX_26255-26260)	This paper
pBG-srp-slv	Km^R, Gm^R, *ori* R6K, pBG-derived, contains *slv* gene pair (RPPX_26255-26260) and *srp* operon (RPPX_27995-27965)	This paper
pBAD18-slvT	Ap^R, ara operon, contains *slvT* (RPPX_26260)	This paper
pUK21-slvA	Km^R, lac operon, contains *slvA* (RPPX_26255)	This paper
pTnS-1	Ap^R, *ori* R6K, TnSABC+D operon	(52)

DNA and RNA methods

All PCRs were performed using Phusion polymerase (Thermo Fisher) according to the manufacturer's manual. Primers used in this paper (Table 4.2) were procured from Sigma-Aldrich. PCR products were checked by gel electrophoresis on 1 % (wt/vol) TBE agarose containing 5 µg ml^{-1} ethidium bromide (110V, 0.5x TBE running buffer). For reverse transcriptase quantitative PCR (RT-qPCR) analysis, RNA was extracted using TRIzol reagent (Invitrogen) according to the manufacturer's manual. The obtained RNA samples were immediately reverse transcribed using iScript cDNA synthesis kit (Bio-Rad), and cDNA may have been stored at -20 °C prior to qPCR analysis. qPCR was performed using iTaq Universal SYBR Green Supermix (Bio-Rad) on a CFX96 Touch real-time PCR Detection System (Bio-Rad). The genome sequence of *P. putida* S12 ΔpTTS12 was analyzed using Illumina HiSeq instrument (GenomeScan BV, The Netherlands) and assembled according to the existing complete genome sequence (GenBank accession no. CP009974 and CP009975) (12).

Table 4.2. Oligos used in this study

Oligos	Sequences (5'-3')	Restriction sites	PCR templates	Description
TS1-srp-for	TATCTGGTACCTTGTCCTGGAAG CCGCTAATGA	KpnI	pTTS12	Construction of pEMG-Δ*srpABC*
TS1-srp-rev	CAGCGGCGGCCGCTTTAACGCA GGAAAGCTGCGAG	NotI	pTTS12	Construction of pEMG-Δ*srpABC*
TS2-srp-for	CCGAAGCGGCCGCCAGCGCAG TTAAGGGGATTACC	NotI	pTTS12	Construction of pEMG-Δ*srpABC*
TS2-srp-rev	TCAGCTCTAGAGCGCAGGTAAG GCTTCACC	XbaI	pTTS12	Construction of pEMG-Δ*srpABC*
srpO_F	TGCGAATTCGGTATCGCACATG GCATTGG	EcoRI	pTTS12	Construction of pBG-srp
srpO_R	TGCTCTAGAGCCTCACACCTGG TGTACC	XbaI	pTTS12	Construction of pBG-srp
slv_F	ATGCTTAATTAACTTTTGCTGCG GTCTACACAGG	PacI	pTTS12	Construction of pBG-slv
slv_R	AGCGGGAATTCCTCCAAAACCG GTTCTGAAGCC	EcoRI	pTTS12	Construction of pBG-slv
slvA_F	AGAGAGCTCCATAGTAAGTGCA ATCCTAAAG	SacI	pTTS12	Construction of pUK21-*slvA*
slvA_R	GTCTAGACTCCAGCTCCAGATG TAG	XbaI	pTTS12	Construction of pUK21-*slvA*
slvT_F	GGTGCTCTAGAATGAAAATCATC GGAGTG	XbaI	pTTS12	Construction of pBAD18-*slvT*
slvT_R	GGAAGGAGCTCGTACGTGTAAG GCGCTAC	SacI	pTTS12	Construction of pBAD18-*slvT*
TS1_slv_F	TGCTGGAATTCCTTTTGCTGCGG TCTACACAGG	EcoRI	pTTS12	Construction of pEMG-Δ*slvAT*
TS1_slv_R	GGCAACTGATCGGTGAAAAGCAC TTTGAGAGCGTCCATCAAGCC	-	pTTS12	Construction of pEMG-Δ*slvAT*
TS2_slv_F	GGCTTGATGGACGCTCTCAAAGT GCTTTTCACCGATCAGTTGC	-	pTTS12	Construction of pEMG-Δ*slvAT*
TS2_slv_R	GCCCAGGATCCCGAATGTCCATA ATCCAGGCGC	KpnI	pTTS12	Construction of pEMG-Δ*slvAT*
TS1_slvT_F	GCATAGGATCCGAGAATTGTGCAT AGTAAGTG	KpnI	pTTS12	Construction of pEMG-Δ*slvT*
TS1_slvT_R	GATCGTTGACCACAATATCTCCAG CTCCAGATGTAG	-	pTTS12	Construction of pEMG-Δ*slvT*
TS2_slvT_F	CTACATCTGGAGCTGGAGATATTG TGGTCAACGATC	-	pTTS12	Construction of pEMG-Δ*slvT*
TS2_slvT_R	AGGTTAAGCTTGTCTGCAGTGTCT ATTCC	HindIII	pTTS12	Construction of pEMG-Δ*slvT*
eco_gyrB_F	CGATAATTTTGCCAACCAC-GAT	-	gyrB	qPCR, reference gene
eco_gyrB_R	GAAATTCTCCTCCCAGAC-CAAA	-	gyrB	qPCR, reference gene

Oligos	Sequences (5'-3')	Restriction sites	PCR templates	Description
eco_rpoB_F	AACACGAGTTC-GAGAAGAAACT	-	rpoB	qPCR, reference gene
eco_rpoB_R	CGTTTAACCGCCAGA-TATACCT	-	rpoB	qPCR, reference gene
ppu_gyrB_F	GCTTCGACAAGATGATTTC-GTC	-	gyrB	qPCR, reference gene
ppu_gyrB_R	GCAGTTTGTCGATGTTG-TACTC	-	gyrB	qPCR, reference gene
ppu_rpoB_F	GACAAGGAATCGTCGAA-CAAAG	-	rpoB	qPCR, reference gene
ppu_rpoB_R	GAAGGTACCGTTCTCAGT-CATC	-	rpoB	qPCR, reference gene
srpA_F	CTCGGAAAACTTCA-GAGTTCCT	-	srpA	qPCR, target gene
srpA_R	AAAGCTTCTTGGTCTG-CAAAAG	-	srpA	qPCR, target gene
srpB_F	TACATGACCAGGAAGACCAG-TA	-	srpB	qPCR, target gene
srpB_R	GTGGAGGTCATTTATC-CCTACG	-	srpB	qPCR, target gene
srpC_F	GCCATAAGTTGATGTTCAG-CAG	-	srpC	qPCR, target gene
srpC_R	ATTCCAACGGATTTGC-CAAAAA	-	srpC	qPCR, target gene

Curing and complementation of megaplasmid pTTS12 from *P. putida* S12

P. putida S12 was grown in LB to reach early exponential phase (approximately 3 h or OD_{600} 0.4-0.6). Subsequently, mitomycin C was added to the liquid LB culture to a final concentration of 10, 20, 30, 40, or 50 μg ml^{-1}. These cultures were grown for 24 h and plated on M9 minimal media supplemented with indole to select for the absence of megaplasmid. Loss of megaplasmid was confirmed by loss of other phenotypes connected with the megaplasmid, such as MIC reduction of potassium tellurite and solvent sensitivity under toluene atmosphere, as well as through genomic DNA sequencing. Complementation of megaplasmid pTTS12 was performed using biparental mating between *P. putida* S12-1 (pTTS12 Km^R) and plasmid-cured genotypes *P. putida* S12 ΔpTTS12 (Gm^R :: Tn7) and followed by selection on LB agar supplemented with kanamycin and gentamicin.

Plasmid cloning

Deletion of *srpABC*, *slvT*, and *slvAT* genes was performed using homologous recombination between free-ended DNA sequences that are generated by cleavage at unique I-SceI sites

(37). Two homologous recombination sites were chosen downstream (TS-1) and upstream (TS-2) of the target genes. TS-1 and TS-2 fragments were obtained by performing PCR using primers listed in Table 4.2. Constructs were verified by DNA sequencing. Mating was performed as described by Wynands and colleagues (27). Deletion of *srpABC*, *slvT*, and *slvAT* was verified by PCR and Sanger sequencing (Macrogen B.V., Amsterdam, The Netherlands).

Introduction of the complete *srp* operon (*srpRSABC*) and *slvAT* was accomplished using the mini-Tn7 delivery vector backbone of pBG35 developed by Zobel and colleagues (46). The DNA fragments were obtained by PCR using primer pairs listed on Table 4.2 and ligated into pBG35 plasmid at PacI and XbaI restriction site. This construct generated a Tn7 transposon segment in pBG35 containing gentamicin resistance marker and *srp* operon with Tn7 recognition sites flanking on 5' and 3' sides of the segment. Restriction analysis followed by DNA sequencing (Macrogen, The Netherlands) were performed to confirm the correct pBG-srp, pBG-slv, and pBG-srp-slv construct. The resulting construct was cloned in *E. coli* WM3064 and introduced into *P. putida* or *E. coli* strains with the help of *E. coli* WM3064 pTnS-1. Integration of construct into the Tn7 transposon segment was confirmed by gentamicin resistance, PCR, and the ability of the resulting transformants to withstand and grow under toluene atmosphere conditions.

Toxin-antitoxin assay

Bacterial growth during toxin-antitoxin assay was observed on LB medium supplemented with 100 mg liter^{-1} ampicillin and 50 mg liter^{-1} kanamycin. Starting cultures were inoculated from a 1:100 dilution of overnight culture (OD_{600} 0.1) into a microtiter plate (96 well), and bacterial growth was measured using a Tecan Spark 10M instrument. To induce toxin and antitoxin, a total concentration of 0.8% (wt/vol) arabinose and 2 mM IPTG were added to the culture, respectively. Cell morphology was observed using light microscope (Zeiss Axiolab 5) at a magnification of x100. A final concentration of 2.5x SYBR Green I (10000x stock; New England Biolabs) was applied to visualize DNA, followed by two times washing with 1x phosphate-buffer saline (PBS), and analyzed using a Guava easyCyte single sample flow cytometer (Millipore). At indicated time points, NAD^+ levels were measured using NAD/NADH-Glo assay kit (Promega) according to the manufacturer's manual. The percentage of NAD^+ level was calculated by dividing the measured luminescence of tested strains with that of the control strains at the same timepoints. RPPX_26255 and RPPX_26260 were modelled using I-TASSER server

(35) and visualized using PyMol (version 2.3.1). Phylogenetic trees of toxin-antitoxin module derived from COG5654-COG5642 family were constructed using MEGA (version 10.0.5) as a maximum likelihood tree with 100 bootstraps and visualized using iTOL webserver (https://itol.embl.de) (47).

Data availability

The sequence data for wild-type *P. putida* S12 and plasmid-cured genotypes of *P. putida* S12 ΔpTTS12 have been submitted to the SRA database under accession number PRJNA602416.

References

1. Aono R, Kobayashi H. 1997. Cell surface properties of organic solvent-tolerant mutants of *Escherichia coli* K-12. Appl Environ Microbiol 63:3637–3642.
2. Kabelitz N, Santos PM, Heipieper HJ. 2003. Effect of aliphatic alcohols on growth and degree of saturation of membrane lipids in *Acinetobacter calcoaceticus*. FEMS Microbiol Lett 220:223–227.
3. Hartmans S, van der Werf MJ, de Bont JA. 1990. Bacterial degradation of styrene involving a novel flavin adenine dinucleotide-dependent styrene monooxygenase. Appl Environ Microbiol 56:1347–1351.
4. Heipieper HJ, Weber FJ, Sikkema J, Keweloh H, de Bont JAM. 1994. Mechanisms of resistance of whole cells to toxic organic solvents. Trends Biotechnol 12:409–415.
5. Wierckx NJP, Ballerstedt H, de Bont JAM, Wery J. 2005. Engineering of solvent-tolerant *Pseudomonas putida* S12 for bioproduction of phenol from glucose. Appl Environ Microbiol 71:8221–8227.
6. Verhoef S, Wierckx N, Westerhof RGM, de Winde JH, Ruijssenaars HJ. 2009. Bioproduction of p-hydroxystyrene from glucose by the solvent-tolerant bacterium *Pseudomonas putida* S12 in a two-phase water-decanol fermentation. Appl Environ Microbiol 75:931–936.
7. Verhoef S, Ruijssenaars HJ, de Bont JAM, Wery J. 2007. Bioproduction of p-hydroxybenzoate from renewable feedstock by solvent-tolerant *Pseudomonas putida* S12. J Biotechnol 132:49–56.
8. Ruijssenaars HJ, Sperling EMGM, Wiegerinck PHG, Brands FTL, Wery J, de Bont JAM. 2007. Testosterone 15beta-hydroxylation by solvent tolerant *Pseudomonas putida* S12. J Biotechnol 131:205–208.
9. Koopman F, Wierckx N, de Winde JH, Ruijssenaars HJ. 2010. Efficient whole-cell biotransformation of 5-(hydroxymethyl)furfural into FDCA, 2,5-furandicarboxylic acid. Bioresour Technol 101:6291–6296.
10. Volkers RJM, de Jong AL, Hulst AG, van Baar BLM, de Bont JAM, Wery J. 2006. Chemostat-based proteomic analysis of toluene-affected *Pseudomonas putida* S12. Environ Microbiol 8:1674–1679.
11. Volkers RJM, Snoek LB, Ruijssenaars HJ, de Winde JH. 2015. Dynamic Response of *Pseudomonas putida* S12 to Sudden Addition of Toluene and the Potential Role of the

Solvent Tolerance Gene trgI. PLoS One 10:e0132416.

12. Kuepper J, Ruijssenaars HJ, Blank LM, de Winde JH, Wierckx N. 2015. Complete genome sequence of solvent-tolerant *Pseudomonas putida* S12 including megaplasmid pTTS12. J Biotechnol 200:17–18.
13. Kieboom J, Dennis JJ, de Bont JAM, Zylstra GJ. 1998. Identification and Molecular Characterization of an Efflux Pump Involved in *Pseudomonas putida* S12 Solvent Tolerance. J Biol Chem 273:85–91.
14. Kieboom J, Dennis JJ, Zylstra GJ, de Bont JA. 1998. Active efflux of organic solvents by *Pseudomonas putida* S12 is induced by solvents. J Bacteriol 180:6769–6772.
15. Garikipati SVBJ, McIver AM, Peeples TL. 2009. Whole-Cell Biocatalysis for 1-Naphthol Production in Liquid-Liquid Biphasic Systems. Appl Environ Microbiol 75:6545–6552.
16. Janardhan Garikipati SVB, Peeples TL. 2015. Solvent resistance pumps of *Pseudomonas putida* S12: Applications in 1-naphthol production and biocatalyst engineering. J Biotechnol 210:91–99.
17. O'Connor KE, Dobson ADW, Hartmans S. 1997. Indigo formation by microorganisms expressing styrene monooxygenase activity. Appl Environ Microbiol 63:4287–4291.
18. Isken S, de Bont JAM. 2000. The solvent efflux system of *Pseudomonas putida*. Appl Microbiol Biotechnol 54:711–714.
19. Shao Y, Harrison EM, Bi D, Tai C, He X, Ou HY, Rajakumar K, Deng Z. 2011. TADB: A web-based resource for Type 2 toxin-antitoxin loci in bacteria and archaea. Nucleic Acids Res.
20. Xie Y, Wei Y, Shen Y, Li X, Zhou H, Tai C, Deng Z, Ou HY. 2018. TADB 2.0: An updated database of bacterial type II toxin-antitoxin loci. Nucleic Acids Res 46:D749–D753.
21. Harms A, Brodersen DE, Mitarai N, Gerdes K. 2018. Toxins, Targets, and Triggers: An Overview of Toxin-Antitoxin Biology. Mol Cell 70:768–784.
22. Maisonneuve E, Gerdes K. 2014. Molecular mechanisms underlying bacterial persisters. Cell 157:539–548.
23. McKenzie JL, Robson J, Berney M, Smith TC, Ruthe A, Gardner PP, Arcus VL, Cook GM. 2012. A VapBC toxin-antitoxin module is a posttranscriptional regulator of metabolic flux in *Mycobacteria.* J Bacteriol 194:2189–2204.
24. Pinto UM, Pappas KM, Winans SC. 2012. The ABCs of plasmid replication and seg-

regation. Nat Rev Microbiol 10:755–765.

25. Trevors JT. 1986. Plasmid curing in bacteria. FEMS Microbiol Lett 32:149–157.
26. Chakrabarty AM. 1972. Genetic basis of the biodegradation of salicylate in *Pseudomonas*. J Bacteriol 112:815–823.
27. Wynands B, Lenzen C, Otto M, Koch F, Blank LM, Wierckx N. 2018. Metabolic engineering of *Pseudomonas taiwanensis* VLB120 with minimal genomic modifications for high-yield phenol production. Metab Eng 47:121–133.
28. Nikel PI, de Lorenzo V. 2018. *Pseudomonas putida* as a functional chassis for industrial biocatalysis: From native biochemistry to trans-metabolism. Metab Eng 50:142–155.
29. Studier FW, Moffatt BA. 1986. Use of bacteriophage T7 RNA polymerase to direct selective high-level expression of cloned genes. J Mol Biol 189:113–130.
30. Puigbò P, Bravo IG, Garcia-Vallve S. 2008. CAIcal: A combined set of tools to assess codon usage adaptation. Biol Direct 3:38.
31. Makarova KS, Wolf YI, Koonin E V. 2009. Comprehensive comparative-genomic analysis of Type 2 toxin-antitoxin systems and related mobile stress response systems in prokaryotes. Biol Direct 4:19.
32. Piscotta FJ, Jeffrey PD, Link AJ. 2019. ParST is a widespread toxin–antitoxin module that targets nucleotide metabolism. Proc Natl Acad Sci 116:826–834.
33. Skjerning RB, Senissar M, Winther KS, Gerdes K, Brodersen DE. 2018. The RES domain toxins of RES-Xre toxin-antitoxin modules induce cell stasis by degrading NAD. Mol Microbiol 66:213.
34. Freire DM, Gutierrez C, Garza-Garcia A, Grabowska AD, Sala AJ, Ariyachaokun K, Panikova T, Beckham KSH, Colom A, Pogenberg V, Cianci M, Tuukkanen A, Boudehen YM, Peixoto A, Botella L, Svergun DI, Schnappinger D, Schneider TR, Genevaux P, de Carvalho LPS, Wilmanns M, Parret AHA, Neyrolles O. 2019. An NAD^+ Phosphorylase Toxin Triggers *Mycobacterium tuberculosis* Cell Death. Mol Cell 73:1–10.
35. Yang J, Yan R, Roy A, Xu D, Poisson J, Zhang Y. 2015. The I-TASSER suite: Protein structure and function prediction. Nat Methods 12:7–8.
36. Murphy JR. 2011. Mechanism of diphtheria toxin catalytic domain delivery to the eukaryotic cell cytosol and the cellular factors that directly participate in the process. Toxins (Basel) 3:294–308.

37. Martínez-García E, de Lorenzo V. 2011. Engineering multiple genomic deletions in Gram-negative bacteria: analysis of the multi-resistant antibiotic profile of *Pseudomonas putida* KT2440. Environ Microbiol 13:2702–2716.

38. Holtwick R, Meinhardt F, Keweloh H. 1997. cis-trans isomerization of unsaturated fatty acids: Cloning and sequencing of the cti gene from *Pseudomonas putida* P8. Appl Environ Microbiol 63:4292–4297.

39. Pullinger GD, Lax AJ. 1992. A *Salmonella dublin* virulence plasmid locus that affects bacterial growth under nutrient-limited conditions. Mol Microbiol 6:1631–1643.

40. Zhang YX, Guo XK, Wu C, Bi B, Ren SX, Wu CF, Zhao GP. 2004. Characterization of a novel toxin-antitoxin module, VapBC, encoded by *Leptospira interrogans* chromosome. Cell Res 14:208–216.

41. Sun C, Guo Y, Tang K, Wen Z, Li B, Zeng Z, Wang X. 2017. MqsR/MqsA toxin/antitoxin system regulates persistence and biofilm formation in *Pseudomonas putida* KT2440. Front Microbiol 8:840.

42. Tamman H, Ainelo A, Ainsaar K, Hõrak R. 2014. A moderate toxin, GraT, modulates growth rate and stress tolerance of *Pseudomonas putida*. J Bacteriol 196:157–169.

43. Page R, Peti W. 2016. Toxin-antitoxin systems in bacterial growth arrest and persistence. Nat Chem Biol 12:208–214.

44. Muthuramalingam M, White JC, Bourne CR. 2016. Toxin-antitoxin modules are pliable switches activated by multiple protease pathways. Toxins 8:214.

45. Abril MA, Michan C, Timmis KN, Ramos JL. 1989. Regulator and enzyme specificities of the TOL plasmid-encoded upper pathway for degradation of aromatic hydrocarbons and expansion of the substrate range of the pathway. J Bacteriol 171:6782–6790.

46. Zobel S, Benedetti I, Eisenbach L, de Lorenzo V, Wierckx N, Blank LM. 2015. Tn7-Based Device for Calibrated Heterologous Gene Expression in *Pseudomonas putida*. ACS Synth Biol 4:1341–1351.

47. Letunic I, Bork P. 2019. Interactive Tree Of Life (iTOL) v4: recent updates and new developments. Nucleic Acids Res 47:W256–W25.

48. Bagdasarian M, Lurz R, Rückert B, Franklin FCH, Bagdasarian MM, Frey J, Timmis KN. 1981. Specific-purpose plasmid cloning vectors II. Broad host range, high copy number, RSF 1010-derived vectors, and a host-vector system for gene cloning in *Pseudomonas*. Gene 16:237–247.

49. Boyer HW, Roulland-dussoix D. 1969. A complementation analysis of the restriction and modification of DNA in *Escherichia coli*. J Mol Biol 41:459–472.

50. Herrero M, De Lorenzo V, Timmis KN. 1990. Transposon vectors containing non-antibiotic resistance selection markers for cloning and stable chromosomal insertion of foreign genes in gram-negative bacteria. J Bacteriol 172:6557–6567.

51. Figurski DH, Helinski DR. 1979. Replication of an origin-containing derivative of plasmid RK2 dependent on a plasmid function provided in trans. Proc Natl Acad Sci 76:1648–1652.

52. Choi K-H, Gaynor JB, White KG, Lopez C, Bosio CM, Karkhoff-Schweizer RR, Schweizer HP. 2005. A Tn7-based broad-range bacterial cloning and expression system. Nat Methods 2:443–448.

Supplementary Materials

Table 4.S1. Expression of *srpABC* genes in *P. putida* and *E. coli* strains in basal level and in the presence of 0.1% (vol/vol) toluene with *gyrB* and *rpoB* as reference genes

Genes	Strains	Basal expression	Toluene induced expression	Fold change
srpA	*P. putida* S12	1.69 ± 0.31	4.08 ± 0.79	2.44 ± 0.50
	P. putida S12-6.1	2.27 ± 0.36	4.56 ± 1.08	1.99 ± 0.28
	P. putida KT2440-srp	2.84 ± 0.92	5.60 ± 1.79	1.99 ± 0.28
	E. coli BL21(DE3)-srp	3.30 ± 0.43	6.60 ± 2.06	1.98 ± 0.45
	E. coli TG1-srp	5.28 ± 1.76	11.06 ± 4.10	2.10 ± 0.36
srpB	*P. putida* S12	1.92 ± 0.36	3.83 ± 0.76	2.02 ± 0.42
	P. putida S12-6.1	2.57 ± 0.33	5.49 ± 1.13	2.15 ± 0.46
	P. putida KT2440-srp	3.51 ± 1.22	6.59 ± 1.87	1.91 ± 0.20
	E. coli BL21(DE3)-srp	3.69 ± 0.58	7.52 ± 2.26	2.01 ± 0.36
	E. coli TG1-srp	5.35 ± 1.97	11.52 ± 4.84	2.21 ± 0.75
srpC	*P. putida* S12	2.01 ± 0.28	3.96 ± 0.75	1.97 ± 0.29
	P. putida S12-6.1	2.32 ± 0.27	4.45 ± 0.99	1.91 ± 0.35
	P. putida KT2440-srp	2.07 ± 0.68	5.13 ± 1.55	2.50 ± 0.22
	E. coli BL21(DE3)-srp	3.41 ± 0.52	6.70 ± 1.67	1.95 ± 0.25
	E. coli TG1-srp	4.18 ± 1.40	9.78 ± 5.23	2.32 ± 0.92

Table 4.S2. Codon adaptation index of *srp* operon in *E. coli* and *P. putida* reference strains

Genes	Length	CAI	%G+C	Nc	Species	Strain
srpA	1170	0.598	56.5	57.2	*E.coli*	K12
	1170	0.6	56.5	57.2	*E.coli*	B
	1170	0.742	56.5	57.2	*E.coli*	N/A
	1170	0.442	56.5	57.2	*P.putida*	F1
	1170	0.468	56.5	57.2	*P.putida*	N/A
	1170	0.372	56.5	57.2	*P.putida*	GB1
srpB	3150	0.662	56.5	46.1	*E.coli*	K12
	3150	0.67	56.5	46.1	*E.coli*	B
	3150	0.749	56.5	46.1	*E.coli*	N/A
	3150	0.565	56.5	46.1	*P.putida*	F1
	3150	0.587	56.5	46.1	*P.putida*	N/A
	3150	0.502	56.5	46.1	*P.putida*	GB1
srpC	1413	0.62	54.2	51.3	*E.coli*	K12
	1413	0.628	54.2	51.3	*E.coli*	B
	1413	0.735	54.2	51.3	*E.coli*	N/A
	1413	0.456	54.2	51.3	*P.putida*	F1
	1413	0.483	54.2	51.3	*P.putida*	N/A
	1413	0.394	54.2	51.3	*P.putida*	GB1
srpR	642	0.604	54.5	59.8	*E.coli*	K12
	642	0.622	54.5	59.8	*E.coli*	B
	642	0.724	54.5	59.8	*E.coli*	N/A
	642	0.464	54.5	59.8	*P.putida*	F1
	642	0.491	54.5	59.8	*P.putida*	N/A
	642	0.399	54.5	59.8	*P.putida*	GB1
srpS	780	0.636	55.4	55.5	*E.coli*	K12
	780	0.638	55.4	55.5	*E.coli*	B
	780	0.737	55.4	55.5	*E.coli*	N/A
	780	0.47	55.4	55.5	*P.putida*	F1
	780	0.496	55.4	55.5	*P.putida*	N/A
	780	0.399	55.4	55.5	*P.putida*	GB1

Table 4.S3. Putative COG5654-COG5642 RES-Xre toxin-antitoxin from NCBI RefSeq (31)

Strain	Protein ID	
	Toxin	Antitoxin
Acidovorax sp. JS42	YP_984893.1	YP_984894.1
Mycobacterium bovis BCG str. Pasteur 1173P2	YP_978095.1	YP_978096.1
Marinobacter hydrocarbonoclasticus VT8	YP_958617.1	YP_958618.1
Mycobacterium sp. KMS	YP_935598.1	YP_935597.1
Shewanella amazonensis SB2B	YP_928802.1	YP_928803.1
Shewanella sp. ANA-3	YP_863727.1	YP_863728.1
Gramella forsetii KT0803	YP_862703.1	YP_862704.1
Ralstonia eutropha H16	YP_840783.1	YP_840782.1
Burkholderia cenocepacia HI2424	YP_839838.1	YP_839837.1
Burkholderia cenocepacia HI2424	YP_837474.1	YP_837473.1
Rhodopseudomonas palustris BisA53	YP_780344.1	YP_780345.1
Rhodopseudomonas palustris BisA53	YP_778971.1	YP_778972.1
Burkholderia ambifaria AMMD	YP_777867.1	YP_777868.1
Burkholderia ambifaria AMMD	YP_777448.1	YP_777447.1
Burkholderia ambifaria AMMD	YP_777114.1	YP_777115.1
Rhizobium leguminosarum bv. viciae 3841	YP_771125.1	YP_771124.1
Rhizobium leguminosarum bv. viciae 3841	YP_771096.1	YP_771097.1
Rhizobium leguminosarum bv. viciae 3841	YP_765386.1	YP_765385.1
Rhizobium leguminosarum bv. viciae 3841	YP_764601.1	YP_764602.1
Nitrosomonas eutropha C91	YP_748179.1	YP_748180.1
Alkalilimnicola ehrlichii MLHE-1	YP_741338.1	YP_741337.1
Ralstonia eutropha H16	YP_725909.1	YP_725910.1
Trichodesmium erythraeum IMS101	YP_721262.1	YP_721261.1
Alcanivorax borkumensis SK2	YP_693226.1	YP_693225.1
Chelativorans sp. BNC1	YP_673203.1	YP_673204.1
Yersinia pestis Antiqua	YP_651606.1	YP_651605.1
Yersinia pestis Nepal516	YP_647735.1	YP_647734.1
Burkholderia cenocepacia AU 1054	YP_625684.1	YP_625683.1
Burkholderia cenocepacia AU 1054	YP_624375.1	YP_624376.1
Cupriavidus metallidurans CH34	YP_583373.1	YP_583374.1
Nitrobacter hamburgensis X14	YP_578969.1	YP_578968.1
Burkholderia xenovorans LB400	YP_552488.1	YP_552489.1
Polaromonas sp. JS666	YP_551796.1	YP_551795.1
Rhodopseudomonas palustris BisB18	YP_533769.1	YP_533770.1
Rhodopseudomonas palustris BisB18	YP_531278.1	YP_531277.1
Rhodoferax ferrireducens T118	YP_524055.1	YP_524056.1
Rhodopseudomonas palustris HaA2	YP_487787.1	YP_487786.1
Rhodopseudomonas palustris HaA2	YP_483989.1	YP_483990.1

Strain	Toxin	Antitoxin
Rhizobium etli CFN 42	YP_472228.1	YP_472227.1
Anaeromyxobacter dehalogenans 2CP-C	YP_464961.1	YP_464960.1
Erythrobacter litoralis HTCC2594	YP_457022.1	YP_457021.1
Salinibacter ruber DSM 13855	YP_446753.1	YP_446752.1
Salinibacter ruber DSM 13855	YP_444335.1	YP_444336.1
Rhodospirillum rubrum ATCC 11170	YP_428817.1	YP_428816.1
Rhodospirillum rubrum ATCC 11170	YP_428306.1	YP_428307.1
Rhodospirillum rubrum ATCC 11170	YP_427975.1	YP_427974.1
Rhodospirillum rubrum ATCC 11170	YP_425903.1	YP_425904.1
Brucella abortus 2308	YP_419077.1	YP_419076.1
Nitrosospira multiformis ATCC 25196	YP_411613.1	YP_411612.1
Synechococcus elongatus PCC 7942	YP_399513.1	YP_399514.1
Geobacter metallireducens GS-15	YP_384617.1	YP_384616.1
Burkholderia lata	YP_373007.1	YP_373008.1
Burkholderia lata	YP_366311.1	YP_366310.1
Rhodobacter sphaeroides 2.4.1	YP_353530.1	YP_353531.1
Pseudomonas fluorescens Pf0-1	YP_348851.1	YP_348852.1
Rhodobacter sphaeroides 2.4.1	YP_345300.1	YP_345299.1
Nitrosococcus oceani ATCC 19707	YP_342684.1	YP_342683.1
Thiobacillus denitrificans ATCC 25259	YP_315251.1	YP_315252.1
Ralstonia eutropha JMP134	YP_295535.1	YP_295536.1
Ralstonia eutropha JMP134	YP_293190.1	YP_293191.1
Pseudomonas syringae pv. phaseolicola 1448A	YP_273196.1	YP_273197.1
Pseudomonas protegens Pf-5	YP_257886.1	YP_257887.1
Pseudomonas syringae pv. syringae B728a	YP_233980.1	YP_233981.1
Brucella abortus bv. 1 str. 9-941	YP_223658.1	YP_223657.1
Aromatoleum aromaticum EbN1	YP_195457.1	YP_195458.1
Synechococcus elongatus PCC 6301	YP_171736.1	YP_171735.1
Aromatoleum aromaticum EbN1	YP_160869.1	YP_160870.1
Legionella pneumophila str. Paris	YP_123890.1	YP_123891.1
Burkholderia pseudomallei K96243	YP_111824.1	YP_111825.1
Legionella pneumophila subsp. pneumophila str. Philadelphia 1	YP_095631.1	YP_095632.1
Yersinia pseudotuberculosis IP 32953	YP_070779.1	YP_070778.1
Leifsonia xyli subsp. xyli str. CTCB07	YP_063014.1	YP_063013.1
Pectobacterium atrosepticum SCRI1043	YP_050894.1	YP_050895.1
Geobacter bemidjiensis Bem	YP_002136885.1	YP_002136886.1
Anaeromyxobacter sp. K	YP_002134448.1	YP_002134449.1
Cupriavidus taiwanensis LMG 19424	YP_002007827.1	YP_002007826.1
Cupriavidus taiwanensis LMG 19424	YP_002005344.1	YP_002005345.1
Chloroherpeton thalassium ATCC 35110	YP_001997574.1	YP_001997575.1

Strain	Toxin	Antitoxin
Rhodopseudomonas palustris TIE-1	YP_001992552.1	YP_001992551.1
Rhizobium etli CIAT 652	YP_001985675.1	YP_001985674.1
Burkholderia multivorans ATCC 17616	YP_001948023.1	YP_001948022.1
Burkholderia multivorans ATCC 17616	YP_001941953.1	YP_001941954.1
Brucella abortus S19	YP_001932799.1	YP_001932798.1
Methylobacterium populi BJ001	YP_001924424.1	YP_001924425.1
Burkholderia phytofirmans PsJN	YP_001890479.1	YP_001890478.1
Yersinia pseudotuberculosis PB1/+	YP_001872759.1	YP_001872758.1
Burkholderia phymatum STM815	YP_001863413.1	YP_001863414.1
Burkholderia phymatum STM815	YP_001863338.1	YP_001863339.1
Burkholderia phymatum STM815	YP_001860557.1	YP_001860558.1
Beijerinckia indica subsp. indica ATCC 9039	YP_001832632.1	YP_001832633.1
Burkholderia ambifaria MC40-6	YP_001815841.1	YP_001815840.1
Burkholderia ambifaria MC40-6	YP_001815740.1	YP_001815741.1
Burkholderia ambifaria MC40-6	YP_001812408.1	YP_001812407.1
Burkholderia ambifaria MC40-6	YP_001810424.1	YP_001810423.1
Burkholderia cenocepacia MC0-3	YP_001777325.1	YP_001777326.1
Burkholderia cenocepacia MC0-3	YP_001774298.1	YP_001774297.1
Shewanella woodyi ATCC 51908	YP_001761847.1	YP_001761846.1
Shewanella woodyi ATCC 51908	YP_001760834.1	YP_001760833.1
Yersinia pseudotuberculosis YPIII	YP_001720644.1	YP_001720645.1
Caulobacter sp. K31	YP_001686389.1	YP_001686390.1
Pseudomonas putida GB-1	YP_001668316.1	YP_001668315.1
Brucella suis ATCC 23445	YP_001622109.1	YP_001622110.1
Yersinia pestis Angola	YP_001606943.1	YP_001606942.1
Brucella canis ATCC 23365	YP_001594232.1	YP_001594233.1
Burkholderia multivorans ATCC 17616	YP_001585295.1	YP_001585294.1
Azorhizobium caulinodans ORS 571	YP_001527226.1	YP_001527227.1
Vibrio campbellii ATCC BAA-1116	YP_001447766.1	YP_001447765.1
Parvibaculum lavamentivorans DS-1	YP_001413635.1	YP_001413636.1
Xanthobacter autotrophicus Py2	YP_001409444.1	YP_001409443.1
Xanthobacter autotrophicus Py2	YP_001409339.1	YP_001409340.1
Yersinia pseudotuberculosis IP 31758	YP_001400767.1	YP_001400768.1
Ochrobactrum anthropi ATCC 49188	YP_001371470.1	YP_001371469.1
Sinorhizobium medicae WSM419	YP_001314122.1	YP_001314121.1
Sinorhizobium medicae WSM419	YP_001313272.1	YP_001313271.1
Sinorhizobium medicae WSM419	YP_001312332.1	YP_001312331.1
Mycobacterium tuberculosis F11	YP_001287957.1	YP_001287958.1
Mycobacterium tuberculosis H37Ra	YP_001283324.1	YP_001283325.1
Pseudomonas putida F1	YP_001268571.1	YP_001268572.1
Sphingomonas wittichii RW1	YP_001262457.1	YP_001262456.1

Strain	Toxin	Antitoxin
Sphingomonas wittichii RW1	YP_001260351.1	YP_001260352.1
Brucella ovis ATCC 25840	YP_001257308.1	YP_001257309.1
Legionella pneumophila str. Corby	YP_001250345.1	YP_001250346.1
Geobacter uraniireducens Rf4	YP_001231219.1	YP_001231220.1
Pseudomonas stutzeri A1501	YP_001172612.1	YP_001172613.1
Rhodobacter sphaeroides ATCC 17025	YP_001168572.1	YP_001168573.1
Novosphingobium aromaticivorans DSM 12444	YP_001166184.1	YP_001166185.1
Yersinia pestis Pestoides F	YP_001162176.1	YP_001162177.1
Polynucleobacter necessarius subsp. asymbioticus QLW-P1DM-WA-1	YP_001155131.1	YP_001155130.1
Mycobacterium gilvum PYR-GCK	YP_001136659.1	YP_001136660.1
Burkholderia vietnamiensis G4	YP_001115251.1	YP_001115250.1
Burkholderia vietnamiensis G4	YP_001114818.1	YP_001114817.1
Burkholderia vietnamiensis G4	YP_001114692.1	YP_001114691.1
Burkholderia vietnamiensis G4	YP_001110405.1	YP_001110406.1
Burkholderia vietnamiensis G4	YP_001109906.1	YP_001109907.1
Burkholderia pseudomallei 1106a	YP_001076500.1	YP_001076501.1
Mycobacterium sp. JLS	YP_001072829.1	YP_001072830.1
Mycobacterium sp. JLS	YP_001072800.1	YP_001072801.1
Burkholderia pseudomallei 668	YP_001063601.1	YP_001063602.1
Rhodobacter sphaeroides ATCC 17029	YP_001043985.1	YP_001043986.1
Methylibium petroleiphilum PM1	YP_001021529.1	YP_001021528.1
Yersinia enterocolitica subsp. enterocolitica 8081	YP_001006356.1	YP_001006355.1
Yersinia pestis biovar Microtus str. 91001	NP_993465.1	NP_993464.1
Rhodopseudomonas palustris CGA009	NP_948506.1	NP_948505.1
Ralstonia eutropha H16	NP_942832.1	NP_942831.1
Photorhabdus luminescens subsp. laumondii TTO1	NP_929604.1	NP_929603.1
Gloeobacter violaceus PCC 7421	NP_925671.1	NP_925670.1
Gloeobacter violaceus PCC 7421	NP_924158.1	NP_924159.1
Chromobacterium violaceum ATCC 12472	NP_899706.1	NP_899705.1
Bordetella bronchiseptica RB50	NP_889433.1	NP_889434.1
Bordetella parapertussis 12822	NP_885120.1	NP_885121.1
Bordetella pertussis Tohama I	NP_880058.1	NP_880057.1
Mycobacterium bovis AF2122/97	NP_855661.1	NP_855662.1
Nitrosomonas europaea ATCC 19718	NP_842117.1	NP_842116.1
Vibrio parahaemolyticus RIMD 2210633	NP_800280.1	NP_800279.1
Pseudomonas syringae pv. tomato str. DC3000	NP_790873.1	NP_790874.1
Pseudomonas putida KT2440	NP_744582.1	NP_744581.1
Brucella suis 1330	NP_699467.1	NP_699468.1
Yersinia pestis KIM10+	NP_669301.1	NP_669302.1
Brucella melitensis bv. 1 str. 16M	NP_541956.1	NP_541955.1

Strain	Toxin	Antitoxin
Sinorhizobium meliloti 1021	NP_437942.1	NP_437943.1
Sinorhizobium meliloti 1021	NP_437247.1	NP_437246.1
Sinorhizobium meliloti 1021	NP_436473.1	NP_436474.1
Sinorhizobium meliloti 1021	NP_436040.1	NP_436041.1
Yersinia pestis CO92	NP_405883.1	NP_405882.1
Agrobacterium fabrum str. C58	NP_353871.2	NP_353870.2
Mycobacterium tuberculosis CDC1551	NP_336505.1	NP_336506.1
Mycobacterium tuberculosis H37Rv	NP_216505.1	NP_216506.1
Mesorhizobium loti MAFF303099	NP_103613.1	NP_103614.1
Mesorhizobium loti MAFF303099	NP_085650.1	NP_085649.1
Sphingobium sp. YBL2	AJR25280.1	AJR25281.1
Pseudomonas putida S12	AJA16860.1	AJA16859.1

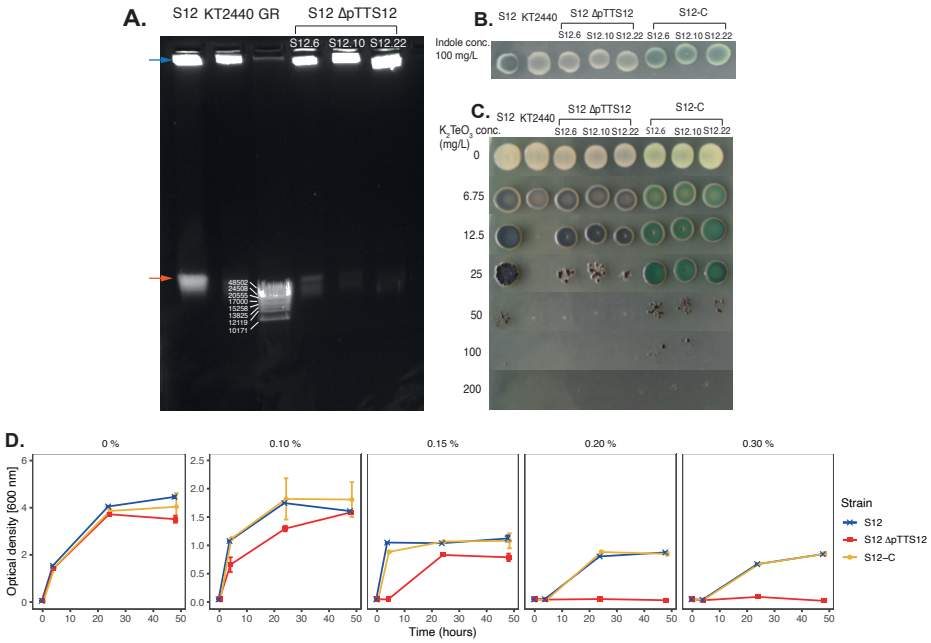

Fig. 4.S1. Removal and complementation of the megaplasmid pTTS12 from *P. putida* S12.

A. The loss of the megaplasmid band in megaplasmid-cured *P. putida* S12 proven by electrophoresis of agarose embedded genomic DNA. Megaplasmid band (orange arrow) was visible in the positive control *P. putida* S12 and absent in negative control *P. putida* KT2440 and Mitomycin C treated strains (strain S12-6, S12-10, and S12-22). Blue arrow indicates bacterial chromosome.

B. Activity of styrene monooxygenase (SMO) and styrene oxide isomerase (SOI) for indigo formation from indole in *P. putida* strains. Enzyme activity was lost in the megaplasmid-cured strains S12 ΔpTTS12 (white colonies) and restored with the complementation of megaplasmid in the strains S12-C (blue colonies). Indole (100 mg L^{-1}) was supplemented in M9 minimum media.

C. K_2TeO_3 resistance of *P. putida* strains on lysogeny broth (LB) agar. Tellurite resistance was reduced in the megaplasmid-cured strains S12 ΔpTTS12 (MIC 50 mg L^{-1}) and restored with the complementation of megaplasmid in the strains S12-C (MIC 200 mg L^{-1}).

D. Solvent tolerance analysis was performed on *P. putida* S12, *P. putida* S12 ΔpTTS12, and *P. putida* S12-C growing in liquid LB media with 0, 0.10, 0.15, 0.20 and 0.30 % v/v toluene. The removal of the megaplasmid pTTS12 clearly caused a significant reduction in the solvent tolerance of *P. putida* S12 ΔpTTS12. Complementation of pTTS12 restores the solvent tolerance trait in *P. putida* S12-C. This figure displays the mean of three independent replicates and error bars indicate standard deviation. The range of y-axis is different in the first panel (0 - 6) than the rest of the panels (0 - 2.5).

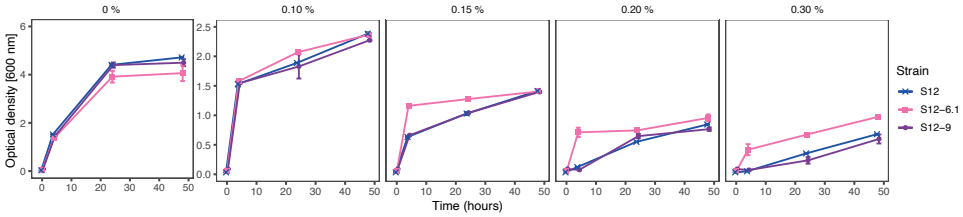

Fig. 4.S2. Metabolic burden of megaplasmid pTTS12 during growth in the presence of organic solvent.

Solvent tolerance was compared between *P. putida* S12, *P. putida* S12-6.1 (S12-6 srp::attn7), and *P. putida* S12-9 (S12-6 srp::attn7, pTTS12 tet::srp) in liquid LB media with 0, 0.10, 0.15, and 0.20 % v/v toluene. This figure displays the mean of three independent replicates and error bars indicate standard deviation. The range of y-axis is different in the first panel (0 - 6) than the rest of the panels (0 - 2.5).

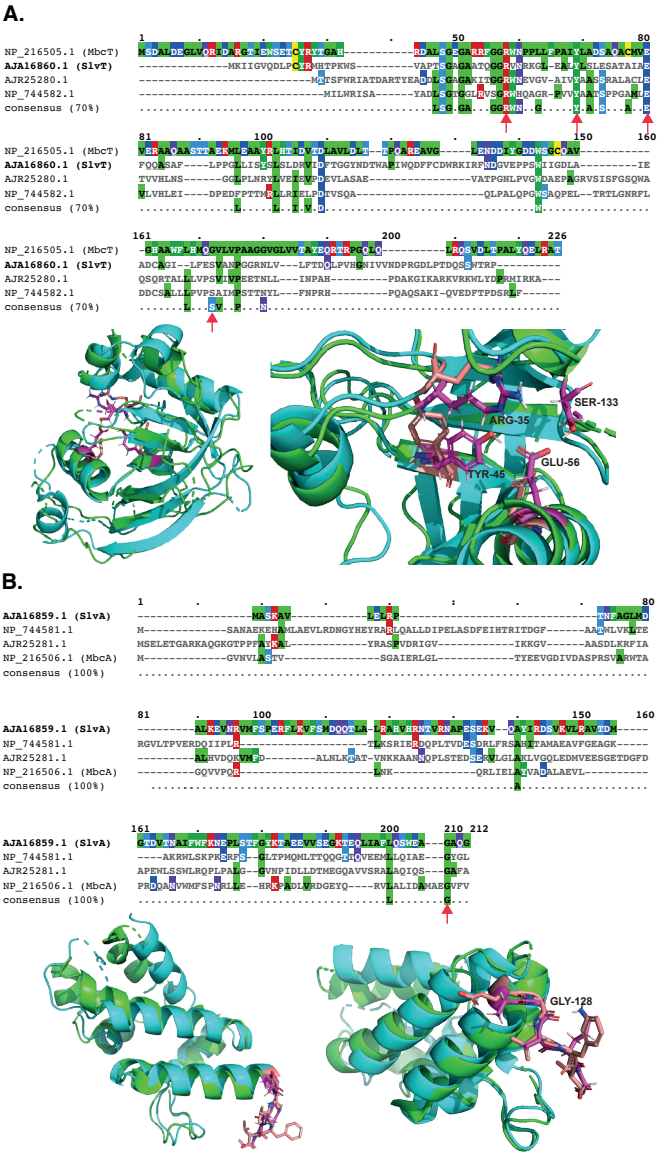

Fig. 4. S3. Multiple alignment of SlvT and SlvA with characterized toxin-antitoxin of COG5654- COG5642 family

A. Sequence similarity of SlvT from *P. putida* S12 with several characterized COG5654-family toxin protein and overlay of the predicted structure of SlvT (green) against the crystal structure of MbcT (turqoise). B. Sequence similarity of the SlvA from *P. putida* S12 with several characterized COG5642-family antitoxin protein and overlay of the predicted structure of SlvA (green) against the crystal structure of MbcA (turqoise). Putative active site residues which showed >70% similarities are indicated by arrows in the alignment or as magenta (SlvTA) and beige (MbcTA) sticks in the protein 3D structure overlay.

CHAPTER 5

Adaptive laboratory evolution restores solvent tolerance in plasmid-cured *Pseudomonas putida* S12; a molecular analysis

Hadiastri Kusumawardhani, Benjamin Furtwängler, Matthijs Blommestijn, Adelė Kaltenytė, Jaap van der Poel, Jan Kolk, Rohola Hosseini, Johannes H. de Winde

Submitted for publication.

DOI: 10.1101/2020.08.01.232264

Abstract

Pseudomonas putida S12 is intrinsically solvent-tolerant and constitutes a promising platform for biobased production of aromatic compounds and biopolymers. The genome of *P. putida* S12 consists of a 5.8 Mbp chromosome, and a 580 kbp megaplasmid pTTS12 that carries several gene clusters involved in solvent tolerance. Removal of pTTS12 caused a significant reduction in solvent tolerance. In this study, we succeeded in restoring solvent tolerance in plasmid-cured *P. putida* S12 using adaptive laboratory evolution (ALE), underscoring the innate solvent-tolerance of this strain.

Whole genome sequencing revealed several single nucleotide polymorphisms (SNPs) and a mobile element insertion, enabling ALE-derived strains to survive and sustain growth in the presence of a high toluene concentration (10% (vol/vol)). Mutations were identified in an RND efflux pump regulator *arpR*, resulting in constitutive upregulation of the multifunctional efflux pump ArpABC. SNPs were also found in the intergenic region and subunits of ATP synthase, RNA polymerase subunit β', global two-component regulatory system (GacA/GacS) and a putative AraC-family transcriptional regulator Afr. RNA-seq analysis further revealed a constitutive down-regulation of energy consuming activities in ALE-derived strains, including flagellar assembly, F0F1 ATP synthase, and membrane transport proteins. Our results indicate that constitutive expression of an alternative solvent extrusion pump in combination with high metabolic flexibility ensures restoration of solvent-tolerance in *P. putida* S12 lacking its megaplasmid.

Introduction

Pseudomonas putida is a promising microbial host for biobased production of valuable chemicals and biopolymer compounds (1). Endowed with its natural versatility, *P. putida* is robust towards toxic compounds which may arise in whole-cell biocatalysis processes as substrates, intermediates, or products. *P. putida* displays a remarkable intrinsic oxidative stress- and solvent-tolerance. This may be further optimized for utilization of secondary feedstock as carbon source and production of various aromatic compounds and bioplastics monomers (2–9). Moreover, several metabolic models and genetic tools are currently available for the design and implementation of novel biosynthetic pathways in *P. putida* (10–12).

P. putida S12 was isolated from soil on minimal media to use styrene as its sole carbon source (13). It is highly tolerant towards organic solvents and aromatic compounds which are often toxic towards microbial hosts. As such, this strain has been used to produce a variety of high value aromatic compounds (6, 8, 9, 14). Organic solvents and aromatic compounds are toxic to most bacteria as these compounds are able to accumulate in the bacterial membrane and thus alter membrane integrity (15), resulting in damage and loss of various membrane functions such as permeability barrier, matrix for protein and metabolic reaction, energy transduction and denaturation of essential enzymes.

The *P. putida* S12 genome comprises of a 5.8 Mbp chromosome and a single-copy 583 kbp megaplasmid pTTS12 (16). Plasmid pTTS12 encodes, among others, an RND efflux pump (SrpABC), a styrene–phenylacetate degradation pathway, and a toxin-antitoxin module slvTA are responsible for high solvent tolerance of *P. putida* S12 (13, 17, 18). A significant reduction of solvent-tolerance was previously demonstrated when *P. putida* S12 was cured from its megaplasmid. As a result of plasmid-curing, *P. putida* S12 ΔpTTS12 could only survive and sustain growth in a maximum of 0.15% (vol/vol) toluene (18). As a comparison, wildtype S12 can sustain growth in 0.30% toluene and survive up to 10% toluene. However, as was previously demonstrated, the expression of SrpABC efflux pump in *E. coli* and the non-solvent-tolerant *P. putida* KT2440 instigated still a lower solvent-tolerance than in *P. putida* S12, indicating the intrinsic solvent-tolerance of *P. putida* S12 (18).

In this paper, we further addressed the intrinsic solvent tolerance of *P. putida* S12. Megaplasmid pTTS12 may confer genetic adaptation towards environmental chemical stressors like organic solvents and aromatic compounds, through horizontal gene transfer. Here, we examined the ability of plasmid-cured *P. putida* S12 to survive and sustain growth in the

presence of toluene. Using adaptive laboratory evolution (ALE), we were able to restore the solvent tolerance in *P. putida* S12 lacking the megaplasmid. Specific mutations putatively responsible for the restored solvent-tolerance trait were characterized. Moreover, RNA-seq transcriptional analysis revealed the constitutive responses of the plasmid-cured *P. putida* S12 after adaptation to the elevated toluene concentration.

Materials and Methods

Strains and culture conditions

Strains and plasmids used in this paper are listed in Table 5.S1. *P. putida* strains were grown in Lysogeny Broth (LB) on 30 °C with 200 rpm shaking. *E. coli* strains were cultivated in LB on 37 °C with 250 rpm. For solid cultivation, 1.5 % (wt/vol) agar was added to LB. When required, gentamycin (25 mg l^{-1}), ampicillin (100 mg l^{-1}), kanamycin (50 mg l^{-1}), and streptomycin (50 mg l^{-1}) were added to the media. Hartman's minimal medium (13) was supplemented with 2 mg $MgSO_4$ and 0.2 % (wt/vol) of citrate, 0.4% (wt/vol) of glycerol, or 0.2% (wt/vol) of glucose may be added as sole carbon source. Growth parameters were measured in a 96-well plates using a Tecan Spark 10M instrument and calculated using growthcurver R-package ver.0.3.0 (19). Maximum growth rate (μmax) was calculated as the fastest growth rate when there were no restrictions imposed on total population size (t = 2-5 hours). Maximum OD_{600} (maxOD) was defined as the OD_{600} measurement after the stationary phase was reached (t ~ 10 hours). Solvent tolerance analysis was performed by growing 20 ml of *P. putida* culture (starting OD_{600} ± 0.1) on LB with the addition of toluene (0.15 – 10% (vol/vol) in 250 ml Boston glass bottles with Mininert® valve (Sigma-Aldrich) bottle caps. Cell turbidity (OD600) was measured at timepoint 0, 4, 24, and 48 hours to indicate biomass growth. If biomass growth could not be observed, 1 ml of the liquid culture was plated with serial dilution to determine the bacterial survival (viable cell count).

Adaptive Laboratory Evolution

P. putida strains were grown overnight on LB, 30 °C with 200 rpm shaking. Starting cultures were diluted 100 times with LB (starting OD_{600} ± 0.05) and 20 ml of this diluted cultures were placed in Boston bottles. Toluene was added (0.15% (vol/vol)) into the cultures and the bottles were immediately closed using Mininert® bottle caps. These cultures were grown on 30 °C with 200 rpm shaking for approximately 24-48 hours to allow the strains to reach stationary

phase. The toluene-adapted cultures were then diluted 100 times with LB and grown overnight on 30 °C with 200 rpm shaking. Stocks were made from this LB culture and the cycle of toluene adaptation were continued with higher toluene concentration (0.2% (vol/vol)). This cycle was repeated up to 8 cycles with the addition of 0.5% (vol/vol) toluene as shown on Fig. 5.1A.

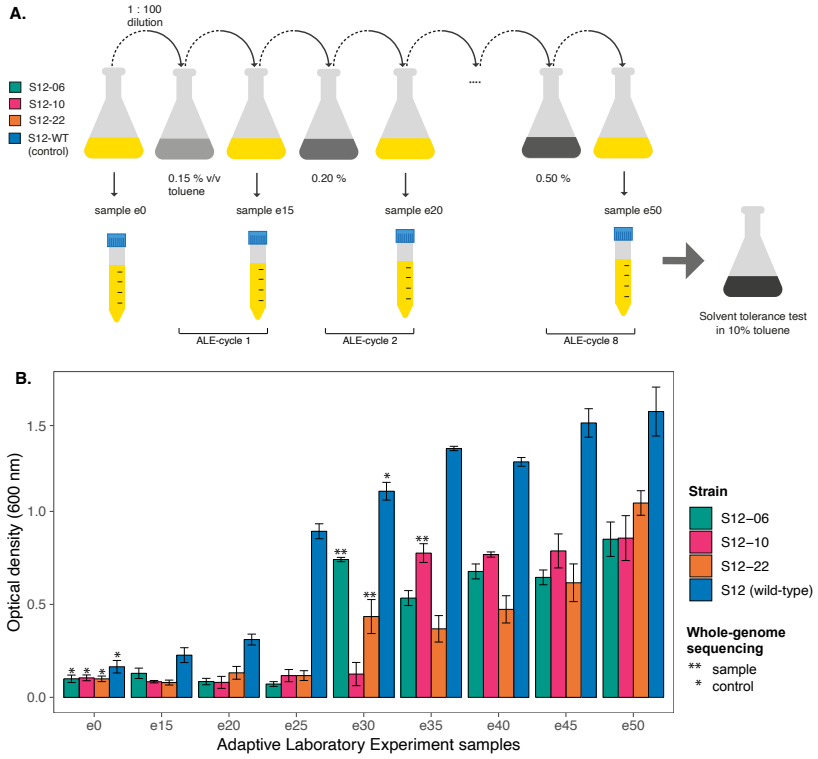

Fig. 5.1. Adaptive laboratory evolution (ALE) experiment of the plasmid-cured *P. putida* S12 to increasing concentration of toluene

A. Experimental design of ALE. ALE was performed on three plasmid-cured *P. putida* S12 strains (S12-06, S12-10, and S12-11). In the ALE experiment, LB media (yellow) was used as the growth media with the addition of increasing toluene concentration 0.05% (vol/vol) every cycle (grey).

B. Plasmid-cured *P. putida* S12 regained the ability to grow on high toluene concentration. The solvent-tolerance phenotype of ALE-derived strains was tested by observing strain growth on LB with 10% (vol/vol) toluene within 48 hours. The asterisks (*) and double asterisk (**) indicate the control and sample strains that were taken for whole genome sequencing. This experiment was performed with three biological replicates and error bars indicate standard deviation.

PCR and cloning methods

PCR reactions were performed using Phusion polymerase (Thermo Fisher) according to the manufacturer's manual. Oligos used in this paper (Table 5.S2) were procured from Sigma-Aldrich. PCR products were analysed by gel electrophoresis on 1 % (wt/vol) TBE agarose containing 5 μg mL^{-1} ethidium bromide (110V, 0.5x TBE running buffer).

Deletion of *arpR*, *gacA*, *gacS*, and *afr* genes and restoration of mutations on ALE-derived strains were performed using homologous recombination between free-ended DNA sequences that are generated by cleavage on unique I-SceI sites (20). Two homologous recombination fragments (TS-1 and TS-2) were obtained by performing PCR using oligos listed in Table 5.S2. Reverse engineering of the point mutations at ATP synthase subunit α (RPPX_09510) and RNA polymerase subunit β' (RPPX_06985) loci were performed using CRISPR-cas9 enhanced single stranded DNA (ssDNA) recombineering method (21, 22). Spacers and ssDNA repair fragments were created using oligos listed in Table 5.S2. All of the obtained plasmid constructs, deletion, and restoration of the selected genes were verified by Sanger sequencing (Macrogen BV., Amsterdam).

Whole-genome sequencing of plasmid-cured and ALE-derived strains

For whole genome sequencing, DNA was extracted by phenol-chloroform extraction followed by column clean-up using NucleoSpin® DNA Plant II kit (Macherey-Nagel). Clustering and DNA sequencing of wildtype, plasmid-cured, and ALE-derived *P. putida* S12 strains were performed using Illumina cBot and HiSeq 4000 (GenomeScan BV, The Netherlands). Image analysis, base calling, and quality check were performed with the Illumina data analysis pipeline RTA v.2.7.7 and Bcl2fastq v.2.17. Raw-data reads were assembled according to the existing complete genome sequence (Accession no. CP009974 and CP009975) in Geneious software (16).

RNA sequencing of plasmid-cured and ALE-derived strains

Wildtype, plasmid-cured, and ALE-derived *P. putida* S12 cultures were grown from overnight culture (100 times diluted) on 20 ml LB for 2 hours (30 °C, 200rpm) with and without the addition of 0.1% (vol/vol) toluene to bacterial cell cultures. RNA was extracted using TRIzol reagent (Invitrogen) according to the manufacturer's manual. The obtained RNA samples were cleaned-up using NucleoSpin® RNA Plant and Fungi kit (Macherey-Nagel). RNA libraries

were prepared for sequencing using standard Illumina protocols and paired-end sequence reads were generated using the Illumina MiSeq system (BaseClear BV, The Netherlands). Initial quality assessment was based on data passing the Illumina Chastity filtering. Subsequently, reads containing PhiX control signal were removed using an in-house filtering protocol. In addition, reads containing (partial) adapters were clipped (up to a minimum read length of 50 bp). The second quality assessment was based on the remaining reads using the FASTQC quality control tool version 0.11.5. Tophat2 version 2.1.1 aligned RNA-seq reads to a reference genome (Acc. No. CP009974 and CP009975) using the ultra-high-throughput short read aligner Bowtie version 2.2.6 (23, 24). Cufflink was used to test for differential expression and regulation in RNA-Seq samples. Cuffdiff then estimated the relative abundances of these transcripts.

Microtiter dish biofilm formation assay

To quantify biofilm formation, crystal-violet based assay on 96-well plate was performed as described by O'Toole (25). Overnight cultures of *P. putida* S12 (100 times diluted) were grown in flat bottomed 96-well microtiter plate with 100 μl LB media (30 °C) for 6 hours without shaking. After 6 hours, OD_{600} was measured using Tecan Spark® 10M (Tecan) to ensure the growth of *P. putida* S12. Liquid cultures were removed from 96-well microtiter plate and followed by two-times washing with water. Crystal violet solution (0.1% (vol/vol)) 125 μl was added to each well followed by 10-15 minutes of incubation. After incubation, crystal violet solution was removed and the wells were washed with water to remove the excess crystal violet. Microtiter plate was then turned upside-down and dried. Acetic acid solution (30% (vol/vol)) 125 μl were added to solubilized biofilm stained crystal violet and incubated for 10-15 minutes. The absorbance at 550 nm was measured to represent biofilm formation using Tecan Spark® 10M (Tecan) and acetic acid solution as blank.

Swimming motility assay

As starting culture, *P. putida* S12 strains were streaked and grown on LB agar overnight (30 °C). Single colonies were picked and stab-inoculated on to low viscosity LB agar (0.3% (wt/vol) agar). This agar was incubated cap-side up for 24 hours at 30 °C. Radial growth of *P. putida* S12 on low-viscosity agar was measured with three replicates to represent swimming motility.

Data availability

Whole genome sequencing data for the wild-type, plasmid-cured genotypes, and ALE-derived *P. putida* S12 have been submitted to the SRA database under accession number PRJNA602416. Datasets generated from RNA-seq experiment have been submitted to the GEO database under accession number GSE144045.

Results

Plasmid-cured Pseudomonas putida S12 can regain the ability to tolerate high-concentration toluene

To investigate the intrinsic solvent-tolerance of *P. putida* S12, we performed adaptive laboratory evolution (ALE) experiment on plasmid-cured *P. putida* S12. Three biological replicates of plasmid-cured *P. putida* S12 (strain S12-06, S12-10, and S12-22) and a wildtype *P. putida* S12 as control were set up to grow on lysogeny broth (LB) media with the addition of 0.15% (vol/vol) toluene; the initial maximum concentration that can be tolerated by plasmid-cured *P. putida* S12 (Fig. 5.1A). At stationary phase (typically after 24-48 hours), these cultures were transferred (1:100 dilution) to grow overnight on fresh LB media. Overnight LB media cultures were transferred into LB media containing toluene 0.20% (increase of 0.05% toluene) to continue with the next ALE cycle. While plasmid-cured *P. putida* S12 was unable to grow on LB with 0.20% (vol/vol) toluene directly, after adaptation to LB with 0.15% (vol/vol) toluene these cultures are able to grow on LB with 0.20% (vol/vol) toluene. We repeated this growth cycle with increasing concentration every cycle until plasmid-cured *P. putida* S12 strains were able to grow on LB with 0.50% (vol/vol) toluene (Fig. 5.1A). All samples from every ALE-cycle were collected and tested for their ability to survive 10% (vol/vol) toluene on LB for 48 hours. This concentration was chosen to represent a high toluene concentration which creates a distinct second phase layer in the culture medium.

Initially, the plasmid-cured *P. putida* S12 did not show growth and survival in the presence of 10% toluene, while the wild-type *P. putida* S12 can survive ($(2.52 \pm 0.31) \times 10^{-2}$ survival frequency) although it did not show any growth in 10% toluene (Fig. 5.1B). After the adaptation with a moderate toluene concentration (0.30-0.35%), both wild-type and plasmid-cured *P. putida* S12 showed a significant increase in their ability to withstand and sustain growth in 10% toluene. ALE-derived strains S12-06e30, S12-10e35, and S12-22e30 were

able to grow on LB media with 10% (vol/vol) toluene, reaching final OD_{600} of 0.741 ± 0.02, 0.776 ± 0.08, and 0.434 ± 0.158 respectively after 48 hours. These three samples were taken for whole genome sequencing to map the occurring mutations important for the solvent-tolerance phenotype. Wildtype *P. putida* S12, S12e30, and the initial plasmid-cured *P. putida* S12 strains were sequenced as controls.

Common mutations were identified in solvent-tolerant strains obtained from ALE

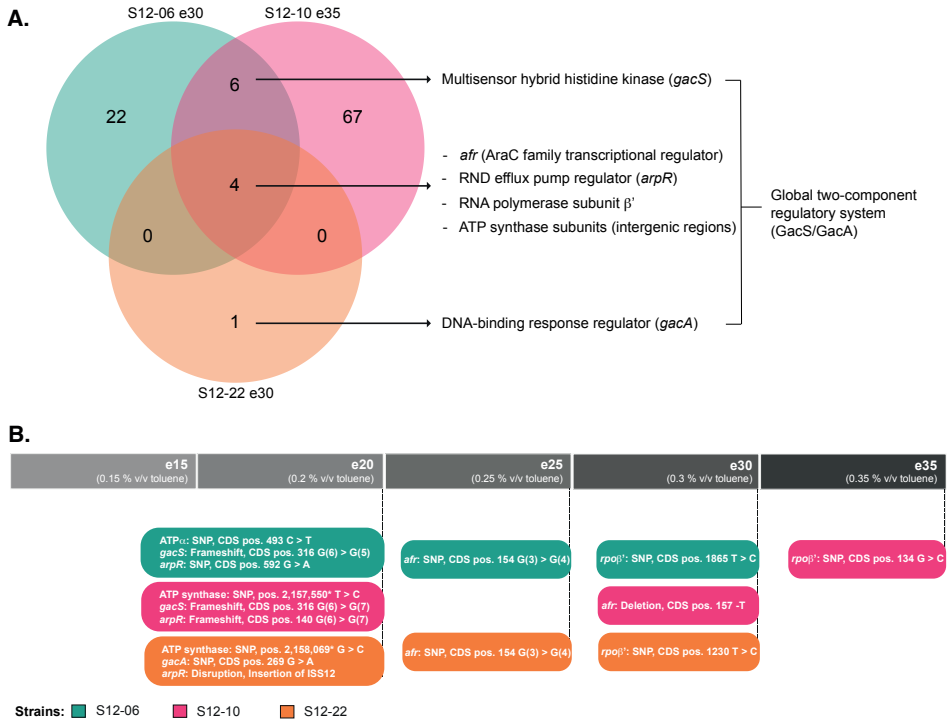

Fig. 5.2. Common mutated loci were identified in the ALE-derived *P. putida* S12 strains.

A. Venn diagram of mutated loci in the ALE-derived *P. putida* S12 strains. The colors indicate the three ALE-derived strains. Common mutated loci were identified among ALE-derived strains on an AraC family transcriptional regulator (Afr), RND efflux pump regulator (ArpR), RNA polymerase subunit β', intergenic region of F0F1 ATP synthase subunits, and global two-component regulatory system GacS/GacA.

B. ALE-derived *P. putida* S12 strains accumulated key mutations in a stepwise manner. ALE-derived strains were probed for key mutations accumulation with PCR and Sanger sequencing. The colors indicate the three ALE-derived strains and the grey bar indicate the ALE cycles which the strains were originating from. The position of the occurring SNPs or indels are indicated as CDS position of each mutated loci, except

for the SNPs within the intergenic regions of ATP synthase which positions are indicated relative to the chromosome sequence.

We performed whole genome sequencing of ALE-derived strains S12-06e30, S12-10e35, and S12-22e30 to map the occurring mutations that may lead to increased solvent tolerance in the evolved strains. We identified 32, 77, and 5 mutations (SNPs, insertions/deletions, and mobile element ISS12 insertion) respectively, in S12-06e30, S12-10e35, and S12-22e30 (Fig. 5.2A). Among these mutations, four common mutated loci were identified in all strains. These mutations occurred in an AraC-family transcriptional regulator Afr (RPPX_14685), in a RND efflux pump regulator ArpR (RPPX_14650), in RNA polymerase subunit β' *rpoB*' (RPPX_06985), and in the intergenic regions and subunits of ATP synthase (RPPX_09480-09510) (Fig. 5.2A). Six mutated loci were shared only between S12-06e30 and S12-10e35. Among these six loci, indels occurred within *gacS* locus (RPPX_15700) in S12-06e30 and S12-10e35 while S12-22e30 had a unique SNP within *gacA* locus (RPPX_00635). In *Pseudomonas*, GacS and GacA proteins are known to constitute a two-component regulatory system which regulates biofilm formation, cell motility, and secondary metabolism (26).

Since the ALE-derived strains showed a sudden increase in their ability to tolerate high toluene concentrations, we investigated the order of accumulation of key mutations in ALE-derived strains. Key mutations accumulated in a stepwise manner rather than emerging simultaneously in one cycle (Fig. 5.2B). In the second ALE-cycle, three key mutations occurred under the exposure to 0.20% (vol/vol) toluene in all strains (S12-06e20, S12-10e20, and S12-22e20). The first accumulated mutations occurred on the intergenic regions between ATP synthase subunits, *gacS*/*gacA* loci, and *arpR* locus. In the subsequent cycle, S12-06e25, S12-10e30, and S12-22e25 accumulated additional key mutations in the *afr* locus. The final key mutations *on rpoB'* locus were accumulated by strain S12-06e30, S12-10e35, and S12-22e30, in which the sudden increase of solvent tolerance were observed.

Contribution of key mutations to increased solvent-tolerance of ALE-derived strains

To study the contribution and impact of each mutated locus, single knock-out strains of *arpR* (RPPX_14650), *afr* (RPPX_14685), *gacA* (RPPX_00635), and *gacS* (RPPX_15700) were created in plasmid-cured *P. putida* S12. In the ALE-derived strains, the acquired mu-

tations (indels and mobile element insertion) in *arpR* (RPPX_14650), *afr* (RPPX_14685), and *gacS* (RPPX_15700) caused truncation of the encoded protein, while the SNP in *gacA* (RPPX_00635) caused an amino acid residue change (P90L). The SNPs acquired in ATP synthase and in RNA polymerase subunit β' loci were not addressed with this single knock-out approach since knocking out these genes would have deleterious effects. Solvent-tolerance analysis of the single knock-out strains indicated that deletion of each of those genes improved the growth of plasmid-cured *P. putida* S12 strains on LB with 0.15% (vol/vol) toluene (Fig. 5.3A). However, single knock-out of these genes did not enable plasmid-cured *P. putida* S12 strains to grow on higher toluene concentration than 0.15% (vol/vol).

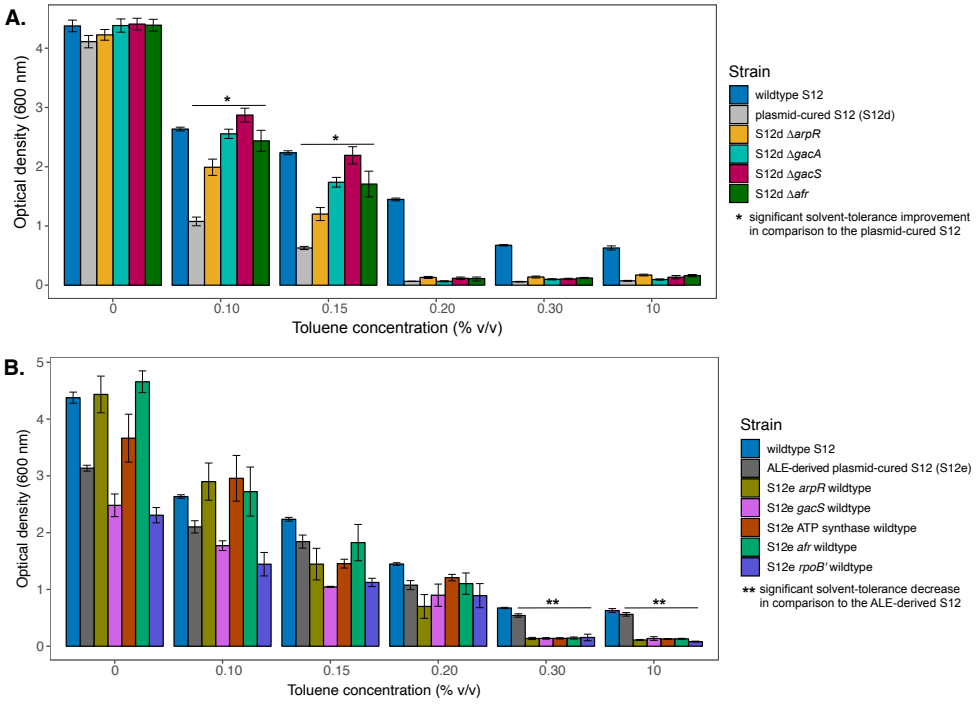

Fig 5.3. Accumulated key mutations contributed to solvent-tolerance phenotype of ALE-derived *P. putida* S12 strains.

A. Single-knockout of common mutated loci in the plasmid-cured *P. putida* S12 improved strain growth on LB with low toluene concentration (0.1-0.15% (vol/vol)). The colors indicate the control strains and the plasmid-cured S12 with deleted loci. This experiment was performed with three biological replicates and error bars indicate standard deviation.

B. Single-restoration of common mutated loci in the ALE-derived *P. putida* S12 reduced solvent-tolerance phenotype. The colors indicate the control strains and the ALE-derived S12 with restored loci. The restored

strains can grow on LB with a maximum of 0.20% (vol/vol) toluene. This experiment was performed with three biological replicates and error bars indicate standard deviation.

Individual restoration of common mutated loci in the ALE-derived strains to their wild-type sequence caused these strains to lose the ability to withstand the presence of moderate and high toluene concentration (0.30% and 10% (vol/vol) toluene) (Fig. 5.3B). These strains can sustain growth on LB with maximum 0.20% (vol/vol) toluene. Therefore, we concluded that each of the common mutated loci is important for the solvent-tolerance phenotype in ALE-derived strains.

Reverse engineering of key mutations on plasmid-cured S12 successfully restore solvent-tolerance

To confirm the important contribution of key mutations, we introduced these mutations on a plasmid-cured S12 strain and analyse the growth parameters of the resulting strains in the presence and absence of toluene (Fig. 5.4 and Table 5.S3). Strain S12-10 was chosen to represent the plasmid-cured S12 in this experiment. A knock-out of *arpR* (RPPX_14650) locus was performed resulting in the first reverse engineering strain (RE1). Second knock-out mutation at *gacS* (RPPX_15700) locus was performed on strain RE1, resulting in the strain RE2. It is interesting to note that strain RE2 exhibit significantly better growth parameters in LB and minimal media compared to its parent strains RE1 and S12-10 (Table 5.S3). The third mutation was introduced at the ATP synthase subunit alpha (RPPX_09510) to strain RE2, resulting in the strain RE3. This mutation caused an amino acid substitution from arginine to cysteine at position 165 (R165C), mimicking the mutation found in the strain S12-06e30. Indeed, the introduction of this mutation caused a severe reduction of growth parameters in LB and minimal media (Table 5.S3). Fourth knock-out mutation at *afr* (RPPX_14685) locus was performed on strain RE3, resulting in the strain RE4. Finally, a point mutation was introduced to strain RE4 at *rpoB'* (RPPX_06985) locus to construct strain RE5 which caused an amino acid substitution from aspartic acid to glycine at position 622 (D622G) mimicking the mutation found in the strain S12-06e30.

Reverse engineering strains and its parent, strain S12-10, were tested for their ability to survive and sustain growth in the presence of toluene (Fig. 5.4). Strain S12-10, RE1, and RE2 were only able to withstand and sustain growth in the presence of 0.15% (vol/vol) toluene. Nevertheless, strain RE1 and RE2 showed growth improvement in comparison to strain

S12-10 (Fig. 5.4, panel 2). Strain RE3 and RE4 were able to withstand and sustain growth in a slightly higher toluene concentration, 0.20% and 0.25% (vol/vol) toluene respectively. Finally, strain RE5 were able to sustain growth in the presence of high toluene concentration (10% (vol/vol) toluene). These results confirm that the key mutations are indeed important for the restoration of solvent tolerance in plasmid-cured S12.

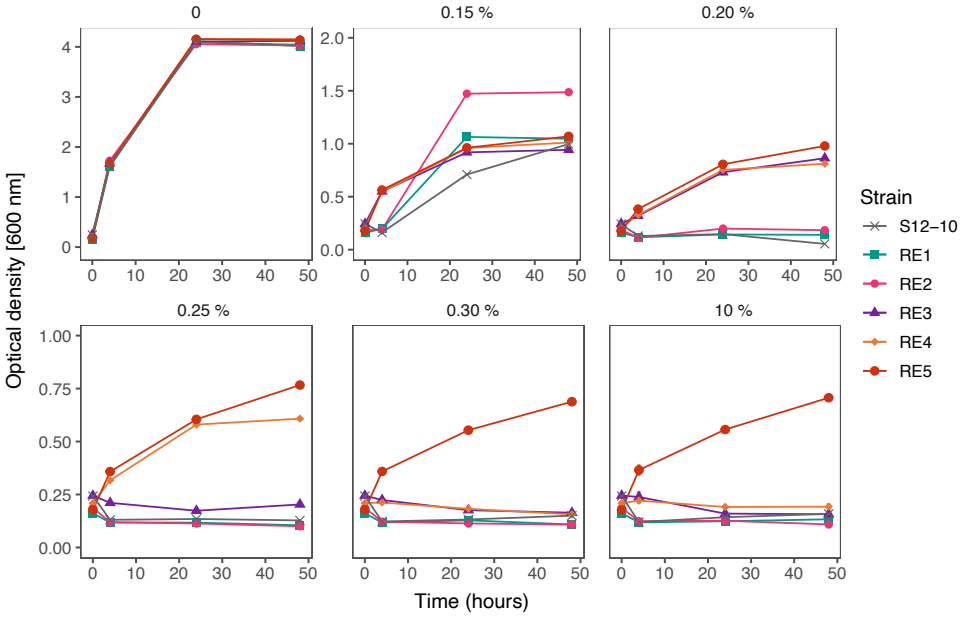

Fig. 5.4. Reverse engineering of the key mutations found in ALE-derived strains

Reverse engineering of the key mutations found in the ALE-derived *P. putida* S12 successfully restores the solvent-tolerance phenotype in the plasmid-cured strain S12-10. The colors indicate the control strain S12-10 and the reverse engineering strains (RE). This experiment was performed with three biological replicates and error bars indicate standard deviation. The y-axis may be different for the presented panels.

Restoration of solvent-tolerance involved a constitutive downregulation of energy consuming activities in ALE-derived strains

Global transcriptional analysis (RNA sequencing) was performed to probe the response of ALE-derived *P. putida* S12 in comparison with wildtype and plasmid-cured *P. putida* S12 in the presence of toluene (LB with 0.1% (vol/vol) toluene). As a response to toluene addition, ALE-derived strains showed differential expression only of 14 loci. This response was in stark contrast to the wild-type S12 and plasmid-cured S12 which differentially expressed more than 500 loci as a response to toluene addition (Fig. 5.S1). Comparisons of gene expression be-

tween ALE-derived strains with plasmid-cured and wildtype *P. putida* S12 growing on LB in the absence of toluene indicated that the mutations which occurred in the ALE-derived strains caused constitutive differential expression of ± 900 genes which play a role in restoring solvent tolerance (Fig. 5.5).

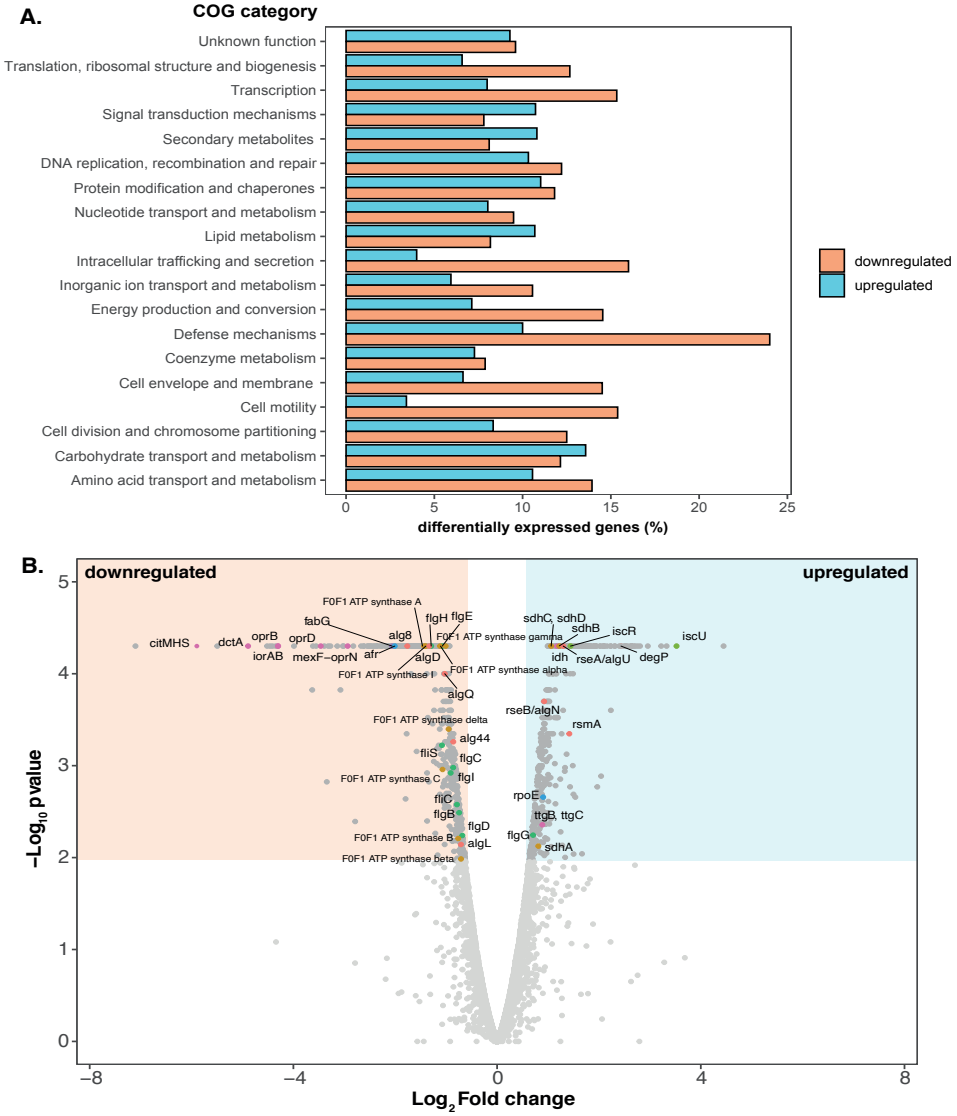

Fig. 5.5. Visualization of differentially expressed genes on ALE-derived *P. putida* S12 strains in comparison to its parental strain growing on LB.

A. COG classification of differential gene expression in ALE-derived strains in comparison to plasmid-cured *P. putida* S12. COG classification was performed using eggNOG 5.0 mapper (http://eggnogdb.embl.de/#/app/emapper). The percentages of up-regulated genes in each class are represented by the blue bar and the

percentages of down-regulated genes are represented by the red bar.

B. Volcano plot of differential gene expression in ALE-derived strains in comparison to the plasmid-cured *P. putida* S12 growing on LB. Blue area indicates the significantly upregulated genes and beige area indicates the significantly downregulated genes (cut-off: Log_2 Fold Change ≥ 1 for up-regulated genes or ≤ 1 for down-regulated genes and p-value ≤ 0.01). The colored dots represent the significantly up-/down-regulated genes discussed in this paper. The colors correspond to the functions of each genes: red represents biofilm and alginate production genes; orange represents the genes involved in oxidative phosphorylation process; light green represents the genes involved in energy production process; green represents flagellar assembly gene clusters; blue represents sigma factor and transcriptional regulator; and magenta represents the genes which constitute membrane transporters.

Constitutive differentially expressed genes in ALE-derived strains in comparison to parental plasmid-cured *P.putida* S12 were classified based of COG categorization. Several classes of genes were downregulated in ALE-derived strains compared to plasmid-cured S12, for example, genes constituting cell motility, intracellular trafficking and secretion, and defence mechanism functions (Fig. 5.5A). In general, ALE-derived strains appeared to constitutively shut-down energy consuming activities, such as flagella biosynthesis, F0F1 ATP synthase, and membrane transport proteins which are energized through proton (H^+) influx. Additionally, genes related to biofilm formation were constitutively down-regulated. Here, we focused on several classes of genes that were differentially expressed in ALE-derived strains compared to its parental strain.

Membrane proteins and efflux pumps

ArpABC efflux pump (RPPX_14635-14640) is a multi-functional RND efflux pump homologous to TtgABC from *P. putida* DOT-T1E. This locus was moderately upregulated in ALE-derived strains (Fig. 5.5B; *ttgB* and *ttgC*). While the upregulation of this pump is a common response to toluene in wildtype *P. putida* S12, ALE-derived strains constitutively upregulate ArpABC by SNPs and mobile element insertion in its negative regulator gene *arpR* (RPPX_14650). Interestingly, almost all of the other RND efflux pumps encoded in the chromosome of *P.putida* S12 were downregulated in ALE-derived strains. In the ALE-derived strains, lacking the pTTS12-encoded SrpABC solvent pump, ArpABC is the only remaining efflux pump that may extrude toluene, albeit with a much lower affinity (27). Downregulation of other efflux pumps is likely to be important to preserve the required proton motive force.

The genes associated with porin function were downregulated in ALE-derived strains as exemplified by RPPX_10240, RPPX_14820, and RPPX_17640 which encodes OprD porin

family proteins. This response was similar to previous proteomics study (28) which noted the downregulation of porins to avoid toluene leakage into the cell through these porins. In addition to porins downregulation, several membrane transport proteins like *dctA* (H^+/C4-dicarboxylate symporters, RPPX_17630) and *citMHS* (citrate-divalent cation/H^+ symporter, RPPX_17635) were constitutively downregulated.

Energy production and conversion

In ALE-derived strains, F0F1 ATP synthase subunits were constitutively downregulated (Fig. 5.5B). This was in-line with our finding of the SNPs which occurred on the intergenic regions between F0F1 ATP synthase subunits (RPPX_09480-RPPX_09510). F0F1 ATP synthase generates 1 ATP from ADP in bacteria by pumping out 3 H^+ molecule and thus downregulation of this loci may also contributed to the preservation of proton motive force.

Succinate dehydrogenase (SdhABCD) gene cluster (RPPX_01070-RPPX_01085) were constitutively upregulated in ALE-derived strains. Succinate dehydrogenase is responsible as complex II in oxidative phosphorylation process. Cytochrome C oxidase subunit II (RPPX_08860) and its assembly protein (RPPX_08850), composing complex IV, were also constitutively upregulated in ALE-derived strains. Taken together, these findings underlined the importance of electron transport chain in maintaining proton motive force during solvent-stress.

Biofilm formation

In ALE-derived strains, we observed a constitutive upregulation of the *rsmA* locus (RPPX_02245). Upregulation of *rsmA* locus may be caused by the mutations found in *gacS*/*gacA* locus and is known to promote motile lifestyle in *Pseudomonas* (26). Downregulation of alginate biosynthesis pathway as the main polysaccharide matrix in *Pseudomonas* biofilm was also observed. Alg44 (RPPX_14155), which upon its interaction with c-di-GMP is known to positively regulate alginate production (29), was constitutively downregulated in ALE-derived strains. Other loci which are involved in alginate biosynthesis and export were also down regulated e.g. *algL* (RPPX_14130), *alg8* (RPPX_14160), *algD* (RPPX_14165), and *algE* (RPPX_21545). Taken together, these findings pointed to reduction of biofilm formation capacity in the ALE-derived strains.

To confirm this result, we applied a microtiter dish biofilm formation assay (25) to assess the biofilm formation in ALE-derived strains (Fig. 5.6A). Biofilm formation was indeed

clearly lower in ALE-derived strains compared to the wildtype and plasmid-cured *P. putida* S12. This tendency was reversed when the indel mutation in the *gacS* locus was restored to the wildtype sequence. While biofilm may protect bacteria from external stressors, nutrient and oxygen depletion during sessile lifestyle may be disadvantageous in solvent-stress and therefore constitutive downregulation of biofilm-related genes was beneficial in ALE-derived strain.

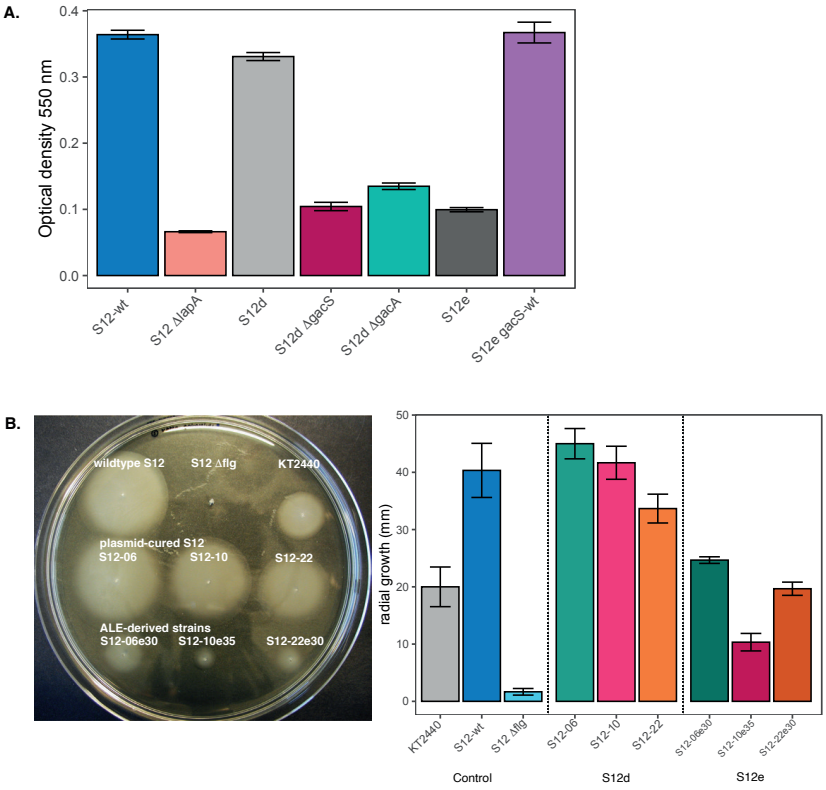

Fig. 5.6. Biofilm formation and cell motility were reduced in ALE-derived *P. putida* S12 strains

A. Microtiter biofilm formation assay of *P. putida* S12. Plasmid-cured *P. putida* S12 (S12d) Δ*gacS* and Δ*gacA* showed similar reduction as ALE-derived *P. putida* S12 (S12e) strains. Restoration of *gacS* locus to wild-type sequence (S12e *gacS*-wt) also restore biofilm formation in ALE-derived *P. putida* S12 (S12e). The measurement of biofilm formation was performed by measuring optical density at 500nm as previously described (25) with Δ*lapA* (adhesin) taken as negative control. This experiment was performed with three biological replicates and error bars indicate standard deviation.

B. Swimming motility assay of *P. putida* S12 in low viscosity agar (LB + 0.3% agar). ALE-derived *P. putida* S12 strains (S12e) showed a reduced radial growth in low viscosity agar indicating lower swimming motility.

The Δ*flg* (flagella gene cluster) was taken as a negative control. On the second panel, the bars represent an average of radial growth of at least three biological replicates of each strains and error bars indicate standard deviation.

Cell motility

Flagellar biosynthesis loci (RPPX_02045-RPPX_02125) were constitutively downregulated in ALE-derived strains (Fig. 5.5B). Consequently, this may lead to reduced swimming motility in ALE-derived strains. We confirmed this finding by measuring the radial growth of ALE-derived strains in comparison to the wildtype and plasmid-cured *P. putida* S12 on low-viscosity agarose (Fig. 5.6B). Indeed, ALE-derived strains showed a significant reduction of radial growth. Downregulation of flagella may be a strategy of ALE-derived strains to maintain proton motive force and reroute its energy towards extrusion of toluene since both RND efflux pump ArpABC and flagella utilize H^+ influx as energy source.

Chaperones

We also observed the constitutive upregulation of loci RPPX_14680-14875 which encode homologs of sigma factor E (RpoE), anti-sigma factor RseAB, and DegP protein respectively. This cluster is known to orchestrate the expression of chaperone proteins as a stress response to the elevated amount of misfolded proteins in *E.coli* (30). Additionally, these sigma factors are known to negatively regulate alginate biosynthesis in *P. aeruginosa* (31). Other chaperone protein, like Hsp20 protein (RPPX_17155) was also constitutively upregulated in ALE-derived strains. Constitutive upregulation of these genes suggested an important role of chaperones in the adaptive response to high toluene concentration.

Discussion

Solvent tolerance can be restored in a relatively small number of generations

The single copy megaplasmid pTTS12 plays an essential role in the solvent-tolerance trait of *P. putida* S12. An efficient solvent extrusion pump SrpABC (homologous to TtgGHI), styrene-phenylacetate degradation pathway, and the recently-identified toxin-antitoxin SlvTA are encoded within this megaplasmid (16). Unlike *P. putida* DOT-T1E, *P. putida* S12 does not encode toluene degradation pathway within its genome and thus, its solvent-tolerance heavily relies on the gene clusters encoded in pTTS12 as mentioned above (32). However, previous

attempts expressing SrpABC in other non-solvent tolerance bacteria like *E. coli* were unsuccessful to incite the same level of solvent-tolerance as with *P. putida*. This may indicate that *P. putida* S12 is intrinsically solvent tolerant to begin with (33, 34). Hence, in this paper, we further scrutinized this putative intrinsic solvent tolerance in *P. putida* S12 using Adaptive Laboratory Evolution (ALE).

Upon curing of megaplasmid pTTS12, solvent-tolerance of *P. putida* S12 was significantly reduced. After 4-5 adaptation cycles (± 7 generations per growth cycle) to increasing toluene concentrations, solvent-tolerance trait of plasmid-cured *P. putida* S12 could be restored. Relatively short adaptation to alternating cycles of LB in the presence or absence of toluene can restore solvent-tolerance to elevated concentration of toluene due to the stringent selection pressure elicited by this experimental set-up. However, we also observed a severe reduction in growth parameters on the resulting ALE-derived strains grown in the absence of toluene compared to wildtype *P. putida* S12 undergoing the same adaptation cycles to toluene. Several common mutated loci were identified between replicates of ALE-derived *P. putida* S12. Whole genome sequencing revealed SNPs, indels, and an insertion of mobile genetic element ISS12 occurred in a negative regulator of RND efflux pump ArpR, an uncharacterized AraC family transcriptional regulator Afr, RNA polymerase subunit β', intergenic region of F0F1 ATP synthase subunits and global two-components regulatory system GacS/GacA. Each of these mutations were demonstrated to be essential in restoring solvent-tolerance of the plasmid-cured *P. putida* S12.

Up-regulation of solvent efflux pump is compensated by down-regulation of other membrane proteins

RNA-sequencing revealed constitutive differential changes of gene expression in ALE-derived strains caused by the observed mutations. Truncation of ArpR caused a moderate upregulation of ArpBC locus, confirming the promiscuous function of ArpABC efflux pump as antibiotic pump and solvent pump as was previously described (35). However, other RND efflux pumps were generally downregulated in ALE-derived strains. Indeed, it has been described that a combination of different efflux pumps expression can be toxic to bacteria (36). While there are multifactorial causes of efflux pumps toxicity, including membrane composition changes and insertion machinery overload (36–38), we propose that the cause of efflux pump toxicity may be due to a high demand of proton motive force. In ALE-derived strains, F0F1 ATP syn-

thase subunits, flagella and other H^+ influx-dependent membrane transporters were severely downregulated following the moderate upregulation of ArpBC locus. Downregulation of F0F1 ATP synthase subunits may contribute to the observed fitness reduction and at the same time, required as a strategy in ALE-derived strains to overcome efflux pump toxicity in supporting the immense effort of solvent extrusion.

Truncation of putative regulator Afr in ALE-derived strains reduces expression of membrane proteins

Indel mutations were observed in a hitherto uncharacterized AraC-family transcriptional regulator (Afr), causing it to be truncated in the ALE-derived strains. In *P.putida* KT2440, a homolog of Afr encoded by PP1395 (100% identity, 100% coverage) was found to be responsible for a decrease in glycerol uptake (39), while in *P. aeruginosa* PA14, Afr homolog (63% identity, 88% coverage) encoded by PA14_38040 (PA2074 in strain PAO1) was reported to regulate the expression of RND efflux pump MexEF-OprN (40). Further characterization of Afr is underway. Since the above mentioned homologs of Afr pointed to a function regulation of transporters, truncation/deletion of Afr may contribute to the maintenance of proton motive force in ALE-derived strains.

Mutations in the *gacS*/*gacA* loci as a common strategy for swift phenotypic switching in Pseudomonads

Truncation of GacS protein and a SNP at *gacA* locus in ALE-derived strains resulted in the observed upregulation of its target, *rsmA* locus. Alginate biosynthesis genes, the main polysaccharide constituting Pseudomonas biofilm (29), were constitutively downregulated in ALE-derived strains. Indeed, we observed reduced biofilm formation in ALE-derived strains, which could be reversed when the mutation in *gacS* locus was complemented with wildtype sequence. In *P. aeruginosa*, biofilm dispersion can be triggered by carbon starvation and involves proton motive force dependent step(s) (41). During solvent-stress, efficient carbon catabolism and energy production is essential for the extrusion of solvent and survival of *P. putida* S12, therefore biofilm formation causing carbon starvation and oxygen depletion will be disadvantageous.

In the reverse engineering strain RE2, the deletion of *gacS* locus resulted in a significant improvement of growth parameters in the presence and absence of toluene. This mutation may have been selected for to compensate for the mutations that severely affect the

growth of ALE-derived strains, for example, the mutations at F0F1 ATP synthase loci. Similar observation was also reported in previous studies, e.g. the loss of function mutation at the *gacS*/*gacA* loci increased the fitness of plasmid-carrying bacterial strain (42) and improved growth characteristics and efficient root colonization (43, 44). The GacS/GacA two-component system may have a pleiotropic effect since this system regulates a large set amount of genes as a response to environmental stimuli. Additionally, *gacA*/*gacS* loci may constitute a commonly mutated loci which have an elevated mutation rate to allow for a swift phenotypic switching in the environmental dynamics (42–44).

General summary

In summary, ALE presents a powerful combination of mutation selection and construction of beneficial genetic variation in many different genes and regulatory regions in parallel (45, 46), for the restoration of solvent-tolerance in plasmid-cured *P. putida* S12. Through ALE, we gained insight into intrinsically promoting solvent-tolerance of *P. putida* S12. High metabolic flexibility of *P. putida* S12, e.g. ability to maintain proton motive force, indeed proved essential to incite solvent-tolerance with the availability of a solvent extrusion pump. This may very well be under the control of *gacA*/*gacS* loci and may involve the putative regulator Afr. Further characterization of the efficiency of solvent extrusion pumps and their impact and demand on proton motive force is required for the application of solvent-tolerant strains, especially in the bioproduction of high-value chemicals and biofuels.

References

1. Nikel PI, de Lorenzo V. *Pseudomonas putida* as a functional chassis for industrial biocatalysis: From native biochemistry to trans-metabolism. *Metab Eng* 2018; **50**: 142–155.
2. Kohlstedt M, Starck S, Barton N, Stolzenberger J, Selzer M, Mehlmann K, et al. From lignin to nylon: Cascaded chemical and biochemical conversion using metabolically engineered *Pseudomonas putida*. *Metab Eng* 2018; **47**: 279–293.
3. Wynands B, Lenzen C, Otto M, Koch F, Blank LM, Wierckx N. Metabolic engineering of *Pseudomonas taiwanensis* VLB120 with minimal genomic modifications for high-yield phenol production. *Metab Eng* 2018; **47**: 121–133.
4. Borrero-de Acuña JM, Bielecka A, Häussler S, Schobert M, Jahn M, Wittmann C, et al. Production of medium chain length polyhydroxyalkanoate in metabolic flux optimized *Pseudomonas putida*. *Microb Cell Fact* 2014; **13**: 88.
5. Poblete-Castro I, Becker J, Dohnt K, dos Santos VM, Wittmann C. Industrial biotechnology of *Pseudomonas putida* and related species. *Appl Microbiol Biotechnol* 2012; **93**: 2279–2290.
6. Verhoef S, Wierckx N, Westerhof RGM, de Winde JH, Ruijssenaars HJ. Bioproduction of p-hydroxystyrene from glucose by the solvent-tolerant bacterium *Pseudomonas putida* S12 in a two-phase water-decanol fermentation. *Appl Environ Microbiol* 2009; **75**: 931–936.
7. Meijnen JP, De Winde JH, Ruijssenaars HJ. Engineering *Pseudomonas putida* S12 for efficient utilization of D-xylose and L-arabinose. *Appl Environ Microbiol* 2008; **74**: 5031–5037.
8. Verhoef S, Ruijssenaars HJ, de Bont JAM, Wery J. Bioproduction of p-hydroxybenzoate from renewable feedstock by solvent-tolerant *Pseudomonas putida* S12. *J Biotechnol* 2007; **132**: 49–56.
9. Wierckx NJP, Ballerstedt H, de Bont JAM, Wery J. Engineering of solvent-tolerant *Pseudomonas putida* S12 for bioproduction of phenol from glucose. *Appl Environ Microbiol* 2005; **71**: 8221–8227.
10. Loeschcke A, Markert A, Wilhelm S, Wirtz A, Rosenau F, Jaeger K-E, et al. TREX: A Universal Tool for the Transfer and Expression of Biosynthetic Pathways in Bacteria. *ACS Synth Biol* 2012; **2**: 22–33.

11. Silva-Rocha R, Martínez-García E, Calles B, Chavarría M, Arce-Rodríguez A, de las Heras A, et al. The Standard European Vector Architecture (SEVA): a coherent platform for the analysis and deployment of complex prokaryotic phenotypes. *Nucleic Acids Res* 2013; **41**: D666–D675.

12. Kampers LFC, van Heck RGA, Donati S, Saccenti E, Volkers RJM, Schaap PJ, et al. In silico-guided engineering of *Pseudomonas putida* towards growth under micro-oxic conditions. *Microb Cell Fact* 2019; **18**: 179.

13. Hartmans S, Smits JP, van der Werf MJ, Volkering F, de Bont JA. Metabolism of Styrene Oxide and 2-Phenylethanol in the Styrene-Degrading *Xanthobacter* Strain 124X. *Appl Environ Microbiol* 1989; **55**: 2850–2855.

14. Koopman F, Wierckx N, de Winde JH, Ruijssenaars HJ. Efficient whole-cell biotransformation of 5-(hydroxymethyl)furfural into FDCA, 2,5-furandicarboxylic acid. *Bioresour Technol* 2010; **101**: 6291–6296.

15. Kusumawardhani H, Hosseini R, de Winde JH. Solvent Tolerance in Bacteria: Fulfilling the Promise of the Biotech Era? *Trends Biotechnol* 2018; **36**: 1025–1039.

16. Kuepper J, Ruijssenaars HJ, Blank LM, de Winde JH, Wierckx N. Complete genome sequence of solvent-tolerant *Pseudomonas putida* S12 including megaplasmid pTTS12. *J Biotechnol* 2015; **200**: 17–18.

17. Kieboom J, Dennis JJ, de Bont JAM, Zylstra GJ. Identification and Molecular Characterization of an Efflux Pump Involved in *Pseudomonas putida* S12 Solvent Tolerance. *J Biol Chem* 1998; **273**: 85–91.

18. Kusumawardhani H, van Dijk D, Hosseini R, de Winde JH. A novel toxin-antitoxin module SlvT–SlvA regulates megaplasmid stability and incites solvent tolerance in *Pseudomonas putida* S12. *Appl Environ Microbiol* 2020; **86**: e00686-20.

19. Sprouffske K, Wagner A. Growthcurver: An R package for obtaining interpretable metrics from microbial growth curves. *BMC Bioinformatics* 2016; **17**: 172.

20. Martínez-García E, de Lorenzo V. Engineering multiple genomic deletions in Gram-negative bacteria: analysis of the multi-resistant antibiotic profile of *Pseudomonas putida* KT2440. *Environ Microbiol* 2011; **13**: 2702–2716.

21. Aparicio T, de Lorenzo V, Martínez-García E. CRISPR/Cas9-enhanced ssDNA recombineering for *Pseudomonas putida*. *Microb Biotechnol* 2019; **12**: 1076– 1089.

22. Aparicio T, de Lorenzo V, Martínez-García E. CRISPR/Cas9-Based Counterselection

Boosts Recombineering Efficiency in *Pseudomonas putida*. *Biotechnol J* 2017; **13**: e1700161.

23. Kim D, Pertea G, Trapnell C, Pimentel H, Kelley R, Salzberg SL. TopHat2: Accurate alignment of transcriptomes in the presence of insertions, deletions and gene fusions. *Genome Biol* 2013; **14**: R36.
24. Langmead B, Salzberg SL. Fast gapped-read alignment with Bowtie 2. *Nat Methods* 2012; **9**: 357–359.
25. O'Toole GA. Microtiter dish Biofilm formation assay. *J Vis Exp* 2010; **47**: 2437.
26. Nadal Jimenez P, Koch G, Thompson JA, Xavier KB, Cool RH, Quax WJ. The Multiple Signaling Systems Regulating Virulence in *Pseudomonas aeruginosa*. *Microbiol Mol Biol Rev* 2012; **76**: 46–65.
27. Kieboom J, de Bont JAM. Identification and molecular characterization of an efflux system involved in *Pseudomonas putida* S12 multidrug resistance. *Microbiology* 2001; **147**: 43–51.
28. Wijte D, van Baar BLM, Heck AJR, Altelaar AFM. Probing the proteome response to toluene exposure in the solvent tolerant *Pseudomonas putida* S12. *J Proteome Res* 2011; **10**: 394–403.
29. Whitney JC, Whitfield GB, Marmont LS, Yip P, Neculai AM, Lobsanov YD, et al. Dimeric c-di-GMP is required for post-translational regulation of alginate production in *Pseudomonas aeruginosa*. *J Biol Chem* 2015; **290**: 12451–12462.
30. Hews CL, Cho T, Rowley G, Raivio TL. Maintaining Integrity Under Stress: Envelope Stress Response Regulation of Pathogenesis in Gram-Negative Bacteria. *Front Cell Infect Microbiol* 2019; **9**: 313.
31. Yorgey P, Rahme LG, Tan MW, Ausubel FM. The roles of mucD and alginate in the virulence of *Pseudomonas aeruginosa* in plants, nematodes and mice. *Mol Microbiol* 2001; **41**: 1063–1076.
32. Molina-Santiago C, Udaondo Z, Gómez-Lozano M, Molin S, Ramos JL. Global transcriptional response of solvent-sensitive and solvent-tolerant *Pseudomonas putida* strains exposed to toluene. *Environ Microbiol* 2017; **19**: 645–658.
33. Garikipati SVBJ, McIver AM, Peeples TL. Whole-Cell Biocatalysis for 1-Naphthol Production in Liquid-Liquid Biphasic Systems. *Appl Environ Microbiol* 2009; **75**: 6545–6552.

34. Janardhan Garikipati SVB, Peeples TL. Solvent resistance pumps of *Pseudomonas putida* S12: Applications in 1-naphthol production and biocatalyst engineering. *J Biotechnol* 2015; **210**: 91–99.

35. Rojas A, Duque E, Mosqueda G, Golden G, Hurtado A, Ramos JL, et al. Three efflux pumps are required to provide efficient tolerance to toluene in *Pseudomonas putida* DOT-T1E. *J Bacteriol* 2001; **183**: 3967–3973.

36. Turner WJ, Dunlop MJ. Trade-Offs in Improving Biofuel Tolerance Using Combinations of Efflux Pumps. *ACS Synth Biol* 2015; **4**: 1056–1063.

37. Alsaker K V, Paredes C, Papoutsakis ET. Metabolite stress and tolerance in the production of biofuels and chemicals: gene-expression-based systems analysis of butanol, butyrate, and acetate stresses in the anaerobe *Clostridium acetobutylicum*. *Biotechnol Bioeng* 2010; **105**: 1131–1147.

38. Wagner S, Baarst L, Ytterberg AJ, Klussmerer A, Wagner CS, Nord O, et al. Consequences of membrane protein overexpression in *Escherichia coli*. *Mol Cell Proteomics* 2007; **6**: 1527−1550.

39. Beckers V, Poblete-Castro I, Tomasch J, Wittmann C. Integrated analysis of gene expression and metabolic fluxes in PHA-producing *Pseudomonas putida* grown on glycerol. *Microb Cell Fact* 2016; **15**: 73.

40. Juarez P, Jeannot K, Plésiat P, Llanes C. Toxic Electrophiles Induce Expression of the Multidrug Efflux Pump MexEF-OprN in *Pseudomonas aeruginosa* through a Novel Transcriptional Regulator, CmrA. *Antimicrob Agents Chemother* 2017; **61**: e00585-17.

41. Huynh TT, McDougald D, Klebensberger J, Al Qarni B, Barraud N, Rice SA, et al. Glucose starvation-induced dispersal of *Pseudomonas aeruginosa* biofilms is camp and energy dependent. *PLoS One* 2012; **7**: e42874.

42. Harrison E, Guymer D, Spiers AJ, Paterson S, Brockhurst MA. Parallel Compensatory Evolution Stabilizes Plasmids across the Parasitism-Mutualism Continuum. *Curr Biol* 2015; **25**: 2034–2039.

43. Van Den Broek D, Bloemberg G V., Lugtenberg B. The role of phenotypic variation in rhizosphere Pseudomonas bacteria. *Environ Microbiol* 2005; **7**: 1686–1697.

44. Seaton SC, Silby MW, Levy SB. Pleiotropic effects of GacA on *Pseudomonas fluorescens* Pf0-1 in vitro and in soil. *Appl Environ Microbiol* 2013; **79**: 5405–5410.

45. Dragosits M, Mattanovich D. Adaptive laboratory evolution -- principles and applications for biotechnology. *Microb Cell Fact* 2013; **12**: 64.

46. Portnoy VA, Bezdan D, Zengler K. Adaptive laboratory evolution — harnessing the power of biology for metabolic engineering. *Curr Opin Biotechnol* 2011; **22**: 590–594.

47. Hartmans S, van der Werf MJ, de Bont JA. Bacterial degradation of styrene involving a novel flavin adenine dinucleotide-dependent styrene monooxygenase. *Appl Environ Microbiol* 1990; **56**: 1347–1351.

Supplementary Materials

Table 5.S1. Strains and plasmids used in this paper

Strain	Characteristics	Ref.
P. putida S12	Wild type *P. putida* S12 (ATCC 700801), harboring megaplasmid pTTS12, solvent-tolerant strain	(47)
P. putida S12d (S12-06/ S12-10/ S12-22)	*P. putida* S12 ΔpTTS12, non-solvent-tolerant strains	(18)
P. putida S12e (S12-06e30/ S12-10e35/ S12-22e30)	ALE-derived *P. putida* S12 ΔpTTS12, solvent-tolerant strain	This paper
P. putida S12d Δ*arpR*	*P. putida* S12 ΔpTTS12 ΔRPPX_14650	This paper
P. putida S12d Δ*afr*	*P. putida* S12 ΔpTTS12 ΔRPPX_14685	This paper
P. putida S12d Δ*gacA*	*P. putida* S12 ΔpTTS12 ΔRPPX_00635	This paper
P. putida S12d Δ*gacS*	*P. putida* S12 ΔpTTS12 ΔRPPX_15700	This paper
P. putida S12e *arpR*-wt	ALE-derived *P. putida* S12 ΔpTTS12 RPPX_14650-wt	This paper
P. putida S12e *afr*-wt	ALE-derived *P. putida* S12 ΔpTTS12 RPPX_14685-wt	This paper
P. putida S12e *gacS*-wt	ALE-derived *P. putida* S12 ΔpTTS12 RPPX_15700-wt	This paper
P. putida S12e *rpoB'*-wt	ALE-derived *P. putida* S12 ΔpTTS12 RPPX_06985-wt	This paper
P. putida S12e ATP-wt	ALE-derived *P. putida* S12 ΔpTTS12 RPPX_09480-09510-wt	This paper
P. putida S12 Δ*lapA*	*P. putida* S12 ΔRPPX_08475	This paper
P. putida S12 Δ*flg*	*P. putida* S12 ΔRPPX_02040-02125	This paper
P. putida S12-RE1	*P. putida* S12-10 (ΔpTTS12) Δ*arpR*	This paper
P. putida S12-RE2	*P. putida* S12-10 (ΔpTTS12) Δ*arpR; ΔgacS*	This paper
P. putida S12-RE3	*P. putida* S12-10 (ΔpTTS12) Δ*arpR; ΔgacS; atp*α (R165C)	This paper
P. putida S12-RE4	*P. putida* S12-10 (ΔpTTS12) Δ*arpR; ΔgacS; atp*α (R165C); Δ*afr*	This paper
P. putida S12-RE5	*P. putida* S12-10 (ΔpTTS12) Δ*arpR; ΔgacS; atp*α (R165C); Δ*afr; rpoB'* (D622G)	This paper
E. coli WM3064	*thrB1004 pro thi rpsL hsdS lacZ*ΔM15 RP4-1360 Δ(*araBAD*)567 Δ*dapA1341*::[erm pir]	William Metcalf
Plasmid	**Description**	**Ref.**
pEMG	Km^R, Ap^R, *ori* R6K, *lacZ*α MCS flanked by two I-SceI sites	(20)
pEMG-Δ*arpR*	pEMG plasmid for constructing *P. putida* S12d Δ*afr*	This paper
pEMG-Δ*afr*	pEMG plasmid for constructing *P. putida* S12d Δ*afr*	This paper

Plasmid	Description	Ref.
pEMG-Δ*gacA*	pEMG plasmid for constructing *P. putida* S12d Δ*gacA*	This paper
pEMG-Δ*gacS*	pEMG plasmid for constructing *P. putida* S12d Δ*gacS*	This paper
pEMG-Δ*lapA*	pEMG plasmid for constructing *P. putida* S12 Δ*lapA*	This paper
pEMG-Δ*flg*	pEMG plasmid for constructing *P. putida* S12 Δ*flg*	This paper
pEMG-c-*arpR*	pEMG plasmid for constructing *P. putida* S12e *arpR*-wt	This paper
pEMG-c-*afr*	pEMG plasmid for constructing *P. putida* S12e *afr*-wt	This paper
pEMG-c-*gacS*	pEMG plasmid for constructing *P. putida* S12e *gacS*-wt	This paper
pEMG-c-*rpoB'*	pEMG plasmid for constructing *P. putida* S12e *rpoB'*-wt	This paper
pEMG-c-ATP	pEMG plasmid for constructing *P. putida* S12e ATP-wt	This paper
pSW-2	Gm^R, *ori* RK2, *xylS*, Pm ® I-sceI	(20)
p421-cas9	Cas9 and tracrRNA; oriV RK2; Sm^R/Sp^R	(22)
p658-ssr	xylS -Pm → ssr , oriV RSF1010; Gm^R	(22)
p2316	SEVA CRISPR array; oriV pBBR1; Km^R	(21)
p2316-ATPsyn	pSEVA2316 derivative containing the ATP synthase spacer	This paper
p2316-rpoB'-622	pSEVA2316 derivative containing the rpoB' spacer (substitution of amino acid D622G)	This paper

Table 5.S2. Oligos used in this study

Oligos	Sequence	Purpose
Afr_test_F	gaaacgaccatgtaatgc	PCR and sanger sequencing of mutated region within RPPX_14685
Afr_test_R	gaggaaagccatcatgac	PCR and sanger sequencing of mutated region within RPPX_14685
ArpR_test_F	gtcgaaccaaagaagaag	PCR and sanger sequencing of mutated region within RPPX_14650
ArpR_test_R	gctgaagactacgcaatc	PCR and sanger sequencing of mutated region within RPPX_14650
ATP_test_F	ggttattcgctacaactc	PCR and sanger sequencing of mutated region in the intergenic region of RPPX_09485-09490
ATP_test_R	gaagatcaacaggaagatc	PCR and sanger sequencing of mutated region in the intergenic region of RPPX_09485-09490
ATPa_test_F	aaaggtcctctgggtaac	PCR and sanger sequencing of mutated region within RPPX_09510
ATPa_test_R	gacagcaacataaacacag	PCR and sanger sequencing of mutated region within RPPX_09510
GacA_test_F	atctgcgggctgatatag	PCR and sanger sequencing of mutated region within RPPX_000635
GacA_test_R	gttgtgctgatggatgtg	PCR and sanger sequencing of mutated region within RPPX_000635
GacS_test_F	cgacagctcgatctctac	PCR and sanger sequencing of mutated region within RPPX_15700
GacS_test_R	caactggagagaattgcc	PCR and sanger sequencing of mutated region within RPPX_15700
rpoB1_test_45_F	acttcaacgccgcacttc	PCR and sanger sequencing of mutated region within RPPX_06985, for the mutation N45S
rpoB1_test_45_R	cttgaaagacctactgaatttgc	PCR and sanger sequencing of mutated region within RPPX_06985, for the mutation N45S
rpoB1_test_410_F	ttaccttcgatcagtacgg	PCR and sanger sequencing of mutated region within RPPX_06985, for the mutation D622G
rpoB1_test_410_R	ggtaagcgtgttgactactcc	PCR and sanger sequencing of mutated region within RPPX_06985, for the mutation D622G
rpoB1_test_622_F	gtactggctctcgatttc	PCR and sanger sequencing of mutated region within RPPX_06985, for the mutation D410E
rpoB1_test_622_R	ttgtactgggtctgtactacat	PCR and sanger sequencing of mutated region within RPPX_06985, for the mutation D410E
Flg_test_F	catacatttcgcggtagac	PCR and sanger sequencing of the knocked-out flagella gene cluster

Oligos	Sequence	Purpose
Flg_test_F	agaataagcagtacctggtttc	PCR and sanger sequencing of the knocked-out flagella gene cluster
KO_TS1_ArpR_F	cgggcgaattctcttctttcttacagccact	ΔRPPX_14650
KO_TS1_ArpR_R	aacagatcgacactgtcagcttgtagaaggccctttc	ΔRPPX_14650
KO_TS2_ArpR_F	gaaagggccttctacaagctgacagtgtcgatctgtt	ΔRPPX_14650
KO_TS2_ArpR_R	cggactctagactacaaaccacagatcctg	ΔRPPX_14650
KO_TS1_Afr_F	cctcaggatccctcagtcgaaggtatgcaagtcca	ΔRPPX_14685
KO_TS1_Afr_R	Ttcttcacctttatgaattcccatgatcatgatggctttc ctctgctgaccg	ΔRPPX_14685
KO_TS2_Afr_F	Cgcacggcatggatgaactctacaaataaagct-caa cattcgcctgcaccg	ΔRPPX_14685
KO_TS2_Afr_R	ggcgatctagaccaacctgtgtataccggcaacct	ΔRPPX_14685
KO_TS1_GacA_F	tagtagctatcttcgcactg	ΔRPPX_00635
KO_TS1_GacA_R	ctcatgtcccaagtcttt	ΔRPPX_00635
KO_TS2_GacA_F	accactaagaccctaatcaa	ΔRPPX_00635
KO_TS2_GacA_R	catagtgaatccatacgtttac	ΔRPPX_00635
KO_TS1_GacS_F	gagttcgtcattgatgaag	ΔRPPX_15700
KO_TS1_GacS_R	ctgacatgctgagtatgct	ΔRPPX_15700
KO_TS2_GacS_F	atccttgagctgattgac	ΔRPPX_15700
KO_TS2_GacS_R	ggtagctatttcacctgg	ΔRPPX_15700
KO_TS1_lapA_F	agattgaattcaagtacaaccatataactgtcc	knocking-out lapA/adhesin, negative control for biofilm assay
KO_TS1_lapA_R	gtggcgtaatcgtttataatcatcatccacaacaag	knocking-out lapA/adhesin, negative control for biofilm assay
KO_TS2_lapA_F	cttgttgtggatgatgattataaacgattacgccac	knocking-out lapA/adhesin, negative control for biofilm assay
KO_TS2_lapA_R	gggcatctagagtgtacttatcgaaggtgac	knocking-out lapA/adhesin, negative control for biofilm assay
KO_TS1_flg_F	ggcagggatccggaagaaatttcacctaaaagc	knocking-out flagella gene cluster, negative control for swimming motility assay
KO_TS1_flg_R	ctataccttgctcaacgaaattgaagagatgatg-cagatcaatc	knocking-out flagella gene cluster, negative control for swimming motility assay
KO_TS2_flg_F	gattgatctgcatcatctcttcaatttcgttgagcaag-gtatag	knocking-out flagella gene cluster, negative control for swimming motility assay
KO_TS2_flg_R	cgtgttctagaggaatgtgctgatctatttctc	knocking-out flagella gene cluster, negative control for swimming motility assay
c_Afr_F	gcaatgaattcatctgtgcaaaaacctgta	complementation of RPPX_14685 to the wild-type sequence in the evolved strains
c_Afr_R	agggttctagaacaatctccttgaagcag	complementation of RPPX_14685 to the wild-type sequence in the evolved strains
c_ArpR_F	ccttcgaattccgaagagcgaccgatacgg	complementation of RPPX_14650 to the wild-type sequence in the evolved strains
c_ArpR_R	ttctttctagacttccagtccatttcgctgacc	complementation of RPPX_14650 to the wild-type sequence in the evolved strains

Oligos	Sequence	Purpose
c_ATPa_F	cgaaagaattcgaagcattgaaatcttgag	complementation of RPPX_09510 to the wild-type sequence in the evolved strains
c_ATPa_R	tgatgtctagaatcttactgcgaatctcttt	complementation of RPPX_09510 to the wild-type sequence in the evolved strains
c_GacA_F	gcgctgaattcaaagacttgggacatgag	complementation of RPPX_00635 to the wild-type sequence in the evolved strains
c_GacA_R	gaggtggatccttgattagggtcttagtggt	complementation of RPPX_00635 to the wild-type sequence in the evolved strains
c_GacS_F	cagccgaattcaagctttcctgatcgtag	complementation of RPPX_15700 to the wild-type in the evolved strains
c_GacS_R	ggcaatctagaataacacgtactaaagagatgc	complementation of RPPX_15700 to the wild-type in the evolved strains
c_ATP_F	gcactggatccacaacttaaggaatccgtat	complementation of RPPX_09485-09490 to the wild-type sequence in the evolved strains
c_ATP_R	gtcagtctagacaagtggtgctggatatag	complementation of RPPX_09485-09490 to the wild-type sequence in the evolved strains
c_rpoB1_F	ccaaaggatccggtacaaaagtctaaagaggat	complementation of RPPX_06985 to the wild-type sequence in the evolved strains
c_rpoB1_R	aggagtctagaccttgaaagacctactgaat	complementation of RPPX_06985 to the wild-type sequence in the evolved strains
cr-rpoBWT-622-1-S	aaacagtaagcgaaaccggtgtacatcagctggtg	spacer fragment for introducing D622G point mutation at RPPX_06985
cr-rpoBWT-622-1-AS	aaaacaccagctgatgtacaccggtttcgcttact	spacer fragment for introducing D622G point mutation at RPPX_06985
RpoB-622e-1	Gaaatggtcgagtaagcgaaaccggtgtacat-cagctggccggcgaagataacggtctctttcagac-caaccacgcggtag	repair fragment for introducing D622G point mutation at RPPX_06985
cr-ATPWT-1-S	aaacatctgacggtcgccaatgatcagctcacgcg	spacer fragment for introducing R165C point mutation at RPPX_09510
cr-ATPWT-1-AS	aaaacgcgtgagctgatcattggcgaccgtcagat	spacer fragment for introducing R165C point mutation at RPPX_09510
ATP-09510e-1	Gtcttgccgatctgacggtcgccaatgatcagctca-cactggccacggccgacagggatcatggcgtc-gacggatttgtaaccag	repair fragment for introducing R165C point mutation at RPPX_09510

Table 5.S3. Growth parameters of ALE-derived and reverse engineering strains

Strains	Media	Lag time (minutes)	μmax (h^{-1})		maxOD	
			μmax	sd	maxOD	sd
ALE						
S12	LB	180	1.18	0.090	0.90	0.038
S12e30		180	1.02*	0.021	0.87	0.027
S12-06		180	1.14	0.026	0.88	0.048
S12-06e30		180	0.80*	0.029	0.82*	0.036
S12-10		180	1.15	0.038	0.89	0.039
S12-10e35		180	0.78*	0.030	0.83*	0.032
S12-22		195	1.07	0.037	0.88	0.045
S12-22e30		180	0.79*	0.018	0.82*	0.034
S12	MM + citrate	180	1.02	0.105	0.88	0.064
S12e30		180	1.05	0.044	0.86	0.027
S12-06		165	1.01	0.095	0.83	0.027
S12-06e30		225	0.48*	0.058	0.54*	0.130
S12-10		165	1.02	0.141	0.83	0.032
S12-10e35		255	0.47*	0.044	0.37*	0.145
S12-22		165	0.99	0.078	0.84	0.019
S12-22e30		240	0.41*	0.049	0.30*	0.115
S12	MM + glucose	150	0.89	0.072	1.00	0.024
S12e30		150	1.06*	0.021	0.99	0.009
S12-06		150	0.95	0.027	1.02	0.033
S12-06e30		180	0.71*	0.028	0.66*	0.074
S12-10		150	0.97	0.058	1.03	0.033
S12-10e35		195	0.70*	0.032	0.70*	0.199
S12-22		150	0.94	0.033	1.02	0.022
S12-22e30		210	0.73*	0.019	0.62*	0.161
S12	MM + glycerol	195	1.16	0.119	1.04	0.006
S12e30		195	1.04	0.010	0.89*	0.046
S12-06		195	1.11	0.138	1.09	0.051
S12-06e30		255	0.54*	0.044	0.82*	0.010
S12-10		180	1.11	0.159	1.08	0.046
S12-10e35		315	0.50*	0.011	0.79*	0.031
S12-22		195	1.17	0.119	1.10	0.044
S12-22e30		300	0.52*	0.029	0.80*	0.011

Strains	Media	Lag time (minutes)	μmax (h^{-1})		maxOD	
			μmax	sd	maxOD	sd
Reverse engineering						
RE1	LB	195	0.88	0.013	0.93	0.0498
RE2		105**	0.96**	0.017	0.96	0.0468
RE3		135*	0.88*	0.035	1.07	0.1016
RE4		135	0.89	0.035	1.07	0.0985
RE5		135	0.94	0.029	1.04	0.0937
RE1	MM + citrate	195	1.02	0.048	0.85	0.0605
RE2		150**	0.97	0.025	0.94	0.0460
RE3		240*	0.54*	0.106	0.51*	0.1681
RE4		240	0.57	0.096	0.40	0.0698
RE5		240	0.49	0.067	0.44	0.1328
RE1	MM + glucose	120	0.98	0.031	1.02	0.0326
RE2		120	1.04	0.018	1.00	0.0399
RE3		165*	0.84*	0.077	0.64*	0.0917
RE4		165	0.78	0.083	0.63	0.1286
RE5		165	0.93	0.140	0.59	0.1101
RE1	MM + glycerol	150	1.10	0.044	1.00	0.0958
RE2		120**	1.14	0.072	0.99	0.1264
RE3		180*	0.78*	0.101	1.06	0.2613
RE4		180	0.79	0.098	1.02	0.2867
RE5		180	0.87	0.098	1.10	0.2124

*) significant reduction of growth parameter in comparison to its parent strain

**) significant improvement of growth parameter in comparison to its parent strain

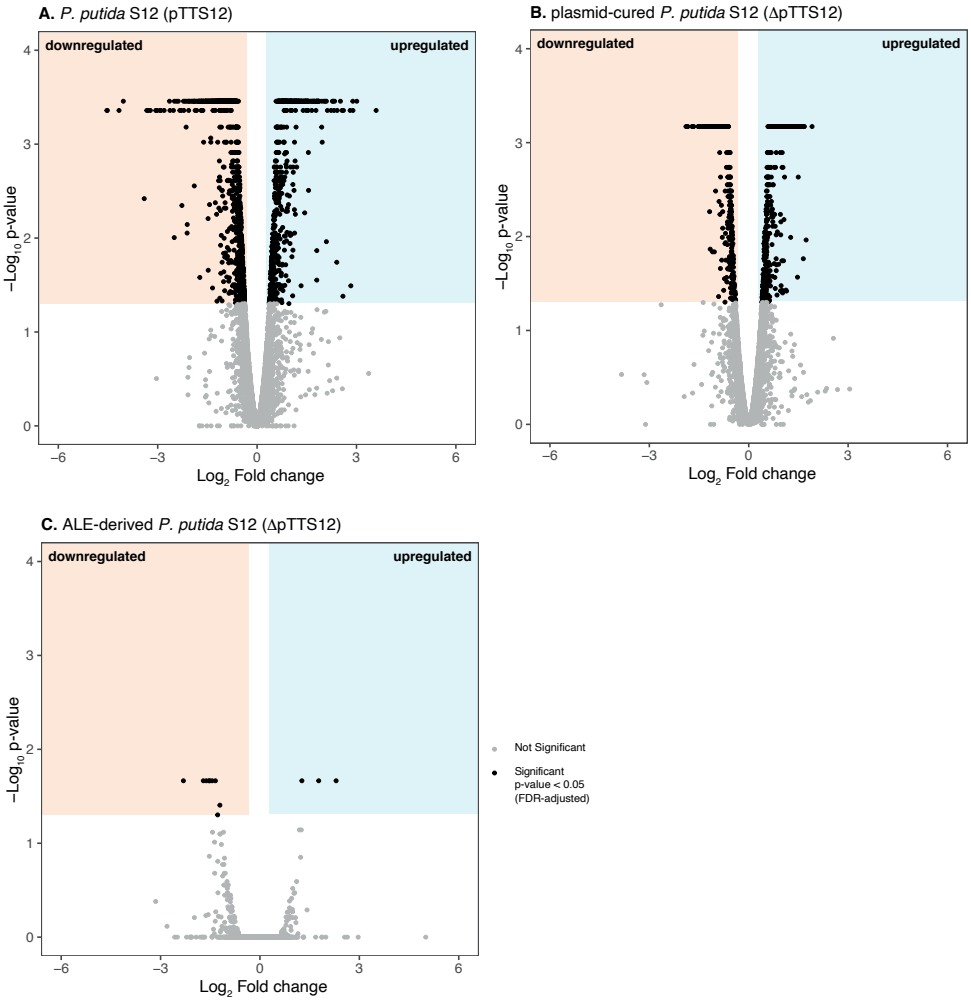

Fig. 5.S1. Volcano plot of differential gene expression in P. putida S12, S12 ΔpTTS12, and ALE-derived strains in the presence of toluene.

Control strains were refers on LB medium for 2 hours before sampling and sample strains were grown on LB medium with 0.1% (vol/vol) toluene for 2 hours before sampling. Blue area indicates the significantly upregulated genes and beige area indicates the significantly downregulated genes (cut-off: Log_2 Fold Change ≥ 1 for up-regulated genes or ≤ 1 for down-regulated genes and FDR-adjusted p-value ≤ 0.05).

CHAPTER 6

Characterization of an AraC family transcriptional regulator Afr in *Pseudomonas putida* S12

Hadiastri Kusumawardhani, Aditi Yadav, Adelė Kaltenytė, Benjamin Furtwängler, Rohola Hosseini, Johannes H. de Winde

Manuscript in preparation.

Abstract

Megaplasmid curing in *Pseudomonas putida* S12 caused a specific mutation at RPPX_14685 locus, putatively encoding for an AraC family transcriptional regulator (proposed name Afr). Furthermore, during the adaptive laboratory evolution (ALE) experiment to recover solvent tolerance in the plasmid-cured *P. putida* S12, SNPs which cause a frameshift occurred at the *afr* locus. Therefore, Afr seems to play an important role to enable plasmid-curing and regain the solvent tolerance trait in the plasmid-cured strain, however its function remained elusive. In this chapter, we characterize the function and role of Afr. Transcriptional analysis (RNA-seq) and a confirmatory RT-qPCR experiment indicated that Afr positively regulates 32 loci which consist of membrane transporters, porins, and dehydrogenases; including the MexEF-OprN multidrug efflux pump. Remarkably, the mutation and truncation of Afr were able to change the antibiotic resistance profile, underscoring the central role of Afr as a stress-response regulator in *P. putida* S12.

Introduction

The AraC family transcriptional regulators (AFTR) are among the largest families of prokaryotic transcription factors (1). Members of the AFTR typically consist of 250-350 amino acid residues and are ubiquitous in gamma proteobacteria. AFTR proteins contain a variable N-terminal domain and a conserved C-terminal domain, the latter being responsible for DNA binding activity. This regulator family is involved in controlling a wide variety of functions, such as carbon utilization, pathogenesis and stress responses (2). Most AFTRs play a role as positive activators and may respond directly to the environmental signalling molecules which diffused into the bacterial cell or controlled by another regulator (1, 2).

The mechanism of AFTR is modelled after the transcriptional activator AraC of arabinose catabolism gene cluster *ara*BAD. Signalling molecules may interact with the N-terminal effector binding domain (EBD), causing a conformational change of the AFTR dimer and subsequently allows the C-terminal helix-turn-helix (HTH) domain to bind the promoter region (3–5). The proposed mechanism of the AraC transcriptional regulator, called the 'light switch' model, requires the availability of arabinose as an environmental signalling molecule (4). In the absence of arabinose, the AraC dimer will bind the O_2 and I_1 promoter regions. In the presence of arabinose, this dimer undergoes conformational and binding site changes to the I_1 and I_2 promoter regions. This change enables the expression of the *ara*BAD gene cluster and consequently, arabinose utilization; hence the 'light switch' analogy. Other members of AFTRs, such as RegA and ToxT, were also reported to respond to their respective effectors in a similar manner as the 'light switch' model (3, 5). More recently, CmrA was identified to be an AFTR responsible for the antibiotic resistance phenotype of the *nfxC2* mutant *Pseudomonas aeruginosa* PA14 and requires electrophilic molecules to be activated (6).

In previous experiments, we successfully removed the megaplasmid of solvent-tolerant *Pseudomonas putida* S12 and studied its effect on inciting solvent tolerance trait (7). However, the resulting strains carry an identical SNP at RPPX_14685 locus (CDS position 157) which putatively substitutes an amino acid on its N-terminal region. BLASTp searches and protein modelling revealed that RPPX_14685 putatively encodes for an AFTR (proposed gene name *afr*). In this chapter, we characterize the function of this transcriptional regulator and identify the genes regulated by Afr in *P. putida* S12.

Results

A point mutation at the RPPX_14685 locus occurred during plasmid curing with mitomycin C

The megaplasmid pTTS12 was cured from *P. putida* S12 using an intercalating agent, mitomycin C (30 μg ml^{-1}) (7). Following the curing of pTTS12, we performed whole genome sequencing on the plasmid-cured strains to map the mutations that can be caused by plasmid curing using an intercalating agent. The three different plasmid-cured isolates; S12-06, S12-10, and S12-22 contain a limited amount of SNPs (Table 6.1). However, all of the plasmid-cured isolates carry a SNP at the RPPX_14685 locus which resulted in a codon change of ACC into CCC, substituting the 53rd amino acid from threonine into proline (T53P). Upon the repetition of the plasmid curing experiment, all of the plasmid-cured strains were found to contain the same ACC → CCC point mutation (Table 6.2).

Table 6.1. The genetic variants found in the plasmid-cured strains of *P. putida* S12.

Strain	Locus tag	Product	Variant type	Protein effect	Codon change	Amino acid change	CDS pos.	Variant Frequency
S12-06	RPPX_14685	AraC family transcriptional regulator	SNP (transversion)	Substitution	ACC → CCC	T → P	157	100%
S12-10	RPPX_14685	AraC family transcriptional regulator	SNP (transversion)	Substitution	ACC → CCC	T → P	157	100%
S12-22	RPPX_14685	AraC family transcriptional regulator	SNP (transversion)	Substitution	ACC → CCC	T → P	157	100%
S12-22	RPPX_19665	GCN5 family acetyltransferase	Insertion of mobile element	Disruption	-	-	-	-
S12-06	RPPX_05325 - 05330	Intergenic region	SNP (transversion)	-	-	-	-	100%

The recurring ACC → CCC point mutation at the RPPX_14685 locus might give an advantage regarding mitomycin C resistance and might actually be important for losing the

megaplasmid pTTS12. Therefore, we compared the survival rate on mitomycin C and plasmid-curing rate between wild-type S12 and S12c, a S12 strain with the ACC → CCC mutation at RPPX_14685 locus. The strain S12c showed more surviving colonies after mitomycin C treatment, suggesting a higher mitomycin C resistance. All of the surviving colonies of S12c after mitomycin C treatment showed a loss of megaplasmid. In the wild-type S12 strain, only 2.48% of the surviving colonies lost the megaplasmid pTTS12 (Table 6.2). Therefore, the point mutation at the RPPX_14685 locus increased survival and plasmid curing rate during mitomycin C treatment.

Table 6.2. Survival and plasmid curing rate of the wild-type *P. putida* S12 and *P. putida* S12c, carrying ACC → CCC point mutation at the RPPX_14685 locus.

Strain	Survival rate on Mitomycin C (30 μg ml^{-1})	pTTS12 curing rate	Variant frequency at RPPX_14685 locus
S12	2.48 (± 0.58) x 10^{-8}	2.48 (± 0.5) %	100%
S12c	1.44 (±0.51) x 10^{-4}	100%	-

The protein encoded on RPPX_14685 constitutes an AraC family transcriptional regulator (Afr)

Based on our BLASTp search, RPPX_14685 seemed to encode for an **A**raC **f**amily transcriptional **r**egulator and therefore we propose to name this protein Afr. Afr is widely distributed among the *Pseudomonas* genus (Fig 6.1). The best characterized homologue of Afr is CmrA (63% identity, 88% coverage), a transcriptional activator of the MexEF-OprN antibiotic pump found in *Pseudomonas aeruginosa* PA14 (6). *P. putida* S12 also contains another putative AraC family transcriptional regulator encoded on RPPX_17385 locus which shares 58.84% identity and 95% coverage with Afr. This transcriptional regulator is more closely related to CmrA (67% identity, 91% coverage) than Afr, as it belongs to the same clade with CmrA (Fig 6.1). It is interesting to note that other *P. putida* strains (e.g. F1, GB-1, ND6, and DOT-T1E) also contain two Afr-like proteins, one belonging to the same clade as Afr and another to the same clade as CmrA and RPPX_17385.

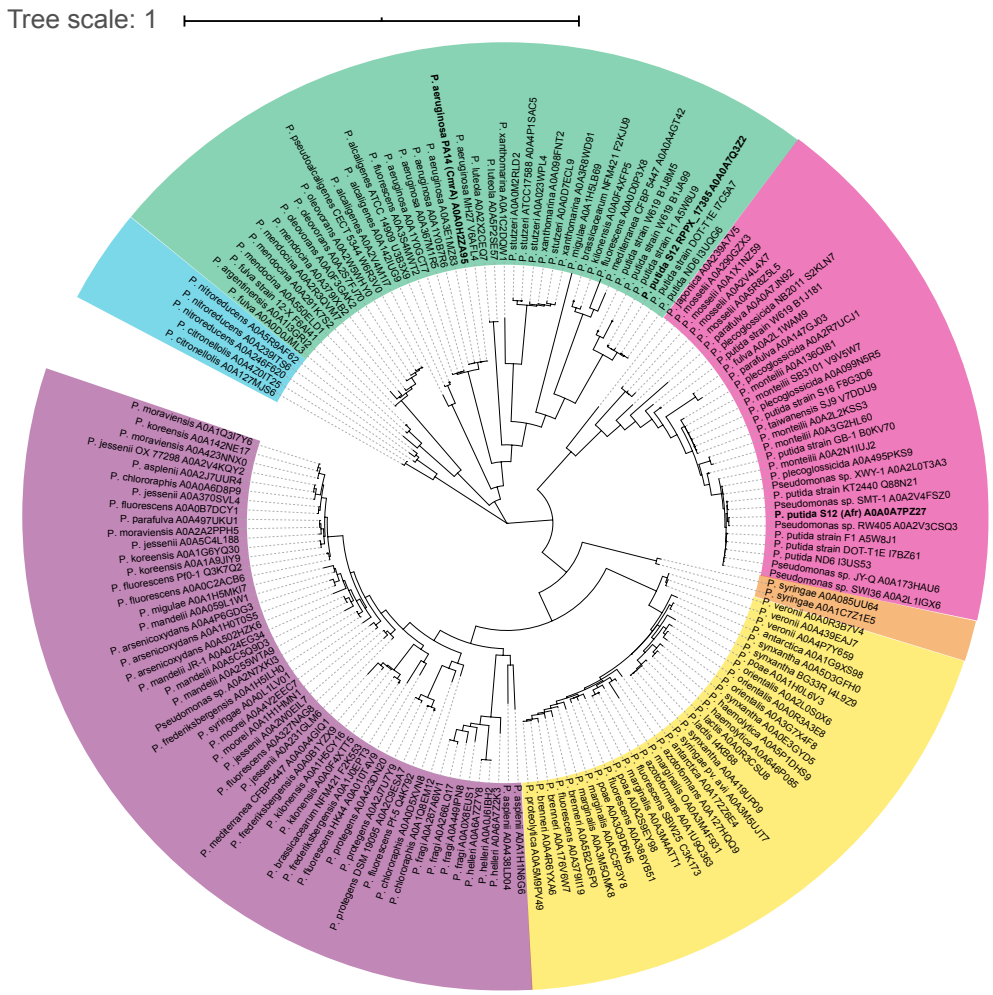

Fig. 6.1. Phylogenetic tree of 165 Afr-like proteins encoded on the genome of various Pseudomonas species. Different colours represent different clades. Afr and CmrA are indicated with bold text, belonging to the magenta and green clade respectively.

Analysis of 165 Afr homologues from different *Pseudomonas* species revealed a high degree of conservation on its C-terminal domain while the N-terminal domain of Afr was highly variable (Fig. 6.2A). The substituted Threonine-53 occurred on this variable N-terminal region (Fig. 6.2A, indicated by the red arrow). It is interesting to note that the HTH-2 C-terminal domain is highly conserved among Afr homologues from different *Pseudomonas* species (Fig. 6.2A). To understand the effect of T53P substitution on Afr, we predicted the structure of Afr using online protein prediction tool I-TASSER (8). Afr was modelled after ToxT from *Vibrio cholerae*, an AFTR which positively regulates the cholera toxin and type VI secretion system

(T6SS), the main characteristics for virulence in *V. cholerae* (5). Afr contains a N-terminal effector binding domain (EBD) and two regions of helix-turn-helix (HTH), which are putatively responsible for DNA binding and the dimerization of the Afr protein (Fig. 6.1B). The substituted Threonine-53 occurred in the middle of the EBD region, at a linker between β-sheets that are largely present on the N-terminal domain (Fig. 6.2B).

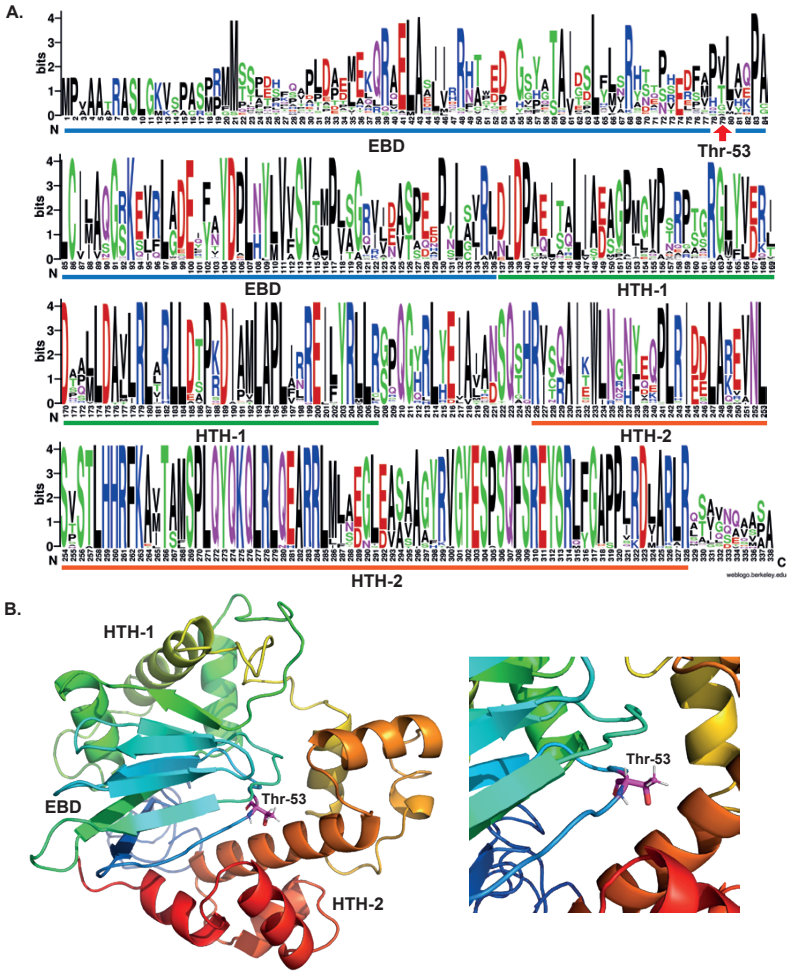

Fig. 6.2. A. Weblogo representation of the amino acid conservation among 165 Afr homologues from different Pseudomonas species.

Different domains of Afr are indicated with colored lines. The substituted Threonine-53 (Thr-53) is indicated with a red arrow. B. I-TASSER prediction of the Afr structure. According to the protein structure of ToxT (PDB ID 3GBG) from Vibrio cholera. Afr contains an effector binding domain (EBD) which consists of parallel beta-sheets and two helix-turn-helix (HTH) regions. The substituted Threonine-53 (Thr-53) is located at the EBD, as indicated in this figure.

Table 6.3. Putative Afr-regulated loci

Locus tag	Annotation	Plasmid-cured S12		Confirmatory RT-qPCR log_2FC; normalized to S12-wt		
		log_2FC	p_value	S12-10	S12-10Δ	S12-10wt
RPPX_14685 *)	AraC family transcriptional regulator	2.20414	5.00E-05	2.448	N/A	-0.006
RPPX_14930	Quinoprotein glucose dehydrogenase	2.07601	5.00E-05	2.377	-0.205	0.078
RPPX_14935	OprB family porin	3.67882	5.00E-05	3.632	0.184	-0.085
RPPX_16940, RPPX_16945	MetNI (methionine importer)	1.32573	5.00E-05	1.590	-0.170	0.336
RPPX_17365	SDR family oxidoreductase	1.72841	5.00E-05	1.700	0.045	0.042
RPPX_17630	DctA (aerobic C4-dicarboxylate transport protein)	5.18095	5.00E-05	3.775	-0.140	-0.197
RPPX_17635	Citrate-divalent cation : H^+ symporter	5.80933	5.00E-05	5.039	-0.087	0.009
RPPX_17640	OprD family porin	3.32728	5.00E-05	3.354	-0.039	0.096
RPPX_17645	CsbD family protein	2.02353	5.00E-05	2.245	0.062	0.082
RPPX_17650	SoxR (bacterial sensor of oxidative stress)	2.06389	5.00E-05	2.076	-0.026	0.024
RPPX_17720	RNA polymerase sigma factor (σ^{70} family)	2.89481	5.00E-05	2.061	-0.012	0.020
RPPX_17725	Diaminopimelate decarboxylase	1.75665	5.00E-05	1.913	0.079	-0.001
RPPX_21210, RPPX_21215 *)	RND efflux pump MexF-OprN	3.9932	5.00E-05	3.772	0.003	-0.043
RPPX_21545	Alginate export family protein	5.14782	5.00E-05	4.432	0.020	-0.005
RPPX_21550	3-(3-hydroxy-phenyl)propionate transporter	2.35045	5.00E-05	2.046	-0.089	-0.131
RPPX_21555	RbdA	3.50752	5.00E-05	3.778	-0.178	0.237
RPPX_21560, RPPX_21565	TonB-dependent receptor	3.61084	5.00E-05	3.515	0.032	-0.045
RPPX_24075	Zinc-dependent alcohol dehydrogenase	2.2774	5.00E-05	2.225	0.115	0.012
RPPX_24520	Quinoprotein dehydrogenase	2.24277	5.00E-05	2.227	0.091	0.008
RPPX_24525	Arginine binding protein	1.82785	5.00E-05	1.737	-0.013	0.249
RPPX_24930, RPPX_24935 *)	IorAB (Isoquinoline 1-oxidoreductase)	5.37876	5.00E-05	4.836	-0.278	0.011
RPPX_25035	Methyl-accepting chemotaxis protein	3.56493	5.00E-05	3.704	-0.012	0.057
RPPX_25340	Enoyl-CoA hydratase	5.01552	5.00E-05	4.937	-0.080	0.073
RPPX_25345, RPPX_25350, RPPX_25355	Putative ABC transport system	1.73293	5.00E-05	1.912	0.140	0.227

**) homologs of these genes were also regulated by CmrA from PA14 (6)*

***) Colours indicate putative gene clusters*

Identification of the genes regulated by Afr

Previous RNA-seq experimental data were analysed to identify the genes regulated by Afr. In this experiment, we compare the wild-type S12 with the plasmid-cured S12, the latter contains the T53P substitution at Afr locus (see Chapter 5). The RNA-seq data were screened for the genes that are differentially expressed in the plasmid-cured S12 compared to the wild-type S12. We found 32 loci differentially expressed in this comparison and all of these loci were upregulated in the plasmid-cured S12 compared to the wild-type S12 (Table 6.3).

We performed RT-qPCR to confirm our findings of the genes putatively regulated by Afr. For this experiment, we used the wild-type S12 as the control strain. Strain S12-10 represented the plasmid-cured strains, containing only the point mutation ACC → CCC at *afr* locus. Strain S12-10wt represented the plasmid-cured strain without the point mutation at the *afr* locus (wild-type Afr). Strain S12-10Δ represented the strain with a deleted *afr* locus in the absence of pTTS12 plasmid. The 32 loci were upregulated in the strain S12-10 while there were no observed differences in the expression of these loci in the strains S12-10wt and S12-10Δ compared to the wild-type S12. Indeed, all of the 32 loci that are putatively regulated by Afr according to the RNA-seq data were confirmed to be regulated by Afr in our RT-qPCR experiment.

Many of these loci appear to constitute putative gene clusters, indicated by different colours on Table 6.3. Moreover, several loci belong to polycistronic mRNA, for instance, RPPX_16940-RPPX_16945, RPPX_21210-21215, RPPX_24930-RPPX_24935, and RPPX_25345-RPPX_25355. Among the 32 loci regulated by Afr, the genes encoded by RPPX_14685 (Afr), RPPX_21210 & RPPX_21215 (MexF-OprN), and RPPX_24930 & RPPX_24935 (aldehyde dehydrogenase & oxidoreductase) are homologs to the genes regulated by CmrA from *P. aeruginosa* PA14 (6), as indicated by asterisks on Table 6.3.

The T53P substitution of Afr affected antibiotic resistance profile of *P. putida* S12

Based on the RNA-seq and RT-qPCR findings, the substitution T53P at the Afr locus (strain S12-10) seemed to cause an upregulation of RPPX_21210 and RPPX_21215 which encode for MexF and OprN, the inner and outer membrane components of the MexEF-OprN efflux pump respectively. Therefore, the point mutation at the *afr* locus may change the antibiotic resistance of the plasmid-cured S12 strain. Indeed, we demonstrated an increase in the survival rate of the strain S12c during mitomycin C treatment (Table 6.2). To characterize the effect of

the T53P substitution in Afr, we quantified the minimum inhibitory concentration (MIC assay) of several antibiotics on the strains S12, S12-10, S12-10wt, and S12-10Δ (Table 6.4).

The strain S12-10 showed an increase in its antibiotic resistance against Mitomycin C (8 times), ciprofloxacin (8 times) and chloramphenicol (4 times) compared to the wild-type S12 strain (Table 6.4). Ciprofloxacin and chloramphenicol have been previously identified as substrates of the MexEF-OprN pump (6). The strains S12-10wt and S12-10Δ showed a similar antibiotic resistance profile as the wild-type S12 strain, which confirms the RNA-seq and RT-qPCR findings that in these strains the expression level of the MexEF-OprN efflux pump was similar to the wild-type S12. This indicates that in the strain S12-10, the MexEF-OprN was indeed upregulated. However, a decrease in antibiotic resistance against carbenicillin, kanamycin, and streptomycin was observed in the strain S12-10. These antibiotics are not the substrates of MexEF-OprN; they are the substrates of ArpABC, a homolog to TtgABC from *P. putida* DOT-T1E and MexAB-OprM from *P. aeruginosa* (9, 10).

Table 6.4. Minimum inhibitory concentration of several antibiotics in *P. putida* S12 strains

Antibiotic	Minimum inhibitory concentration (μg ml^{-1})			
	S12-wt	S12-10wt	S12-10	S12-10Δ
Mitomycin C	32	32	256	32
Carbenicillin	256	256	64	256
Cefotaxime	16	16	16	16
Kanamycin	32	32	16	32
Ciprofloxacin	0.125	0.125	1	0.125
Trimethoprim	4096	4096	4096	4096
Aztreonam	32	32	16	32
Imipenem	2	2	2	2
Chloramphenicol	128	128	512	128
Streptomycin	64	64	32	64
Tetracycline	16	16	16	16

Discussion

The substitution T53P putatively caused a constitutive activation of Afr

Similar to CmrA (6) and ToxT (5), Afr seemed to constitute a positive regulator in the family of

AraC transcriptional regulators. This family of transcriptional regulators requires an induction, e.g. Arabinose for the model AraC transcriptional regulator in *E. coli* (11) and cinnamaldehyde for CmrA in *P. aeruginosa* PA14 (6). In our findings, S12-10wt and S12-10Δ did not seem to show a differential expression on the 32 loci putatively regulated by Afr relative to the wild-type S12 strain. Indeed, this may indicate that in the wild-type S12 and S12-10wt, Afr is present in an inactive form. The substitution T53P occurred at the effector binding domain (EBD) region of Afr. The EBD region is important for the binding to the inducer and thus drives the activity of an AraC family transcriptional regulator (AFTR) to form a dimer and bind to the promoter regions (5, 11). Our data indicated that the T53P substitution caused Afr to be in a constitutively active form, overriding the need for an inducer, and therefore causing a constitutive upregulation of its target loci.

BLASTp analysis revealed that the Afr protein is ubiquitous in *Pseudomonas* species. Indeed, several *Pseudomonas putida* strains even contain two Afr proteins, e.g. RPPX_14685 and RPPX_17385 from *P. putida* S12. The C-terminal region composing an HTH-2 domain exhibits a high amino acid sequence conservation. This region is responsible for DNA binding, while the effector binding domain (EBD) and the HTH-1 domain is responsible for the dimerization of Afr-like protein (3, 5, 12). Due to the high conservation of the HTH-2 domain and the low conservation of EBD, it is possible that the two Afr-like proteins in *P. putida* strains recognize the same promoter regions and regulate the same set of genes while responding to different environmental effectors. It is interesting to study the cross-recognition among similar AFTRs which exist in one strain.

Afr regulates a plethora of membrane-bound proteins

Several Afr-regulated genes share homology with the genes regulated by CmrA from *P. aeruginosa* PA14. RPPX_21210 and RPPX_21215, which encode for MexF and OprN respectively, are among the Afr-regulated loci. In the strain S12-10 with T53P substitution on Afr, we could observe an increase of the minimum inhibitory concentration (MIC) of MexEF-OprN substrates like ciprofloxacin and chloramphenicol. Afr seemed to be self-regulating similar to its homolog CmrA in *P. aeruginosa* PA14 (6). In addition, Afr and CmrA also seem to regulate a putative membrane-bound isoquinoline-1-oxidoreductase (*iorAB*) encoded on RPPX_24930 and RPPX_24935 in *P. putida* S12 or PA1881 and PA1880 in *P. aeruginosa* PA14. This reductase was characterized for its ability to catalyse the hydroxylation of isoquinoline to

1-oxo-1,2-dihydroxyquinoline (13). A recent study also identified this reductase to be responsible for vanillin utilization in *P. putida* KT2440 as an alternative vanillin dehydrogenase (14).

Our RNA-seq and RT-qPCR data suggested that Afr regulates other membrane proteins like porins and transporters that are responsible for the transport of carbon sources and amino acids. RPPX_14635 and RPPX_17640 are predicted to encode for a carbohydrate-specific OprB porin and an amino acid porin OprD, respectively (15, 16). RPPX_16940 and RPPX_16945 are predicted to encode for the homolog of MetNI, a high-affinity methionine ABC transporter previously described in *E. coli* (17). Furthermore, RPPX_17630 and RPPX_17635 appear to encode for proton-dependent C4-dicarboxylate and citrate-Mg^{2+}/Ca^{2+} symporters, respectively (18). We attempted to predict the DNA binding sites of Afr using MEMEsuite (http://meme-suite.org/) based on the upstream regions of the Afr-regulated gene clusters. However, we could not identify any putative binding site from this analysis. Indeed, Afr may not directly regulate the expression of these transporters and membrane proteins. Further binding site analysis (e.g. CHIP-seq) may be beneficial to elucidate the regulation mechanism of Afr.

The role of Afr in enabling plasmid-curing and restoring solvent tolerance in ALE-derived strains

Previous attempts reported success in curing *Pseudomonas* plasmids using Mitomycin C treatment with a plasmid curing rate of 5-7% (19, 20). In the plasmid-cured strains, a point mutation occurred at *afr* locus causing the S12c strain to have a higher tolerance towards mitomycin C and subsequently, a higher plasmid-curing efficiency. This mutation seemed to be strongly selected for by mitomycin C treatment, possibly caused by its role in increasing tolerance towards mitomycin C. Upregulation of the MexEF-OprN antibiotic pump regulated by Afr caused the increase of surviving colonies after mitomycin C treatment.

A frameshift at the *afr* locus is among the key mutations required for the restored tolerance towards high toluene concentrations in ALE-derived strains (Chapter 5). Truncation of the Afr protein and downregulation of the loci it is regulating, are therefore essential for the restoration of the solvent tolerance trait. Afr regulates an antibiotic efflux pump and several transporters which require H^+ influx to energize these systems, thus competing with the ArpABC efflux pump for toluene extrusion. Moreover, Afr positively regulates several porins which can be the entry channel for organic solvent into cytoplasm and membrane lipid bilay-

er. While the wild-type Afr requires an induction for upregulating these loci, the mutated Afr (T53P) is constitutively active and therefore these loci are constitutively overexpressed. The frameshift at the *afr* locus in ALE derived strains probably is required to maintain proton motive force and reduce toluene influx through porins.

Interplay between MexEF-OprN and ArpABC is mediated by Afr

In our plasmid-cured strains, the substitution T53P at Afr caused an increase in the MIC value of chloramphenicol and ciprofloxacin, the known substrates of MexEF-OprN. However, the MIC values for carbenicillin, kanamycin and streptomycin, which are the substrates of ArpABC, were decreased even though the expression level of ArpABC was not affected. In the ALE-derived strains, the ArpABC efflux pump was upregulated while other RND efflux pumps and proton-dependent membrane transporters were downregulated, including the MexEF-OprN. A previous study in *P. aeruginosa nfxC* mutant having the overexpression of MexEF-OprN pump, described a decreased production of C4-HSL which causes the downregulation of MexAB-OprM pump (homolog to ArpABC) (10). Taken together, there seems to be a competition between the efflux pumps ArpABC and the MexEF-OprN mediated by genetic regulatory elements like Afr and C4-HSL.

A previous study indicated that the expression of multiple pumps can cause a deleterious effect on the strain harbouring them (21). The cause of this toxicity may be due to the maintenance of proton motive force or the spatial competition since these pumps are embedded on the limited surface of the cell membrane. Afr seems to have a central role in the interplay between ArpABC and MexEF-OprN by positively regulating the expression of MexEF-OprN. Differential expression of MexEF-OprN, and perhaps also other membrane-bound transporters, can affect the performance of ArpABC in conferring antibiotic resistance or solvent tolerance to *P. putida* S12.

Materials and Methods

Strains and culture conditions

Strains and plasmids used in this chapter are listed in Table 6.5. All *P. putida* strains were grown in Lysogeny Broth (LB) at 30 °C with 200 rpm shaking and *E. coli* strains were cultivated in LB at 37 °C. For solid cultivation, 1.5 % (wt/vol) agar was added to LB. When required, gentamicin (25 mg liter^{-1}), carbenicillin (32 - 4096 mg liter^{-1}), kanamycin (1 - 128 mg liter^{-1}),

cefotaxime (2 – 256 mg liter^{-1}), ciprofloxacin (0.0625 – 8 mg liter^{-1}), trimethoprim (0.128 – 16.384 g liter^{-1}), aztreonam (2 - 256 mg liter^{-1} in DMSO), chloramphenicol (32 - 4096 mg liter^{-1} in methanol), streptomycin (8 – 1024 mg liter^{-1}), tetracycline (0.5 – 64 mg liter^{-1}), were added to the media.

Table 6.5. Strains and plasmids used in this chapter

Strain	**Characteristics**	**Ref.**
P. putida S12	Wild-type *P. putida* S12 (ATCC 700801), harboring megaplasmid pTTS12	(22)
P. putida S12c	*P. putida* S12, contains the point mutation ACC → CCC at RPPX_14685 locus (CDS. position 157)	(7)
P. putida S12-10	*P. putida* S12 ΔpTTS12, contains the point mutation ACC → CCC at RPPX_14685 locus (CDS. position 157)	(7)
P. putida S12-10wt	*P. putida* S12 ΔpTTS12, contains the wild-type RPPX_14685 locus (CDS. position 157)	This paper
P. putida S12-10Δ	*P. putida* S12 ΔpTTS12 ΔRPPX_14685	This paper
E. coli WM3064	*thrB1004 pro thi rpsL hsdS lacZ*ΔM15 RP4-1360 Δ(*araBAD*)567 Δ*dapA1341*::[erm pir]	William Metcalf
Plasmid	**Descriptions**	**Ref.**
pEMG	Km^R, Ap^R, *ori* R6K, *lacZ*α MCS flanked by two I-SceI sites	(23)
pEMG-Δ*afr*	pEMG plasmid for constructing *P. putida* S12-10Δ	This paper
pEMG-*afr*_wt	pEMG plasmid for constructing *P. putida* S12-10wt	This paper
pSW-2	Gm^R, *ori* RK2, *xylS*, Pm → I-SceI	(23)

DNA and RNA methods

All PCRs were performed using Phusion polymerase (Thermo Fisher) according to the manufacturer's manual. Primers used in this chapter (Table 6.6) were procured from Sigma-Aldrich. PCR products were visualized by gel electrophoresis on 1 % (w/v) TBE agarose containing 5 µg ml^{-1} ethidium bromide (110V, 0.5x TBE running buffer). For whole genome sequencing, DNA was extracted and the obtained data was processed as described in Chapter 5. The genome sequence of the plasmid-cured *P. putida* S12 have been submitted to the SRA database under accession number PRJNA602416.

For RT-qPCR analysis, RNA was extracted using TRIzol reagent (Invitrogen) according to the manufacturer's manual. The obtained RNA samples were cleaned-up using NucleoSpin® RNA Plant and Fungi kit (Macherey-Nagel) and immediately reverse transcribed using iScript™ cDNA synthesis kit (BioRad). cDNA may be stored at -20 °C prior to qPCR analysis. qPCR was performed using iTaq™ Universal SYBR Green Supermix (BioRad) on CFX96 Touch™ Real-Time PCR Detection System (BioRad). Data analysis was performed to calculate the $\log_2$ fold-change value as described by Taylor and colleagues (24), using the wild-type S12 strain as the control strain where *rpoB* and *gyrB* were chosenas the control household genes. For RNA-seq, the experiment was carried out as described in Chapter 5. Datasets generated from the RNA-seq experiment have been submitted to the GEO database under accession number GSE144045.

Table 6.6. Oligos used in this study

Oligos	Sequence	Purpose
KO_TS1_Afr_F	CCTCAGGATCCCTCAGTCGAAGGTATGCAAGTC-CA	knocking-out RPPX_14685
KO_TS1_Afr_R	TTCTTCACCTTTATGAATTCCCATGATCATGATG-GCTTTCCTCTGCTGACCG	knocking-out RPPX_14685
KO_TS2_Afr_F	CGCACGGCATGGATGAACTCTACAAATAAAGCT-CAACATTCGCCTGCACCG	knocking-out RPPX_14685
KO_TS2_Afr_R	GGCGATCTAGACCAACCTGTGTATACCGG-CAACCT	knocking-out RPPX_14685
c_Afr_F	GCAATGAATTCATCTGTGCAAAAACCTGTA	complementation of RPPX_14685 to the wild-type sequence in S12-10wt strain
c_Afr_R	AGGGTTCTAGAACAATCTCCTTGAAGCAG	complementation of RPPX_14685 to the wild-type sequence in S12-10wt strain
eco_gyrB_F	CGATAATTTTGCCAACCACGAT	qPCR, reference gene
eco_gyrB_R	GAAATTCTCCTCCCAGACCAAA	qPCR, reference gene
eco_rpoB_F	AACACGAGTTCGAGAAGAAACT	qPCR, reference gene
eco_rpoB_R	CGTTTAACCGCCAGATATACCT	qPCR, reference gene
ppu_gyrB_F	GCTTCGACAAGATGATTTCGTC	qPCR, reference gene
ppu_gyrB_R	GCAGTTTGTCGATGTTGTACTC	qPCR, reference gene
ppu_rpoB_F	GACAAGGAATCGTCGAACAAAG	qPCR, reference gene
ppu_rpoB_R	GAAGGTACCGTTCTCAGTCATC	qPCR, reference gene
14685_F	GCAGTTGCTTCTGGTACTGA	qPCR, target gene

Oligos	Sequence	Purpose
14685_R	GCTCAACAACAACTTCCAAC	qPCR, target gene
14930_F	GATGATGTAATCGCCCATCT	qPCR, target gene
14930_R	CAAGGAGTTGTGGAAAGCTC	qPCR, target gene
14935_F	CAAGGGAAGCTGTTGAAGTC	qPCR, target gene
14935_R	GATGTGGATCAAGCAGAAGTAC	qPCR, target gene
16940_F	CTGATCCTGGACGAACCTAC	qPCR, target gene
16940_R	GTTCAGCCTCTTCCAGGTAGT	qPCR, target gene
16945_F	GATCACCATGGTCCTGTACTT	qPCR, target gene
16945_R	ATGTACTGCATGTAGGTGAAGC	qPCR, target gene
17365_F	TGCAGCAATACCGTGTAGTAC	qPCR, target gene
17365_R	GTCGACGTACTCATCAACAATG	qPCR, target gene
17630_F	GAGAAACTCGAGAAGCTTGG	qPCR, target gene
17630_R	AACGACAGATAGATGGCAGTAC	qPCR, target gene
17635_F	CACCACGACTTACATGATTACC	qPCR, target gene
17635_R	CTCATGATGCTCAATGACAG	qPCR, target gene
17640_F	CAACGTGTACTTCAACGAGA	qPCR, target gene
17640_R	GTAATCGAGCAGAAAGCCTT	qPCR, target gene
17645_F	GTAGGTCTTGGTCACCTGG	qPCR, target gene
17645_R	ATCGAAGGTGTAGCAGAAGAC	qPCR, target gene
17650_F	CTGGGCTACCTTGATGATC	qPCR, target gene
17650_R	CTGCACTTCTACGAAACCAAG	qPCR, target gene
17720_F	CCACCAGCATTTCTATGATG	qPCR, target gene
17720_R	CCTTCTGATAGACAAAGCTCG	qPCR, target gene
17725_F	CTGTTGTAGTTCGACGACATC	qPCR, target gene
17725_R	GTGTTCACTCAGGATGACCA	qPCR, target gene
21210_F	AGTACCAGGTAGTCCACGGTAC	qPCR, target gene
21210_R	TCAGCGATTACGACAAGAC	qPCR, target gene
21215_F	GTGTACAGTGAACCCAGGTAAAC	qPCR, target gene
21215_R	CTGTTTACCAGCTACCAGGT	qPCR, target gene
21220_F	TGTCGACGAAGTTCATCTG	qPCR, target gene
21220_R	GTACCTCAAGTACACCCAGCT	qPCR, target gene
21545_F	CTGAACGACGATTCCTATCT	qPCR, target gene
21545_R	GAGTACAAGTCCTTGCCAAAG	qPCR, target gene
21550_F	GTGTGCTTACCCAACTGTTC	qPCR, target gene
21550_R	GCAACATGTACAACACTGTCAG	qPCR, target gene
21555_F	GAACGTGTCGTTGATCTGTT	qPCR, target gene
21555_R	AACTGACTGGTCTGAACAACC	qPCR, target gene
21560_F	CTTCCAGGGTGAATAGACAAC	qPCR, target gene
21560_R	GACTTCACCAACGAGATGAC	qPCR, target gene

Oligos	Sequence	Purpose
21565_F	GTAGTGGTAGAAGGTATTACGCAG	qPCR, target gene
21565_R	CACTCTGCACATCGACAAG	qPCR, target gene
24075_F	GGTACACCTTGATGATCTGC	qPCR, target gene
24075_R	CAGTTCTATGTGCACTGCATC	qPCR, target gene
24520_F	GTCGATCTCCAGCGGTAC	qPCR, target gene
24520_R	CTTCTGTGATGTGGGACTTCTAC	qPCR, target gene
24525_F	GTCATCGTCGAGCTTTTCTC	qPCR, target gene
24525_R	CCTACAGTTTCCAGGACCAC	qPCR, target gene
24930_F	CATCAACCAGAAGACCTATCAG	qPCR, target gene
24930_R	GCAGCCATACTTGGTGC	qPCR, target gene
24935_F	ATGCAGGTAGACTGGAAAGAAC	qPCR, target gene
24935_R	ATATCCCCTTCGTTCTCTTC	qPCR, target gene
25035_F	AACTGCACACTGTCACTGAAG	qPCR, target gene
24035_R	GCAGTCATCTGGTTCACC	qPCR, target gene
25340_F	GAACGACCTGATCACACG	qPCR, target gene
25340_R	GTACATGGCAGTGTTCAGG	qPCR, target gene
25345_F	CTGTAATAGTACGAAGCCTGG	qPCR, target gene
25345_R	GTATTGAACAGCTACAGATGGG	qPCR, target gene
25350_F	GAACACATAGAGCGGTAACC	qPCR, target gene
25350_R	CAGACACTCATGCTCAGCA	qPCR, target gene
25355_F	GATCAGGTTGTACTGCTGAAAC	qPCR, target gene
25355_R	GTATTCTGATCGACGACGTTC	qPCR, target gene

Curing and complementation of megaplasmid pTTS12 from *P. putida* S12

P. putida S12 was grown in LB to reach early exponential phase (± 3 hours or OD_{600} = 0.4-0.6). Subsequently, mitomycin C was added to the liquid culture to a final concentration of 10, 20, 30, 40, or 50 μg ml^{-1}. These cultures were grown for 24 hours and plated on M9 minimal media plated supplemented with indole to select for the absence of the megaplasmid. Complementation of the megaplasmid pTTS12 was performed using bi-parental mating between *P. putida* S12 (pTTS12 Km^R) and plasmid-cured strain *P. putida* S12 ΔpTTS12 (Gm^R :: Tn7) and followed by selection on LB agar supplemented with kanamycin and gentamicin.

MIC assay

The quantification of minimum inhibitory concentration (MIC) values were performed using broth microdilution on a 96-well plate. Overnight starting culture was diluted with LB media to reach 0.5 McFarland or approximately 10^8 CFUs ml^{-1}. A mixture of 95 µl LB media and 5 µl of

the inoculum suspension was placed in each well of a 96-well plate. Each column represented a different sample to be analyzed, with column 1-3 representing the wild-type S12, column 4-6 representing strain S12-10wt, column 7-9 representing strain S12-10, and column 10-12 representing strain S12-10Δ. Antibiotic solution (100 µl, diluted from the stock solution accordingly) was placed in row A and thoroughly mixed by pipetting. From the first row of wells, 100 µl of the mixture was added to the second row and mixed, and this serial dilution procedure was repeated up to row H; after which the excess 100-µl mixture was discarded. The microplate was incubated at 30°C for 24 h and the bacterial growth in the wells was assessed by measuring absorbance at 600nm (OD_{600}) using Tecan Spark plate reader.

Plasmid cloning

Deletion and complementation of the *afr* locus (RPPX_14685) was performed using homologous recombination between free-ended DNA sequences that are generated by cleavage at unique I-SceI sites (23). Two homologous recombination sites were chosen downstream (TS-1) and upstream (TS-2) of the target genes. TS-1 and TS-2 fragments were obtained by performing PCR using primers listed in Table 6.6. The obtained plasmid constructs were verified by DNA sequencing. Mating was performed as described by Wynands and colleagues (25). Deletion and complementation of the *afr* locus were verified by PCR and Sanger sequencing (Macrogen B.V., Amsterdam).

References

1. Yang J, Tauschek M, Robins-Browne RM. 2011. Control of bacterial virulence by AraC-like regulators that respond to chemical signals. Trends Microbiol 19:128–135.
2. Gallegos MT, Schleif R, Bairoch A, Hofmann K, Ramos JL. 1997. Arac/XylS family of transcriptional regulators. Microbiol Mol Biol Rev 61:393–410.
3. Yang J, Dogovski C, Hocking D, Tauschek M, Perugini M, Robins-Browne RM. 2009. Bicarbonate-Mediated Stimulation of RegA, the Global Virulence Regulator from *Citrobacter rodentium*. J Mol Biol 394:591–599.
4. Schleif R. 2000. Regulation of the L-arabinose operon of *Escherichia coli*. Trends Genet 16:559–565.
5. Cruite JT, Kovacikova G, Clark KA, Woodbrey AK, Skorupski K, Kull FJ. 2019. Structural basis for virulence regulation in *Vibrio cholerae* by unsaturated fatty acid components of bile. Commun Biol 2:440.
6. Juarez P, Jeannot K, Plésiat P, Llanes C. 2017. Toxic Electrophiles Induce Expression of the Multidrug Efflux Pump MexEF-OprN in *Pseudomonas aeruginosa* through a Novel Transcriptional Regulator, CmrA. Antimicrob Agents Chemother 61:e00585-17.
7. Kusumawardhani H, van Dijk D, Hosseini R, de Winde JH. 2020. A novel toxin-antitoxin module SlvT–SlvA regulates megaplasmid stability and incites solvent tolerance in *Pseudomonas putida* S12. Appl Environ Microbiol 86:e00686-20.
8. Yang J, Yan R, Roy A, Xu D, Poisson J, Zhang Y. 2015. The I-TASSER suite: Protein structure and function prediction. Nat Methods 12:7–8.
9. Rojas A, Duque E, Mosqueda G, Golden G, Hurtado A, Ramos JL, Segura A. 2001. Three efflux pumps are required to provide efficient tolerance to toluene in *Pseudomonas putida* DOT-T1E. J Bacteriol 183:3967–3973.
10. Maseda H, Sawada I, Saito K, Uchiyama H, Nakae T, Nomura N. 2004. Enhancement of the mexAB-oprM Efflux Pump Expression by a Quorum-Sensing Autoinducer and Its Cancellation by a Regulator, MexT, of the mexEF-oprN Efflux Pump Operon in *Pseudomonas aeruginosa*. Antimicrob Agents Chemother 48:1320–1328.
11. Miyada CG, Stoltzfus L, Wilcox G. 1984. Regulation of the araC of *Escherichia coli*: Catabolite repression, autoregulation, and effect on araBAD expression. Proc Natl Acad Sci U S A 81:4120–4124.
12. Issa KHB, Phan G, Broutin I. 2018. Functional mechanism of the efflux pumps tran-

scription regulators from *Pseudomonas aeruginosa* based on 3D structures. Front Mol Biosci.

13. Lehmann M, Tshisuaka B, Fetzner S, Lingens F. 1995. Molecular cloning of the isoquinoline 1-oxidoreductase genes from *Pseudomonas diminuta* 7, structural analysis of IorA and IorB, and sequence comparisons with other molybdenum-containing hydroxylases. J Biol Chem 270:14420–14429.
14. Price MN, Ray J, Iavarone AT, Carlson HK, Ryan EM, Malmstrom RR, Arkin AP, Deutschbauer M. 2019. Oxidative Pathways of Deoxyribose and Deoxyribonate Catabolism. mSystems 4:e00297-18.
15. Wylie JL, Worobec EA. 1995. The OprB porin plays a central role in carbohydrate uptake in *Pseudomonas aeruginosa*. J Bacteriol 177:3021–3026.
16. Li H, Luo YF, Williams BJ, Blackwell TS, Xie CM. 2012. Structure and function of OprD protein in *Pseudomonas aeruginosa*: From antibiotic resistance to novel therapies. Int J Med Microbiol 302:63–68.
17. Kadaba NS, Kaiser JT, Johnson E, Lee A, Rees DC. 2008. The high-affinity *E. coli* methionine ABC transporter: Structure and allosteric regulation. Science (80-) 321:250–253.
18. Zhou YF, Nan B, Nan J, Ma Q, Panjikar S, Liang YH, Wang Y, Su XD. 2008. C4-Dicarboxylates Sensing Mechanism Revealed by the Crystal Structures of DctB Sensor Domain. J Mol Biol 383:49–61.
19. Tenneson ME, Bilton RF, Drasar BS, Mason AN. 1979. The possible role of catabolic plasmids in bacterial steroid degradation. FEBS Lett 102:311–315.
20. Franklin FC, Bagdasarian M, Bagdasarian MM, Timmis KN. 1981. Molecular and functional analysis of the TOL plasmid pWWO from *Pseudomonas putida* and cloning of genes for the entire regulated aromatic ring meta cleavage pathway. Proc Natl Acad Sci 78:7458–7462.
21. Turner WJ, Dunlop MJ. 2015. Trade-Offs in Improving Biofuel Tolerance Using Combinations of Efflux Pumps. ACS Synth Biol 4:1056–1063.
22. Hartmans S, van der Werf MJ, de Bont JA. 1990. Bacterial degradation of styrene involving a novel flavin adenine dinucleotide-dependent styrene monooxygenase. Appl Environ Microbiol 56:1347–1351.
23. Martínez-García E, de Lorenzo V. 2011. Engineering multiple genomic deletions in

Gram-negative bacteria: analysis of the multi-resistant antibiotic profile of *Pseudomonas putida* KT2440. Environ Microbiol 13:2702–2716.

24. Taylor SC, Nadeau K, Abbasi M, Lachance C, Nguyen M, Fenrich J. 2019. The Ultimate qPCR Experiment: Producing Publication Quality, Reproducible Data the First Time. Trends Biotechnol.

25. Wynands B, Lenzen C, Otto M, Koch F, Blank LM, Wierckx N. 2018. Metabolic engineering of *Pseudomonas taiwanensis* VLB120 with minimal genomic modifications for high-yield phenol production. Metab Eng 47:121–133.

CHAPTER 7

Discussion

Pseudomonas putida as a robust microbial host for the production of high-value chemicals

The transition from a fossil-fuel to a bio-based economy is necessary to tackle the current environmental issues and ensure the sustainable economic growth. Current high demands in the production of value added products (e.g. food, energy, high-value chemicals) from renewable biological resources needs to be followed by system innovations in biotechnology fields. Recent developments in microbial physiology and metabolic engineering enable the production of biobased chemicals to become economically competitive with the petrochemical-based production (1–4).

Industrial microbial hosts need to fulfill a number of key performance indicators; for instance straightforward handling, reproducible production behavior, and more importantly, natural robustness to bioprocessing conditions (5). *Pseudomonas putida* meets these criteria due to its fast growth, high biomass yields, and low maintenance demands (6). This bacterium lacks a functional Embden-Meyerhof-Parnas (EMP) pathway and therefore, glycolysis occurs via Entner-Doudoroff (ED) pathway (7). Indeed, 90% of the consumed sugar is converted into gluconate and enters central carbon metabolism as 6-phosphogluconate (ED pathway) (8). However, 10% of the triose phosphates were found to be recycled back to form hexose phosphates, which evidently, merges ED, EMP, and pentose phosphate (PP) pathways into an EDEMP pathway (8). As the result, this bacterium exhibits an overflow metabolism which results in a surplus of ATP production and high NAD(P)H regeneration rates (8, 9). In addition, *P. putida* has been successfully engineered for efficient utilization of alternative carbon sources (e.g. D-xylose and L-arabinose), underlining its versatile metabolic constitution (10).

The remarkable solvent tolerance trait of *P. putida* S12 offers a greater degree of freedom in bioprocess development for aromatic chemicals (11). Therefore, *P. putida* S12 has been exploited for bioproduction of various aromatic chemicals, e.g. phenol, p-hydroxybenzoate, p-hydroxystyrene, and FDCA (4, 12–14). In this chapter, the genetic interplay of the advantageous solvent tolerance trait in *P. putida* S12 will be discussed.

Immediate and adaptive responses are required to circumvent solvent toxicity

Organic solvents ($LogP_{o/w}$ 1-4) may directly diffuse through the membrane or enter the cyto-

plasmic compartment through membrane porins and subsequently accumulate in bacterial membrane (Fig. 7.1). This accumulation leads to the increase of fluidity and disruption of the membrane. Damaged macromolecules and cellular components upon exposure to organic solvent may elicit a variety of cellular responses (15). Such responses can be divided into immediate and adaptive responses (15, 16). Immediate responses are a first line defence to solvent stress which are induced very rapidly or within minutes following the addition of organ-ic solvent. While such responses ensure the survival to solvent-shock, but they may not be sufficient to support long term growth in the presence of solvent. For this, adaptive responses ultimately take over after hours or generations of solvent exposure in bacterial cultures. In this chapter, the time frame of various cellular responses toward solvent stress in *P. putida* S12 will be addressed.

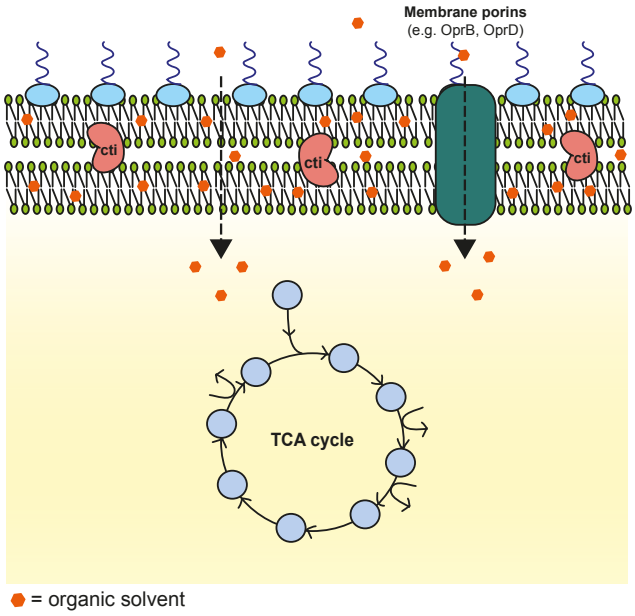

Fig. 7.1. Illustration of bacterial cells experiencing solvent stress.

Solvent tolerance mechanisms in *Pseudomonas putida* S12

Membrane lipid bilayer

Membrane compaction is important for the tolerance of *P. putida* S12 against organic solvents. By compacting the membrane, *P. putida* S12 reduces the internalization of organic solvent into the cells. As extensively discussed by Rühl and colleagues, trans-unsaturated

fatty acid concentrations were increased in *P. putida* S12 treated with 1-butanol, reducing the "kink" caused by the cis-conformation of unsaturated fatty acid (17). However, previous transcriptomic studies (18, 19) nor the transcriptomic data in this thesis (Chapter 5) did not show an increase in the expression of cis-trans isomerase (cti) during elevated temperature and solvent stress. Eberlein and colleagues argued that cti is constitutively expressed in a sufficient amount and its activity is controlled by the change of membrane fluidity as an immediate response to stress (20). A recent model of cti's mode of action by Eberlein and colleagues illustrate that in the presence of organic solvent, the membrane bilayer becomes more fluid and thus allow cti to access the membrane and change the cis-unsaturated fatty acid into its trans-conformation (Fig. 7.1, Ref. (20)). Introduction of cti into *E. coli*, a non-solvent-tolerant microbial host, significantly improved its solvent tolerance towards n-butanol (21).

In addition to cti activity, an increase of phosphatidylethanolamine (PE) and cardiolipin (CL) head groups was observed as a response to sudden 1-butanol addition at the expense of phosphatidylglycerol (PG) in *P. putida* S12 (17). However, variation of headgroup species was not observed when *P. putida* S12 was previously adapted to the presence of 1-butanol. Similar to cti activity, headgroup shift may play a role as an immediate response to stabilize bacterial membrane in the presence of organic solvent.

Bioenergetics and redox balance

During solvent stress, tricarboxylic acid (TCA) cycle components are upregulated, the NAD(P) H/NAD(P)$^+$ ratio is increased, but cell growth is typically reduced (Fig. 7.2, Ref. (16, 22–25)). Upregulation of the TCA cycle and subsequent increase of the NAD(P)H/NAD(P)$^+$ ratio enable the cells to cope with the demand of active solvent extrusion by the efflux pumps in maintaining proton motive force. When plasmid-cured *P. putida* S12 was adapted to high toluene concen-tration (ALE-derived strains), we observed the downregulation of F0F1 ATP synthase follow-ing the mutations found in the intergenic regions and subunits of this gene cluster (Chapter 5). Apparently, the demand of solvent extrusion pump requires the repression of other membrane proteins which are also energized by H^+ influx. On the other hand, respiratory proteins such as succinate dehydrogenase and cytochrome C oxidase were upregulated, presumably as an attempt to maintain redox balance and intracellular pH (Chapter 5, Ref. (24)). This remarkable metabolic flexibility allows *P. putida* S12 to survive the addition of high toluene concentration, even in the absence of its megaplasmid containing its main solvent pump.

Membrane proteins

P. putida S12, like other *P. putida* strains, contains multiple **r**esistance, **n**odulation, and cell-**d**ivision (RND) efflux pumps encoded on its chromosome and megaplasmid. Among these pumps, SrpABC, a homologue to TtgGHI of *P. putida* DOT-T1E and *Pseudomonas taiwanensis* VLB120, is the main solvent extrusion pump. SrpABC expression can be induced by organic solvents, which in turn will be extruded by this pump (26, 27). The *srpRSABC* operon is encoded on pTTS12 megaplasmid, along with a 3-phenylpropionate degradation gene cluster adjacent to it (Chapter 3). Identical arrangement of the *srpRSABC* operon and the 3-phenylpropionate degradation gene cluster was also found in *P. taiwanensis* VLB120, suggesting that these gene clusters were recently disseminated, presumably through horizontal gene transfer.

In *P. putida* S12, another RND efflux pump, ArpABC (homologue to TtgABC *P. putida* DOT-T1E and MexAB-OprM in *P. aeruginosa* (28, 29)), plays a role as a secondary extrusion pump to organic solvents. Notably, the role of this extrusion pump was initially unclear in *P. putida* S12 since megaplasmid removal or *srpABC* deletion would render the strain to be non-solvent-tolerant (Chapter 4) (30, 31). Kieboom and colleagues hypothesized that ArpABC may have a lower affinity towards organic solvent compared to SrpABC (31). Further analysis on the pumps efficiency and specific affinity to organic solvent however, remains of interest.

In the ALE-derived strains (Chapter 5), we observed that mutations occurred at the *arpR* locus which encodes for the repressor to ArpABC efflux pump. These mutations subsequently caused moderate upregulation of *arpBC* (*ttgBC*) loci. However, to achieve tolerance to a high toluene concentration, upregulation of this pump was not sufficient. Downregulation of other membrane proteins which are energized by H^+ influx, such as flagellar assembly, F0F1 ATP synthase, and transporters, is also appears necessary. Indeed, downregulation of membrane proteins, such as flagellar assembly gene clusters, was also reported by Molina and colleagues in their study regarding the response of *P. putida* strains towards solvent stress (22). This may be to accommodate the demand of ArpABC pump on proton motive force and due to the spatial restriction of the membrane surface in which these proteins are embedded.

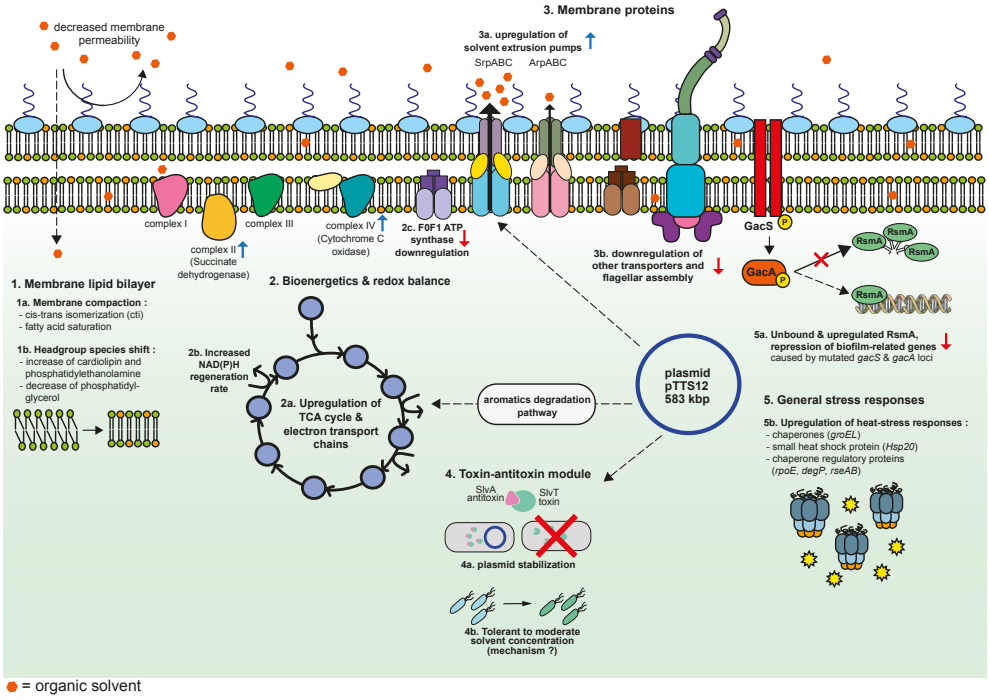

Fig. 7.2. Schematic representation of the solvent tolerance mechanism in *P. putida* S12

Toxin-antitoxin module

Bacterial toxin-antitoxins (TA) are ubiquitous systems that can be found encoded on bacterial chromosomes and plasmids; their role has been a controversial subject in recent years. TA modules have been reported to be important for the bacterial defence mechanisms, for instance in antibiotic resistance, bacterial persister formation, and more recently, as a predecessor to CRISPR-Cas systems as a phage defence system (32–35). However, Rosendahl and colleagues argued that most of the chromosomal TA systems do not demonstrate any clear benefit to their host and that they are maintained due to their low fitness cost (36).

In Chapter 4, a novel SlvT-SlvA TA module was identified to play a role in solvent stress response of *P. putida* S12. The polycistronic SlvT-SlvA TA mRNA was upregulated in transcriptomic data of *P. putida* S12 growing in the presence of toluene (Chapter 5 and Ref. (16)). Further scrutiny on this TA module revealed a role in stabilizing and maintaining the pTTS12 megaplasmid, especially during solvent stress when this plasmid may cause metabolic burden to *P. putida* S12 (Fig. 7.2). Moreover, chromosomal introduction of the SlvT-SlvA TA module in the plasmid-cured *P. putida* and *E. coli* strains slightly improved solvent

tolerance in these strains. This TA system is likely to act in the immediate response towards solvent stress by stalling cell growth. This would allow the bacteria to quickly adapt to its environment. Several proteases were found to be upregulated during solvent stress (16), that potentially may degrade SlvA antitoxin and subsequently release the SlvT toxin in its active form. Once active, SlvT toxin degrades NAD^+, thus affecting intracellular cofactor levels causing cell growth to be stalled.

General stress response and biofilm formation

One of the main stress responses in *P. putida* is the formation of biofilm. Biofilm formation occurs as a series of highly regulated steps: attachment, microcolony formation, maturation and dispersal (37). Reversible apical attachment of bacterial cells occurs to a surface upon initial contact, followed by irreversible lateral interaction. These attached cells rapidly multiplied into clonal microcolonies which then produce the biofilm matrix, consisting of exopolysaccharide (EPS), extracellular DNA and proteins (38). However, it was unclear whether biofilm formation is actually beneficial for constituting a high solvent tolerance phenotype. In addition, unintentional biofilm formation maybe disadvantageous in a fermenter set-up as previously described (39). Adherent cell layers in bioreactors may cause a negative effect on mass, energy and momentum transfer; creating an atypical econiche within the bioreactor; and inaccurate culture stoichiometric and kinetic parameters estimation (39).

The formation of biofilm in *P. putida* is regulated by the GacS/GacA two component system (37). Upon sensing the environmental signal, GacS becomes phosphorylated, which in turn, causes GacA to also become phosphorylated. GacA phosphorylation stimulates production of the small RNAs RsmZ and RsmY, which bind to the RsmA protein, releasing the repression of the biofilm matrix, quorum sensing signalling, and Type VI secretion system gene clusters (37). Both *gacS* and *gacA* loci were truncated or mutated in our ALE-derived strains with enhanced solvent tolerance (Chapter 5). In addition, RsmA was upregulated, probably unbound to RsmZ or RsmY, due to the disruption of *gacS* or mutated *gacA* loci. As the result, a significant reduction of biofilm formation was observed in our ALE-derived strains (Fig. 7.2). Reverse engineering of the key mutations revealed that after deletion of the *gacS* locus, solvent tolerance and growth parameters were generally improved (Chapter 5) while no biofilm formation occurred during solvent stress. It appears that in *P. putida* S12, it is essential to escape biofilm-forming tendency to adapt to high solvent concentration.

Several stress-related proteins were differentially expressed during solvent stress in *P. putida* S12 (Fig. 7.2). A previous chemostat-based proteomic study reported upregulation of heat shock protein GroEL caused by the addition of 5 mM toluene (24). In the ALE-derived strains, upregulation of another heat shock protein, Hsp20 (RPPX_17155), was observed (Chapter 5). Moreover, constitutive upregulation of the putative sigma factor E (RpoE), anti-sigma factor RseAB, and DegP, known to regulate chaperone proteins expression in *E. coli* (40), were observed in ALE-derived strains. Upregulation of several heat shock proteins and chaperones indicates the involvement of general stress responses, that are similar between heat and solvent stress. Heat stress primarily inactivate microbial activity through general protein unfolding. Thermophile bacteria respond to this stress by expressing chaperones and heat shock proteins to aid protein refolding (41–43). Similarly, solvent stress causes the release of membrane-bound proteins due to the membrane disruption (44). Thus, similar responses (e.g. chaperones and heat shock proteins upregulation) can be observed between thermophile and solvent-tolerant bacteria, aimed at refolding denatured proteins.

Regulating solvent tolerance mechanisms

Due to the high energy demand and potential toxicity of RND efflux pumps (45), such systems are typically tightly regulated. The SrpABC efflux pump is regulated by a pair of repressor and antirepressor, SrpS and SrpR respectively (46). The repression imposed by SrpS binding to the promoter region of srpABC operon can be subjugated by organic solvent binding to SrpS, or binding of SrpS to its antirepressor SrpR. The ArpABC efflux pump is regulated by a single repressor system, ArpR, which is a member of the TetR family regulators (31). Crystal structure analysis of TtgR (homologue of ArpR regulator in *P. putida* DOT-T1E) indicates the occurrence of two distinct binding sites within its large pocket (47). These binding sites allow the interaction between TtgR and antibiotics, solvents, or toxic plant secondary metabolites which are also extruded by the efflux pump. In addition to these repressor systems, mobile elements have been described to play an important role in regulating solvent efflux pumps. ISS12 and ISPpu21 were reported to disrupt the repressors of the *srpABC* and *arpABC* operons after prolonged exposure to organic solvent, thus enabling constitutive expression of the solvent extrusion pumps (Chapter 5, Ref. (48, 49)). On the other hand, prolonged storage in the absence of organic solvent was reported to cause ISS12 disruption of the *srpA* locus, rendering *P. putida* S12 to be less solvent-tolerant (50).

Other regulatory mechanisms have been described to be involved in the solvent stress response in *P. putida* S12. A putative modulator, TrgI, was found to be immediately repressed upon exposure to organic solvent (51). A knock-out of this gene causes a significant increase in solvent tolerance followed by differential expression of many genes, especially upregulation of the proteins related to the posttranslational modification, protein turnover, and molecular chaperones (16). In Chapter 5, an AraC family transcriptional regulator Afr, was found to be truncated in all of the ALE-derived strains. Afr positively regulates a number of membrane-bound proteins, including the MexEF-OprN antibiotic efflux pump (Chapter 6). Downregulation of TrgI and Afr regulatory proteins in *P. putida* S12 seemed to be important for the rewiring of metabolism during solvent stress.

Conclusion and future outlook

P. putida S12 circumvents the solvent stress through environmentally acquired mechanisms (e.g. solvent extrusion pumps and aromatic degradation pathway) in combination with inherent metabolic flexibility which allows this strain to adapt to the high energy demand of solvent extrusion pumps. While solvent extrusion pumps are indeed the main mechanisms to survive solvent stress, other accessory factors (e.g. membrane compaction, NAD(P)H regeneration rate, general stress responses) need to be taken into account to model and efficiently engineer the solvent tolerance trait in other non-solvent-tolerant microbial strains. Alternative mechanisms for cellular solvent removal, like outer membrane vesicle formation, have been described in other *P. putida* strains (52, 53) but requires further analysis in *P. putida* S12. Moreover, the works in this thesis indicate that there is a difference between SrpABC and ArpABC efflux pump in their ability to extrude solvent molecules. Further scrutiny on this difference; whether it is caused by pump specificity or affinity, membrane localization and other factors, may be beneficial for understanding and constructing a solvent-tolerant microbial cell factory.

References

1. Wynands B, Lenzen C, Otto M, Koch F, Blank LM, Wierckx N. 2018. Metabolic engineering of *Pseudomonas taiwanensis* VLB120 with minimal genomic modifications for high-yield phenol production. Metab Eng 47:121–133.
2. Kuepper J, Dickler J, Biggel M, Behnken S, Jäger G, Wierckx N, Blank LM. 2015. Metabolic Engineering of *Pseudomonas putida* KT2440 to Produce Anthranilate from Glucose. Front Microbiol 6:1310.
3. Wangrangsimagul N, Klinsakul K, Vangnai AS, Wongkongkatep J, Inprakhon P, Honda K, Ohtake H, Kato J, Pongtharangkul T. 2012. Bioproduction of vanillin using an organic solvent-tolerant *Brevibacillus agri* 13. Appl Microbiol Biotechnol 93:555–563.
4. Koopman F, Wierckx N, de Winde JH, Ruijssenaars HJ. 2010. Efficient whole-cell biotransformation of 5-(hydroxymethyl)furfural into FDCA, 2,5-furandicarboxylic acid. Bioresour Technol 101:6291–6296.
5. Weimer A, Kohlstedt M, Volke DC, Nikel PI, Wittmann C. 2020. Industrial biotechnology of *Pseudomonas putida*: advances and prospects. Appl Biochem Biotechnol.
6. Poblete-Castro I, Becker J, Dohnt K, dos Santos VM, Wittmann C. 2012. Industrial biotechnology of *Pseudomonas putida* and related species. Appl Microbiol Biotechnol 93:2279–2290.
7. Conway T. 1992. The Entner-Doudoroff pathway: history, physiology and molecular biology. FEMS Microbiol Lett 9:1–27.
8. Nikel PI, Chavarría M, Fuhrer T, Sauer U, De Lorenzo V. 2015. *Pseudomonas putida* KT2440 strain metabolizes glucose through a cycle formed by enzymes of the Entner-Doudoroff, embden-meyerhof-parnas, and pentose phosphate pathways. J Biol Chem 290:25920–25932.
9. Kohlstedt M, Wittmann C. 2019. GC-MS-based 13C metabolic flux analysis resolves the parallel and cyclic glucose metabolism of *Pseudomonas putida* KT2440 and *Pseudomonas aeruginosa* PAO1. Metab Eng 54:35–53.
10. Meijnen JP, De Winde JH, Ruijssenaars HJ. 2008. Engineering *Pseudomonas putida* S12 for efficient utilization of D-xylose and L-arabinose. Appl Environ Microbiol 74:5031–5037.
11. Kusumawardhani H, Hosseini R, de Winde JH. 2018. Solvent Tolerance in Bacteria: Fulfilling the Promise of the Biotech Era? Trends Biotechnol 36:1025–1039.

12. Wierckx NJP, Ballerstedt H, de Bont JAM, Wery J. 2005. Engineering of solvent-tolerant *Pseudomonas putida* S12 for bioproduction of phenol from glucose. Appl Environ Microbiol 71:8221–8227.
13. Verhoef S, Ruijssenaars HJ, de Bont JAM, Wery J. 2007. Bioproduction of p-hydroxybenzoate from renewable feedstock by solvent-tolerant *Pseudomonas putida* S12. J Biotechnol 132:49–56.
14. Verhoef S, Wierckx N, Westerhof RGM, de Winde JH, Ruijssenaars HJ. 2009. Bioproduction of p-hydroxystyrene from glucose by the solvent-tolerant bacterium *Pseudomonas putida* S12 in a two-phase water-decanol fermentation. Appl Environ Microbiol 75:931–936.
15. Nicolaou SA, Gaida SM, Papoutsakis ET. 2010. A comparative view of metabolite and substrate stress and tolerance in microbial bioprocessing: From biofuels and chemicals, to biocatalysis and bioremediation. Metab Eng 12:307–331.
16. Volkers RJM, Snoek LB, Ruijssenaars HJ, de Winde JH. 2015. Dynamic Response of *Pseudomonas putida* S12 to Sudden Addition of Toluene and the Potential Role of the Solvent Tolerance Gene trgI. PLoS One 10:e0132416.
17. Rühl J, Hein E-M, Hayen H, Schmid A, Blank LM. 2012. The glycerophospholipid inventory of *Pseudomonas putida* is conserved between strains and enables growth condition-related alterations. Microb Biotechnol 5:45–58.
18. Kiran MD, Prakash JSS, Annapoorni S, Dube S, Kusano T, Okuyama H, Murata N, Shivaji S. 2004. Psychrophilic *Pseudomonas syringae* requires trans-monounsaturated fatty acid for growth at higher temperature. Extremophiles 8:401–410.
19. Kiran MD, Annapoorni S, Suzuki I, Murata N, Shivaji S. 2005. Cis-trans isomerase gene in psychrophilic *Pseudomonas syringae* is constitutively expressed during growth and under conditions of temperature and solvent stress. Extremophiles 9:117–125.
20. Eberlein C, Baumgarten T, Starke S, Heipieper HJ. 2018. Immediate response mechanisms of Gram-negative solvent-tolerant bacteria to cope with environmental stress: *cis-trans* isomerization of unsaturated fatty acids and outer membrane vesicle secretion. Appl Microbiol Biotechnol 102:2583–2593.
21. Tan Z, Yoon JM, Nielsen DR, Shanks J V., Jarboe LR. 2016. Membrane engineering via trans unsaturated fatty acids production improves *Escherichia coli* robustness and

production of biorenewables. Metab Eng 35:105–113.

22. Molina-Santiago C, Udaondo Z, Gómez-Lozano M, Molin S, Ramos JL. 2017. Global transcriptional response of solvent-sensitive and solvent-tolerant *Pseudomonas putida* strains exposed to toluene. Environ Microbiol 19:645–658.
23. Udaondo Z, Duque E, Fernández M, Molina L, de la Torre J, Bernal P, Niqui J-L, Pini C, Roca A, Matilla MA, Molina-Henares MA, Silva-Jiménez H, Navarro-Avilés G, Busch A, Lacal J, Krell T, Segura A, Ramos JL. 2012. Analysis of solvent tolerance in *Pseudomonas putida* DOT-T1E based on its genome sequence and a collection of mutants. FEBS Lett 586:2932–2938.
24. Volkers RJM, de Jong AL, Hulst AG, van Baar BLM, de Bont JAM, Wery J. 2006. Chemostat-based proteomic analysis of toluene-affected *Pseudomonas putida* S12. Environ Microbiol 8:1674–1679.
25. Segura A, Godoy P, van Dillewijn P, Hurtado A, Arroyo N, Santacruz S, Ramos J-L. 2005. Proteomic analysis reveals the participation of energy- and stress-related proteins in the response of *Pseudomonas putida* DOT-T1E to toluene. J Bacteriol 187:5937–5945.
26. Kieboom J, Dennis JJ, Zylstra GJ, de Bont JA. 1998. Active efflux of organic solvents by *Pseudomonas putida* S12 is induced by solvents. J Bacteriol 180:6769–6772.
27. Kieboom J, Dennis JJ, de Bont JAM, Zylstra GJ. 1998. Identification and Molecular Characterization of an Efflux Pump Involved in *Pseudomonas putida* S12 Solvent Tolerance. J Biol Chem 273:85–91.
28. Rojas A, Duque E, Mosqueda G, Golden G, Hurtado A, Ramos JL, Segura A. 2001. Three efflux pumps are required to provide efficient tolerance to toluene in *Pseudomonas putida* DOT-T1E. J Bacteriol 183:3967–3973.
29. Tsutsumi K, Yonehara R, Ishizaka-Ikeda E, Miyazaki N, Maeda S, Iwasaki K, Nakagawa A, Yamashita E. 2019. Structures of the wild-type MexAB–OprM tripartite pump reveal its complex formation and drug efflux mechanism. Nat Commun. 10: 1520
30. Kusumawardhani H, van Dijk D, Hosseini R, de Winde JH. 2020. A novel toxin-antitoxin module SlvT–SlvA regulates megaplasmid stability and incites solvent tolerance in *Pseudomonas putida* S12. Appl Environ Microbiol 86:e00686-20.
31. Kieboom J, de Bont JAM. 2001. Identification and molecular characterization of an efflux system involved in *Pseudomonas putida* S12 multidrug resistance. Microbiology

147:43–51.

32. Yang QE, Walsh TR. 2017. Toxin-antitoxin systems and their role in disseminating and maintaining antimicrobial resistance. FEMS Microbiol Rev 41:343–353.
33. Maisonneuve E, Gerdes K. 2014. Molecular mechanisms underlying bacterial persisters. Cell 157:539–548.
34. Page R, Peti W. 2016. Toxin-antitoxin systems in bacterial growth arrest and persistence. Nat Chem Biol 12:208–214.
35. Song S, Wood TK. 2020. A Primary Physiological Role of Toxin/Antitoxin Systems Is Phage Inhibition. Front Microbiol 11:1895.
36. Rosendahl S, Tamman H, Brauer A, Remm M, Hõrak R. 2020. Chromosomal toxin-antitoxin systems in *Pseudomonas putida* are rather selfish than beneficial. Sci Rep 10:9230.
37. Nadal Jimenez P, Koch G, Thompson JA, Xavier KB, Cool RH, Quax WJ. 2012. The Multiple Signaling Systems Regulating Virulence in *Pseudomonas aeruginosa*. Microbiol Mol Biol Rev 76:46–65.
38. Martínez-Gil M, Ramos-González MI, Espinosa-Urgel M. 2014. Roles of cyclic Di-GMP and the Gac system in transcriptional control of the genes coding for the *Pseudomonas putida* adhesins LapA and LapF. J Bacteriol 196:1484–1495.
39. Bryers JD. 1991. Understanding and controlling detrimental bioreactor biofilms. Trends Biotechnol 9:422–426.
40. Hews CL, Cho T, Rowley G, Raivio TL. 2019. Maintaining Integrity Under Stress: Envelope Stress Response Regulation of Pathogenesis in Gram-Negative Bacteria. Front Cell Infect Microbiol 9:313.
41. Shockley KR, Ward DE, Chhabra SR, Conners SB, Montero CI, Kelly RM. 2003. Heat shock response by the hyperthermophilic archaeon *Pyrococcus furiosus*. Appl Environ Microbiol 69:2365–2371.
42. Johnson MR, Conners SB, Montero CI, Chou CJ, Shockley KR, Kelly RM. 2006. The Thermotoga maritima phenotype is impacted by syntrophic interaction with *Methanococcus jannaschii* in hyperthermophilic coculture. Appl Environ Microbiol 72:811–818.
43. Wang Q, Cen Z, Zhao J. 2015. The survival mechanisms of thermophiles at high temperatures: An angle of omics. Physiology 30:97–106.
44. Volkers R. 2012. Systems analysis of solvent tolerance mechanisms in *Pseudomonas*

putida S12 - Importance of energy metabolism and functional identification of the TrgI regulator. Delft University of Technology.

45. Turner WJ, Dunlop MJ. 2015. Trade-Offs in Improving Biofuel Tolerance Using Combinations of Efflux Pumps. ACS Synth Biol 4:1056–1063.
46. Sun X, Zahir Z, Lynch KH, Dennis JJ. 2011. An Antirepressor, SrpR, Is Involved in Transcriptional Regulation of the SrpABC Solvent Tolerance Efflux Pump of *Pseudomonas putida* S12. J Bacteriol 193:2717–2725.
47. Alguel Y, Meng C, Terán W, Krell T, Ramos JL, Gallegos MT, Zhang X. 2007. Crystal Structures of Multidrug Binding Protein TtgR in Complex with Antibiotics and Plant Antimicrobials. J Mol Biol 369:829–840.
48. Wery J, Hidayat B, Kieboom J, de Bont JA. 2001. An insertion sequence prepares *Pseudomonas putida* S12 for severe solvent stress. J Biol Chem 276:5700–5706.
49. Sun X, Dennis JJ. 2009. A Novel Insertion Sequence Derepresses Efflux Pump Expression and Preadapts *Pseudomonas putida* S12 for Extreme Solvent Stress. J Bacteriol 191:6773–6777.
50. Hosseini R, Kuepper J, Koebbing S, Blank LM, Wierckx N, de Winde JH. 2017. Regulation of solvent tolerance in *Pseudomonas putida* S12 mediated by mobile elements. Microb Biotechnol 10:1558–1568.
51. Volkers RJM, Ballerstedt H, Ruijssenaars H, de Bont JAM, de Winde JH, Wery J. 2009. TrgI, toluene repressed gene I, a novel gene involved in toluene-tolerance in *Pseudomonas putida* S12. Extremophiles 13:283–297.
52. Baumgarten T, Sperling S, Seifert J, von Bergen M, Steiniger F, Wick LY, Heipieper HJ. 2012. Membrane vesicle formation as a multiple-stress response mechanism enhances *Pseudomonas putida* DOT-T1E cell surface hydrophobicity and biofilm formation. Appl Environ Microbiol 78:6217–6224.
53. Eberlein C, Starke S, Doncel ÁE, Scarabotti F, Heipieper HJ. 2019. Quantification of outer membrane vesicles: a potential tool to compare response in *Pseudomonas putida* KT2440 to stress caused by alkanols. Appl Microbiol Biotechnol 103:4193–4201.

Summary

Bacterial biocatalysis constitutes a sustainable alternative for high-value chemicals production by enabling the utilization of renewable feedstocks. However, biobased production of aromatic compounds and biopolymers requires a specialized microbial cell factory. Microbial hosts may experience cell toxicity caused by the solvent-like compounds that emerge as products, substrates or intermediates during the production process. Therefore, solvent tolerance is an essential trait for the microbial hosts used in biobased production of aromatic chemicals and biopolymers. The work described in this thesis focused on identifying and characterizing genes/gene clusters which are involved in conferring solvent tolerance trait in bacteria.

Pseudomonas putida S12 is inherently solvent-tolerant and, therefore, constitutes a promising platform for biobased production of aromatic compounds and biopolymers (overview in **chapter 2**). The genome of *P. putida* S12 consists of a 5.8-Mbp chromosome and a 580-kbp megaplasmid pTTS12. In **chapter 3**, systematic analysis of the genes encoded on pTTS12 revealed that a large fraction of these genes is involved in stress response, increasing survival under harsh conditions like heavy metal and solvent stress. Comparative analysis of pTTS12 provides a thorough insight into its structural and functional build-up. This plasmid is highly stable and carries a complex arrangement of transposable elements containing heavy metal resistance clusters and several aromatic degradation pathways.

In **chapter 4**, we revisit the essential role of pTTS12 for molecular adaptation to solvent stress in *P. putida* S12. In addition to the solvent extrusion pump (SrpABC), we identified a novel toxin-antitoxin module (SlvAT) which contributes to the short-term tolerance in moderate solvent concentrations and to the stability of pTTS12. Indeed, toxin-antitoxin modules have been reported to be involved in survival strategies, such as stress response, biofilm formation, and antimicrobial persistence in *Pseudomonas*. SlvT toxin expression causes NAD^+ degradation which leads to the arrest of cell division. The expression of SlvA antitoxin immediately restores NAD^+ levels. This toxin-antitoxin module may act as an immediate response towards solvent stress by stalling cell growth, allowing the bacteria to quickly adapt to their environment. The solvent tolerance gene clusters from pTTS12: *slvAT* and *srp* operon, were successfully expressed in the non-solvent-tolerant strains of *P. putida* and *Escherichia coli* strains to confer and enhance their solvent tolerance.

Removal of pTTS12 caused a significant reduction in the solvent tolerance of *P. putida* S12. In **chapter 5**, we succeeded in restoring solvent tolerance in the plasmid-cured *P. putida* S12 using adaptive laboratory evolution (ALE). We further investigate the intrinsic solvent tolerance of *P. putida* S12 (in the absence of pTTS12). Whole genome sequencing identified several single nucleotide polymorphisms (SNPs) and a mobile element insertion, which allow the solvent-adapted strains to grow in the presence of 10% (vol/vol) toluene. Mutations were identified on an RND efflux pump regulator *arpR*, resulting in a constitutive upregulation of the multifunctional efflux pump ArpABC. Single nucleotide polymorphisms (SNPs) were also found in the intergenic regions and subunits of ATP synthase, RNA polymerase subunit β', the global two-component regulatory system (*gacA*/*gacS*), and a putative AraC family transcriptional regulator *afr* loci. Transcriptome analysis further revealed a constitutive down-regulation of proton-influx dependent activities in ALE-derived strains; such as flagellar assembly, F0F1 ATP synthase, and membrane transport proteins.

Our experiments pointed to the importance of the *afr* locus in enabling the plasmid curing and recovery of solvent tolerance. However, the role of this putative transcriptional regulator remained elusive. In **chapter 6**, the role of Afr was further characterized. Transcriptional analysis (RNA-seq) and confirmatory RT-qPCR experiments indicated that Afr positively regulates at least 32 loci. These genes/gene clusters putatively encode for membrane transporters, porins, and dehydrogenases; including the MexEF-OprN multidrug efflux pump known to be involved in active export of several antibiotics. Moreover, the mutation and truncation of Afr changed the antibiotic resistance profile, underscoring the central role of Afr as a stress-response regulator in *P. putida* S12.

The work described in this thesis further enhanced our knowledge and insight into the mechanisms operating in *P. putida* to establish solvent tolerance. Adaptability of *P. putida* S12 is dependent on the ability to cope with the high energy demand of solvent stress. The inherent metabolic flexibility of *P. putida* S12 has partly been developed through horizontally transferred traits, such as aromatic degradation pathways and solvent extrusion pumps.

Samenvatting

Bacteriële biokatalyse vormt een duurzaam alternatief voor de productie van waardevolle chemicaliën doordat er gebruik wordt gemaakt van hernieuwbare grondstoffen. Echter, voor het biologisch produceren van aromatische stoffen en biopolymeren is een gespecialiseerde microbiologische celfabriek nodig. De oplosmiddel-achtige stoffen die als product, substraat of tussenproduct aanwezig kunnen zijn of gevormd kunnen worden tijdens productie, worden door de microbiële gastheer mogelijk als toxisch ervaren. Daarom is 'oplosmiddel tolerantie' een essentiële eigenschap voor de microbiële gastheerorganismen die gebruikt worden voor de biologische productie van aromatische stoffen en biopolymeren. Het werk beschreven in dit proefschrift focust op het identificeren en karakteriseren van genen en genclusters die betrokken zijn bij oplosmiddeltolerantie in bacteriën.

Pseudomonas putida S12 is intrinsiek oplosmiddel tolerant en vormt daarom een veelbelovend platform voor de biologische productie van aromatische stoffen en biopolymeren (overzicht in **hoofdstuk 2**). Het genoom van *P. putida* S12 bestaat uit een 5,8-Mbp chromosoom en een 580-kbp megaplasmide pTTS12. In **hoofdstuk 3** wordt beschreven hoe een systematische analyse van genen gecodeerd op pTTS12 liet zien dat een groot gedeelte van deze genen betrokken is bij de algemene stress respons, wat de overlevingskans tegen heftige stressoren zoals zware metalen en oplosmiddelen vergroot. Een vergelijkende analyse van pTTS12 gaf nieuwe inzichten in de structurele en functionele opbouw van dit plasmide. Het plasmide is erg stabiel en draagt een complexe verzameling van transponeerbare elementen bestaand uit genclusters voor resistentie tegen zware metalen en meerdere afbraakroutes van aromatische verbindingen.

In **hoofdstuk 4** herbeschouwen we de essentiële rol van pTTS12 voor moleculaire adaptatie van *P. putida* S12 tegen oplosmiddel stress. Naast de oplosmiddel extrusiepomp (SrpABC) hebben we een nieuwe toxine-antitoxine module geïdentificeerd (SlvAT) welke bijdraagt aan de korte termijn tolerantie in gematigde oplosmiddel concentraties en bijdraagt aan de stabiliteit van plasmide pTTS12. Inderdaad, toxine-antitoxine modules werden ook eerder genoemd als betrokken bij microbiële overlevingsstrategieën, zoals stress respons, vorming van biofilms en antimicrobiële resistentie in *Pseudomonas* soorten. Expressie van het SlvT toxine leidt tot NAD^+ degradatie, wat op zijn beurt leidt tot het stop zetten van celdel-

ing. Expressie van het antitoxine SlvA herstelt de NAD^+ concentratie binnen korte tijd weer. Deze toxine-antitoxine module zou kunnen dienen als een onmiddellijke reactie tegen oplosmiddel stress door celgroei te remmen, wat de bacteriën in staat stelt en tijd geeft om zich aan te passen aan hun omgeving. De genclusters betrokken bij oplosmiddel resistentie gecodeerd op plasmide pTTS12 (*slvAT* en het *srp* operon) zijn succesvol overgebracht en tot expressie gebracht in van nature niet-oplosmiddel-resistente stammen van *P. putida* en *E. coli*, om zo de oplosmiddel resistente eigenschap over te brengen en te versterken in deze stammen. Dit onderzoek laat zien dat deze oplosmiddel resistentie, inderdaad in bepaalde mate overdraagbaar is aan andere bacteriën.

Het verwijderen van pTTS12 uit *P. putida* S12 leidt tot een significante reductie in oplosmiddel resistentie. In **hoofdstuk 5** laten we zien hoe de oplosmiddel resistente eigenschap hersteld kan worden een stam waaruit het plasmide werd verwijderd, aan de hand van adaptieve laboratorium evolutie (ALE). Vervolgens onderzochten we in meer detail de intrinsieke oplosmiddel resistentie van *P. putida* S12 (in de afwezigheid van pTTS12). Door het genoom volledig te sequencen kwamen we er achter dat mutaties van maar enkele basen in het DNA (SNPs) en een insertie van een mobiel element de (geringe) veranderingen waren op het genoom die er samen voor hebben gezorgd dat de geëvolueerde stammen konden groeien in de aanwezigheid van 10% (vol/vol) tolueen. Mutaties zaten onder andere in een RND-type extrusiepomp regulator genaamd *arpR*; deze mutatie leidde tot een constitutieve opregulatie van de multifunctionele extrusiepomp ArpABC. Mutaties zijn ook gevonden in de intergene regio's en subunits van ATP synthase, RNA polymerase subunit β', het algemene twee-componenten regulatie system (*gacA*/*gacS*) en op het locus van een nog onbekende regulator van transcriptie behorende tot de AraC familie. Uit analyse van het transcriptoom bleek dat er constitutieve downregulatie plaatsvindt van activiteiten die afhankelijk zijn van proton-instroom in alle ALE-verkregen stammen zoals de assemblage van flagella, F0F1 ATP synthase en membraan transport eiwitten.

Uit onze experimenten bleek het belang van het *afr* locus bij het wel of niet kunnen verliezen van het pTTS12 plasmide alsmede het herstellen van oplosmiddel resistentie in de geëvolueerde stammen. Echter, de rol van deze mogelijke regulator van transcriptie bleef tot nog toe onbekend. In **hoofdstuk 6** wordt de rol van Afr verder gekarakteriseerd. Transcriptoom analyse (RNA-seq) en bevestiging middels RT-qPCR experimenten duidde aan dat regulator Afr op zijn minst 32 loci aanstuurt. Deze genen dan wel genclusters coderen

vermoedelijk voor membraan transporters, porines, en dehydrogenases; waaronder de MexEF-OprN multidrug extrusiepomp waarvan bekend is dat deze meerdere soorten antibiotica actief de cel uit exporteert. Tevens, de mutatie en truncatie van Afr veranderde het antibiotica resistentie profiel van *P. putida S12*, wat nogmaals onderstreept dat Afr een centrale rol speelt als stress-response regulator in deze bacterie.

Het werk in dit proefschrift verbreedt en verruimt onze kennis en inzichten in de mechanismen die *P. putida* in staat stellen diens karakteristieke oplosmiddel resistente eigenschappen tot uiting te brengen. Het flexibele en adaptieve karakter van *P. putida* S12 is afhankelijk van het vermogen om aan de sterk verhoogde enrgievraag tijdens oplosmiddel stress te voldoen. De intrinsieke metabole flexibiliteit van *P. putida* S12 is gedeeltelijk tot stand gekomen door horizontale genoverdracht, zoals van aromatische afbraakroutes en van de oplosmiddel extrusiepompen.

Ringkasan

Biokatalisis bakteri merupakan upaya keberlanjutan alternatif dalam produksi bahan kimia bernilai tinggi karena melalui proses ini, bahan baku terbarukan dapat dimanfaatkan. Namun, produksi senyawa aromatik dan biopolimer berbasis biologi membutuhkan pabrik sel mikroba tersendiri. Pada umumnya, inang mikroba akan mengalami toksisitas yang disebabkan oleh senyawa-senyawa dengan sifat seperti pelarut (organik) yang timbul sebagai produk, substrat, atau zat antara selama proses produksi. Oleh karena itu, ketahanan terhadap pelarut merupakan sifat penting bagi inang mikroba yang akan digunakan dalam produksi bahan kimia aromatik dan biopolimer berbasis biologi. Penelitian yang diuraikan dalam disertasi ini berfokus pada identifikasi dan karakterisasi beberapa gen/klaster gen yang terlibat dalam pemberian sifat toleransi terhadap pelarut pada bakteri.

Pseudomonas putida S12 secara inheren memiliki sifat tahan terhadap pelarut, sehingga bakteri ini merupakan inang/*platform* yang sesuai untuk memproduksi senyawa aromatik dan biopolimer berbasis biologi (ikhtisar dalam **bab 2**). Genom *P. putida* S12 terdiri dari sebuah kromosom berukuran 5,8-Mbp dan sebuah megaplasmid pTTS12 berukuran 580-kbp. Dalam **bab 3**, analisis sistematis terhadap plasmid pTTS12 mengungkapkan bahwa sebagian besar gen-gen dalam plasmid ini terlibat dalam respons stres, meningkatkan ketahanan terhadap berbagai logam berat dan pelarut. Analisis komparatif ini memberikan pemahaman yang menyeluruh mengenai struktur dan fungsi plasmid pTTS12. Plasmid ini sangat stabil dan mengandung beberapa elemen transposabel kompleks yang berisi klaster-klaster gen resistensi logam berat dan sejumlah jalur degradasi aromatik.

Dalam **bab 4**, kami meninjau kembali peran penting pTTS12 sebagai adaptasi molekuler terhadap stres yang disebabkan oleh pelarut pada *P. putida* S12. Selain pompa ekstrusi pelarut (SrpABC), kami mengidentifikasi modul toksin-antitoksin baru (SlvAT) yang berkontribusi pada toleransi jangka pendek dalam konsentrasi pelarut sedang dan pada stabilitas pTTS12. Pada beberapa penelitian sebelumnya, modul toksin-antitoksin telah diketahui terlibat dalam strategi bertahan hidup seperti respons stres, pembentukan *biofilm*, dan persistensi terhadap antimikroba pada bakteri *Pseudomonas*. Ekspresi toksin SlvT menyebabkan degradasi NAD^+ yang diikuti dengan terhentinya pembelahan sel. Sebaliknya, ekspresi antitoksin SlvA dapat segera memulihkan kadar NAD^+ dalam sel. Modul toksin-antitoksin

ini bertindak sebagai respon langsung terhadap stres pelarut dengan menghambat pertumbuhan sel, sehingga memungkinkan sel bakteri beradaptasi dengan cepat terhadap lingkungannya. Klaster gen toleransi pelarut dari plasmid pTTS12 (*slvAT* dan operon *srp*) berhasil diekspresikan dalam beberapa galur *P. putida* dan *Escherichia coli* yang pada mulanya tidak tahan terhadap pelarut. Kedua klaster gen ini dapat meningkatkan toleransi pelarut pada beberapa galur *P. putida* dan *Escherichia coli*.

Penghapusan pTTS12 menyebabkan penurunan yang signifikan terhadap toleransi pelarut pada *P. putida* S12. Dalam **bab 5**, kami dapat memulihkan toleransi pelarut pada *P. putida* S12 yang tidak mengandung plasmid melalui eksperimen evolusi adaptif dalam laboratorium (ALE). Kami menyelidiki lebih lanjut toleransi pelarut intrinsik pada *P. putida* S12 yang tidak mengandung plasmid pTTS12. Melalui analisis pengurutan genom secara menyeluruh, beberapa polimorfisme nukleotida tunggal (SNP) dan penyisipan *mobile element* yang memungkinkan galur turunan ini beradaptasi dan tumbuh dalam media dengan 10% (vol / vol) toluena dapat diidentifikasi. Mutasi ditemukan pada gen *arpR*, yang merupakan regulator pompa efluks RND, dan menghasilkan peningkatan ekspresi secara konstitutif terhadap pompa ekstrusi antibiotik ArpABC. Beberapa SNP juga ditemukan pada bagian antargen dan subunit ATP sintase, pada subunit RNA polimerase β', pada sistem pengaturan global dengan dua komponen (gen *gacA*/*gacS*), dan pada regulator transkripsi gen *afr*. Analisis transkriptom mengungkapkan penurunan regulasi secara konstitutif pada beberapa klaster gen dengan aktivitas yang bergantung pada masuknya proton ke dalam sel; seperti flagela, F0F1 ATP sintase, dan protein transpor membran.

Eksperimen kami menunjukkan pentingnya gen *afr* dalam penghapusan plasmid dan pemulihan toleransi pelarut. Namun, aktivitas protein yang diduga berperan sebagai regulator transkripsi ini belum sepenuhnya dipahami. Dalam **bab 6**, peran protein Afr dikarakterisasi lebih jauh. Analisis transkriptom (RNA-seq) dan eksperimen konfirmasi menggunakan RT-qPCR menunjukkan bahwa Afr mengatur setidaknya 32 loci secara positif. Gen-gen ini mengkodekan protein transpor membran, porin, enzim-enzim dehydrogenase, dan pompa ekstrusi antibiotik MexEF-OprN, yang telah dikenal dalam ekspor aktif antibiotik. Selain itu, mutasi dan interupsi protein Afr dapat mengubah profil resistensi antibiotik sehingga menonjolkan peran Afr sebagai regulator respon stres pada *P. putida* S12.

Penelitian yang dijelaskan dalam disertasi ini bermanfaat untuk meningkatkan pengetahuan dan wawasan kita tentang mekanisme sifat ketahanan terhadap pelarut dalam bak-

teri *P. putida*. Adaptasi terhadap pelarut dalam *P. putida* S12 bergantung pada kemampuan bakteri ini untuk memenuhi kebutuhan energi yang tinggi dari stres yang diakibatkan oleh pelarut. Fleksibilitas metabolik yang melekat pada *P. putida* S12 sebagian dibentuk oleh gen-gen yang didapatkan secara horizontal, seperti jalur degradasi aromatik dan pompa ekstrusi pelarut.

Curriculum vitae

Hadiastri Kusumawardhani (Astri) was born on September 6th, 1991 in Bandung, Indonesia. She graduated from SMA Negeri 3 Bandung (high school) in 2009 and continued her study in pharmaceutical science and technology at the School of Pharmacy, Institut Teknologi Bandung (ITB) in Indonesia (2009-2013, cum laude). During her internship and final project, she became interested in the field of biotechnology. This interest motivated her to continue on her master degree (2012-2014, cum laude) in pharmaceutical biotechnology field at the School of Pharmacy, ITB, supported by a scholarship grant for fast-track program from the Ministry of Research, Technology, and Higher Education (DIKTI), Indonesia. After completing her pharmacist professional degree (2014-2015), she started her PhD with Prof. J.H. de Winde, at the Institute of Biology, Leiden University, The Netherlands, to study solvent tolerance mechanisms in industrial strains of *Pseudomonas*. This was supported by the Indonesia Endowment Fund for Education (LPDP) as scholarship provider from the Ministry of Finance, Indonesia. This work is described in this thesis. Astri is now going to continue her research trajectory as a post-doctoral fellow at Prof. Yolanda Schaerli's lab, University of Lausanne, Switzerland.

Publications

Kusumawardhani H, Hosseini R, de Winde JH. 2018. Solvent Tolerance in Bacteria: Fulfilling the Promise of the Biotech Era? Trends Biotechnol 36:1025–1039.
(DOI: 10.1016/j.tibtech.2018.04.007)

Kusumawardhani H, van Dijk D, Hosseini R, de Winde JH. 2020. A novel toxin-antitoxin module SlvT–SlvA regulates megaplasmid stability and incites solvent tolerance in *Pseudomonas putida* S12. Appl Environ Microbiol 86:e00686-20.
(DOI: 10.1128/AEM.00686-20)

Kusumawardhani H*, Hosseini R*, de Winde JH. Comparative analysis reveals the modular functional build-up of megaplasmid pTTS12 of *Pseudomonas putida* S12: a paradigm for transferable traits, plasmid stability and inheritance? *Submitted for publication.*
(DOI: 10.1101/2020.06.19.162511)
*shared first author

Kusumawardhani H, Furtwängler B, Blommestijn M, Kaltenytė A, van der Poel J, Kolk J, Hosseini R, de Winde J H. Adaptive laboratory evolution restores solvent tolerance in plasmid-cured *Pseudomonas putida* S12; a molecular analysis. *Submitted for publication.*
(DOI: 10.1101/2020.08.01.232264)

Kusumawardhani H, Yadav A, Kaltenytė A, Furtwängler B, Hosseini R, de Winde JH. Characterization of an AraC family transcriptional regulator Afr in *Pseudomonas putida* S12. *Manuscript in preparation.*